SEMMELWEIS EGYETEM

DOKTORI ISKOLA

Ph.D. értekezések

3434.

POLLÁK PATRIK

A gyógyszerészeti tudományok korszerű kutatási irányai

című program

Programvezető: Dr. Antal István, egyetemi tanár

Témavezetők: Dr. Milen Mátyás, szenior kutató-fejlesztő vegyész

Dr. Volk Balázs, hatóanyagfejlesztési igazgató

Konzulens: Dr. Mándity István, egyetemi docens

SYNTHESIS OF INDOLE-BASED ALKALOIDS AND THEIR ANALOGUES

PhD thesis

Patrik Pollák

Semmelweis University Doctoral School

Pharmaceutical Sciences and Health Technologies Division

Supervisors: Mátyás Milen, Ph.D
Balázs Volk, D.Sc

Official reviewers: Béla Mátravölgyi, Ph.D
Gábor Krajsovszky, Ph.D

Head of the Complex Examination Committee: Romána Zelkó, D.Sc

Members of the Complex Examination Committee: László Őrfi, Ph.D
Tamás Gáti, Ph.D

Budapest
2026

TABLE OF CONTENTS

LIST OF ABBREVIATIONS

Ac – acetyl

ADME – absorption, distribution, metabolism, and excretion

API – active pharmaceutical ingredient

BBB – blood–brain barrier

Boc – *tert*-butyloxycarbonyl

BOILED – brain or intestina estimated permeation

BPR – back pressure regulator

CBS – Corey–Bakshi–Shibata

CCDC – Cambridge Crystallographic Data Centre

CDI – 1,1'-carbonyldiimidazole

Cy – cyclohexyl

DBU – 1,8-diazabicyclo[5.4.0]undec-7-ene

DCC – *N*,*N*′-dicyclohexylcarbodiimide

DCM – dichloromethane

DDQ – 2,3-dichloro-5,6-dicyano-1,4-benzoquinone

DFT – density functional theory

DIAD – diisopropyl azodicarboxylate

DIPE – diisopropyl ether

DIPEA – *N*,*N*-diisopropylethylamine

DMAP – 4-dimethylaminopyridine

DME – dimethoxyethane

DMF – *N*,*N*-dimethylformamide

DMSO – dimethyl sulfoxide

DPPA – diphenylphosphoryl azide

EDCI – 1-ethyl-3-(3-dimethylaminopropyl)carbodiimide

ee – enantiomeric excess

ESI – electrospray ionization

eq – equivalent

FT-IR – Fourier transform infrared

GI – gastrointestinal

HBTU – (Benzotriazol-1-yl)-*N,N,N′,N′*-tetramethyluronium hexafluorophosphate

HMTA – hexamethylenetetramine

HOBt – hydroxybenzotriazole

HPLC – high-performance liquid chromatography

HPLC-MS – high-performance liquid chromatography - mass spectrometry

Hz – Hertz

IBD – iodobenzene diacetate

IC_{50} – half maximal inhibitory concentration

ID – inner diameter

IR – infrared

LC – liquid chromatography

LED – light-emitting diode

logP – logarithm of the partition coefficient between *n*-octanol and water

Mp – melting point

MS – mass spectrometry

MW – microwave

ND – not determined

NMM – *N*-methylmorpholine

NMR – nuclear magnetic resonance

OD – outer diameter

PE – petroleum ether

Pn – *n*-pentyl

PTSA – *para*-toluenesulfonic acid

Py – pyridine-4-yl

QST3 – Synchronous Transit-Guided Quasi-Newton

R&D – research and development

Red-Al – sodium bis(2-methoxy-ethoxy)aluminium hydride

rt – room temperature

SAR – structure–activity relationship

SMD – solvation model based on density

$t_{1/2}$ – half-life of a reaction

T3P® – propanephosphonic acid anhydride

TBAF – tetrabutylammonium fluoride

TBDPS – *tert*-butyldiphenylsilyl

TEA – triethylamine

Tf – trifluoromethanesulfonate

TFA – trifluoroacetic acid

TFAA – trifluoroacetic anhydride

THF – tetrahydrofuran

TLC – thin-layer chromatography

TPSA – topological polar surface area

TS – transition state

Ts – tosyl

TsDPEN – *N*-tosyl-1,2-diphenyl-ethylenediamine

UPLC – ultra-performance liquid chromatography

UV – ultraviolet

SC-XRD – single crystal X-ray diffraction

1. INTRODUCTION

1.1. Indole-based drug substances and alkaloids

Nowadays, an increasing number of novel compounds containing the indole scaffold are being isolated from natural sources [1]. Furthermore, numerous synthetic indole-based drug candidates are currently undergoing preclinical research and human clinical trials [2]. Several representatives exhibit anticancer [3], antiviral [4], anti-inflammatory [5] activities and some compounds have also proven to be effective for the treatment of depression [6], high blood pressure [7] and migraine [8]. Figure 1 shows a few of the countless chemical structures of indole-containing compounds with medicinal chemistry relevance, which are active pharmaceutical ingredients (also known as drug substances) in clinical use or an investigational new drug. Vilazodone is a serotonin modulator for the treatment of major depressive disorder, pindolol is a non-selective beta blocker used in the treatment of hypertension, and sumatriptan is a serotonin receptor agonist for the treatment of migraine headaches. Indomethacin is a commonly used nonsteroidal anti-inflammatory drug (NSAID), umifenovir is sold and used as an antiviral medication for influenza in Russia and China, and sabazibulin, currently in phase III clinical trials for the treatment of metastatic castration-resistant prostate cancer.

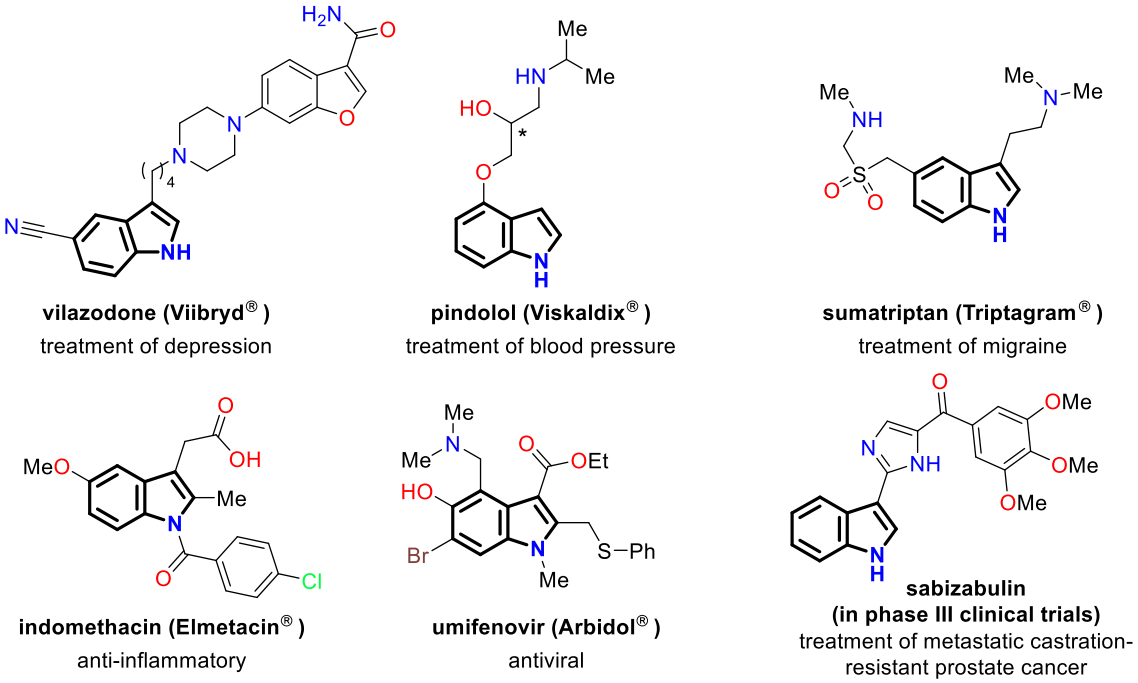

Figure 1. Representatives of indole-based drug substances

Alkaloids, which are defined as naturally occurring, biologically active nitrogen-containing compounds, represent a significant and pharmacologically important class of

drug substances. Figure 2 presents selected examples of indole-based alkaloid structures, several of which also incorporate heteroaromatic moieties such as 1,3-oxazole or 1,3-thiazole rings. Streptochlorin, a 1,3-oxazole-containing alkaloid isolated from the marine bacterium *Streptomyces staurosporeus*, has been reported to induce apoptosis in U937 leukemia cells [9]. Bacillamide A, a 1,3-thiazole-containing metabolite isolated in 2003 from *Bacillus sp.* SY-1, has been identified as an antialgal agent [10]. Camalexin, another 1,3-thiazole-containing compound, was first isolated from *Arabidopsis thaliana* [11] and has been described as a cytotoxic agent [12]. Ellipticine, isolated from *Ochrosia elliptica* [13], acts as a DNA intercalator [14]. Cryptolepinone, obtained from *Cryptolepis sanguinolenta*, has demonstrated antimalarial properties [15]. Finally, echinulin, isolated from *Aspergillus echinulatus* [16], has been reported to possess antiproliferative activity [17].

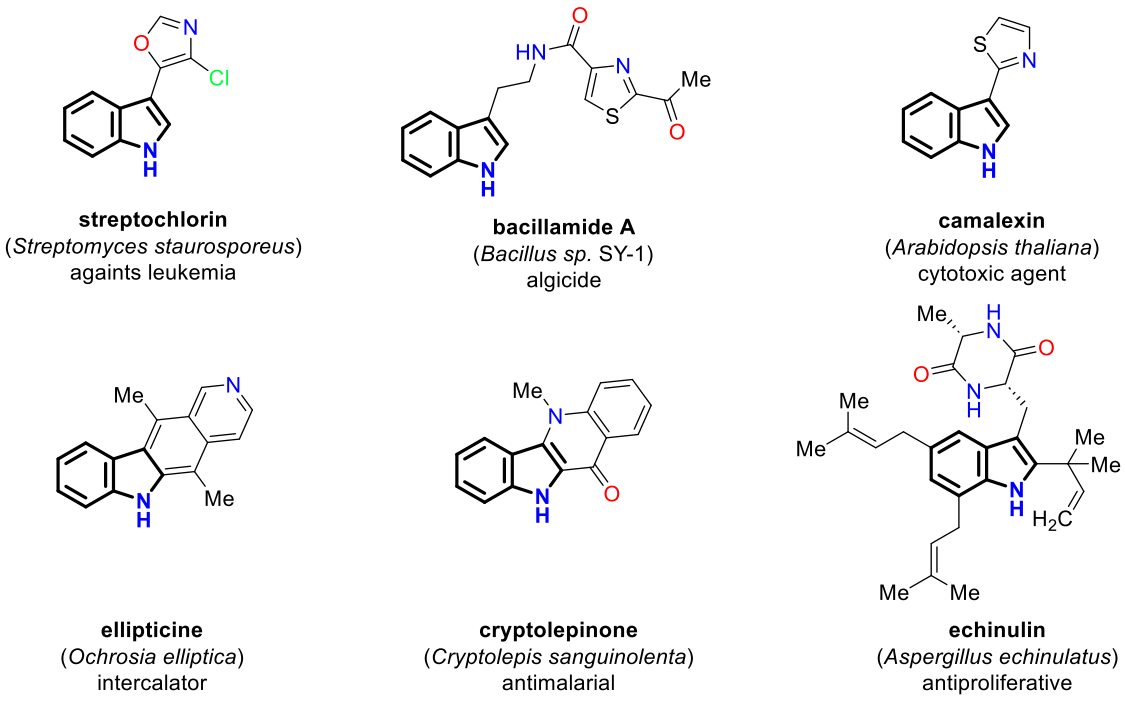

Figure 2. Representatives of indole-based alkaloids

β-Carbolines constitute a structurally distinct class of tricyclic pyridine-fused indole frameworks that are widely found in nature and exhibit remarkable pharmacological potential. This heteroaromatic scaffold is present in several clinically relevant drugs and investigational agents, including vinpocetine, tadalafil, and cipargamin (Figure 3). Notably, vinpocetine holds particular significance in the Hungarian pharmaceutical research, having been developed by Gedeon Richter Plc. (formerly Kőbánya Pharmaceutical Company). Initially synthesized as a semisynthetic derivative of the

natural alkaloid vincamine, vinpocetine is marketed as an over-the-counter medicine under the brand name Cavinton® for the treatment of cerebrovascular disorders [18].

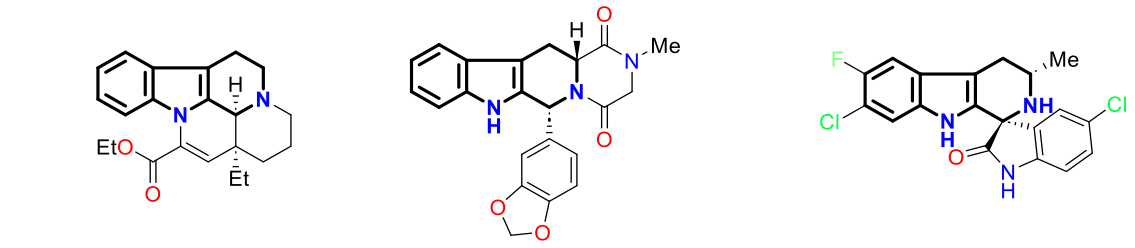

Figure 3. Drug substance representatives of β-carboline type

β-Carboline alkaloids are widely distributed in nature, occurring in diverse biological sources such as plants, foodstuffs, marine organisms, insects, mammals, and even human tissues and body fluids [19]. Representative examples are shown in Figure 4. Yohimbine, isolated from *Pausinystalia johimbe*, is clinically applied for the treatment of sexual dysfunction [20]. Vincamine, first isolated from *Vinca minor*, had its structure elucidated at the Department of Organic Chemistry, Semmelweis University [21], and has been utilized in the treatment of dementia [22]. Reserpine, a natural product present in *Rauvolfia serpentina*, has long been applied in the therapeutic control of hypertension [23].

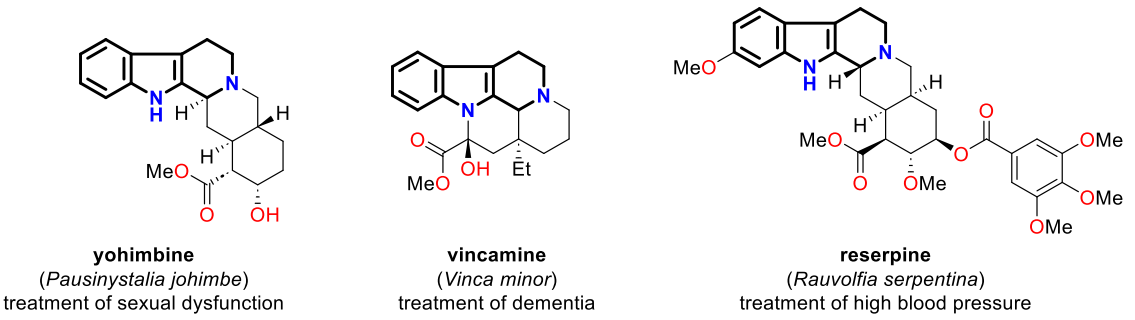

Figure 4. Representatives of β-carboline alkaloids

Given the remarkable biological relevance and structural diversity of indole-based alkaloids, numerous synthetic strategies have been developed to access various functionalized indole derivatives. Among these, the introduction of heteroaromatic substituents, such as oxazole and thiazole rings, has gained particular interest due to their impact on bioactivity and molecular recognition. Therefore, in the following section, the principal synthetic approaches towards oxazolyl- and thiazolylindole systems will be summarized.

1.2. Synthetic approaches towards oxazolyl- and thiazolylindoles

Several naturally occurring oxazolylindole derivatives, notably pimprinine (**1**, R = Me, Scheme 1) and its analogues, differ only in indole and/or oxazole ring substituents [24,25]. The most common synthetic route to the oxazolylindoles involves cyclodehydration (known as Robinson–Gabriel synthesis) of *N*-[2-(1*H*-indol-3-yl)-2-oxoethyl]carboxamides (**2**) in the final step, typically using $POCl_3$. Interestingly, in some cases it slowly occurs just upon boiling in THF. The amides (**2**) are prepared *via* oxidation of *N*-acyltryptamine derivatives (**3**) with DDQ.

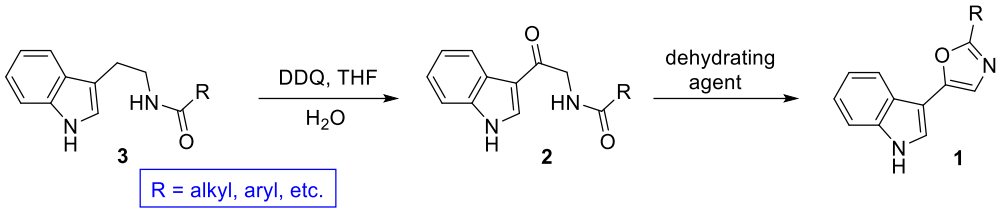

Scheme 1. Representative synthetic route leading to oxazolylindoles (**1**)

Koyama *et al.* reported the synthesis of ketones **2** from ethyl indole-3-carboxylate (**4**, Scheme 2). Reaction of **4** with isocyanomethyllithium in THF afforded 3-(1,3-oxazol-5-yl)-1*H*-indole (**5**), which, after acylation with various carboxylic anhydrides and subsequent hydrolysis, yielded ketones **2**. Cyclization of these intermediates in refluxing $POCl_3$ gave the corresponding substituted oxazolyl–indoles (**1**) [25].

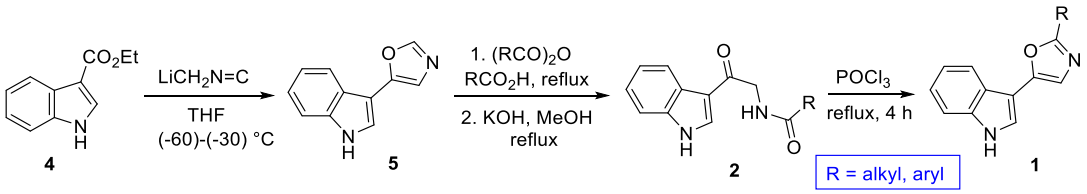

Scheme 2. Synthesis of oxazolylindoles (**5**) from ethyl indole-3-carboxylate (**4**)

Kumar *et al.* synthesized compounds **1** in a five-step sequence (24–32% overall yield) starting from 3-acetyl-1-phenylsulfonylindole (**6**) (Scheme 3). Oxidation with hydroxy(tosyloxy)iodobenzene afforded the tosyloxy derivative (**7**), which was aminated with HMTA to give amine **8**. Subsequent *N*-acylation yielded amides **9**, which underwent cyclodehydration in refluxing EtOH with PTSA to form 5-(3-indolyl)oxazole derivatives **10**. Final removal of the *N*-phenylsulfonyl group led to the target products (**1**) [26].

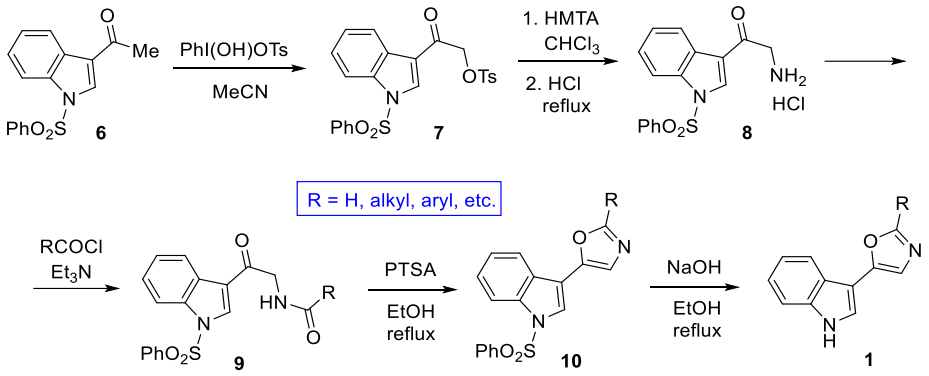

Scheme 3. Synthesis of oxazolylindoles (**1**) from 3-acetyl-1-phenylsulfonylindole (**6**)

A recent study reported the optimization of reaction conditions for the Friedel–Crafts synthesis of acylaminoketone **2** (R = Ph) *via* the reaction of indole (**11**) with 2-phenyl-1,3-oxazol-5(4*H*)-one (**12**), as well as of the Robinson–Gabriel cyclization of **2** (R = Ph) to 3-(2-phenyl-1,3-oxazol-5-yl)-1*H*-indole (**1**, R = Ph) (Scheme 4). Both transformations proceeded in good yields, enabling the development of an efficient one-pot procedure [27].

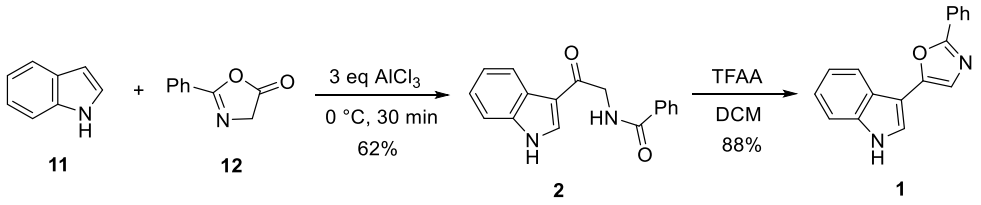

Scheme 4. Synthesis of phenyloxazolylindole **1** *via* Friedel–Crafts acylation of indole followed by Robinson–Gabriel cyclization

Regarding the synthesis of oxazolylindoles bearing a carboxyl group or its derivatives at the 2-position of the oxazole ring, only a single example has been reported. In this study, continuous-flow photoisomerization of isoxazole **13** furnished ethyl 5-(1*H*-indol-3-yl)-1,3-oxazole-2-carboxylate (**1**, Scheme 5) [28].

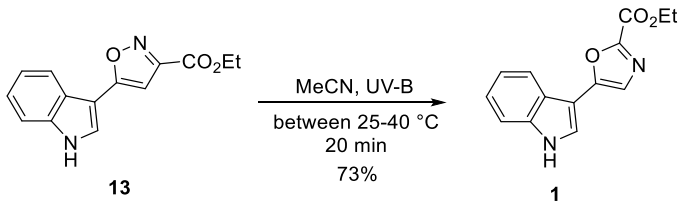

Scheme 5. The sole reported synthetic route to indolyloxazole-carboxylates

The synthesis of certain thiazolylindole derivatives has also been reported. According to a Japanese patent [29], ketone **14** was converted to thiazole **15** *via* treatment with

phosphorus pentasulfide (Scheme 6). Notably, the *in situ* cyclodehydration of intermediate **16** occurred under relatively mild conditions, in refluxing chloroform.

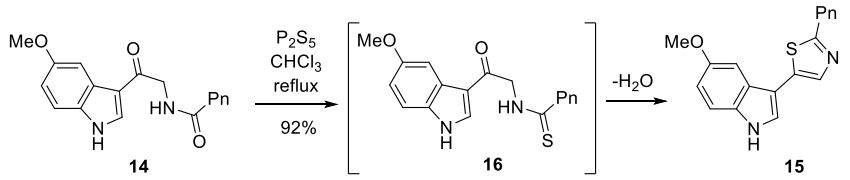

Scheme 6. Synthesis of thiazolylindole **15** from ketone **14**

Similarly, ketone **2** (R = H) reacted with Lawesson's reagent to afford thiazole **17** (R = H) *via* intermediate **18** (R = H, Scheme 7) [30].

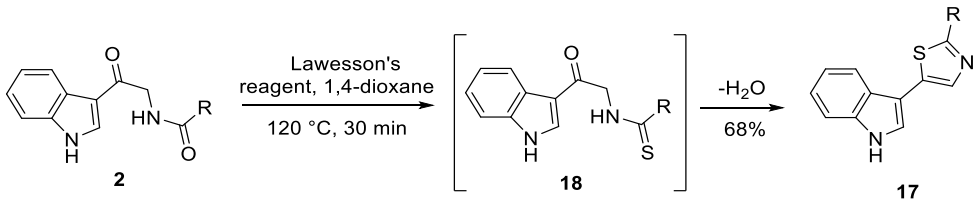

Scheme 7. Synthesis of thiazolylindole **17** (R = H)

Nicolaou *et al.* synthesized key intermediate **18** (R = Ph) *via* thiobenzoylation of amino-ketone **19**. Subsequent cyclization with $POCl_3$ and pyridine under mild conditions afforded thiazolylindole **17** (R = Ph) in good yield (Scheme 8) [31].

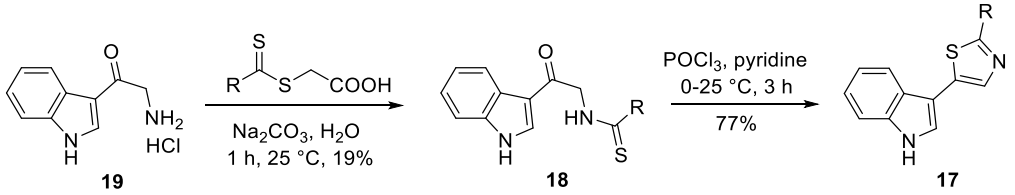

Scheme 8. Two-step synthesis of thiazolylindole **17** (R = Ph) from amino-ketone (**19**)

Al-Azawe reported the synthesis of thiazolylindole **17** (R = Py) *via* the reaction of 3-(2-bromoacetyl)indole (**20**) with pyridine-4-carbothioamide (**21**) (Scheme 9) [32].

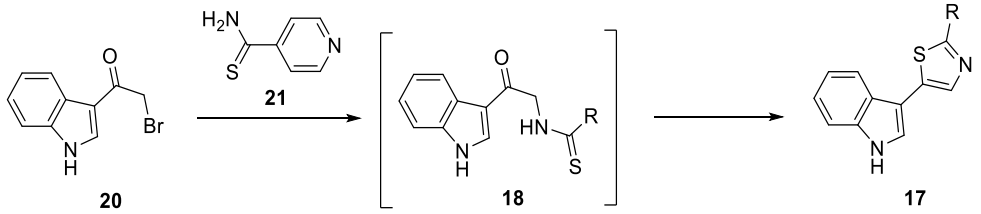

Scheme 9. Synthesis of thiazolylindole (**17**)

As several oxazolyl- and thiazolylindole frameworks occur naturally within bioactive secondary metabolites, these structural motifs have attracted attention in the context of marine and microbial alkaloids. One representative family is the bacillamides, which

combine indole and thiazole moieties in their molecular architecture. To place our synthetic work in a broader biological and chemical context, the next section provides an overview of the literature related to bacillamide-type indole alkaloids.

1.3. Literature summary of bacillamide indole alkaloids

Rising algal blooms have highlighted the algicidal [33–35] and recently discovered anticancer [36] activities of bacillamide alkaloids. The stereostructures and optical rotations of the chiral bacillamides are shown in Figure 5.

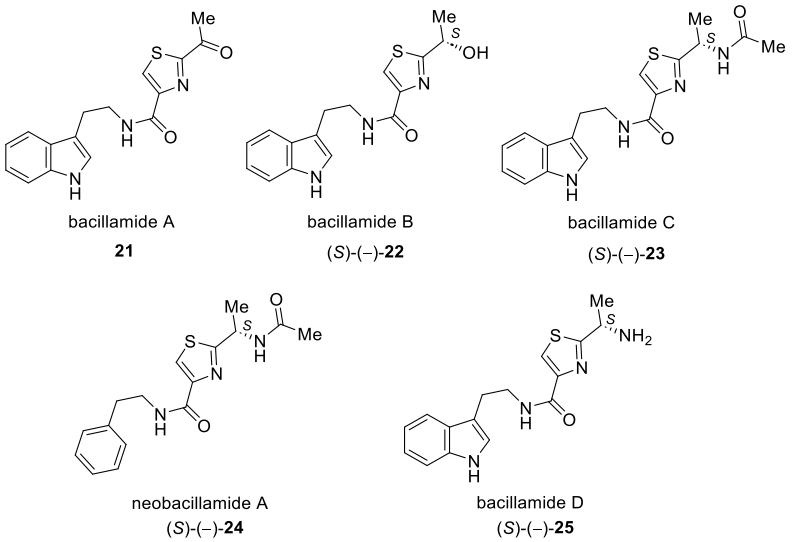

Figure 5. Structure of bacillamide and neobacillamide alkaloids

Okada *et al.* [10] isolated bacillamide A (**21**) from the marine bacterium *Bacillus sp.* SY-1 and elucidated its structure using spectroscopic data. The first synthesis, starting from 4-methylthiazole, was a multistep process with low yields and significant by-product formation due to the use of mixed anhydrides [37]. Later, a more practical route involved cyclization of (*R*)-cysteine ethyl ester hydrochloride (**26**) with pyruvaldehyde (**27**), oxidation of the product with iodobenzene diacetate to yield ethyl 2-acetyl-1,3-thiazole-4-carboxylate (**28**), and amidation with tryptamine (**29a**) to afford bacillamide A (**21**) (Scheme 10) [38].

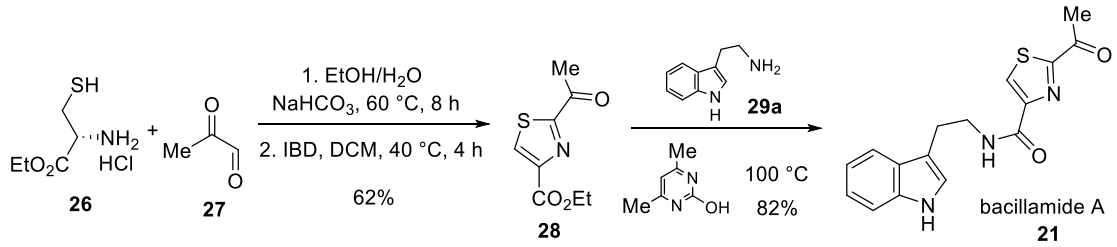

Scheme 10. Synthesis of bacillamide A alkaloid (**21**)

Rowley *et al.* isolated bacillamide B [(*S*)-**22**] from *Bacillus endophyticus*, reporting a positive optical rotation, $[\alpha]_D^{20} = +7.4$ (c 0.095, MeOH), and proposed structure **22** with *R* configuration at the asymmetric center based on circular dichroism comparison with a related compound of known configuration [39]. Bray *et al*. [40] synthesized compound (*S*)-**22** (Scheme 11), *via* reaction of (*S*)-lactic acid derivative **30** with ethyl bromopyruvate (**31**), formation to thiazole **32**, hydrolysis to **33**, and coupling with tryptamine (**29a**). The product optical rotation $[\alpha]_D^{20} = +10.1$ (c 0.10, MeOH), led to a revision of bacillamide B alkaloid's stereochemistry from *R* to *S*.

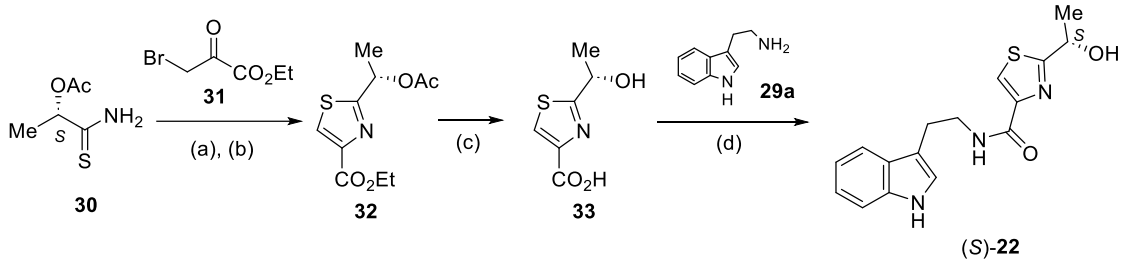

(a) compound **31**, ethyloxirane, *i*-PrOH, 60 °C, 30 min; (b) $(CF_3CO)_2O$, 20 °C, 30 min, 58% (for 2 steps); (c) 2 M LiOH, THF–MeOH; 20 °C, 24 h, 80%; (d) dipyridyl disulfide, Ph_3P, tryptamine (**29a**), CH_2Cl_2, 20 °C, 16 h, 54%.

Scheme 11. The synthesis of bacillamide B [(*S*)-**22**] from (*S*)-lactic acid derivative (**30**) [40]

To resolve the contradictory stereochemical data, Du *et al.* developed syntheses for both enantiomers of compound **22** [41], illustrated in Scheme 12 for (*S*)-**22**. *L*-Cystine (**34**) was converted to β-azidodisulfide **35**, which underwent amidation with tryptamine (**29a**) to afford intermediate **36**. Cyclization yielded thiazoline **38** (diastereomeric ratio not reported), which was dehydrogenated (**39**) and deprotected to give bacillamide B [(*S*)-**22**, $[\alpha]_D^{20} = -1.81$ (c 0.095, MeOH)]. The (*R*)-enantiomer showed $[\alpha]_D^{20} = +2.01$ (c 0.095, MeOH). Reproducing Bray's synthesis, they obtained $[\alpha]_D^{20} = -2.6$ (c 1.0, MeOH), contrary to the $[\alpha]_D^{20} = +10.1$ (c 0.10, MeOH) reported. Re-examination of natural bacillamide B gave $[\alpha]_D^{20} = -1.25$ (c 0.16, MeOH), contrasting with Rowley's $[\alpha]_D^{20} = +7.4$ (c 0.095, MeOH). These results strongly support (*S*)-**22** as the correct structure of bacillamide B.

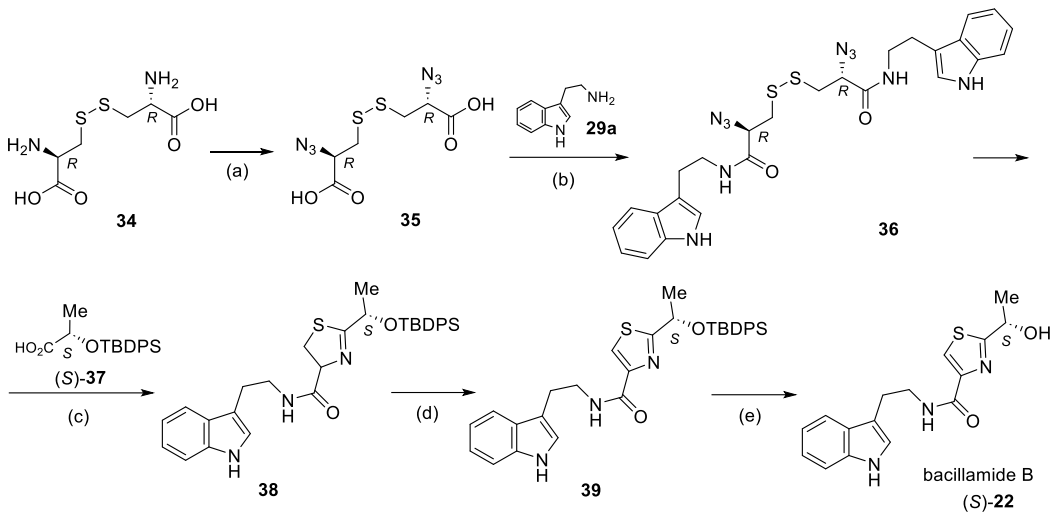

(a) TfN_3, $CuSO_4$, K_2CO_3, 83%; (b) tryptamine (**29a**), DCC, HOBt, rt, 5 h, 85%; (c) EDCI (4.0 eq), DIPEA (8.0 eq), compound **37** (4.0 eq) in DCM, PPh_3 (8.0 eq), reflux, 24 h, 75%; (d) DBU (5.0 eq), $BrCCl_3$ (5.0 eq), DCM, rt, 4 h, 67%; (e) TBAF (1.5 eq), THF, rt, 15 min, 85%.

Scheme 12. Synthesis of bacillamide B [(*S*)-**22**] from (*R*)-cystine (**34**) [41]

Laatsch *et al*. isolated bacillamide C [(*S*)-(–)-**23**], also known as microbiaeratin, from the culture filtrate of *Microbispora aerata* strain IMBAS-11A and elucidated its structure spectroscopically, without addressing stereochemistry or reporting optical rotation [42]. Rowley *et al*. obtained bacillamide C [(*S*)-(–)-**23**] from *Bacillus endophyticus*, measured an optical rotation of $[\alpha]_D^{24} = -15.2$ (c 0.082, MeOH), and proposed an *R* configuration at the asymmetric center based on circular dichroism, as with bacillamide B [39]. Xu *et al*. achieved the first synthesis of (*R*)-**23** and (*R*)-**25** enantiomers of bacillamides C and D, starting from (*R*)-alanine [(*R*)-**40**] (Scheme 13) [43]. This was converted *via* a multistep sequence to thioamide **41**, cyclized to thiazole **42**, hydrolyzed to **43**, and amidated with tryptamine (**29a**) to give compound **44**. Boc deprotection yielded (*R*)-**25**, which underwent *N*-acylation to afford (*R*)-**23**. However, optical rotations of the synthetic products were not determined, so comparison with the natural alkaloids could not be done.

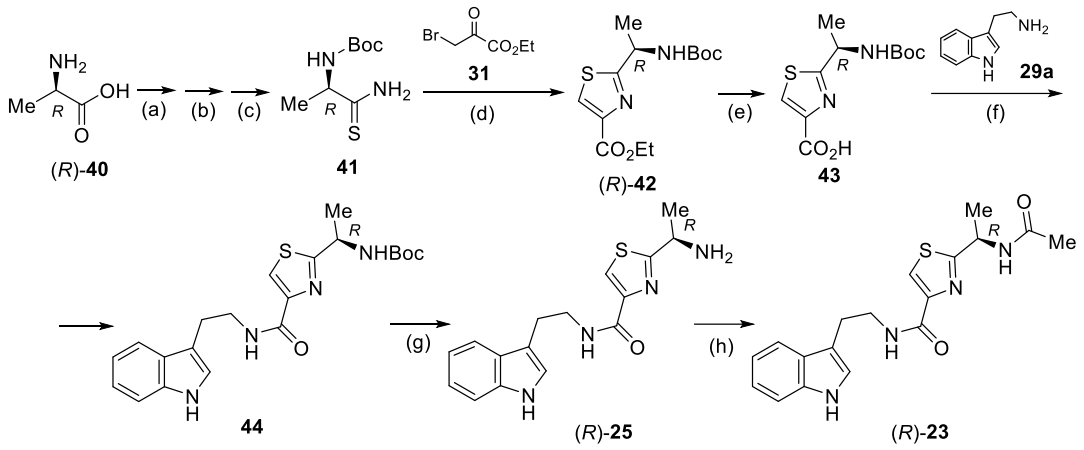

(a) NaOH, 0 °C, $(Boc)_2O$, rt, 92.7%; (b) $(Boc)_2O$, Py, NH_4HCO_3, rt, 92.2%; (c) DME, Lawesson's reagent, rt, 73.4%; (d) 1. $KHCO_3$, DME, −15 °C; 2. compound **31**; 3. TFAA, 2,6-lutidine, −15 °C, 88.7% (for 3 steps); (e) LiOH, THF/MeOH/H_2O; (f) 1. isobutyl chloroformate, NMM, CH_2Cl_2; 2. compound **29a**, NMM, CH_2Cl_2, 56.7% (for 3 steps); (g) AcCl, MeOH, EtOAc, 84.5%; (h) pyridine, Ac_2O, DMAP, 85.4%.

Scheme 13. Synthesis of (*R*)-**23** and (*R*)-**25**, antipodes of bacillamides C and D

Dömling *et al.* [44] reported the synthesis of racemic bacillamide C [(*R*,*S*)-**23**] and its (*R*)-enantiomer [(*R*)-**23**]. The key intermediate thiazole **49** was prepared *via* a multicomponent Ugi reaction (**45**–**48**) employing (*R*)-1-(4-methoxyphenyl)ethylamine (**47**) as the chiral component (Scheme 14). The resulting 1:1 diastereomeric mixture of thiazoles **49** was separated chromatographically. Removal of the chiral auxiliary from (*R*,*R*)-**49** gave ester **50**, which was amidated with tryptamine (**29a**) to yield (*R*)-**23**, exhibiting $[\alpha]_D^{24} = -15.5$ (c 0.155, MeOH). However, as the diastereomers were not rigorously identified, it remains uncertain whether (*R*,*R*)-**49** or (*S*,*R*)-**49** was used in the synthesis, rendering the optical rotation assignment potentially unreliable.

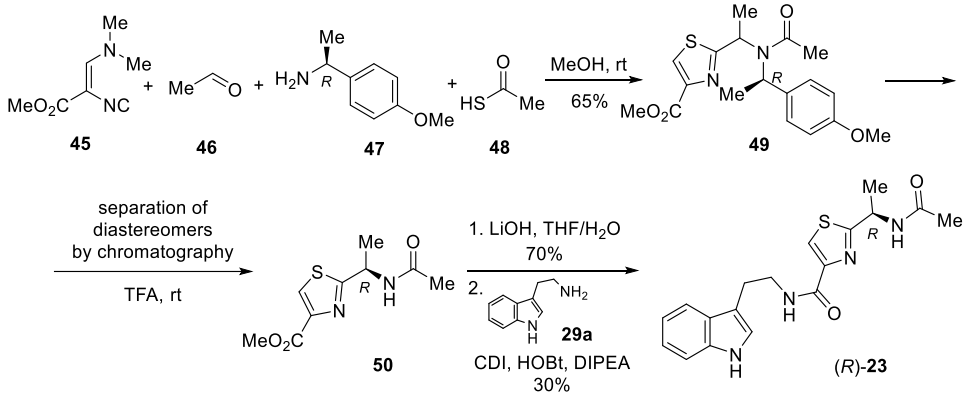

Scheme 14. Synthesis of (*R*)-**23**, antipode of bacillamide C

To resolve the uncertain stereochemical assignment of natural bacillamide C [(*S*)-**23**] [39], Davyt *et al.* synthesized both enantiomers [(*S*)-**23**, (*R*)-**23**] starting from Boc-

protected (*R*)- and (*S*)-alanine (**51**) [45]. Protected (*S*)-alanine (**51**) was converted to nitrile **52**, which reacted with (*R*)-cysteine ethyl ester hydrochloride (**26**) to afford thiazole (*S*)-**42** (Scheme 15). Boc deprotection, *N*-acetylation (**53**), ester hydrolysis (**54**), and amidation with tryptamine (**29a**) yielded bacillamide C [(*S*)-**23**]. These results confirmed that the natural product has (*S*) configuration and a negative optical rotation, $[\alpha]_D^{24} = -23.6$ (c 4.99, MeOH), with its levorotatory character also verified by a biosynthetically produced sample [35].

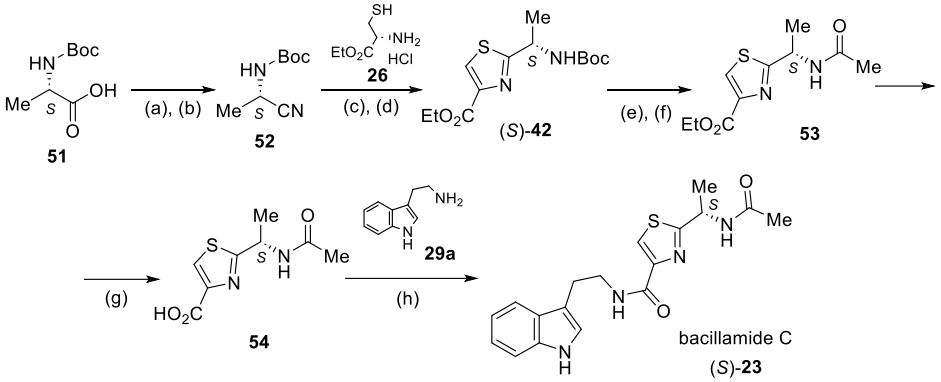

(a) NH_3 gas, $ClCO_2Et$, Et_3N, THF, −10 °C; (b) TFAA, Py, THF, rt, 70% (for two steps); (c) **26**, phosphate buffer pH 7, MeOH, 60 °C; (d) DBU, $BrCCl_3$, CH_2Cl_2, −10 °C, 66% (for two steps); (e) TFA, CH_2Cl_2, rt; (f) Ac_2O, Py, rt, 81% (for two steps); (g) 10% aqueous KOH, THF, rt, 80%; (h) tryptamine (**29a**), HBTU, DIPEA, 0 °C to rt, 29%.

Scheme 15. Synthesis of bacillamide C alkaloid [(*S*)-**23**]

Neobacillamide A [(*S*)-**24**] was isolated from the bacterium *Bacillus vallismortis* C89, and its structure was elucidated by Guo *et al* [46]. Based on previously misassigned literature data [39,42], the authors incorrectly determined the absolute configuration of the levorotatory compound $\{[\alpha]_D^{20} = -16.0$ (c 0.10, MeOH)$\}$. Enantiospecific synthesis of both enantiomers *via* reaction of compound **54** and its antipode with phenylethylamine (**55**, Scheme 16) demonstrated that the levorotatory product, neobacillamide A [(*S*)-**24**, $[\alpha]_D^{24} = -24.1$ (c 7.37, MeOH)] was obtained.

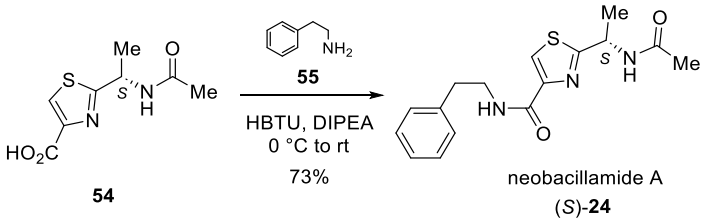

Scheme 16. Synthesis of neobacillamide A alkaloid [(*S*)-**24**]

Bacillamide D [(*S*)-**25**] was the first of the bacillamide alkaloid family to be identified and isolated in 1976 from *Thermoactinomyces* strain TM-6. Its structure was confirmed

by chemical transformations and spectroscopic methods available at that time, and an (*S*) configuration was tentatively assigned to the asymmetric center based on its negative optical rotation, $[\alpha]_D^{20} = -6.0$ (c 1.0, MeOH) [47]. The proposed structure was later confirmed by a synthesis starting from (*S*)-alanine [(*S*)-**40**, Scheme 17] [48]. Conversion to thiazole (**56**) according to established procedures [49] was carried out, followed by *N*-benzyloxycarbonylation (**57**), amidation with tryptamine (**29a**) to give **58**, and deprotection to yield bacillamide D with an optical rotation of $[\alpha]_D^{20} = -2.6$ (c 1.0, EtOH).

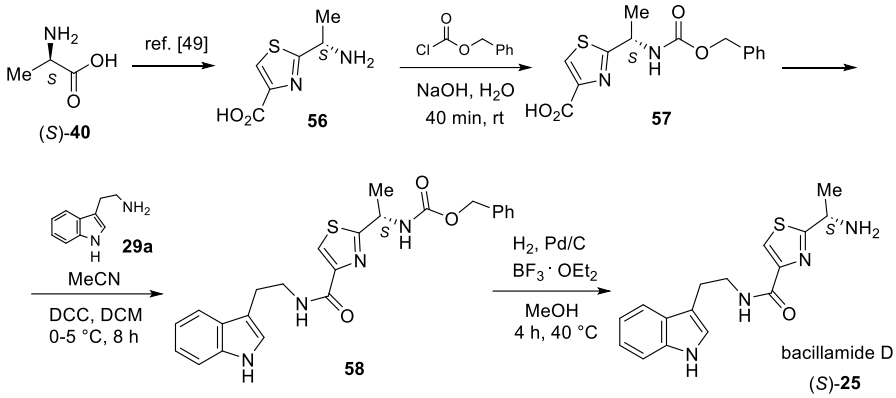

Scheme 17. Synthesis of bacillamide D alkaloid [(*S*)-**25**]

As noted above, Xu *et al.* synthesized (*R*)-**25**, the antipode of bacillamide D [(*S*)-**25**], from (*R*)-alanine [(*R*)-**40**] without reporting optical rotation (Scheme 13) [43] and later prepared (*S*)-**25** from (*S*)-alanine [(*S*)-**40**] [34]. More recently, Gulder *et al.* [36] isolated bacillamide D [(*S*)-**25**] from a bacterial source and converted it to bacillamide C [(*S*)-**23**] by *N*-acetylation. They reported $[\alpha]_D^{20} = -14.7$ (c 2.92, MeOH) for isolated (*S*)-**25** and $[\alpha]_D^{20} = -40.2$ (c 1.02, MeOH) for the synthesized (*S*)-**23**.

1.4. Application of the Bischler–Napieralski reaction in β-carboline synthesis

While the bacillamides illustrate the synthetic and stereochemical challenges associated with thiazolylindole systems, β-carboline alkaloids represent another major subclass of indole-derived natural products with distinct biosynthetic origins and pharmacological profiles. Their synthesis often relies on classical heterocyclization reactions forming the pyridine-fused indole core. One of the most versatile and widely used transformations for this purpose is the Bischler–Napieralski cyclization, which has played a pivotal role in the preparation of β-carboline derivatives. The present section therefore discusses the application of this reaction in β-carboline synthesis.

Discovered in 1893, the Bischler–Napieralski reaction is the key method for synthesizing 3,4-dihydro-β-carbolines (**60**) from tryptamine (**29a**) *via* the corresponding acyltryptamines (tryptamides, **59**, Scheme 18) [50]. Cyclization is typically promoted by dehydrating agents such as $POCl_3$, PCl_5, P_2O_5, etc. [51,52].

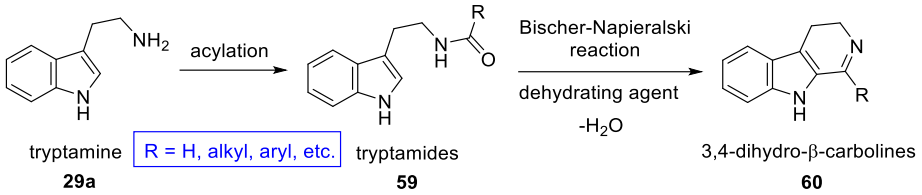

Scheme 18. Preparation of 3,4-dihydro-β-carbolines (**60**) from tryptamine (**29a**) by acylation and subsequent Bischler–Napieralski reaction

Propylphosphonic anhydride (PPAA or T3P®, **61**) is a low-toxicity (compared to other reagents with similar activity), highly soluble coupling agent and water scavenger enabling facile work-up (Scheme 19) [53]. Our research group previously applied T3P® in microwave-assisted Robinson–Gabriel (**62** to **63**) and Bischler–Napieralski reactions of tryptamine derivatives (Scheme 19) [54–56].

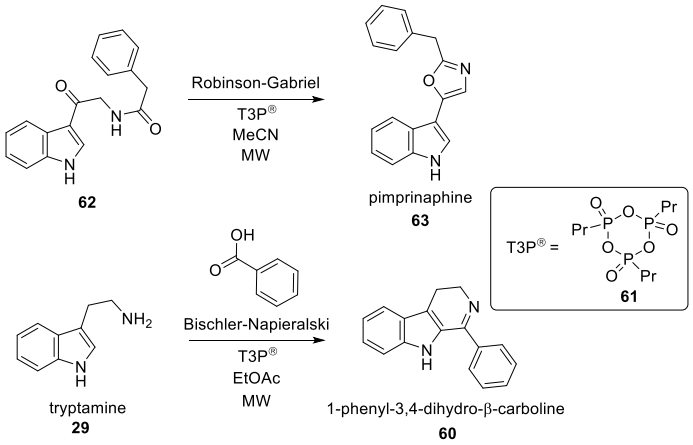

Scheme 19. MW-assisted Robinson–Gabriel synthesis and one-pot acylation-Bischler–Napieralski reaction promoted by T3P®

Microwave treatment of *N*-[2-(1*H*-indol-3-yl)-2-oxoethyl]acetamide (**64**) with T3P® yielded pimprinine (**66**) *via* Robinson–Gabriel synthesis, however there is no data reported about the appropriate Bischler–Napieralski product (**65**) in the literature [54]. In contrast, the analogous reaction of *N*-acetyltryptamine (**67**) is reported to afford harmalan (**68**) through a Bischler–Napieralski pathway (Scheme 20) [55]. In order to clarify the basis of this noteworthy observation, we undertook additional analyses, the outcomes of which are reported in the Results section.

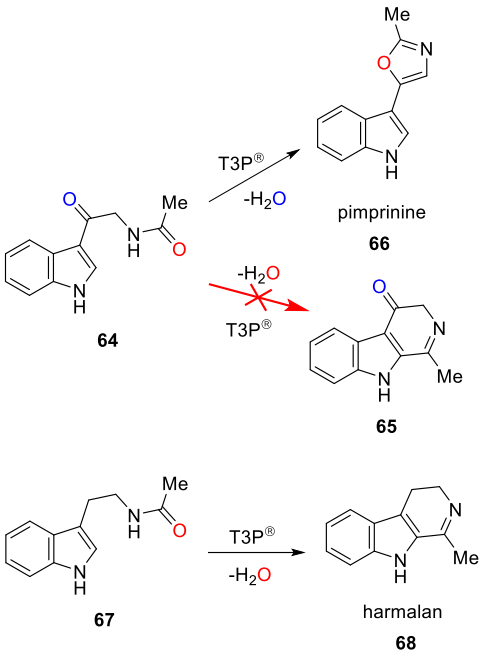

Scheme 20. Experimentally found reactions of **64** and **67** with T3P® reagent

1.5. Overview of β-carboline alkaloids orthoscuticellines A and B

The synthetic utility of the Bischler–Napieralski reaction becomes particularly evident in the preparation of complex natural β-carbolines, including the orthoscuticelline alkaloids. These marine-derived compounds exhibit unique dimeric structures and intriguing stereochemical properties. Consequently, an overview of orthoscuticellines A and B, including their isolation, structural elucidation, and previous synthetic efforts, is provided in the present section.

Several alkaloids, including bis-β-carboline orthoscuticellines A (**69**, meso) and B (**70**, racemate), were recently isolated from the marine bryozoan *Orthoscuticella ventricosa* and structurally characterized (Figure 6) [57]. Both showed modest activity against *Plasmodium falciparum*, the causative agent of malaria.

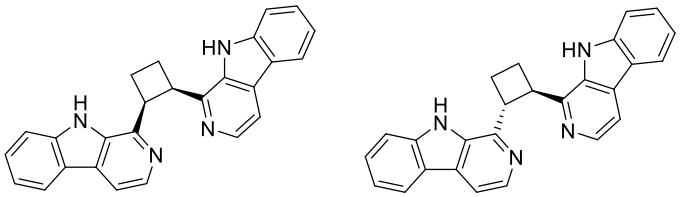

69 (meso form)
orthoscuticelline A

(±)-*trans*-**70**
orthoscuticelline B

Figure 6. Chemical structures of orthoscuticelline A (**69**) and B (**70**) alkaloids

Compounds **69** and (±)-*trans*-**70** were first synthesized by Banwell *et al.* in 2022 [58]. Blue LED irradiation of 1-vinyl-β-carboline (**71**), prepared in four steps from tryptamine

(**29a**) [59], with an iridium(III) catalyst in acetonitrile resulted in a 1:3 mixture of cycloadducts **69** and (±)-*trans*-**70** (Scheme 21) in good yield. The isomers were separated, fully characterized, and the *trans* stereochemistry of (±)-*trans*-**70** was confirmed by SC-XRD. However, the NMR spectra of the isolated compound [57] exhibited significant deviations from those of the synthetic analogue [58], with no explanation provided in the publication.

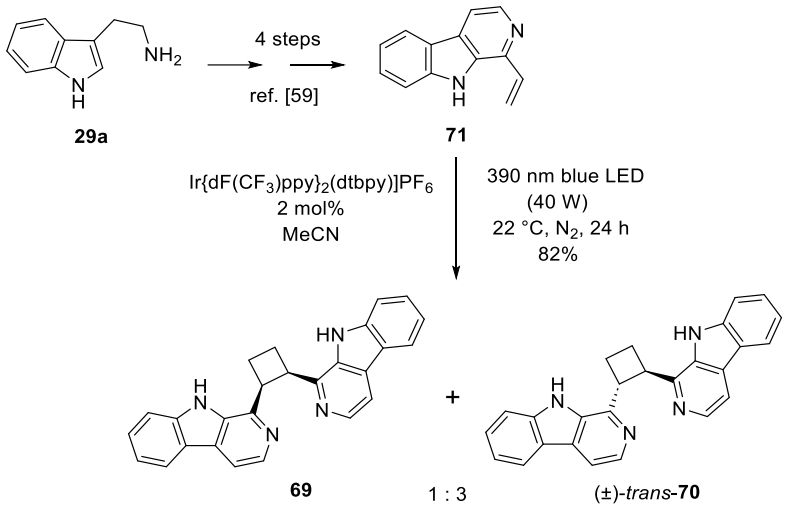

Scheme 21. First total synthesis of orthoscuticelline A (**69**) and B (**70**) alkaloids

Since the photochemical method proved unsuitable for the selective preparation of *cis*- or *trans*-1,2-disubstituted cyclobutanes and the reason for the difference in the NMR spectra was not clear, we aimed the development of an alternative, practical synthetic route to access both stereoisomers, **69** and (±)-*trans*-**70**.

1.6. Literature survey of brevicarine and brevicolline β-carboline alkaloids

Beyond orthoscuticellines, several other β-carboline alkaloids, such as brevicarine and brevicolline, further demonstrate the structural and biosynthetic diversity of this class. Their study also highlights the recurring challenges in regioselective cyclization and oxidation steps characteristic of β-carboline formation. This final section of the introduction therefore summarizes the literature on brevicarine and brevicolline alkaloids, providing additional context for the synthetic investigations presented in this dissertation.

Carex brevicollis DC, a sedge prevalent in Central and South-Eastern Europe, contains several alkaloids, predominantly β-carboline alkaloids (*S*)-brevicolline [(*S*)-**72**] and brevicarine (**73**, Figure 7) [60–62].

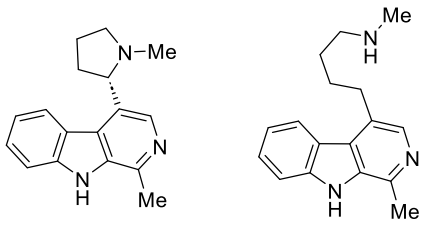

Figure 7. Structure of brevicolline [(*S*)-**72**] and brevicarine (**73**) alkaloids

In a recent study, our research group reported the total synthesis of racemic brevicolline [(±)-**72**] (Scheme 22) [63], enabled by a newly developed triflate intermediate (**74**) suitable for C–C bond formation at position 4 of the β-carboline *via* cross-coupling. Sonogashira coupling of **74** with *N*-(3-butynyl)phthalimide (**75**) afforded **76**, which, after phthalimide cleavage with methylhydrazine, yielded butynylamine **77**. Cyclization to dihydropyrrole **78**, reduction to **79**, and *N*-methylation led to (±)-**72**; chiral chromatography of which provided natural (*S*)-brevicolline [(*S*)-**72**].

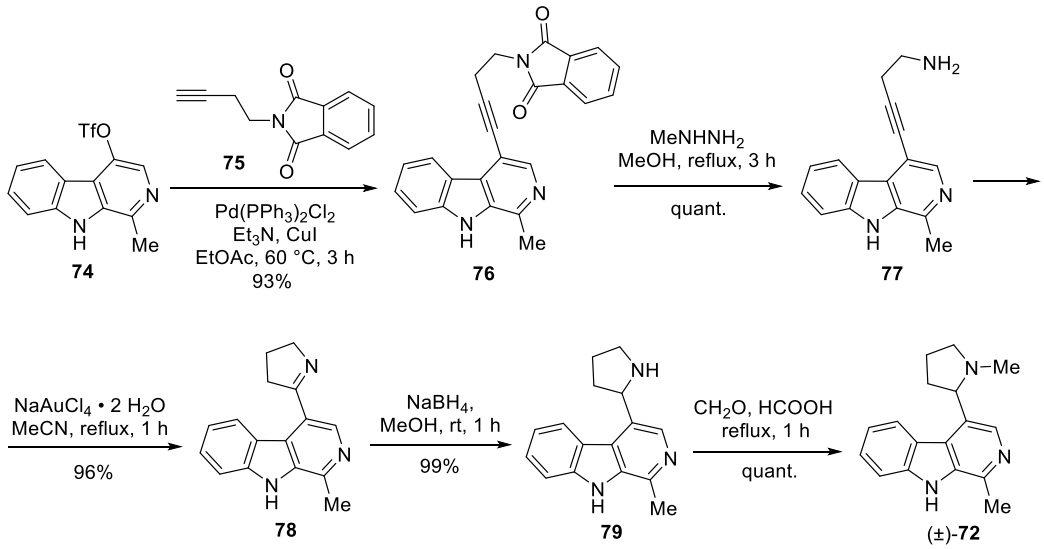

Scheme 22. Synthesis of racemic brevicolline [(±)-**72**] from key triflate intermediate (**74**)

To extend this work, we pursued the synthesis of brevicarine (**73**), a structurally related alkaloid. The first reported semi-synthetic route involved a short sequence from naturally derived (*S*)-brevicolline [(*S*)-**72**] (Scheme 23) [64]. Heating (*S*)-**72** in benzoyl chloride induced pyrrolidine ring opening and *N*-benzoylation to give **80**, which upon debenzoylation yielded **81**. Catalytic hydrogenation of its side-chain C=C bond furnished brevicarine (**73**).

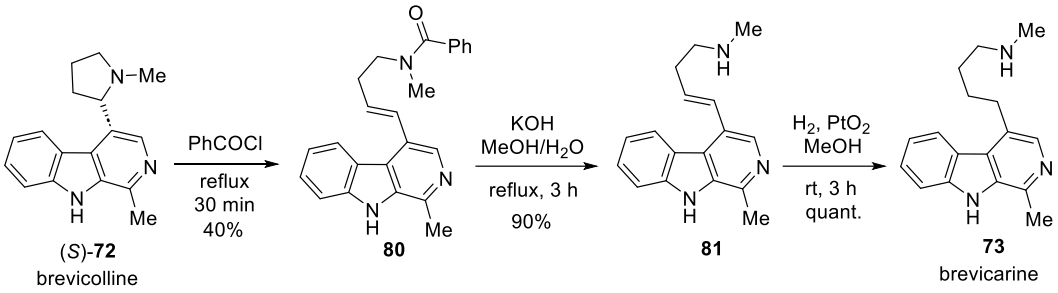

Scheme 23. Semi-synthesis of brevicarine (**73**) from isolated brevicolline [(*S*)-**72**]

The first total synthesis of brevicarine (**73**) is outlined in Scheme 24 [61,65,66]. Condensation of indole (**82**) with 1-methylpiperidone (**83**) afforded **84** [67], which underwent *N*-alkylation with benzyl bromide to give quaternary ammonium salt **85**. Reaction of **85** with the potassium salt of **86** yielded ring-opened derivative **87**. Subsequent removal of the benzylsulfanyl group, Beckmann rearrangement of the oxime derived from ketone **88**, and cyclization produced β-carboline **89**, which was dehydrogenated and debenzylated to brevicarine (**73**), obtained as the dihydrochloride salt.

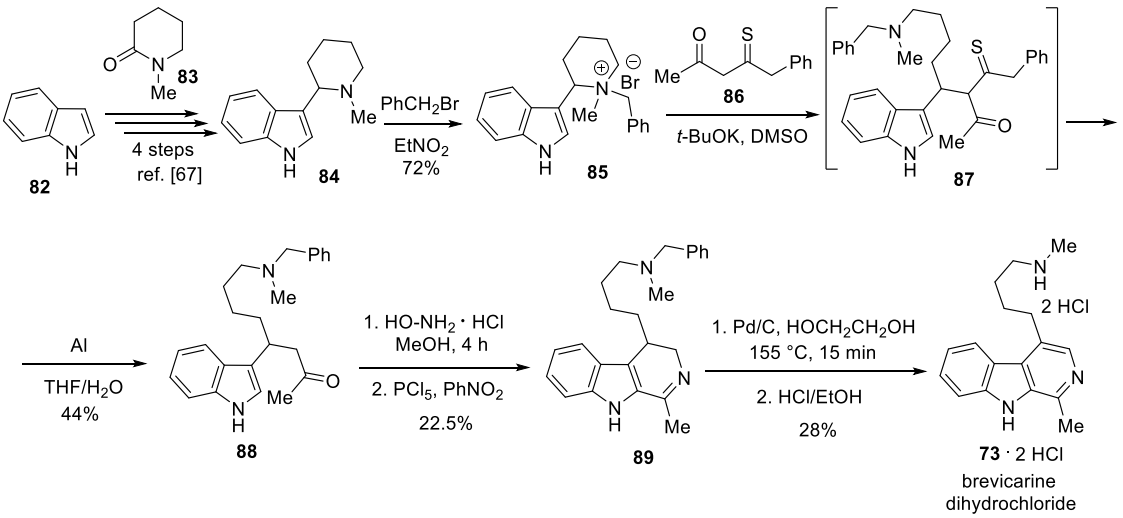

Scheme 24. The first total synthesis of brevicarine (**73**) alkaloid

Müller *et al.* developed an alternative synthesis of brevicarine (**73**, Scheme 25). Treatment of nitrovinylindole (**90**) with *N*-methylpyrrole (**91**) afforded compound **92**, which was hydrogenated under harsh conditions (100 °C, 130 bar) to reduce both the pyrrole ring and the nitro group [68]. *N*-Acetylation yielded a mixture of diastereomeric racemates (**93**), which was cyclized to β-carboline derivatives **94**. Heating **94** in pivalic acid with catalytic trifluoroacetic acid furnished brevicarine (**73**).

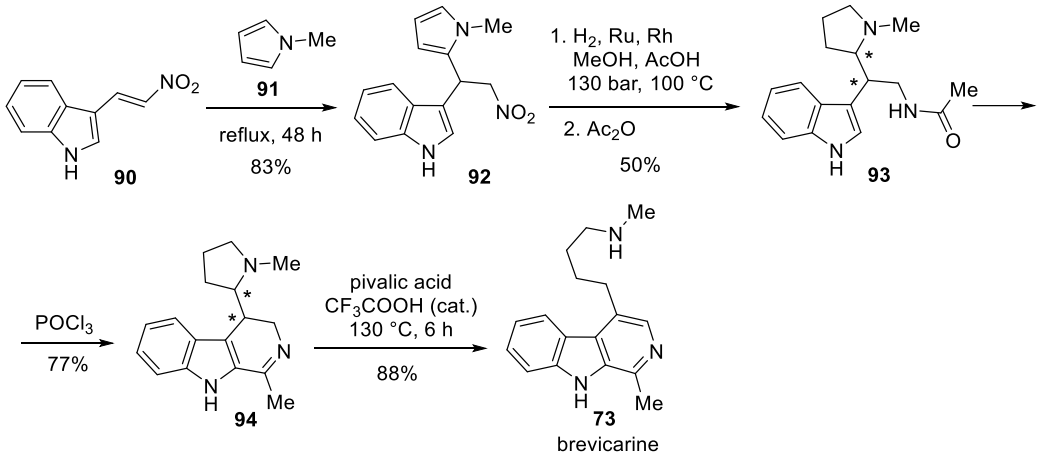

Scheme 25. Synthesis of brevicarine (**73**) from nitrovinylindole (**90**)

The sedge *Carex brevicollis* DC has long been known to induce smooth muscle contraction [61], an effect likely related to the oxytocic activity of (*S*)-brevicolline [(*S*)-**72**], studied in pregnant mammals [69,70]. First isolated in 1960 [62], (*S*)-brevicolline exhibits antibacterial and antifungal activity through photosensitization [71] and has been used in human obstetrics and veterinary infertility treatment [61]. Synthetic and biogenetic studies, including the conversion of (*S*)-**72** to brevicarine (**73**) (Scheme 23), suggest that (*S*)-brevicolline may serve as a biosynthetic precursor of brevicarine in plants [64].

Brevicarine (**73**), first isolated in 1967 from *Carex brevicollis* DC [72], has since been identified in several other natural sources, including *Tambourissa ficus* (Mauritian endemic fruit) [73], *Asparagus racemosus* (linn seed) [74], and extracts of *Phellinus linteus smilax corbularia* and *Phellinus linteus smilax glabra* [75]. Reported pharmacological activities include antioxidant [73], antibacterial against *Mycobacterium tuberculosis* [76], antiproliferative against triple-negative breast cancer [77], anti-Parkinson [74], and skin anti-inflammatory effects [78]. The dihydrochloride salt has shown superior *in vivo* antiarrhythmic efficacy in rats, cats, and rabbits compared to quinidine and novocainamide [79]. *N*-Methylbrevicarine, a semi-synthetic derivative, has demonstrated *in silico* activity as a non-peptide malignant brain tumor antagonist, with hits on three MBT-containing proteins [80]. While *Carex brevicollis* DC has been reported to exhibit teratogenic effects in animals [60,81], possibly linked to its β-carboline alkaloids, further evidence is required. Given their high medicinal potential, the total synthesis of these alkaloids and related analogues remains essential for structural confirmation and securing material for pharmacological evaluation.

2. OBJECTIVES

The primary objective of my PhD research, conducted at the Directorate of Drug Substance Development at Egis Pharmaceuticals PLC and under the academic affiliations of Department of Organic Chemistry and Center of Pharmacology and Drug Research & Development, Semmelweis University, was to contribute to the synthesis and development of novel bioactive compounds with potential pharmaceutical applications. The work was carried out within the framework of the Cooperative Doctoral Program, emphasizing research, development, and innovation, with a strong focus on applicability in industrial settings.

The central aim of the project was the synthesis of natural alkaloids (namely bacillamides, orthoscuticellines A–B, brevicarine, brevicolline) and structurally modified synthetic analogues (oxazolyl- and thiazolylindoles, 1-substituted β-carbolines), with a particular emphasis on compounds containing the indole scaffold as an important skeleton in many biologically active molecules. In line with the growing interest in indole alkaloids as sources of new drug candidates, I set out to develop and optimize synthetic routes that enable the efficient production of such compounds. Where possible, efforts were made to improve existing synthetic methodologies with attention to the principles of green chemistry.

Another key objective was to support pharmacological evaluation of the synthesized new compounds through interdisciplinary collaboration. These studies aimed to assess antiproliferative and cytotoxic activities, providing feedback for further compound optimization and SAR studies in the project of oxazolyl- and thiazolylindoles and 1-substituted β-carbolines.

A further aim was to develop a continuous-flow synthesis of 1-substituted β-carbolines and dihydro-isoquinolines *via* the Bischler–Napieralski reaction and also to model T3P®-induced cyclization reactions in order to understand why, in most cases, the Robinson–Gabriel synthesis proceeds more readily than the Bischler–Napieralski reaction.

Beyond the scientific goals, I prioritized mentoring younger students and fostering knowledge transfer. I involved undergraduate and MSc students in ongoing projects, giving them hands-on experience in an industrial R&D environment and complementing their academic training with practical skills, thereby strengthening the bridge between university education and pharmaceutical industry needs.

3. METHODS

3.1. Reagents, solvents and purification methods

All reagents and solvents were purchased from commercial sources and used without further purification. Purifications by flash column chromatography were carried out using Merck 107736 silica gel 60 H with a hexane–EtOAc, PE–EtOAc, or DCM–MeOH solvent system. Analytical samples of synthesized compounds were obtained by recrystallization from the solvents or solvent mixtures given in the publications or in chapter Discussion. For enantiomer separations, chiral chromatography has been used, the parameters of which are given in the corresponding publications.

3.2. Analytical techniques for compound characterization

Reactions were monitored by TLC carried out on silica gel plates (60 F_{254}) using UV light as visualizing agent, or by HPLC-MS on a Shimadzu LC-40 HPLC equipments (Kyoto, Japan) equipped with diode array detector and an LCMS-2020 quadrupole mass spectrometer. Column: Acquity UPLC bridged ethylene hybrid (BEH) C_{18} 50 × 3 mm, 1.7 μm. All melting points were determined on a Büchi B-540 capillary melting point apparatus and are uncorrected. IR spectra were obtained on a Bruker Alpha FT-IR spectrometer in transmission mode in KBr pellets or film. ^{1}H NMR, ^{13}C NMR and ^{31}P NMR spectra were recorded in DMSO-d_6, $CDCl_3$ or DMSO-d_6 or CD_3OD solution in 5 mm tubes at room temperature, on a Bruker Avance III HD (600, 150 and 242 MHz for ^{1}H, ^{13}C and ^{31}P NMR spectra, respectively) or a Bruker Avance III (400, 100 and 162 MHz for ^{1}H, ^{13}C and ^{31}P NMR spectra, respectively) spectrometer with the deuterium signal of the solvent as the lock and TMS as the internal standard. Chemical shifts (δ) and coupling constants (J) are given in ppm and in Hz, respectively. The following abbreviations are used to designate multiplicities: s = singlet, d = doublet, t = triplet, q = quartet, m = multiplet, br = broad. High-resolution mass spectra (HRMS) were recorded on a Bruker Q-TOF MAXIS Impact mass spectrometer coupled with a Waters I-Class UPLC system (for $[M+H]^+$) or on an Agilent 7250 Q-TOF mass spectrometer coupled to an Agilent 8890 gas chromatographic system (for $[M]^+$). Chiral HPLC measurements were carried out using an Agilent 1200 HPLC instrument. SC-XRD measurements were carried out on a Rigaku R-Axis Spider instrument with image plate detector. SC-XRD structures of compounds have been uploaded to the CCDC database.

3.3. Computational chemistry software

The DFT level computations at the M062X/6–31+G (d,p) level of theory were performed considering the solvent effect (SMD implicit solvent model) of DMF (dielectric constant is 36.71) by the Gaussian 16 program package [82–85] at 120°C. This was followed by single point calculations at the M062X/6-311++G (3df,3pd) level of theory to result in more accurate energy values. The geometries of the molecules were optimized in all cases, and frequency calculations were also performed to assure that the structures are in a local minimum or in a saddle point. The transition states were optimized with the QST3 or the TS (berny) method. Transition states were identified by having one imaginary frequency in the Hessian matrix, and IRC calculations were performed in order to prove that the transition states connect two corresponding minima.

3.4. Flow chemistry apparatus

The continuous flow experiments were performed in a laboratory scale flow reactor system which comprises syringe pumps (manufacturer: H-ION, HI-SY100, 2×5 mL syringe, 0.01–3.50 mL min^{-1}), heated coil reactor (reactor volume: 5 mL, 1.8 mm ID, 1/8" OD, SS316L material, 1.96 m length), back-pressure regulator (manufacturer: H-ION, HI-BP100, 316Ti material, 0.0–100.0 bar) and cooling loop (volume: 0.5 mL, 1 mm ID, 1/16" OD, 0.64 m length) (Figure 8). Before usage and after the reactions, the system was washed thoroughly with MeOH–MeCN 1:1 solution (1 mL min^{-1}). Samples have been collected after reaching stationary conditions (ca. 2 h).

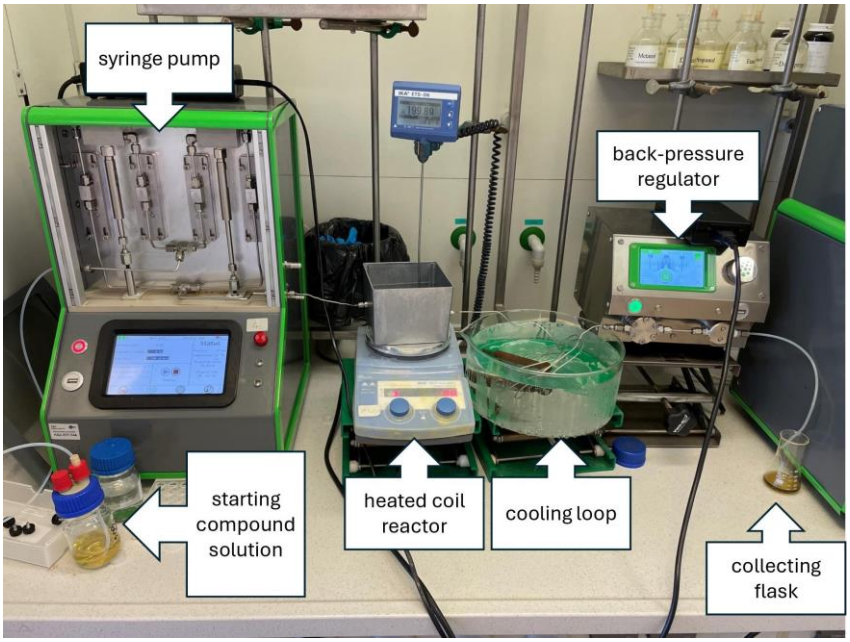

Figure 8. Flow reactor system

4. RESULTS

4.1. Synthesis and SAR studies of novel oxazolyl- and thiazolylindoles

Following an extensive review of the literature, we selected tryptamine (**29a**) as the starting scaffold for the synthesis of the target molecules, employing a Robinson–Gabriel cyclization to construct the oxazole or thiazole ring systems. Condensation of tryptamine (**29a**) and 5-chlorotryptamine (**29b**) with methyl 2-chloro-2-oxoacetate (**95**) furnished oxalamide esters **96a** and **96b** (Scheme 26, pathway A). Subsequent treatment of these intermediates with aqueous ammonia, methylamine, or cyclohexylamine produced the corresponding bis-amides **97a–d**. Oxidation of intermediates **97a** and **97b** with DDQ yielded the α-acylamino ketones **98a** and **98b**, which underwent cyclization to give the target oxazole derivatives **99a** and **99b**. For the cyclization step, TFA and TFAA were used at room temperature for $R^1 = R^2 = H$, whereas $POCl_3$ at 80 °C was required for R^1=H and R^2 = Me. Under the latter conditions, treatment of **98a** (R^1 = H) with $POCl_3$ led to the carbonitrile **100** instead of the amide.

Another synthetic sequence was developed to access oxazoles **99c–e**. In this route, intermediate **96a** was first oxidized with DDQ to ketone **101**, which was subsequently cyclized to indolyloxazole-carboxylic ester **102**, a key intermediate for medicinal chemistry library synthesis. Direct amidation of compound **102** with appropriate amines in methanol at ambient temperature led to oxazole-carboxamides **99c–e**. Finally, conversion of oxazole-carboxamides **99a–e** into the corresponding carbothioamides **103a–e** was achieved in generally high yields by reaction with Lawesson's reagent.

An alternative synthetic pathway (Scheme 26, pathway B) to 1,3-oxazole-2-carbothioamides **103b** and **103c** was established by employing Zavarzin's method to introduce the thioamide functionality. In this approach, 2-chloroacetamide **104**, prepared by the reaction of tryptamine (**29a**) with chloroacetyl chloride, was treated with methylamine or isopropylamine and elemental sulfur, affording 2-oxocarbothioamides **105a** and **105b**. Subsequent DDQ-mediated oxidation yielded the corresponding ketones **106a** and **106b**, which underwent cyclization with $POCl_3$ to furnish the desired products **103b** and **103c**. The application of the Robinson–Gabriel cyclization strategy was justified over the Suzuki coupling by the accessibility of cost-effective starting materials, the opportunity to study mechanistic phenomena such as the spontaneous cyclization of thioamides, and the feasibility of late-stage scaffold diversification.

The molecular structure of the methylamido derivative **103b** (R^1 = H, R^2 = Me) was unambiguously confirmed by SC-XRD as well.

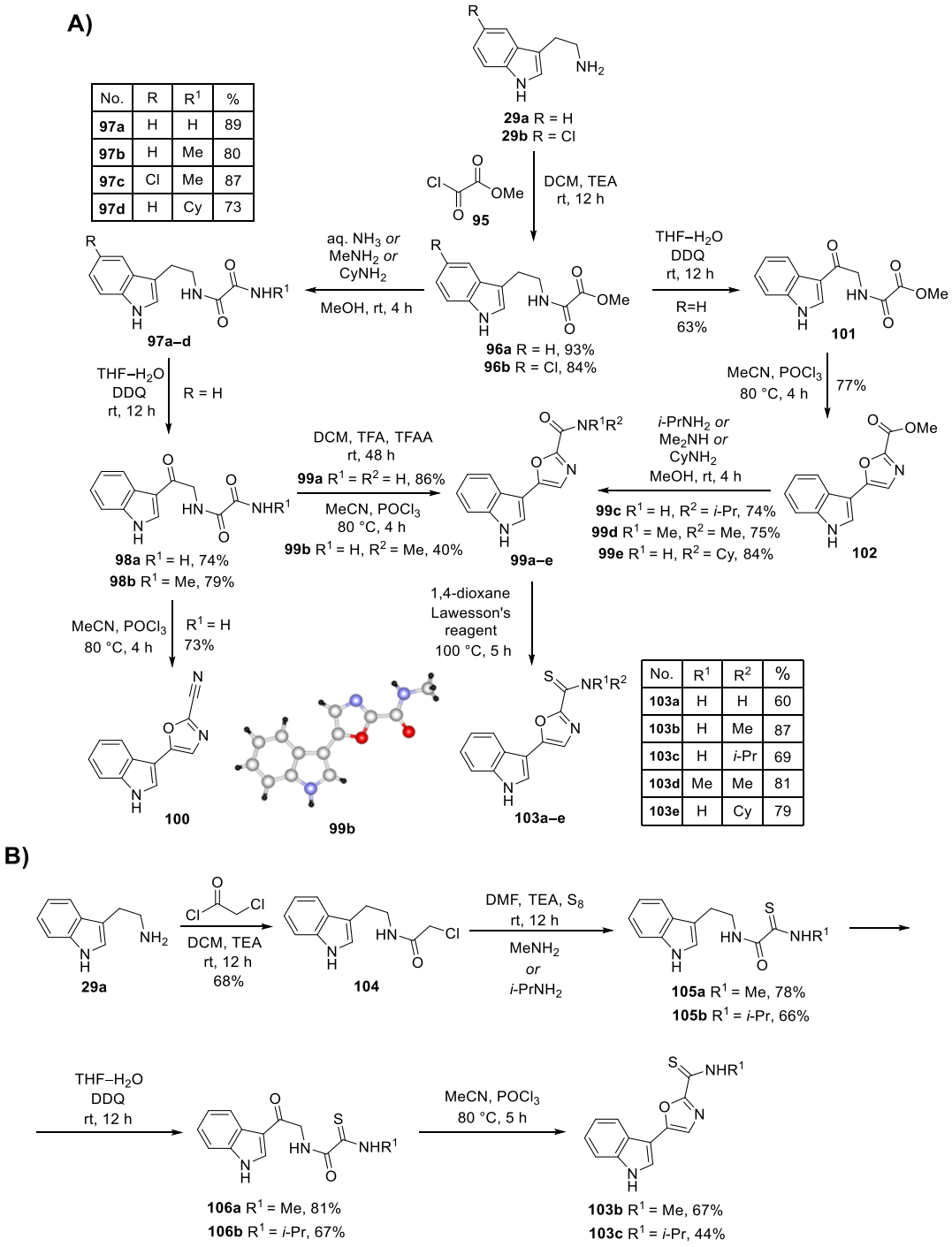

Scheme 26. Synthetic routes leading to indolyloxazole-carboxamides (**99a–e**) and -carbothioamides (**103a–e**)

For the initial step in the synthesis of key intermediates **107a–f** for thiazolylindoles **108a–f** and **109a,b** (Scheme 27), we adopted the procedure of Zavarzin *et al.* for the

convenient preparation of 2-(substituted-amino)-2-thioxoacetamides, which involves treating 2-chloroacetamide with the appropriate amine and elemental sulfur. In our hands, the reaction proved highly effective, providing 2-thioxoacetamides **107a–f** in generally good yields.

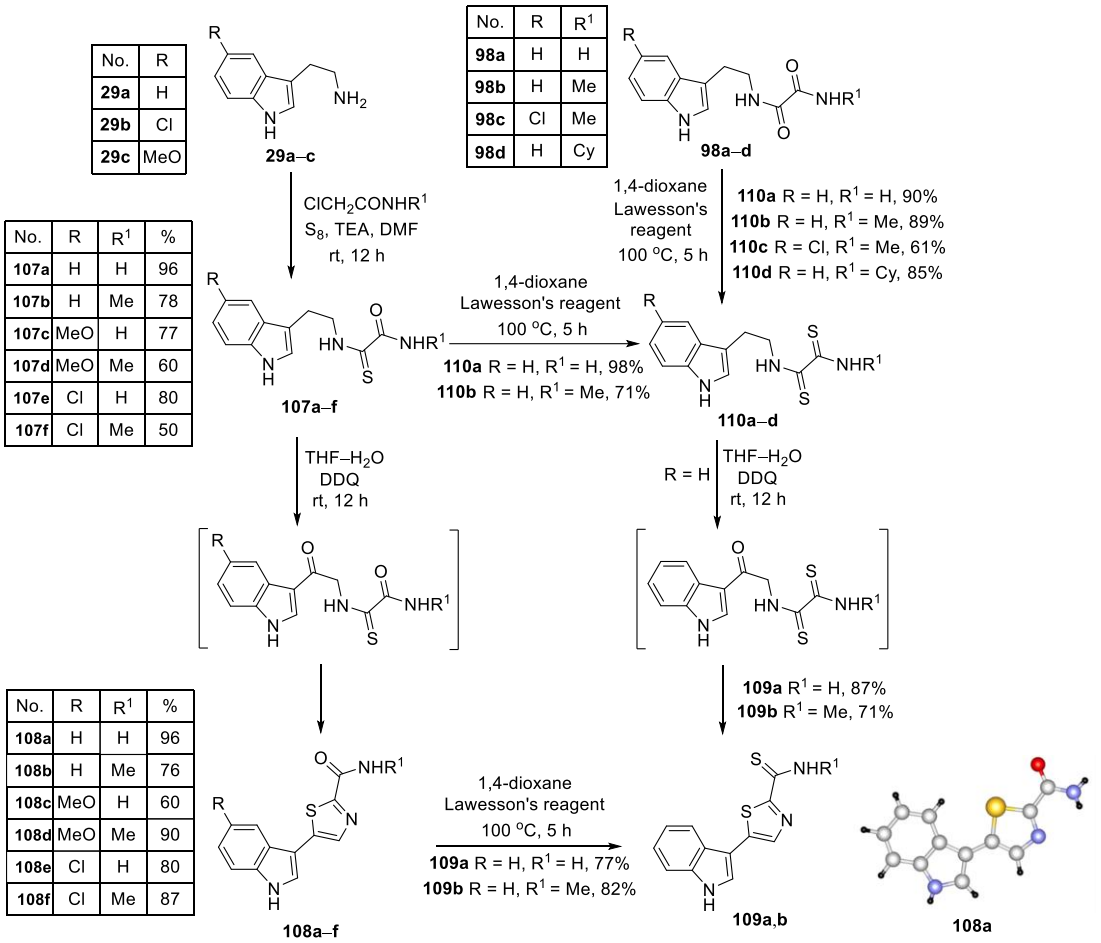

Scheme 27. Synthesis of indolylthiazole-carboxamides (**108a–f**) and -carbothioamides (**109a,b**)

Unexpectedly, DDQ oxidation of **107a–f** in THF at room temperature furnished thiazolylindoles **108a–f** directly, indicating that the ring closure occurred under these mild conditions without the need for a dehydrating reagent – an outcome previously not documented. Further conversion of amides **108a** and **108b** with Lawesson's reagent afforded the corresponding thioamides **109a** and **109b**. The structure of **109a** (R^1 = H) was confirmed by SC-XRD.

Alternatively, **109a** and **109b** could also be obtained *via* DDQ oxidation of bis-thioamide precursors **110a** and **110b**, themselves prepared by treating either **98a–d** or **107a**,**b** with Lawesson's reagent. The application of the Robinson–Gabriel cyclization strategy was justified over the Suzuki coupling by the accessibility of cost-effective

starting materials, the opportunity to study mechanistic phenomena such as the spontaneous cyclization of thioamides, and the feasibility of late-stage scaffold diversification.

In silico ADME profiles of the synthesized compounds were evaluated using SwissADME [86]. Key parameters (molecular weight, H-bond donors, rotatable bonds, Lipinski compliance, TPSA, logP values, solubility, GI absorption, BBB permeability, and lead-likeness) have been studied. All compounds meet Lipinski's rule of five and most show favorable lipophilicity and lead-like properties. BOILED-Egg analysis indicated high GI absorption for all derivatives and predicted good BBB penetration for several ones [87].

The pharmacological evaluation of all synthesized compounds was carried out in collaboration with our partner laboratory, which tested their antiproliferative effects on 3T3 fibroblasts, HL-60 leukemia cells, and C6 glioma cells. The results indicate that only a subset of compounds, primarily thiazoles and oxazoles bearing a thioamide group, reduced cancer cell counts significantly, whereas most acyclic derivatives and oxazoles with a carboxamide group appeared to inhibit proliferation without marked cytotoxicity (Figure 9).

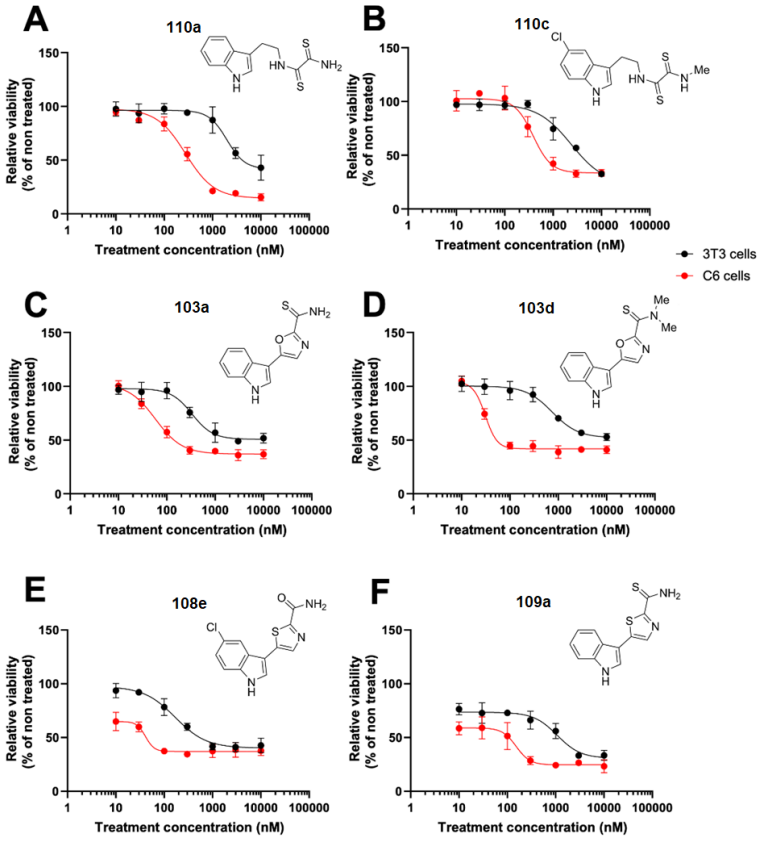

Figure 9. Dose-response curves of the most prominent compounds on C6 and 3T3 cells

Key SAR trends are summarized in Figure 10: thiazole scaffolds were generally more active than oxazoles; carbothioamide substitution further enhanced activity; and chlorine atoms increased both potency and selectivity towards cancer cells. Notably, these compounds and their intermediates present numerous opportunities for further structural optimization.

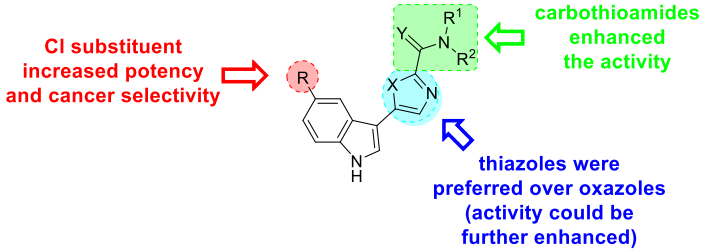

Figure 10. SAR of the prepared compounds

4.2. Synthesis of bacillamide alkaloids

Having established efficient synthetic pathways towards oxazolyl- and thiazolylindole frameworks and identified preliminary structure-activity relationships among these novel compounds, our attention was next directed towards naturally occurring analogues featuring similar heteroaromatic motifs. Among such systems, the bacillamide family of indole and thiazole containing alkaloids represent an intriguing target due to their distinctive biological profiles and unresolved stereochemical questions. Therefore, in the following section, we focused on the asymmetric synthesis of bacillamide alkaloids and their analogues to clarify their absolute configurations and enable stereochemical benchmarking for future studies.

Given the potential ecological relevance of naturally occurring bacillamide alkaloids as algicidal agents, and the complex yet sometimes inconsistent data available on their stereochemistry, we undertook the synthesis of both enantiomeric forms of bacillamides B–D as well as neobacillamide A. For each compound, we determined the absolute configuration and optical rotation. This provides a reference framework: should a natural product of this class be isolated in the future, its optical rotation (or chiral chromatographic behaviour) can be directly compared, enabling straightforward stereochemical assignment. To complement this, chiral HPLC methods were developed, making enantiomer separation and retention time comparison a practical tool for stereochemical determination.

As a preliminary step towards the enantioselective syntheses and the development of chiral analytical methods, we first prepared the racemic forms of the target molecules. In

the following sections, the asymmetric syntheses are described which afforded the enantiomerically enriched final products.

The main intermediates in the syntheses of bacillamides B–D and neobacillamide A are the enantiomeric forms of 2-(1-hydroxyethyl)thiazole (**33**), which were accessed *via* asymmetric transfer hydrogenation or asymmetric hydride transfer reaction of ketone **28**. When employing (*S*)-Me-CBS or (*R*)-Me-CBS as catalysts [88], the reactions afforded 69–71% yields with ee limited to 53–73% (Scheme 28). To improve stereoselectivity, we turned to a Noyori-type catalyst, RuCl(*S*,*S*)-Tsdpen, and its enantiomer [89], which provided the corresponding alcohols in 95–96% ee. An alternative synthetic route to (*S*)-**33** has been reported in the literature [90], supporting the expected stereochemical outcome on the basis of the reaction mechanism [91]. A summary of the asymmetric synthesis results is presented in Table 1.

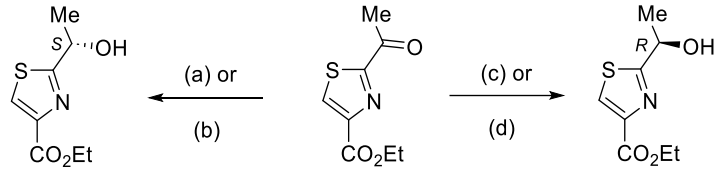

(*S*)-(–)-**33** **28** (see Scheme 10) (*R*)-(+)-**33**

(a) (*R*)-Me-CBS, $NaBH_4$, Me_2SO_4, THF, 69%, ee 73%;
(b) RuCl[(*S*,*S*)-Tsdpen](mesitylene), HCOONa, MeOH, 81%, ee 95%;
(c) (*S*)-Me-CBS, $NaBH_4$, Me_2SO_4, THF, 71%, ee 53%;
(d) RuCl[(*R*,*R*)-Tsdpen](mesitylene), HCOONa, MeOH, 84%, ee 96%.

Scheme 28. Enantioselective synthesis of 2-(1-hydroxyethyl)thiazole **33**

Table 1. Summary of the syntheses of 2-(1-hydroxyethyl)thiazole **33**

catalyst	(*S*)-Me-CBS	(*R*)-Me-CBS	RuCl[(*S*,*S*)-Tsdpen](mesitylene)	RuCl[(*R*,*R*)-Tsdpen](mesitylene)
appropriate product according to mechanism[89]	(*R*)-(+)-**33**	(*S*)-(–)-**33**	(*S*)-(–)-**33**	(*R*)-(+)-**33**
purity by chiral HPLC	ee 53%	ee 73%	ee 95%	ee 96%
yield of reduction	71%	69%	81%	84%
measured optical rotation	ND	ND	$[\alpha]_D^{25} = -19.3$ (*c* 1.20, $CHCl_3$)	$[\alpha]_D^{23} = +20.8$ (*c* 1.20, $CHCl_3$)
literature optical rotation	–	–	$[\alpha]_D^{20} = -19.9$ (*c* 1.20, $CHCl_3$)	–

In the following section, the four synthetic pathways (routes **A–D**) depicted in Scheme 29 are discussed, taking into account that several of the individual transformations are

chemically analogous. In route **A**, the thiazole ester [(*R*)-(+)-**33**] was condensed with tryptamine (**29a**), furnishing the antipode of bacillamide B [(*R*)-(+)-**22**] in 65% yield with 95% ee. Subsequent conversion of this intermediate into bacillamide D [(*S*)-(–)-**25**] was achieved in two steps with an overall yield of 51% and an ee of 87%. The process involved a Mitsunobu reaction to generate the azido intermediate with inverted configuration [(*S*)-**111**], which was directly reduced to yield the target compound. The structure of bacillamide D [(*S*)-(–)-**25**] was confirmed by SC-XRD (Figure 11). Furthermore, *N*-acetylation of bacillamide D [(*S*)-(–)-**25**] led to bacillamide C [(*S*)-(–)-**23**] in 88% yield. These results, corroborated by X-ray analysis, are consistent with the structural and optical rotation data reported by Davyt et al. [45] for bacillamide C [(*S*)-(–)-**23**].

For the synthesis of neobacillamide A (Scheme 29, route **B**), the thiazole ester [(*R*)-(+)-**33**] was subjected to amidation with phenylethylamine (**55**), affording amide (*R*)-(+)-**112** in 79% yield. Subsequent transformation to azido derivative (*S*)-**113**, involving inversion at the stereogenic center, and its subsequent reduction furnished amine (*S*)-(–)-**114** in 40% overall yield for the two steps. Final *N*-acetylation provided neobacillamide A [(*S*)-(–)-**24**] in 80% yield with an ee of 78%.

Bacillamide B [(*S*)-(–)-**22**] was synthesized *via* amidation of the corresponding thiazole ester [(*S*)-(–)-**33**, Scheme 29, route **C**] with tryptamine (**29a**), yielding the product in 89% yield and 96% ee. The literature contains inconsistent data regarding the sign of optical rotation of bacillamide B; our measurements are in agreement with those reported by Du et al [41].

Azidation of bacillamide B [(*S*)-(–)-**22**], accompanied by inversion of configuration to give intermediate (*R*)-**111**, followed by reduction, produced the enantiomer of bacillamide D [(*R*)-(+)-**25**] in 48% yield with 91% ee. The structure of this compound was confirmed by SC-XRD (Figure 12). Subsequent *N*-acetylation led to the corresponding antipode of bacillamide C [(*R*)-(+)-**23**] in 84% yield.

Finally, the enantiomeric counterpart of neobacillamide A [(*R*)-(+)-**24**, Scheme 29, route **D**] was obtained by amidation of the thiazole ester [(*S*)-(–)-**33**] with phenylethylamine (**55**) to form (*S*)-(–)-**112** in 77% yield. Conversion through azide intermediate (*R*)-**113** and reduction afforded amine (*R*)-(+)-**114** in 76% combined yield, which was then *N*-acetylated to yield the target compound in 87% yield with 91% ee.

It is noteworthy that the observed decrease in ee could be attributable to the partial SN_1 character during the Mitsunobu reaction, where the chiral center is directly involved.

Furthermore, minor fluctuations in reaction conditions (such as temperature and reaction time) may have increased this effect and the cumulative impact of which became apparent only in the final products, such as in the case of neobacillamide A ((*R*)-(+)-**24**, ee 78%), due to the lack of systematic chiral HPLC monitoring for every intermediate stage.

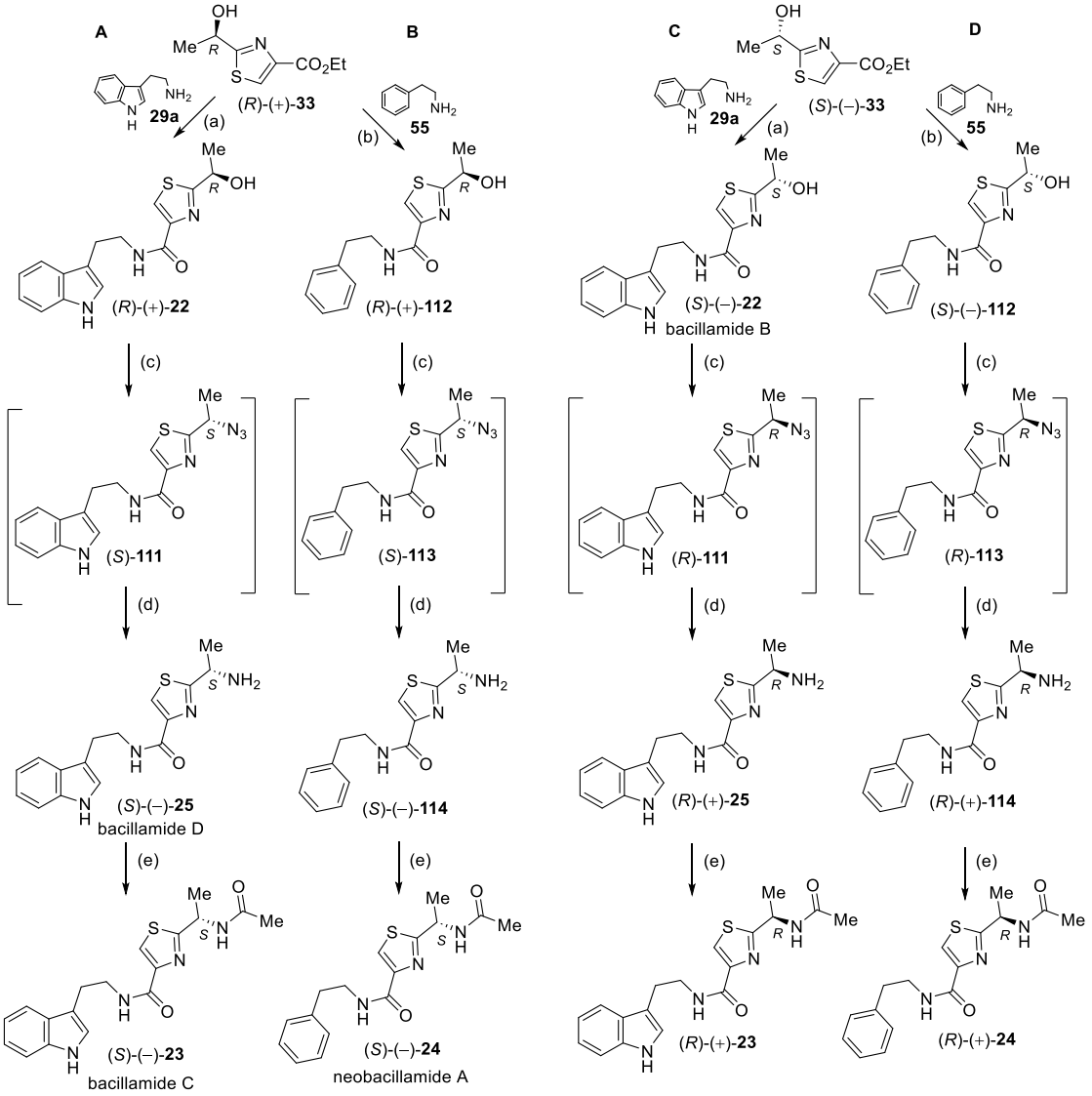

Route A: (a) tryptamine (**29a**), 4,6-dimethylpyrimidin-2-ol, 105 °C, 6 h, 65%, ee 95%; (c) PPh_3, DIPEA, DIAD, THF, DPPA; (d) $NaBH_4$, $NiCl_2 \cdot 6\ H_2O$, MeOH, rt, 51% (for two steps), ee 87%; (e) acetyl chloride, TEA, DCM, 88%, ee 84%. **Route B** (b) phenylethylamine (**55**), 4,6-dimethylpyrimidin-2-ol, 105 °C, 12 h, 79%; (c) PPh_3, DIPEA, DIAD, THF, DPPA; (d) $NaBH_4$, $NiCl_2 \cdot 6\ H_2O$, MeOH, rt, 40% (for two steps); (e) acetyl chloride, TEA, DCM, 80%, ee 78%. **Route C** (a) tryptamine (**29a**), 4,6-dimethylpyrimidin-2-ol, 105 °C, 6 h, 89%, ee 96%; (c) PPh_3, DIPEA, DIAD, THF, DPPA; (d) $NaBH_4$, $NiCl_2 \cdot 6\ H_2O$, MeOH, rt, 48% (for two steps), ee 91%; (e) acetyl chloride, TEA, DCM, 84%, ee 90%. **Route D** (b) phenylethylamine (**55**), 4,6-dimethylpyrimidin-2-ol, 105 °C, 12 h, 77%; (c) PPh_3, DIPEA, DIAD, THF, DPPA; (d) $NaBH_4$, $NiCl_2 \cdot 6\ H_2O$, MeOH, rt, 76% (for two steps); (e) acetyl chloride, TEA, DCM, 87%, ee 91%.

Scheme 29. Synthesis of bacillamide B [(*S*)-(–)-**22**], bacillamide C [(*S*)-(–)-**23**], bacillamide D [(*S*)-(–)-**25**], neobacillamide A [(*S*)-(–)-**24**], and their antipodes.

To the best of our knowledge no SC-XRD analysis of the molecular structures of bacillamides A–D or neobacillamide A has been reported in the literature. In order to prove the configurations of bacillamide D (*S*) and bacillamide D antipode (*R*) and to obtain structural information on the shape of the molecules, crystalline picrate salts [(*S*)-(–)-**25** · $(O_2N)_3C_6H_2OH$] and [(*R*)-(+)-**25** · $(O_2N)_3C_6H_2OH$] have been prepared, yielding crystals suitable for SC-XRD (Figures 11 and 12). The measurements confirm the absolute configuration at the carbon atom of the aminoethyl group attached to the thiazole ring, displaying proper Flack parameters.

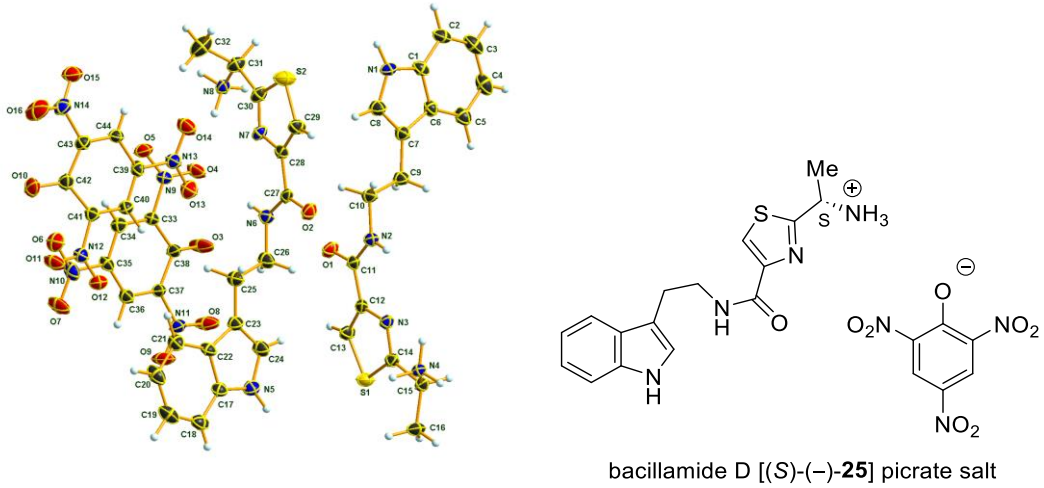

Figure 11. X-ray structure of the picrate salt of bacillamide D [(*S*)-(–)-**25** · $(O_2N)_3C_6H_2OH$]

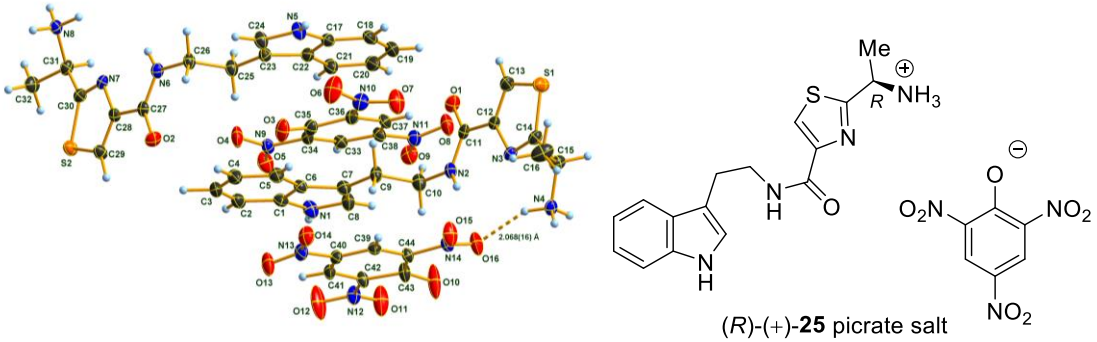

Figure 12. X-ray structure of the picrate salt of bacillamide D antipode [(*R*)-(+)-**25** · $(O_2N)_3C_6H_2OH$].

4.3. Studies on the syntheses of orthoscuticellines A and B

While the synthesis and stereochemical analysis of the bacillamides provided valuable insights into thiazolylindole chemistry and enantioselective transformations, our attention next turned to a structurally distinct group of marine-derived β-carboline dimers: the orthoscuticellines. These compounds represent a unique case where two β-carboline cores

are linked through a cyclobutane unit, posing both synthetic and mechanistic challenges. Building upon the knowledge gained from Bischler–Napieralski cyclizations in the bacillamide project, this section explores our synthetic strategies towards orthoscuticellines A and B.

The synthesis of orthoscuticelline B [(±)-*trans*-**70**] was accomplished in three steps with an overall yield of 58% (Scheme 30). Condensation of tryptamine (**29a**) with (±)-*trans*-1,2-cyclobutanedicarboxylic acid [(±)-*trans*-**115**] in the presence of T3P® as a coupling agent afforded the corresponding dicarboxamide (±)-*trans*-**116** in 83% yield. Subsequent Bischler–Napieralski cyclization produced the bis(dihydro-β-carboline)-substituted cyclobutane derivative (±)-*trans*-**117**, which was then oxidized with DDQ to furnish the target molecule, orthoscuticelline B [(±)-*trans*-**70**]. Remarkably, the trans stereochemistry remained completely intact throughout the sequence, and no formation of the corresponding *cis* isomers was observed in any of the reaction steps.

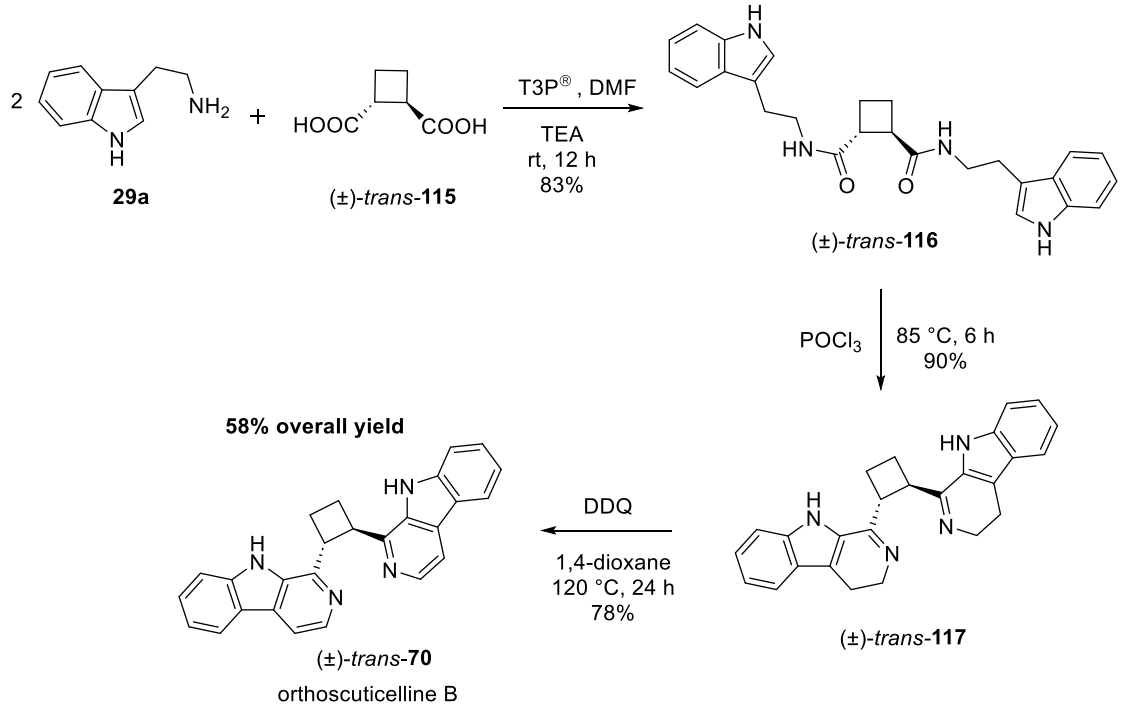

Scheme 30. Synthesis of alkaloid orthoscuticelline B [(±)-*trans*-**70**]

The synthesis of the *cis*-cyclobutane-1,2-dicarboxylic acid (*cis*-**115**, meso form) derivative orthoscuticelline A (**69**) was designed following an analogous strategy to that used for the trans isomer (Scheme 31). In the initial step, condensation of tryptamine (**29a**) with *cis*-**115** yielded the corresponding *cis*-dicarboxamide (*cis*-**116**). The reaction afforded a significantly lower yield (47%) than that obtained for the trans analogue (83%, Scheme 30), which can be attributed to the concurrent formation of the by-product **118**

(meso form) in 19% yield, resulting from the mono-condensation of *cis*-**115** with a single equivalent of tryptamine (**29a**). Subsequent Bischler–Napieralski cyclization of *cis*-**116** produced the bis(dihydro-β-carboline)-substituted cyclobutane intermediate *cis*-**117**. However, the final dehydrogenation step unexpectedly yielded the *trans*-cyclobutane-1,2-dicarboxylic acid (*trans*-**115**) derivative orthoscuticelline B (**70**) instead of the desired orthoscuticelline A (**69**). Attempts to perform the oxidation under milder conditions or using alternative reagents, including oxalyl chloride with iron(III) chloride, T3P®, trifluoromethanesulfonic anhydride (Tf_2O), and polyphosphoric acid (PPA), failed to provide the expected product.

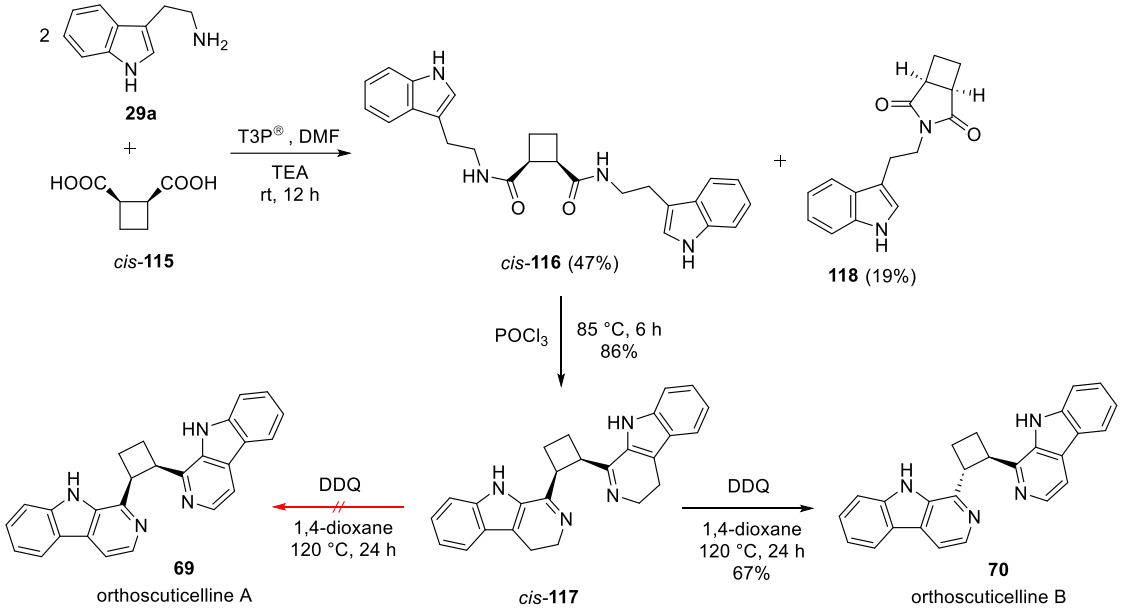

Scheme 31. Synthetic plan for alkaloid orthoscuticelline A (**69**)

The formation of unexpected product **70** is attributable to the conversion of the *cis*-**117** dihydro intermediate into the corresponding (±)-*trans*-**117** isomer through tautomerization of the dihydro-β-carboline ring system under the relatively harsh oxidation conditions (Scheme 32). Experimental evidence supporting this hypothesis was obtained when compound *cis*-**117**, upon stirring overnight at room temperature in 1,4-dioxane, was found to undergo isomerization to yield the (±)-*trans*-**117** derivative.

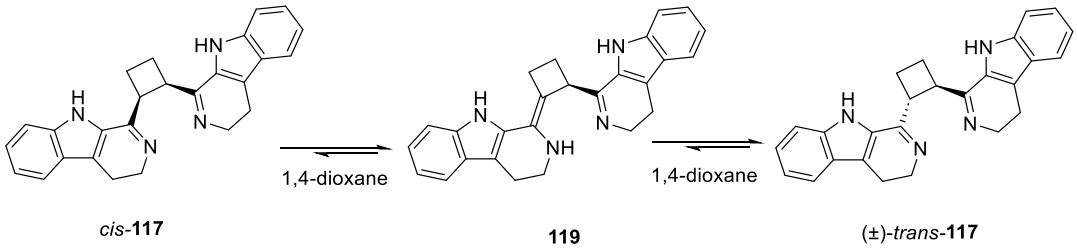

Scheme 32. Proposed tautomerism of *cis*-**117** to (±)-*trans*-**117**

Consequently, an alternative synthetic strategy was explored for the preparation of the *cis* isomer, orthoscuticelline A (**69**), instead of the previously attempted Bischler–Napieralski route. Starting from *cis*-cyclobutane-1,2-dicarboxylic acid (*cis*-**115**), the corresponding *cis*-cyclobutane-1,2-dialdehyde (*cis*-**120**) was obtained in two steps following literature procedures, i.e. *via* acyl chloride formation using thionyl chloride ($SOCl_2$) and subsequent reduction of the diester intermediate (*cis*-**119**) with Red-Al (Scheme 33). However, when conventional Pictet–Spengler cyclization conditions were applied, none of the tested methods afforded the desired tetrahydro derivative (*cis*-**121**) even after 48 hours. The unsuccessful trials included the use of various Brønsted acids (H_2SO_4, trifluoroacetic acid), Lewis acids ($BF_3 \cdot Et_2O$, trimethylsilyl chloride), and other reagents such as 2,4,6-trichloro-1,3,5-triazine, T3P®, and hexafluoro-2-propanol. Following these unsuccessful attempts, the total synthesis of orthoscuticelline A (**69**) was discarded.

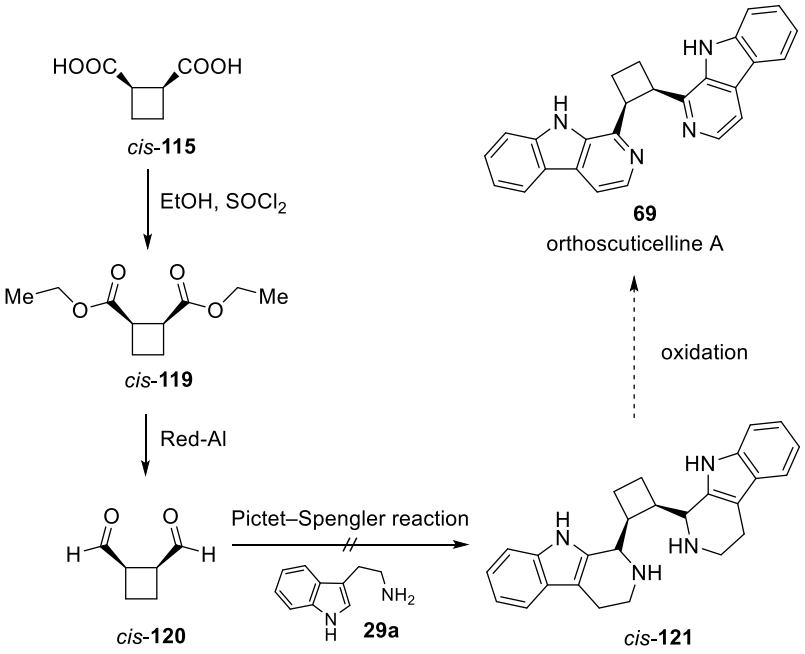

Scheme 33. Alternative synthesis plan for orthoscuticelline A (**69**)

Whereas the initial isolation of orthoscuticelline B [(±)-*trans*-**70**] in the literature from approximately 25 g of freeze-dried bryozoan material yielded only 0.2 mg of product (0.001%) [57], and the first reported total synthesis afforded 31.9 mg of a mixture of orthoscuticellines A (**69**) and B (**70**) over five synthetic steps [58], our optimized synthetic route provided 77 mg of pure orthoscuticelline B (**70**) starting from commercially available tryptamine (**29a**) in only three steps with an overall yield of 58%.

The NMR spectroscopic data of our synthesized (±)-*trans*-**70** were identical to those reported for the synthetic compound by Yi *et al.* [58]. In contrast, the NMR data published by Kleks *et al.* [57] showed significant deviations from those of the synthetic sample. We hypothesized that these discrepancies originated from the formation of a trifluoroacetate salt, as TFA has been used during the isolation procedure in that study. To test this assumption, NMR spectra of our product were recorded in DMSO-d_6 with incremental additions of TFA (0–2 eq). Pronounced changes were observed in both the ^{1}H and ^{13}C NMR chemical shifts with increasing acid concentration. Upon the addition of 0.5 eq of TFA, the resulting spectra matched precisely those reported by Kleks *et al.* [57], thereby confirming our hypothesis.

4.4. Studies on the syntheses of brevicarine and brevicolline

The orthoscuticelline studies highlighted the potential and limitations of classical cyclization reactions in constructing complex β-carboline architectures. To further expand this structural space and connect marine and terrestrial alkaloid chemistry, we next investigated brevicarine and brevicolline, two plant-derived β-carboline alkaloids exhibiting notable pharmacological activities. Their synthesis did not only allow us to compare different β-carboline-forming strategies but also to evaluate scalable, environmentally conscious modifications applicable to natural product synthesis.

In this work, our objective was to establish a novel and scalable synthetic route to brevicarine (**73**) and to design an alternative pathway for the synthesis of brevicolline [(*S*)-**72**], both utilizing a common key intermediate (**74**) [63]. The synthesis of brevicarine (**73**, Scheme 34) commenced with the catalytic hydrogenation of the alkyne moiety in phthaloyl-protected intermediate **76**, affording compound **122**. Subsequent cleavage of the phthalimide protecting group using methylamine furnished the corresponding amine **123**. Alternatively, a modified, environmentally benign protocol was developed, in which the removal of the phthaloyl group from compound **76** to yield amine **77** was achieved with methylamine instead of the previously applied, highly toxic methylhydrazine [92]. This was followed by catalytic reduction of the triple bond, providing the same amine intermediate **123**.

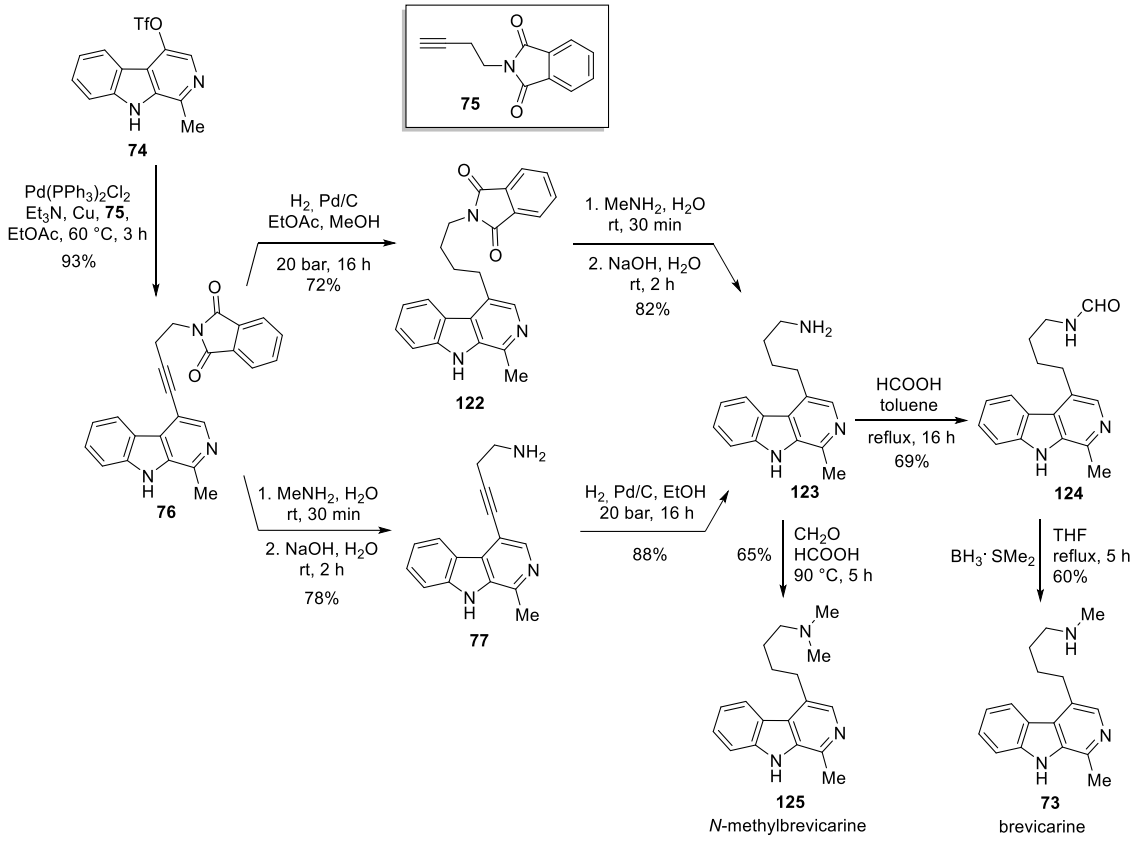

Scheme 34. New synthetic variants for the preparation of brevicarine alkaloid (**73**) and its synthetic derivative *N*-methylbrevicarine (**125**)

Attempts to achieve *N*-monomethylation of the primary amino group in compound **123** through direct alkylation with methyl iodide or *via* the Eschweiler–Clarke reductive amination using formaldehyde and formic acid proved unsuccessful, as the reaction consistently yielded a considerable amount of the undesired dimethylated by-product, even when only one equivalent of the alkylating reagent was employed. Ultimately, a successful strategy was developed to circumvent overmethylation: the methyl group was introduced indirectly by *N*-formylation of compound **123** to afford the formamide intermediate **124**, followed by reduction of the formyl functionality with borane-dimethyl sulfide complex, giving brevicarine (**73**) as its dihydrochloride salt. On the basis of these findings, the Eschweiler–Clarke methylation of primary amine **123** was subsequently applied to prepare *N*-methylbrevicarine (**125**), a close structural analogue of natural alkaloid **73** [93].

Although a preliminary ^{1}H NMR spectrum of isolated brevicarine base (**73**) and partial signal assignments were reported as early as 1969 [93], the data were incomplete. The chemical shifts described in that early report, however, are fully consistent with those of our synthetic compound. Subsequent publications [64,68,69] confirmed the structure of

brevicarine by IR and MS analyses or through its characteristic reactivity but did not include comprehensive NMR characterization. In the present work, we provided the complete and unambiguous assignment of all ^{1}H and ^{13}C NMR resonances for both the free base and the dihydrochloride salt of brevicarine (**73**).

During our investigations aimed at developing an improved and efficient synthetic route to brevicarine (**73**), an unexpected reaction outcome was observed (Scheme 35). According to literature precedents, the reduction of carbamate **126**, prepared from amine **123** *via* ethoxycarbonylation, was anticipated to yield brevicarine (**73**) upon treatment with $LiAlH_4$ [94,95]. Contrary to expectations, the reaction proceeded only as far as the *N*-formyl intermediate (**124**), and no formation of brevicarine (**73**) was detected by LC–MS analysis [96].

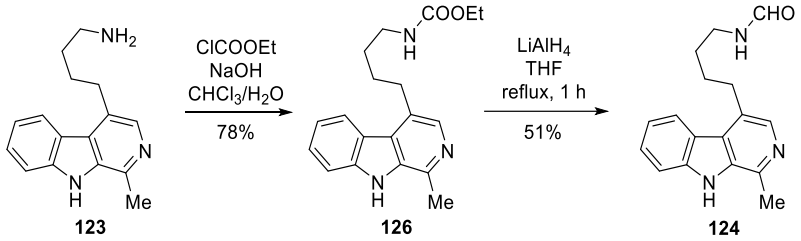

Scheme 35. Synthesis of carbamate **126** and its subsequent reduction with $LiAlH_4$

In designing an alternative synthetic approach towards racemic brevicolline [(±)-**72**], our primary objective was to achieve direct coupling of the pyrrole moiety to compound **74**, rather than constructing the pyrrole ring *via* intramolecular cyclization, as outlined in Scheme 22. The Suzuki–Miyaura cross-coupling reaction of **74** with pyrrole boronic ester **127** proceeded smoothly, affording the pyrrolo-β-carboline derivative **128** in excellent yield (Scheme 36). However, attempts to selectively hydrogenate the pyrrole ring of **128** under various catalytic conditions were unsuccessful. When the reaction was performed under mild conditions (ambient temperature, 15 bar H_2) using platinum(IV) oxide monohydrate (Adams' catalyst, $PtO_2 \cdot H_2O$) as the catalyst, a complete reduction occurred, yielding the overhydrogenated tetrahydro derivative **129**, corresponding to the partially saturated form of racemic brevicolline [(±)-**72**], in 91% yield.

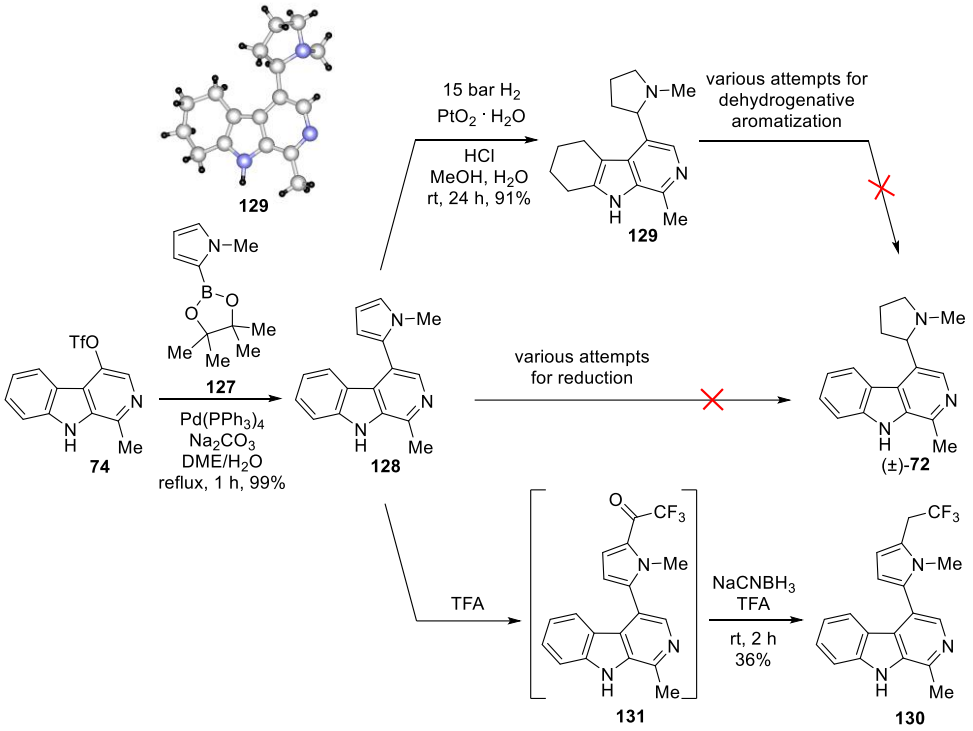

Scheme 36. Experiments on the synthesis of racemic brevicolline [(±)-**72**], and the formation of unexpected products

The structure of compound **129** was further confirmed by SC-XRD analysis. Variation of the hydrogenation catalyst using $Pd(OH)_2$, Ru, or Rh did not alter the course of the reaction; in all cases, compound **129** was obtained exclusively, and the formation of brevicolline [(±)-**72**] could not be detected. Interestingly, attempts to convert compound **129** into brevicolline [(±)-**72**] *via* dehydrogenative aromatization using a range of oxidizing agents (DDQ, Pd/C, MnO_2, $CuCl_2$, I_2, elemental sulfur, and $KMnO_4$) were likewise unsuccessful.

Based on literature precedents [94,95], we next explored the selective reduction of the pyrrole ring in compound **128** with $NaCNBH_3$ in TFA. Unexpectedly, this reaction afforded the trifluoroethylated derivative **130**. The formation of this product can be rationalized by analogy to previously reported examples of TFA-mediated trifluoroacetylation of aromatic systems [97,98]. In our case, however, both trifluoroacetylation of the pyrrole moiety in **128** and subsequent reduction of the resulting carbonyl intermediate **131** with $NaCNBH_3$ occurred in a single reaction vessel – a transformation not previously described in the literature. It is noteworthy that when the same reaction was performed in acetic acid instead of TFA, no conversion was observed,

whereas replacing $NaCNBH_3$ with $NaBH_4$ in TFA again led to the formation of compound **130**.

4.5. Synthesis of 1-substituted β-carbolines *via* multicomponent reactions and SAR studies thereof

Having completed the synthesis of complex β-carboline natural products, our focus shifted towards the development of structurally simplified analogues amenable to high-throughput derivatization and pharmacological screening. To this end, we explored multicomponent reactions as versatile tools for the rapid construction of 1-substituted β-carboline derivatives. These reactions allowed the systematic investigation of substituent effects and the establishment of preliminary structure-activity relationships within a chemically diverse compound library.

In view of the valuable pharmacological potential associated with these structural motifs, we set out to synthesize a series of derivatives of 1-formyl-β-carbolines (**135**), namely α-aminophosphonates (**132**), α-acylamino-α-aryl carboxamides (**133**), and 2-oxo-1,2,3,4-tetrahydropyrimidine-5-acyl derivatives (**134**), employing the Kabachnik–Fields, Ugi, and Biginelli multicomponent reactions, respectively (Scheme 37). The target compounds were designed to incorporate structural features that have frequently been associated with diverse and significant biological activities in the literature.

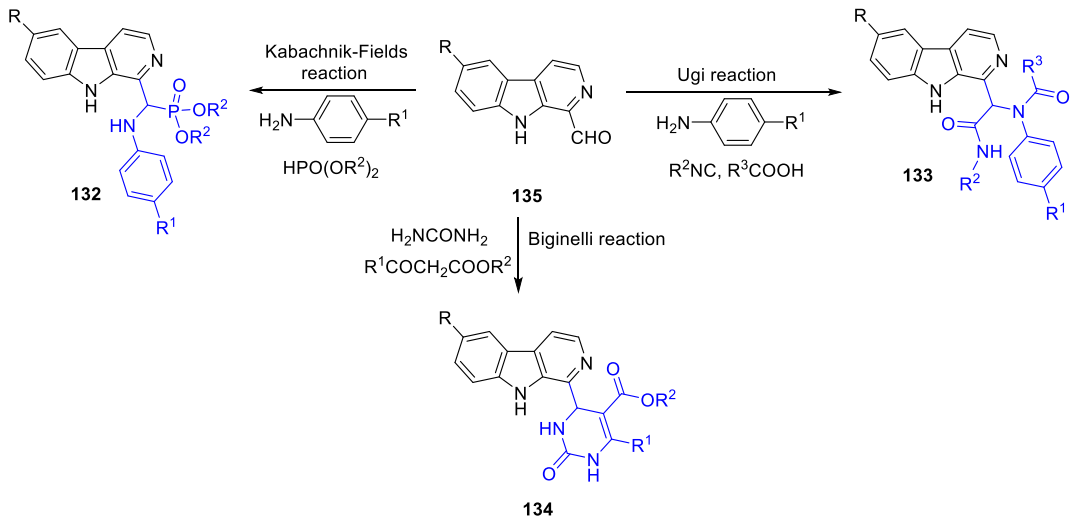

Scheme 37. Multicomponent reactions of 1-formyl-β-carbolines (**135**)

The most widely employed method for the synthesis of α-aminophosphonates is the one-pot, three-component Kabachnik–Fields reaction, which involves the condensation of a carbonyl compound, a primary or secondary amine, and a phosphite. This transformation has been performed under a broad range of experimental conditions,

utilizing various catalysts and solvents [99]. More recently, our group reported a broadly applicable, catalyst- and solvent-free procedure for the Kabachnik–Fields synthesis of α-aminophosphonates under ambient conditions [100]. In the present work, α-aminophosphonates (**132**) incorporating a β-carboline scaffold were synthesized by reacting 1-formyl-β-carbolines (**135**) with aniline or substituted anilines (**136**) and dialkyl phosphites (**137**) in a three-component Kabachnik–Fields condensation carried out at 80 °C in the presence of magnesium perchlorate as the catalyst (Scheme 38) [101].

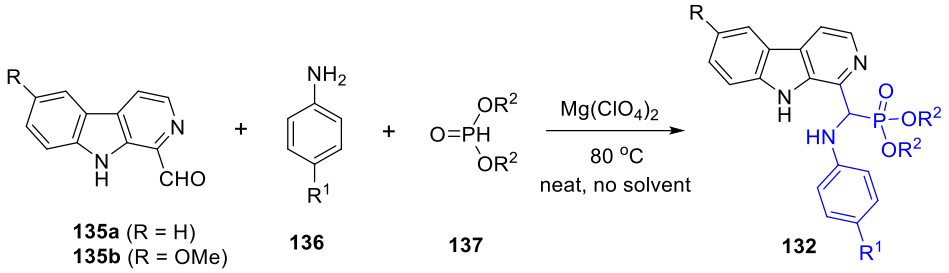

132	R	R^1	R^2	reaction time (h)	yield (%)
a	H	H	Et	2	92
b	H	F	Et	2	94
c	H	Cl	Et	2	80
d	H	Br	Et	4	74
e	H	Me	Et	3	97
f	H	MeO	Et	2.5	98
g	H	CF_3	Et	2	49
h	H	H	*i*-Pr	2	73
i	H	H	Bu	4	49
j	MeO	Br	Et	2	89

Scheme 38. Synthesis of α-aminophosphonate derivatives of β-carboline (**132**)

α-Acylamino-α-aryl carboxamides (**133**) can be synthesized *via* the Ugi multicomponent reaction, which involves the condensation of four components: an amine, an aldehyde or ketone, an isocyanide, and a carboxylic acid. By varying these starting materials, a wide range of substitution patterns can be achieved. In the present work, β-carboline-based α-acylamino-α-aryl carboxamide derivatives (**133**) were obtained through Ugi condensation of 1-formyl-β-carbolines (**135**), aniline or substituted anilines (**136**), alkyl isocyanides (**138**), and carboxylic acids (**139**). The reactions were performed in methanol at room temperature and afforded the desired products in good yields (Scheme 39) [102].

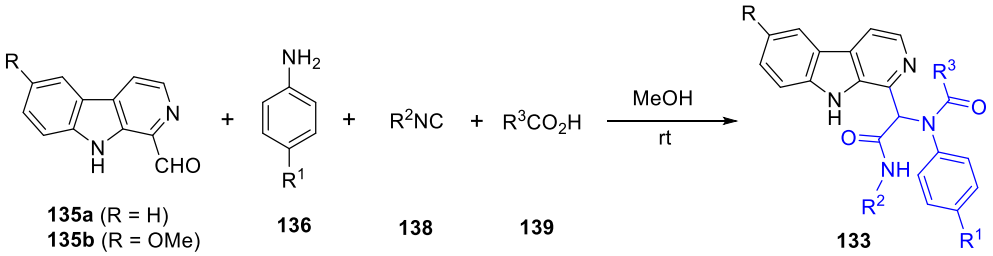

135a (R = H)
135b (R = OMe)

136 **138** **139** **133**

133	R	R^1	R^2	R^3	reaction time (h)	yield (%)
a	H	H	*t*-Bu	Me	24	82
b	H	H	*t*-Bu	*t*-Bu	72	93
c	H	H	*t*-Bu	Ph	48	74
d	H	F	*t*-Bu	Me	48	76
e	H	Cl	*t*-Bu	Me	72	60
f	H	Br	*t*-Bu	Me	48	33
g	H	Me	*t*-Bu	Me	72	90
h	H	MeO	*t*-Bu	Me	48	77
i	H	H	Pn	Me	72	91
j	MeO	H	*t*-Bu	Me	72	80

Scheme 39. Synthesis of α-acylamino-α-aryl carboxamide derivatives of β-carboline (**133**)

The Biginelli reaction is an acid-catalyzed three-component condensation between an aldehyde, a β-ketoester, and urea, leading to the formation of 2-oxo-4-aryl-1,2,3,4-tetrahydropyrimidine-5-carboxylic acid derivatives. In the present work, 2-oxo-1,2,3,4-tetrahydropyrimidine-5-carboxylic acid derivatives bearing a β-carbolin-1-yl substituent at the 4-position (**134**) were synthesized *via* Biginelli reactions by reacting 1-formyl-β-carbolines (**135**) with urea and β-ketoesters (**140**) in various alcohol solvents in the presence of cerium(III) chloride as the catalyst (Scheme 40).

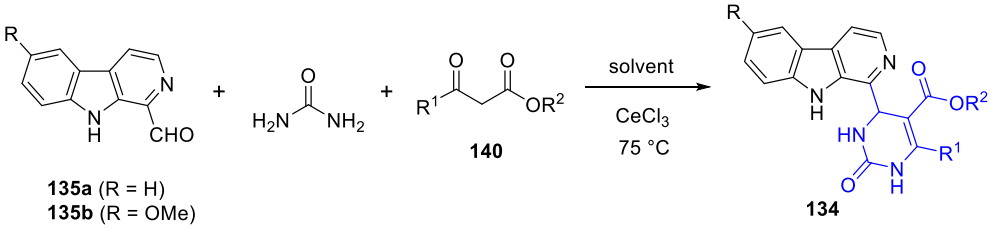

135a (R = H)
135b (R = OMe)

140 **134**

134	R	R^1	R^2	solvent	reaction time (h)	yield (%)
a	H	Me	Me	MeOH	24	59
b	H	Pr	Me	MeOH	24	57
c	H	Ph	Et	EtOH	40	26
d	H	Me	*t*-Bu	*t*-BuOH	24	28
e	H	Me	*i*-Pr	*i*-PrOH	24	82
f	H	Et	Et	EtOH	24	77
g	H	*i*-Pr	Et	EtOH	24	53
h	H	2-Cl-C_6H_4	Me	MeOH	48	35
i	MeO	Me	Me	MeOH	24	33

Scheme 40. Synthesis of 3,4-dihydropyrimidin-2(1*H*)-one derivatives of β-carboline (**134**)

Due to the limitations on dissertation length, only the most promising representatives from each compound class synthesized *via* multicomponent reactions are presented and discussed below. The antiproliferative activities of these compounds were evaluated against two cancer cell lines, HL-60 human promyelocytic leukemia and C6 rat glioma, as well as 3T3 mouse fibroblast cells used as a non-cancerous control to assess selectivity. The HL-60 model represents disseminated hematological malignancies that require systemic pharmacotherapy, while the C6 glioma model serves as a representative for brain tumors, which remain a major therapeutic challenge due to limited efficacy of current treatment options.

Among the compounds tested, Kabachnik–Fields product **132e** exhibited potent activity against HL-60 cells with an IC_{50} of 62.53 nM and demonstrated a 9.0-fold selectivity relative to 3T3 fibroblasts, while showing no measurable activity against C6 glioma cells. Conversely, the Ugi product **133g** showed pronounced cytotoxicity towards C6 cells (IC_{50} = 60.27 nM) with 24.9-fold selectivity and was inactive against HL-60 cells. The Biginelli derivative **134e** displayed dual activity, with IC_{50} values of 136.2 nM on HL-60 cells (14.0-fold selectivity) and 91.83 nM on C6 cells (20.8-fold selectivity). These findings highlight the potential of structurally diverse β-carboline derivatives obtained *via* multicomponent reactions as selective antiproliferative agents with distinct cell-line-specific profiles. Additional *in silico* target docking studies, along with ADME measurements, are currently being conducted.

4.6. Flow synthesis of 1-substituted 3,4-dihydro-β-carbolines

Encouraged by the promising biological results obtained for certain 1-substituted β-carbolines, we next sought to translate batch reactions into continuous-flow processes to enhance efficiency, reproducibility, and scalability. This section presents our efforts towards establishing a robust flow synthesis of 3,4-dihydro-β-carboline intermediates, emphasizing the optimization of reaction parameters and the potential for sustainable production at larger scale.

For the development of a two-step flow synthesis of β-carboline derivatives, harmalan (**68**) was selected as a model compound, starting from tryptamine (**29a**) through T3P® mediated *N*-acetylation to *N*-acetyltryptamine (**67**), followed by Bischler–Napieralski cyclization to yield the corresponding 1-methyl-3,4-dihydro-β-carboline (**68**, Scheme 41).

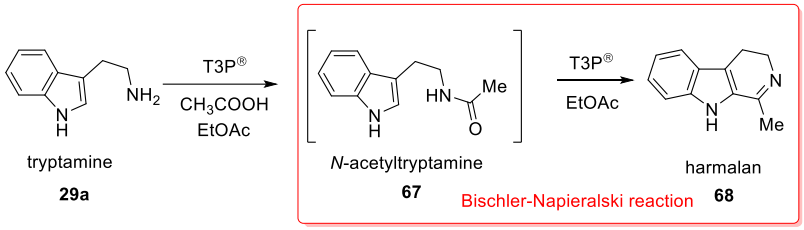

Scheme 41. Synthesis of 1-methyl-3,4-dihydro-β-carboline from tryptamine

Preliminary batch optimization studies were carried out to evaluate the effects of solvent, T3P® excess, temperature, and concentration on reaction efficiency. Initially, DMF was employed as the reaction medium; however, when the reaction time was extended to 1–2 hours, a significant amount of an undesired by-product (**141**) was detected in the mixture and gas formation was observed. The by-product was isolated and characterized, revealing that harmalan (**68**) undergoes overreaction with DMF at elevated temperature in the presence of T3P® (Scheme 42).

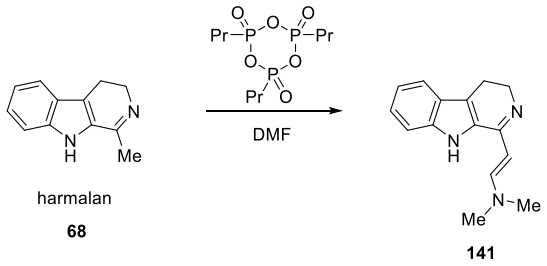

Scheme 42. Unexpected by-product formation from harmalan (**68**)

A solvent mixture of ethyl acetate and acetonitrile was selected after extensive screening, as it provided complete solubility for all reactants and products while eliminating by-product formation observed in DMF. The use of T3P® is advantageous over more aggressive reagents like $POCl_3$ due to its lower toxicity and milder reaction profile. Furthermore, T3P® enables a streamlined process by promoting both the acylation and subsequent cyclization in a single step, while the MeCN/EtOAc solvent system ensures optimal flow compatibility and heat transfer. The model reaction in batch employed tryptamine (**29a**) and a representative carboxylic acid as substrates in a 1:1 ratio, using 2 eq T3P® (50% in EtOAc) as both coupling and cyclization reagent. 0.18 M substrate concentration was needed for full dissolution. The reactions were carried out in the same continuous-flow apparatus described in the Methods section, employing a 5-mL stainless steel coil reactor equipped with a back-pressure regulator (20 bar) to permit operation at 200 °C (Figure 13). Both consecutive reaction steps were performed within

the same coil, immersed in an oil bath and magnetically stirred to ensure uniform temperature distribution.

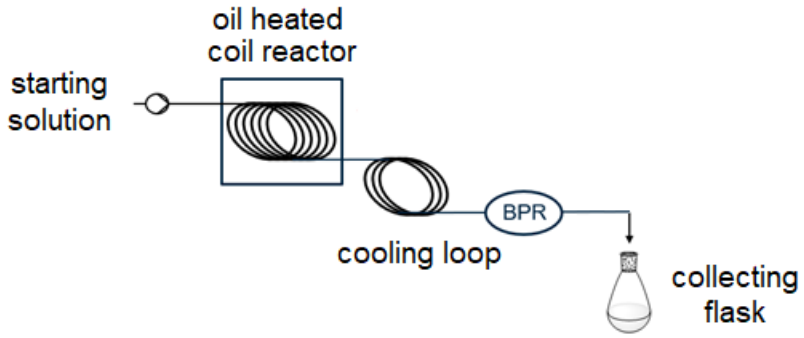

Figure 13. Continuous-flow setup for two-step synthesis of 3,4-dihydro-β-carbolines

The best performance was achieved for the model compound harmalan (**68**) under the following conditions: 200 °C, 20 bar, and a residence time of 4 minutes giving 90% yield (Figure 14). The continuous-flow process demonstrated excellent reproducibility, with consistent yields across multiple runs and no need for chromatographic purification. In most cases of scope expansion, the products could be isolated in high yields by simple solvent evaporation, with only occasional chromatography required when small amounts of intermediates remained (Figure 14).

Compared to the model compound, we extended the reaction by enabling functionalization at both the 1- and 6-positions, thereby broadening the structural diversity and expanding the reaction scope. In some cases (compounds **143**, **145**, **146**), additional MeCN was needed for complete dissolution of the substrates, which can be observed on the concentration data. The high pressure and temperature conditions employed here would be challenging and potentially hazardous in batch mode, but are readily and safely achieved under continuous-flow conditions, illustrating one of the key advantages of the technique.

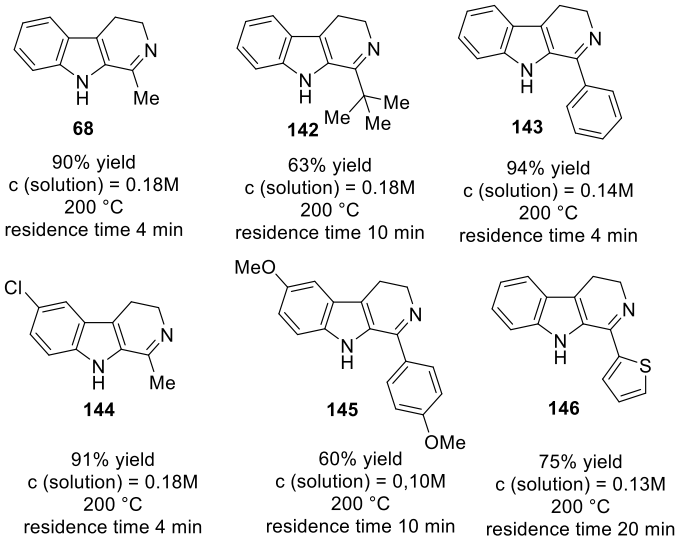

Figure 14. 3,4-dihydro-β-carbolines prepared with flow system

Overall, this work represents the first reported flow synthesis of 3,4-dihydro-β-carbolines starting from tryptamines, providing a reproducible and scalable method with significantly reduced reaction time, simplified workup, and enhanced process safety. The modularity of the approach also allows facile structural diversification by varying the amine or acid components, thereby offering a versatile platform for the rapid generation of β-carboline analogues with potential pharmacological relevance.

4.7. Computational study on the Robinson–Gabriel synthesis and Bischler–Napieralski reaction

To complement the experimental observations obtained from both batch and flow reactions, computational investigations were undertaken to elucidate the mechanistic features governing the key cyclization steps. In particular, DFT calculations were applied to compare the energetics of the Robinson–Gabriel and Bischler–Napieralski reactions, thereby providing theoretical insights that rationalize the distinct outcomes observed in our synthetic studies. The results of these computational analyses are discussed in this section.

To gain insight into the mechanisms of the Robinson–Gabriel and Bischler–Napieralski reactions (for the experimentally found reactions of **64** and **67** with T3P® reagent see Scheme 20 in the Introduction section), DFT calculations were performed using two model substrates, *N*-acetyl-β-oxotryptamine (**64,** Scheme 43) and *N*-acetyltryptamine (**67**, Scheme 44). The computational analysis aimed to rationalize the observed formation of the oxazole product (**66,** Scheme 43) *via* the Robinson–Gabriel

pathway and the absence of the corresponding 3,4-dihydro-β-carboline-4-one (**68**, harmalan, Scheme 44) in the Bischler–Napieralski route.

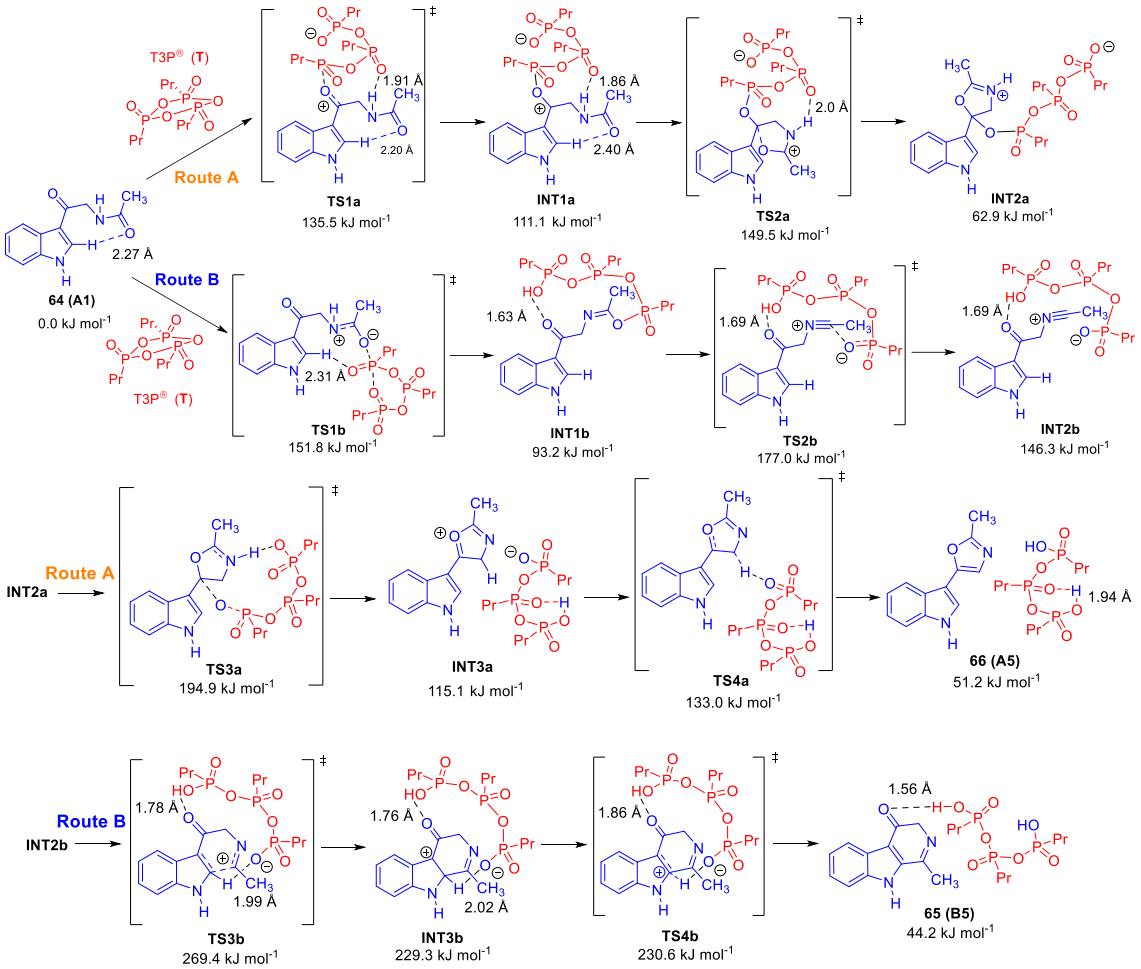

Scheme 43. DFT mapped mechanisms of the Robinson–Gabriel and Bischler–Napieralski reactions from *N*-acetyl-β-oxotryptamine (**64**)

Both mechanisms begin with activation of the amide by T3P®, leading to phosphorus–oxygen adducts. For the β-oxotryptamine model, the carbonyl oxygen proved more reactive than the amide oxygen, favoring the Robinson–Gabriel pathway. Comparison of the calculated activation barriers indicated that the cyclization step forming the oxazole intermediate required substantially less energy than the corresponding step in the Bischler–Napieralski route, which involves nitrilium ion attack on the indole ring.

The overall energy profile revealed that the rate-determining step in the proposed but experimentally unobserved Bischler–Napieralski pathway (TS3b, 269 kJ mol^{-1}) was considerably higher than that of the feasible Robinson–Gabriel cyclization (TS3a, 195 kJ mol^{-1}), explaining why only the latter occurs under the applied conditions. The computed intermediate energies further confirmed that the oxazole ring formation (TS3a) is

exothermic (formation of intermediate INT2a compared to INT1a) and thermodynamically more favorable than β-carboline formation (TS3b).

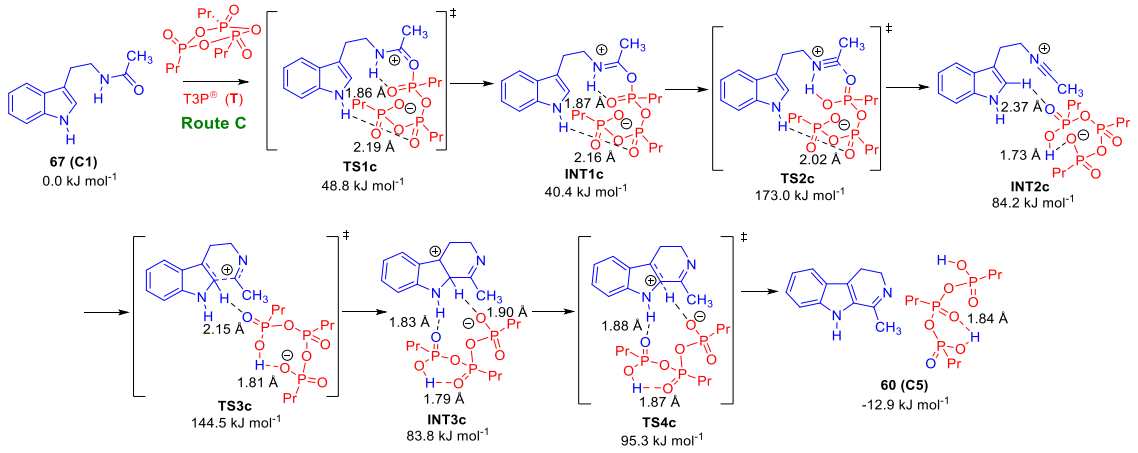

Scheme 44. DFT mapped mechanisms of the Bischler–Napieralski reactions from *N*-acetyltryptamine (**67**)

To evaluate the influence of the carbonyl substituent, the Bischler–Napieralski reaction of *N*-acetyltryptamine (**67**) was also modeled. In this case, the absence of the electron-withdrawing keto group significantly lowered the activation barrier of the cyclization step (144 kJ mol^{-1}), confirming that the carbonyl group in β-oxotryptamine deactivates the indole ring towards electrophilic attack in the Bischler–Napieralski pathway.

The combined energy profiles (Figure 15) clearly demonstrate that the Robinson–Gabriel reaction proceeds *via* a kinetically and thermodynamically more favorable route, while the Bischler–Napieralski pathway of *N*-acetyl-β-oxotryptamine (**64**) is hindered by prohibitively high activation energies, rendering product formation experimentally unfeasible (A6, B6 and C6 are the final products in their lowest energy conformer form without any interactions between them).

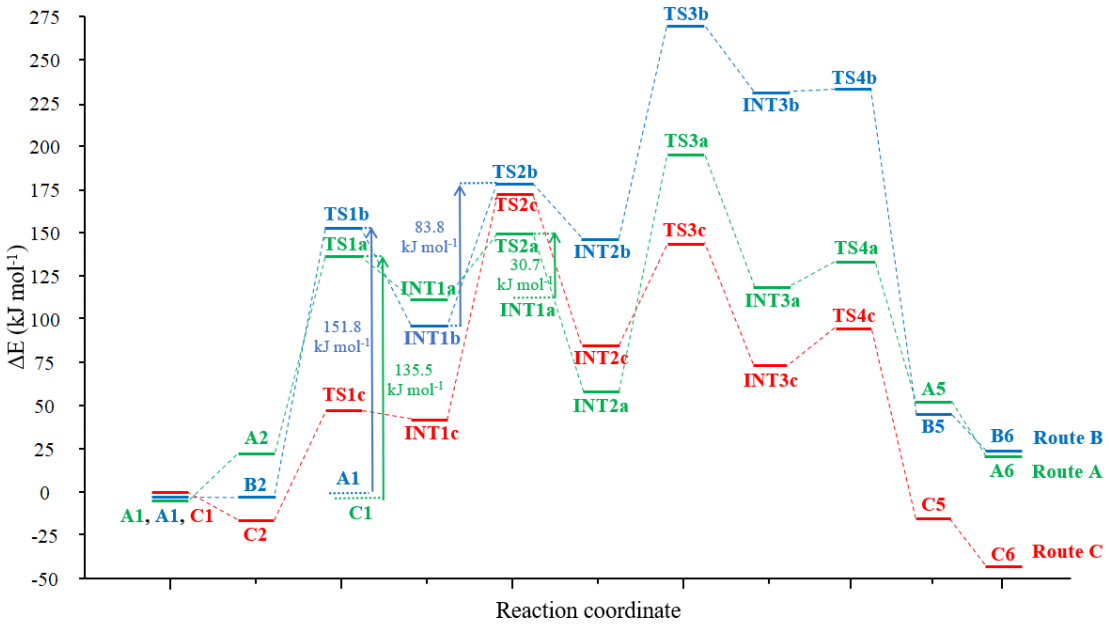

Figure 15. Summarizing diagram for the energetics of the Robinson–Gabriel synthesis (Route A: A1 to A6, green) and Bischler–Napieralski reactions (Route B: A1 to B6, blue and Route C: C1 to C6, red)

To compare the kinetics of the two experimentally feasible reactions, time-resolved HPLC-MS measurements were performed under identical conditions (120°C) to monitor the consumption of *N*-acetyl-β-oxotryptamine (**64**) and *N*-acetyltryptamine (**67**) and the formation of the corresponding Robinson–Gabriel and Bischler–Napieralski products. The Robinson–Gabriel reaction reached 50% conversion after approximately 20 minutes and was complete within 100 minutes, while the Bischler–Napieralski cyclization exhibited a similar profile with a $t_{1/2}$ of 16 minutes and full conversion after about 90 minutes. These comparable reaction rates are consistent with the similar activation barriers calculated for the rate-determining steps (Robinson–Gabriel reaction: TS3a 195 kJ mol^{-1} and Bischler–Napieralski cyclization: TS2c 173 kJ mol^{-1}). While the calculated activation energies appear higher than typically expected for a reaction occurring at 120 °C, it should be noted that such values often reflect the tendency of DFT methods to overestimate activation barriers. Therefore, these results are primarily intended to provide a comparative analysis of energetic trends and mechanistic pathways.

The computational and experimental results are in good agreement, indicating that the electron-withdrawing effect of the keto group in *N*-acetyl-β-oxotryptamine (**64**) alters the charge distribution in the nitrilium intermediate, thereby disfavoring β-carboline ring formation under the applied conditions.

5. DISCUSSION

5.1. Experimental section of compounds

General procedure for the preparation of α-aminophosphonate derivatives of β-carboline (132a–j). The appropriate β-carboline aldehyde (**135a** or **135b**, 0.5 mmol), aniline derivative (**136**, 0.5 mmol), phosphite (**137**, 0.5 mmol) and $Mg(ClO_4)_2$ (10 mol%, 0.05 mmol) were stirred in neat at 80 °C for 2−4 hours (for reaction times, see Scheme 38). After the reaction was complete (or when no more progress was observed in the reaction), the residue was dissolved in a DCM–MeOH 1:1 mixture and it was purified by flash column chromatography on silica gel (DCM–MeOH) to afford pure α-aminophosphonates **132a–j** (for yields, see Scheme 38).

Diethyl [9*H*-β-carbolin-1-yl(phenylamino)methyl]phosphonate (132a). Colourless crystals. Mp 173–175 °C (MeCN) IR (KBr): 3216, 3172, 1601, 1237, 1050, 1020, 971, 752, 742 cm^{-1}. ^1H NMR ($CDCl_3$, 600 MHz): δ 10.25 (br s, 1H), 8.43 (d, J = 5.2 Hz, 1H), 7.97 (m, 1H), 7.87 (dd, J_1 = 1.2 Hz, J_2 = 5.1 Hz, 1H), 7.32 (m, 1H), 7.15 (m, 1H), 7.14 (m, 1H), 7.11 (m, 2H), 6.85 (m, 2H), 6.69 (m, 1H), 5.84 (t, J = 7.3 Hz, 1H), 5.48 (dd, J_1 = 7.0 Hz, J_2 = 20.9 Hz, 1H), 4.17 (m, 1H), 4.12 (m, 1H), 4.07 (m, 1H), 3.96 (m, 1H), 1.26 (t, J = 7.0 Hz, 3H), 1.12 (t, J = 7.0 Hz, 3H) ppm. ^{13}C NMR ($CDCl_3$, 150 MHz): δ 146.9, 140.8, 138.3, 138.1, 134.4, 130.2, 129.1, 128.2, 121.2, 119.7, 118.7, 114.5, 114.2, 111.9, 64.0, 58.1, 57.1, 16.4, 16.2 ppm. ^{31}P NMR ($CDCl_3$, 162 MHz): δ 22.4 ppm. HRMS (ESI) calcd. for $C_{22}H_{25}N_3O_3P^+$ $[M+H]^+$ 410.1628; found: 410.1625.

Diethyl {9*H*-β-carbolin-1-yl[(4-fluorophenyl)amino]methyl}phosphonate (132b). Colourless crystals. Mp 191–193 °C (MeCN) IR (KBr): 3217, 1506, 1237, 1053, 1019, 968, 742 cm^{-1}. ^1H NMR ($CDCl_3$, 400 MHz): δ 10.20 (br s, 1H), 8.43 (d, J = 5.2 Hz, 1H), 8.00 (m, 1H), 7.88 (dd, J_1 = 1.7 Hz, J_2 = 5.2 Hz, 1H), 7.37 (m, 1H), 7.23 (m, 1H), 7.17 (m, 1H), 6.81 (m, 2H), 6.77 (m, 2H), 5.69 (t, J = 7.1 Hz, 1H), 5.38 (dd, J_1 = 7.1 Hz, J_2 = 20.7 Hz, 1H), 4.13 (m, 1H), 4.08 (m, 1H), 4.08 (m, 1H), 3.96 (m, 1H), 1.25 (t, J = 7.1 Hz, 3H), 1.12 (t, J = 7.1 Hz, 3H) ppm. ^{13}C NMR ($CDCl_3$, 100 MHz): δ 156.5, 143.2, 140.9, 138.1, 134.4, 130.3, 128.4, 121.4, 121.3, 119.9, 115.6, 115.3, 114.6, 112.0, 64.0, 64.0, 58.3, 16.4, 16.2 ppm. ^{31}P NMR ($CDCl_3$, 162 MHz): δ 22.3 ppm. HRMS (ESI) calcd. for $C_{22}H_{24}FN_3O_3P^+$ $[M+H]^+$ 428.1534; found: 428.1538.

Diethyl {9*H*-β-carbolin-1-yl[(4-chlorophenyl)amino]methyl}phosphonate (132c). Yellow crystals. Mp 188–190 °C (DIPE) IR (KBr): 3455, 3220, 2994, 1625, 1599, 1491, 1325, 1236, 1201, 1051, 1020, 965 cm^{-1}. ^1H NMR (DMSO-d_6, 600 MHz): δ 11.71 (s,

1H), 8.34 (d, J = 5.2 Hz, 1H), 8.23 (d, J = 7.9 Hz, 1H), 8.07 (d, J = 4.8 Hz, 1H), 7.66 (d, J = 8.2 Hz, 1H), 7.58 (t, J = 7.6 Hz, 1H), 7.26 (t, J =7.4 Hz, 1H), 7.06 (d, J = 8.9 Hz, 2H), 6.88 (d, J = 8.9 Hz, 2H), 6.53 (dd, J_1 = 10.0 Hz, J_2 = 4.6 Hz, 1H), 5.69 (dd, J_1 = 23.0 Hz, J_2 =10.0 Hz, 1H), 4.04 (m, 2H), 3.89 (m, 1H), 3.70 (m, 1H), 1.17 (t, J = 7.0 Hz, 3H), 0.91 (t, J = 7.0 Hz, 3H) ppm. ^{13}C NMR (DMSO-d_6, 150 MHz): δ 146.4, 140.6, 139.5, 137.8, 134.2, 128.7, 128.6, 128.4, 122.1, 120.8, 120.7, 119.7, 115.1, 114.5, 112.0, 62.9, 62.6, 54.0, 16.5, 16.2 ppm. ^{31}P NMR (DMSO-d_6, 242 MHz): δ 21.2 ppm. HRMS (ESI) calcd. for $C_{22}H_{23}ClN_3O_3P^+$ $[M]^+$ 443.1166; found: 443.1171.

Diethyl {[(4-bromophenyl)amino](9*H*-β-carbolin-1-yl)methyl}phosphonate (132d). Colourless crystals. Mp 197–200 °C (MeCN) IR (KBr): 3335, 3241, 2982, 1594, 1503, 1216, 1060, 1028, 968, 812, 738 cm^{-1}. ^{1}H NMR ($CDCl_3$, 600 MHz): δ 10.32 (br s, 1H), 8.43 (d, J = 4.8 Hz, 1H), 7.96 (d, J = 7.8 Hz, 1H), 7.88 (d, J = 4.8 Hz, 1H), 7.32 (m, 1H), 7.17 (m, 1H), 7.13 (m, 1H), 7.11 (m, 1H), 6.73 (d, J = 9.0 Hz, 2H) 5.99 (br s, 1H), 5.48 (d, J = 19.8 Hz, 1H), 4.15 (m, 3H), 3.99 (m, 1H), 2.26 (br s, 1H), 1.26 (t, J = 7.2 Hz, 3H), 1.14 (t, J = 7.2 Hz, 3H) ppm. ^{13}C NMR ($CDCl_3$, 150 MHz): δ 145.8, 141.0, 137.6, 134.2, 131.8, 128.5, 121.3, 121.1, 119.9, 115.7, 114.7, 111.8, 110.4, 64.2, 57.6, 56.6, 16.4, 16.2 ppm. ^{31}P NMR ($CDCl_3$, 242 MHz): δ 21.7 ppm. HRMS (ESI) calcd. for $C_{22}H_{24}BrN_3O_3P^+$ $[M+H]^+$ 488.0733; found: 488.0736.

Diethyl {9*H*-β-carbolin-1-yl[(4-methylphenyl)amino]methyl}phosphonate (132e). Colourless crystals. Mp 138–140 °C (MeCN) IR (KBr): 3354, 3220, 2981, 1614, 1518, 1215, 1059, 1029, 965, 812, 740 cm^{-1}. ^{1}H NMR ($CDCl_3$, 600 MHz): δ 10.15 (br s, 1H), 8.43 (d, J = 4.8 Hz, 1H), 8.00 (d, J = 7.2 Hz, 1H), 7.87 (d, J_1 = 4.2 Hz, 1H), 7.39 (m, 1H), 7.26 (m, 1H), 7.16 (m, 1H), 6.91 (d, J = 7.8 Hz, 2H), 6.75 (d, J = 8.4 Hz, 2H), 5.58 (s, 1H), 5.40 (d, J = 20.4 Hz, 1H), 4.11 (m, 3H), 3.92 (m, 1H), 2.16 (s, 3H), 1.25 (t, J = 7.2 Hz, 3H), 1.10 (t, J = 6.6 Hz, 3H) ppm. ^{13}C NMR ($CDCl_3$, 150 MHz): δ 144.6, 140.9, 138.5, 138.1, 134.4, 130.2, 128.3, 128.1, 121.3, 119.8, 114.4, 112.0, 63.9, 58.7, 57.7, 20.3, 16.4, 16.2 ppm. ^{31}P NMR ($CDCl_3$, 242 MHz): δ 22.5 ppm. HRMS (ESI) calcd. for $C_{23}H_{27}N_3O_3P^+$ $[M+H]^+$ 424.1785; found: 424.1789.

Diethyl {9*H*-β-carbolin-1-yl[(4-methoxyphenyl)amino]methyl}phosphonate (132f). Colourless crystals. Mp 162–165 °C (MeCN) IR (KBr): 3208, 3096, 1625, 1512, 1236, 1033, 960, 828, 748 cm^{-1}. ^{1}H NMR ($CDCl_3$, 600 MHz): δ 10.19 (br s, 1H), 8.43 (d, J = 4.8 Hz, 1H), 8.00 (d, J = 7.8 Hz, 1H), 7.87 (m, 1H), 7.38 (m, 1H), 7.27 (m, 1H), 7.17 (m, 1H), 6.78 (m, 2H), 6.68 (m, 2H), 5.44 (br s, 1H), 5.37 (d, J = 21.0 Hz, 1H), 4.16 (m, 2H),

4.11 (m, 1H), 3.93 (m, 1H), 3.66 (s, 3H), 1.26 (t, J = 7.2 Hz, 3H), 1.11 (t, J = 7.2 Hz, 3H) ppm. ^{13}C NMR ($CDCl_3$, 150 MHz): δ 152.9, 140.9, 138.6, 138.1, 134.4, 130.2, 128.3, 121.3, 119.8, 115.7, 114.6, 114.4, 112.0, 63.9, 59.4, 58.3, 55.6, 16.4, 16.2 ppm. ^{31}P NMR ($CDCl_3$, 242 MHz): δ 22.5 ppm. HRMS (ESI) calcd. for $C_{23}H_{27}N_3O_4P^+$ $[M+H]^+$ 440.1734; found: 440.1737.

Diethyl (9*H*-β-carbolin-1-yl{[4-(trifluoromethyl)phenyl]amino}methyl)phosphonate (132g). Brown crystals. Mp 204–206 °C (DIPE) IR (KBr): 3425, 3252, 1616, 1535, 1433, 1326, 1108, 1059, 825 cm^{-1}. ^{1}H NMR (DMSO-d_6, 600 MHz): δ 11.75 (br s, 1H), 8.36 (d, J = 5.2 Hz, 1H), 8.25 (m, 1H), 8.09 (d, J = 5.0 Hz, 1H), 7.68 (m, 1H), 7.59 (m, 1H), 7.37 (d, J = 8.6 Hz, 2H), 7.27 (m, 1H), 7.07 (dd, J_1 = 4.2 Hz, J_2 = 9.6 Hz, 1H), 7.03 (d, J = 8.6 Hz, 1H), 5.83 (dd, J_1 = 9.6 Hz, J_2 = 22.6 Hz, 1H), 4.04 (m, 2H), 3.90 (m, 1H), 3.74 (m, 1H), 1.16 (t, J = 7.0 Hz, 3H), 0.92 (t, J = 7.0 Hz, 3H) ppm. ^{13}C NMR (DMSO-d_6, 150 MHz): δ 150.7, 140.6, 139.1, 137.8, 134.1, 128.7, 128.5, 126.3, 125.3, 122.1, 120.7, 119.7, 117.1, 114.6, 113.0, 112.1, 62.9, 62.7, 53.4, 16.5, 16.2 ppm. ^{31}P NMR (DMSO-d_6, 242 MHz): δ 20.8 ppm. HRMS (ESI) calcd. for $C_{23}H_{23}F_3N_3O_3P^+$ $[M]^+$ 477.1429; found: 477.1418.

Bis(1-methylethyl) [9*H*-β-carbolin-1-yl(phenylamino)methyl]phosphonate (132h). Colourless crystals. Mp 210–213 °C (DIPE) IR (KBr): 3333, 3217, 3174, 1603, 1503, 1214, 1018, 999, 748 cm^{-1}. ^{1}H NMR (DMSO-d_6, 600 MHz): δ 11.69 (br s, 1H), 8.32 (d, J = 5.2 Hz, 1H), 8.22 (m, 1H), 8.04 (d, J = 5.1 Hz, 1H), 7.66 (m, 1H), 7.57 (m, 1H), 7.24 (m, 1H), 7.01 (m, 2H), 6.85 (m, 2H), 6.53 (m, 1H), 6.19 (dd, J_1 = 5.0 Hz, J_2 = 10.2 Hz, 1H), 5.59 (dd, J_1 = 10.3 Hz, J_2 = 23.9 Hz, 1H), 4.66 (m, 1H), 4.28 (m, 1H), 1.24 (d, J = 6.2 Hz, 3H), 1.20 (d, J = 6.2 Hz, 3H), 1.09 (d, J = 6.1 Hz, 3H), 0.62 (d, J = 6.1 Hz, 3H) ppm. ^{13}C NMR (DMSO-d_6, 150 MHz): δ 147.5, 140.5, 140.2, 137.6, 134.2, 129.0, 128.5, 128.2, 122.0, 120.6, 119.6, 117.5, 114.3, 113.7, 112.0, 71.4, 71.2, 54.6, 24.2, 24.1, 23.7, 23.0 ppm. ^{31}P NMR (DMSO-d_6, 242 MHz): δ 10.9 ppm. HRMS (ESI) calcd. for $C_{24}H_{29}N_3O_3P^+$ $[M+H]^+$ 438.1947; found: 438.1942.

Dibutyl [9*H*-β-carbolin-1-yl(phenylamino)methyl]phosphonate (132i). Yellow oil. IR (KBr): 3220, 3170, 1602, 1502, 1247, 1212, 1063, 1029, 995, 743 cm^{-1}. ^{1}H NMR (DMSO-d_6, 600 MHz): δ 11.73 (br s, 1H), 8.32 (d, J = 5.2 Hz, 1H), 8.22 (m, 1H), 8.05 (dd, J_1 = 1.2 Hz, J_2 = 5.2 Hz, 1H), 7.65 (m, 1H), 7.57 (m, 1H), 7.25 (m, 1H), 7.02 (m, 2H), 6.86 (m, 2H), 6.54 (m, 1H), 6.23 (dd, J_1 = 4.6 Hz, J_2 = 10.1 Hz, 1H), 5.70 (dd, J_1 = 10.1 Hz, J_2 = 23.1 Hz, 1H), 3.98 (m, 2H), 3.82 (m, 1H), 3.61 (m, 1H), 1.50 (m, 2H), 1.23

(m, 2H), 1.20 (m, 2H), 0.98 (m, 2H), 0.77 (t, J = 7.4 Hz, 3H), 0.59 (t, J = 7.4 Hz, 3H) ppm. ^{13}C NMR (DMSO-d_6, 150 MHz): δ 147.4, 140.6, 139.9, 137.7, 134.2, 129.0, 128.5, 128.3, 122.0, 120.7, 119.6, 117.6, 114.4, 113.7, 112.0, 66.4, 66.0, 54.0, 32.2, 31.9, 18.3, 18.1, 13.6, 13.4 ppm. ^{31}P NMR (DMSO-d_6, 242 MHz): δ 21.5 ppm. HRMS (ESI) calcd. for $C_{26}H_{32}N_3O_3P^+$ $[M]^+$ 465.2191; found: 465.2194.

Diethyl {[(4-bromophenyl)amino](6-methoxy-9*H*-β-carbolin-1-yl)methyl}phosphonate (132j). Yellow crystals. Mp 220–223 °C (MeCN) IR (KBr): 3279, 2965, 1672, 1225, 1069, 1013, 967, 746, 576 cm^{-1}. ^{1}H NMR ($CDCl_3$, 600 MHz): δ 10.13 (br s, 1H), 8.39 (d, J = 5.4 Hz, 1H), 7.83 (m, 1H), 7.39 (m, 1H), 7.18 (m, 2H), 6.99 (m, 2H), 6.72 (d, J =9.0 Hz, 2H), 5.96 (br s, 1H), 5.42 (dd, J_1 = 6.0 Hz, J_2 = 27.0 Hz, 1H), 4.14 (m, 3H), 4.08 (m, 1H), 3.88 (s, 3H), 1.25 (t, J = 6.6 Hz, 3H), 1.14 (t, J = 7.2 Hz, 3H) ppm. ^{13}C NMR ($CDCl_3$, 150 MHz): δ 154.0, 145.8, 137.7, 137.4, 135.9, 134.9, 131.8, 130.2, 121.5, 118.6, 115.7, 114.6, 112.7, 110.4, 102.9, 64.1, 64.1, 61.8, 57.6, 56.6, 55.9, 16.4, 16.2 ppm. ^{31}P NMR ($CDCl_3$, 242 MHz): δ 21.5 ppm. HRMS (ESI) calcd. for $C_{23}H_{26}BrN_3O_4P^+$ $[M+H]^+$ 518.0839; found: 518.0841.

General procedure for the preparation of α-acylamino-α-aryl carboxamide derivatives of β-carboline (133a–j). The appropriate β-carboline aldehyde (**135a** or **135b**, 0.250 mmol), aniline derivative (**136**, 0.275 mmol), alkyl isocyanide (**138**, 0.275 mmol) and carboxylic acid (**139**, 0.275 mmol) were stirred in MeOH (2 mL) at room temperature for 24−72 hours (for reaction times, see Scheme 39). After the reaction was complete (or when no more progress was observed in the reaction), water was added, it was extracted with EtOAc and washed with brine. The organic layer was dried over Na_2SO_4 and purified by flash column chromatography on silica gel (DCM–MeOH) to afford pure α-acylamino-α-aryl carboxamides **133a–j** (for yields, see Scheme 39).

2-[Acetyl(phenyl)amino]-*N*-*tert*-butyl-2-(9*H*-β-carbolin-1-yl)acetamide (133a). Colourless crystals. Mp 205–207 °C (hexane). IR (KBr): 3369, 3249, 3057, 1675, 1656, 1495, 1375, 1083, 749, 700 cm^{-1}. ^{1}H NMR ($CDCl_3$, 600 MHz): δ 10.26 (br s, 1H), 9.68 (br s, 1H), 8.20 (d, J = 5.4 Hz, 1H), 8.12 (d, J = 7.8 Hz, 1H), 7.94 (d, J = 4.8 Hz, 1H), 7.62 (m, 1H), 7.59 (m, 1H), 7.31 (m, 1H), 7.26 (m, 1H), 7.20 (m, 2H), 7.20 (br s, 2H), 7.00 (s, 1H), 1.88 (s, 3H), 1.28 (s, 9H) ppm. ^{13}C NMR ($CDCl_3$, 150 MHz): δ 172.7, 165.9, 140.4, 139.6, 138.9, 136.1, 135.2, 129.6, 128.9, 128.8, 128.7, 121.5, 121.3, 120.1, 114.7, 112.4, 58.5, 51.1, 28.4, 22.7 ppm. HRMS (ESI) calcd. for $C_{25}H_{27}N_4O_2^+$ $[M+H]^+$ 415.2129; found: 415.2134.

***N*-[2-(*tert*-Butylamino)-1-(9*H*-β-carbolin-1-yl)-2-oxoethyl]-2,2-dimethyl-*N*-phenyl-propanamide (133b).** Yellow crystals. Mp 76–78 °C (hexane). IR (KBr): 3310, 1670, 1621, 1591, 1495, 1364, 1198, 745, 703 cm^{-1}. ^1H NMR ($CDCl_3$, 600 MHz): δ 10.24 (br s, 1H), 9.53 (br s, 1H), 8.13 (d, J = 5.1 Hz, 1H), 8.12 (m, 1H), 7.88 (d, J = 5.2 Hz, 1H), 7.63 (br s, 1H), 7.61 (m, 1H), 7.58 (m, 1H), 7.30 (m, 1H), 7.29 (br s, 1H), 7.18 (m, 1H), 7.09 (s, 1H), 6.83 (br s, 1H), 5.86 (br s, 1H), 1.34 (s, 9H), 1.02 (s, 9H) ppm. ^{13}C NMR ($CDCl_3$, 150 MHz): δ 180.0, 166.9, 140.3, 139.7, 138.8, 136.0, 135.3, 131.5, 130.8, 129.3, 128.7, 128.6, 128.4, 127.6, 121.5, 121.2, 120.0, 114.6, 112.2, 61.1, 51.2, 41.6, 29.6, 28.5, 27.1 ppm. HRMS (ESI) calcd. for $C_{28}H_{32}N_4O_2^+$ $[M]^+$ 456.2520; found: 456.2532.

***N*-[2-(*tert*-Butylamino)-1-(9*H*-β-carbolin-1-yl)-2-oxoethyl]-*N*-phenylbenzamide (133c).** Colourless crystals. Mp 121–123 °C (hexane). IR (KBr): 3272, 3055, 1673, 1619, 1555, 1493, 1369, 1078, 694 cm^{-1}. ^1H NMR ($CDCl_3$, 600 MHz): δ 10.34 (br s, 1H), 9.67 (br s, 1H), 8.24 (d, J = 5.2 Hz, 1H), 8.13 (m, 1H), 7.94 (d, J = 5.2 Hz, 1H), 7.64 (m, 1H), 7.59 (m, 1H), 7.31 (m, 1H), 7.28 (m, 2H), 7.18 (s, 1H), 7.17 (m, 1H), 7.09 (m, 2H), 7.03 (m, 1H), 6.98 (m, 2H), 6.74 (br s, 2H), 1.31 (s, 9H) ppm. ^{13}C NMR ($CDCl_3$, 150 MHz): δ 172.8, 166.1, 140.5, 139.5, 139.5, 136.4, 135.4, 135.2, 129.9, 129.8, 129.7, 128.8, 128.5, 128.3, 127.7, 127.6, 121.5, 121.3, 120.1, 114.9, 112.4, 59.8, 51.2, 31.6, 28.4, 22.6, 14.1 ppm. HRMS (ESI) calcd. for $C_{30}H_{28}N_4O_2^+$ $[M]^+$ 476.2207; found: 476.2217.

2-[Acetyl(4-fluorophenyl)amino]-*N*-*tert*-butyl-2-(9*H*-β-carbolin-1-yl)acetamide (133d). Yellow crystals. Mp 104–106 °C (hexane). IR (KBr): 3248, 2968, 1647, 1507, 1387, 1217, 1124, 727 cm^{-1}. ^1H NMR ($CDCl_3$, 600 MHz): δ 10.26 (br s, 1H), 9.6 (br s, 1H), 8.21 (d, J = 5.4 Hz, 1H), 8.13 (d, J = 7.8 Hz, 1H), 7.96 (d, J = 4.8 Hz, 1H), 7.61 (m, 2H), 7.31 (m, 1H), 6.99 (s, 1H), 6.89 (br s, 1H), 1.88 (s, 3H), 1.29 (s, 9H) ppm. ^{13}C NMR ($CDCl_3$, 150 MHz): δ 209.8, 208.5, 172.7, 165.9, 163.2, 161.5, 140.7, 138.9, 135.6, 135.1, 134.9, 131.5, 130.2, 129.2, 121.6, 121.1, 120.4, 115.9, 115.0, 112.4, 58.8, 51.3, 42.8, 32.5, 30.0, 28.4, 25.2, 22.7, 18.8 ppm. HRMS (ESI) calcd. for $C_{25}H_{26}FN_4O_2^+$ $[M+H]^+$ 433.2034; found: 433.2041.

2-[Acetyl(4-chlorophenyl)amino]-*N*-*tert*-butyl-2-(9*H*-β-carbolin-1-yl)acetamide (133e). Yellow crystals. Mp 198–200 °C (hexane). IR (KBr): 3283, 2975, 1668, 1556, 1486, 1379, 1303, 1224, 1079, 752 cm^{-1}. ^1H NMR ($CDCl_3$, 600 MHz): δ 10.17 (br s, 1H), 9.66 (br s, 1H), 8.21 (d, J = 5.4 Hz, 1H), 8.13 (d, J = 7.8 Hz, 1H), 7.95 (d, J = 4.8 Hz, 1H), 7.61 (m, 2H), 7.31 (m, 1H), 7.18 (br s, 2H), 6.99 (s, 1H), 1.88 (s, 3H), 1.30 (s, 9H) ppm. ^{13}C NMR ($CDCl_3$, 150 MHz): δ 172.5, 165.7, 140.4, 139.3, 137.4, 136.2, 135.2,

134.7, 131.1, 129.8, 129.2, 128.9, 121.4, 120.2, 114.9, 112.4, 58.3, 51.2, 28.4, 22.7 ppm. HRMS (ESI) calcd. for $C_{25}H_{26}ClN_4O_2^+$ $[M]^+$ 449.1739; found: 449.1738.

2-[Acetyl(4-bromophenyl)amino]-*N*-*tert*-butyl-2-(9*H*-β-carbolin-1-yl)acetamide (133f). Yellow crystals. Mp 212–214 °C (hexane). IR (KBr): 3177, 3098, 1593, 1503, 1291, 1251, 1201, 1042, 971, 789 cm^{-1}. ^1H NMR ($CDCl_3$, 600 MHz): δ 10.16 (br s, 1H), 9.67 (br s, 1H), 8.21 (d, J = 4.8 Hz, 1H), 8.13 (d, J = 7.8 Hz, 1H), 7.95 (d, J = 5.4 Hz, 1H), 7.61 (m, 2H), 7.33 (m, 3H), 6.99 (s, 1H), 1.88 (s, 3H), 1.72 (s, 1H), 1.30 (s, 9H) ppm. ^{13}C NMR ($CDCl_3$, 150 MHz): δ 172.4, 165.7, 140.4, 139.3, 138.0, 136.3, 135.2, 132.3, 131.4, 129.8, 128.9, 122.9, 121.5, 121.3, 120.2, 114.9, 112.4, 58.2, 51.2, 28.4, 22.7 ppm. HRMS (ESI) calcd. for $C_{25}H_{26}BrN_4O_2^+$ $[M+H]^+$ 493.1234; found: 493.1233.

2-[Acetyl(4-methylphenyl)amino]-*N*-*tert*-butyl-2-(9*H*-β-carbolin-1-yl)acetamide (133g). Yellow crystals. Mp 218–220 °C (hexane). IR (film): 3290, 2967, 1646, 1561, 1388, 1226, 909, 730 cm^{-1}. ^1H NMR ($CDCl_3$, 600 MHz): δ 10.27 (br s, 1H), 9.71 (br s, 1H), 8.20 (d, J = 4.8 Hz, 1H), 8.13 (d, J = 7.8 Hz, 1H), 7.93 (d, J = 5.4 Hz, 1H), 7.62 (m, 1H), 7.58 (m, 1H), 7.30 (m, 1H), 7.00 (s, 1H), 6.98 (br s, 1H), 2.29 (s, 3H), 1.87 (s, 3H), 1.30 (s, 9H) ppm. ^{13}C NMR ($CDCl_3$, 150 MHz): δ 172.9, 166.0, 140.4, 139.7, 138.6, 136.2, 136.1, 135.2, 129.6, 129.2, 128.7, 121.5, 121.3, 114.7, 112.4, 58.3, 51.1, 28.4, 22.6, 21.1 ppm. HRMS (ESI) calcd. for $C_{26}H_{29}N_4O_2^+$ $[M+H]^+$ 429.2285; found: 429.2290.

2-[Acetyl(4-methoxyphenyl)amino]-*N*-*tert*-butyl-2-(9*H*-β-carbolin-1-yl)acetamide (133h). Yellow crystals. Mp 145–147 °C (hexane). IR (KBr): 3284, 2965, 1625, 1510, 1389, 1249, 1035, 732 cm^{-1}. ^1H NMR ($CDCl_3$, 600 MHz): δ 10.26 (br s, 1H), 9.73 (br s, 1H), 8.20 (d, J = 5.4 Hz, 1H), 8.13 (d, J = 7.8 Hz, 1H), 7.93 (d, J = 5.4 Hz, 1H), 7.62 (m, 1H), 7.58 (m, 1H), 7.30 (m, 1H), 6.68 (s, 1H), 3.74 (s, 3H), 1.88 (s, 3H), 1.31 (s, 9H) ppm. ^{13}C NMR ($CDCl_3$, 150 MHz): δ 173.2, 166.0, 159.4, 140.4, 139.7, 136.1, 135.2, 131.6, 130.7, 129.6, 128.7, 121.5, 121.3, 120.1, 114.7, 114.0, 112.4, 58.4, 55.3, 51.1, 28.4, 22.6 ppm. HRMS (ESI) calcd. for $C_{26}H_{29}N_4O_3^+$ $[M+H]^+$ 445.2234; found: 445.2235.

2-[Acetyl(phenyl)amino]-2-(9*H*-β-carbolin-1-yl)-*N*-pentylacetamide (133i). Yellow crystals. Mp 66–68 °C (hexane). IR (KBr): 3294, 3061, 1650, 1626, 1494, 1383, 747, 700 cm^{-1}. ^1H NMR ($CDCl_3$, 600 MHz): δ 10.29 (br s, 1H), 9.72 (br s, 1H), 8.21 (d, J = 5.2 Hz, 1H), 8.14 (m, 1H), 7.95 (d, J = 5.2 Hz, 1H), 7.63 (m, 1H), 7.60 (m, 1H), 7.31 (m, 1H), 7.28 (m, 1H), 7.20 (br s, 2H), 7.00 (br s, 2H), 3.26 (m, 1H), 3.20 (m, 1H), 1.88 (s, 3H), 1.38 (m, 2H), 1.25 (m, 2H), 1.15 (m, 2H), 0.84 (t, J = 7.3 Hz, 3H) ppm. ^{13}C NMR ($CDCl_3$, 150 MHz): δ 172.7, 167.0, 140.5, 139.4, 138.9, 136.2, 135.2, 129.8, 129.5, 129.1,

128.9, 128.8, 121.5, 121.3, 120.1, 114.9, 112.4, 58.2, 39.4, 29.0, 28.7, 22.8, 22.3, 14.0 ppm. HRMS (ESI) calcd. for $C_{26}H_{28}N_4O_2^+$ $[M]^+$ 428.2207; found: 428.2217.

2-[Acetyl(phenyl)amino]-*N*-*tert*-butyl-2-(6-methoxy-9*H*-β-carbolin-1-yl)acetamide (133j). Colourless crystals. Mp 193–195 °C (Et_2O). IR (KBr): 3424, 3283, 1675, 1626, 1586, 1494, 1211, 1071, 707 cm^{-1}. ^1H NMR ($CDCl_3$, 600 MHz): δ 10.13 (br s, 1H), 9.70 (br s, 1H), 8.16 (d, J = 5.3 Hz, 1H), 7.89 (d, J = 5.3 Hz, 1H), 7.55 (d, J = 2.4 Hz, 1H), 7.53 (d, J = 8.8 Hz, 1H), 7.28 (m, 2H), 7.25 (dd, J_1 = 2.5 Hz, J_2 = 8.9 Hz, 1H), 7.20 (br s, 2H), 7.20 (br s, 1H), 6.98 (s, 1H), 3.94 (s, 3H), 1.88 (s, 3H), 1.27 (s, 9H) ppm. ^{13}C NMR ($CDCl_3$, 150 MHz): δ 172.7, 165.9, 154.2, 139.8, 138.9, 135.8, 135.6, 135.4, 129.7, 129.4, 128.9, 128.7, 121.6, 118.9, 114.6, 113.2, 103.2, 58.4, 56.0, 51.1, 28.4, 22.7 ppm. HRMS (ESI) calcd. for $C_{26}H_{28}N_4O_3^+$ $[M]^+$ 444.2156; found: 444.2153.

General procedure for the preparation of 3,4-dihydropyrimidin-2(1*H*)-one derivatives of β-carboline (134a–i). The appropriate β-carboline aldehyde (**135a** or **135b**, 0.50 mmol), urea (0.50 mmol), β-ketoester (**140**, 0.90 mmol) and $CeCl_3$ (20 mol%, 0.10 mmol) were stirred in the appropriate solvent (2 mL) at 75 °C for 24−48 hours (for reaction times and solvent, see Scheme 40). After the reaction was complete (or when no more progress was observed in the reaction) the residue was dissolved in a DCM–MeOH 1:1 mixture and it was purified by flash column chromatography on silica gel (DCM–MeOH) to afford pure 3,4-dihydropyrimidin-2(1*H*)-ones **134a–i** (for yields, see Scheme 40).

Methyl4-(9*H*-β-carbolin-1-yl)-6-methyl-2-oxo-1,2,3,4-tetrahydropyrimidine-5-carboxylate (134a). Brown crystals. Mp 290–292 °C (MeCN). IR (KBr): 3310, 3222, 1686, 1658, 1430, 1239, 1103, 746 cm^{-1}. ^1H NMR (DMSO-d_6, 600 MHz): δ 11.61 (br s, 1H), 9.19 (br s, 1H), 8.26 (d, J = 5.2 Hz, 1H), 8.00 (d, J = 5.1 Hz, 1H), 7.63 (m, 1H), 7.62 (m, 1H), 7.55 (m, 1H), 7.23 (m, 1H), 5.94 (d, J = 2.5 Hz, 1H), 3.35 (s, 3H), 2.26 (s, 3H) ppm. ^{13}C NMR (DMSO-d_6, 150 MHz): δ 166.2, 152.6, 149.4, 147.3, 140.9, 138.1, 132.6, 128.3, 128.2, 121.9, 120.8, 119.3, 114.1, 112.0, 97.8, 51.8, 50.8, 18.3 ppm. HRMS (ESI) calcd. for $C_{18}H_{16}N_4O_3^+$ $[M]^+$ 336.1217; found: 336.1219.

Methyl 4-(9*H*-β-carbolin-1-yl)-2-oxo-6-propyl-1,2,3,4-tetrahydropyrimidine-5-carboxylate (134b). Brown crystals. Mp 168–170 °C (MeCN). IR (KBr): 3241, 1697, 1642, 1431, 1233, 1213, 1097, 746 cm^{-1}. ^1H NMR (DMSO-d_6, 600 MHz): δ 11.60 (br s, 1H), 9.14 (br s, 1H), 8.25 (d, J = 5.1 Hz, 1H), 8.21 (m, 1H), 7.99 (d, J = 4.6 Hz, 1H), 7.64 (m, 1H), 7.59 (br s, 1H), 7.55 (m, 1H), 7.23 (m, 1H), 5.93 (s, 1H), 3.34 (s, 3H), 2.78 (m, 1H),

2.53 (m, 1H), 1.58 (m, 2H), 0.94 (t, J = 7.4 Hz, 3H) ppm. ^{13}C NMR (DMSO-d_6, 150 MHz): δ 165.9, 153.6, 152.8, 147.4, 140.8, 138.1, 132.6, 128.3, 128.2, 121.9, 120.8, 119.3, 114.1, 112.0, 97.5, 51.8, 50.8, 45.9, 32.5, 21.8, 13.8 ppm. HRMS (ESI) calcd. for $C_{20}H_{20}N_4O_3^+$ $[M]^+$ 364.1535; found: 364.1538.

Ethyl 4-(9*H*-β-carbolin-1-yl)-2-oxo-6-phenyl-1,2,3,4-tetrahydropyrimidine-5-carboxylate (134c). Brown crystals. Mp 195–197 °C (MeCN). IR (KBr): 3296, 1693, 1693, 1496, 1430, 1371, 1330, 1244, 1189, 1097 cm^{-1}. ^{1}H NMR (DMSO-d_6, 600 MHz): δ 11.67 (s, 1H), 9.24 (br s, 1H), 8.34 (d, J = 5.1 Hz, 1H), 8.23 (d, J = 7.8 Hz, 1H), 8.04 (d, J = 5.1 Hz, 1H), 7.71 (br s, 1H), 7.64 (d, J = 8.2 Hz, 1H), 7.56 (t, J = 7.6 Hz, 1H), 7.40 (m, 1H), 7.39 (m, 2H), 7.30 (m, 2H), 7.24 (t, J = 7.4 Hz, 1H), 6.03 (d, J = 2.4 Hz, 1H), 3.56 (q, J = 7.1 Hz, 2H), 0.52 (t, J = 7.1 Hz, 3H) ppm. ^{13}C NMR (DMSO-d_6, 150 MHz): δ 165.5, 152.6, 149.9, 147.2, 140.8, 138.2, 135.7, 132.7, 128.9, 128.6, 128.3, 128.2, 127.9, 121.9, 120.8, 119.3, 114.2, 112.0, 99.1, 59.0, 52.2, 13.4 ppm. HRMS (ESI) calcd. for $C_{24}H_{20}N_4O_3^+$ $[M]^+$ 412.1530; found: 412.1539.

***tert*-Butyl 4-(9*H*-β-carbolin-1-yl)-6-methyl-2-oxo-1,2,3,4-tetrahydropyrimidine-5-carboxylate (134d).** Gray crystals. Mp 238–240 °C (MeCN). IR (KBr): 3444, 3301, 3242, 3099, 1691, 1636, 1323, 1233, 1093, 741 cm^{-1}. ^{1}H NMR (DMSO-d_6, 600 MHz): δ 11.64 (br s, 1H), 9.00 (br s, 1H), 8.26 (d, J = 5.2 Hz, 1H), 8.21 (m, 1H), 7.99 (d, J = 5.2 Hz, 1H), 7.59 (m, 1H), 7.58 (br s, 1H), 7.53 (m, 1H), 7.22 (m, 1H), 5.92 (br s, 1H), 2.25 (s, 3H), 0.95 (s, 9H) ppm. ^{13}C NMR (DMSO-d_6, 150 MHz): δ 165.3, 152.2, 148.2, 147.5, 140.7, 137.9, 132.9, 128.2, 128.0, 121.9, 120.8, 119.2, 113.9, 112.0, 99.2, 78.8, 52.2, 27.8, 18.2 ppm. HRMS (ESI) calcd. for $C_{21}H_{22}N_4O_3^+$ $[M]^+$ 378.1686; found: 378.1680.

1-Methylethyl 4-(9*H*-β-carbolin-1-yl)-6-methyl-2-oxo-1,2,3,4-tetrahydropyrimidine-5-carboxylate (134e). Grey crystals. Mp 263–265 °C (MeCN). IR (KBr): 3454, 3343, 3167, 3065, 1687, 1636, 1457, 1425, 1372, 1236, 1096, 740 cm^{-1}. ^{1}H NMR (DMSO-d_6, 600 MHz): δ 11.67 (br s, 1H), 9.11 (br s, 1H), 8.26 (d, J = 5.2 Hz, 1H), 8.21 (m, 1H), 7.99 (d, J = 5.1 Hz, 1H), 7.65 (br s, 1H), 7.62 (m, 1H), 7.54 (m, 1H), 7.22 (m, 1H), 5.96 (d, J = 1.9 Hz, 1H), 4.59 (m, 1H), 2.27 (s, 3H), 0.99 (d, J = 6.2 Hz, 3H), 0.33 (d, J = 6.2 Hz, 3H) ppm. ^{13}C NMR (DMSO-d_6, 150 MHz): δ 165.1, 152.3, 149.1, 147.7, 140.7, 138.0, 132.8, 128.2, 127.9, 121.9, 120.8, 119.2, 113.9, 111.9, 98.3, 65.8, 55.1, 51.8 39.8, 39.6, 30.9, 21.7, 21, 18.1 ppm. HRMS (ESI) calcd. for $C_{20}H_{20}N_4O_3^+$ $[M]^+$ 364.1535; found: 364.1536.

Ethyl 4-(9*H*-β-carbolin-1-yl)-6-ethyl-2-oxo-1,2,3,4-tetrahydropyrimidine-5-carboxylate (134f). Brown crystals. Mp 258–260 °C (MeCN). IR (KBr): 3425, 3310, 3227, 3118, 1695, 1661, 1633, 1225, 1097, 748 cm^{-1}. ^1H NMR (DMSO-d_6, 600 MHz): δ 11.63 (br s, 1H), 9.14 (br s, 1H), 8.26 (d, J = 5.1 Hz, 1H), 8.21 (m, 1H), 7.99 (d, J = 5.2 Hz, 1H), 7.62 (m, 1H), 7.61 (br s, 1H), 7.54 (m, 1H), 7.22 (m, 1H), 5.94 (d, J = 2.5 Hz, 1H), 3.77 (m, 2H), 2.89 (m, 1H), 2.45 (m, 1H), 1.14 (t, J = 7.4 Hz, 3H), 0.71 (t, J = 7.1 Hz, 3H) ppm. ^{13}C NMR (DMSO-d_6, 150 MHz): δ 165.3, 154.9, 152.8, 147.6, 140.8, 138.1, 132.7, 128.3, 128.0, 121.9, 120.8, 119.2, 114.0, 111.9, 97.2, 59.1, 51.7, 24.4, 13.8, 13.3 ppm. HRMS (ESI) calcd. for $C_{20}H_{20}N_4O_3^+$ $[M]^+$ 364.1530; found: 364.1528.

Ethyl 4-(9*H*-β-carbolin-1-yl)-6-(1-methylethyl)-2-oxo-1,2,3,4-tetrahydropyrimidine-5-carboxylate (134g). Brown crystals. Mp 236–238 °C (MeCN). IR (KBr): 3372, 2966, 1694, 1664, 1646, 1444, 1326, 1127, 1097 cm^{-1}. ^1H NMR (DMSO-d_6, 600 MHz): δ 11.63 (s, 1H), 8.78 (br s, 1H), 8.26 (d, J = 5.1 Hz, 1H), 8.21 (d, J = 7.9 Hz, 1H), 7.99 (d, J = 5.1 Hz, 1H), 7.62 (m, 2H), 7.54 (~t, J = 8.1 Hz, 1H), 7.22 (t, J = 7.8 Hz, 1H), 5.96 (d, J = 2.6 Hz, 1H), 4.20 (m, 1H), 3.75 (m, 2H), 1.17 (d, J = 7.0 Hz, 3H), 1.16 (d, J = 7.0 Hz, 3H), 0.66 (t, J = 7.1 Hz, 3H) ppm. ^{13}C NMR (DMSO-d_6, 150 MHz): δ 165.7, 157.5, 153.0, 147.6, 140.7, 138.2, 132.7, 128.2, 128.0, 121.9, 120.8, 119.2, 114.0, 111.9, 96.8, 59.2, 51.7, 27.0, 19.5, 19.3, 13.7 ppm. HRMS (ESI) calcd. for $C_{21}H_{22}N_4O_3^+$ $[M]^+$ 378.1692; found: 378.1693.

Methyl 4-(9*H*-β-carbolin-1-yl)-6-(2-chlorophenyl)-2-oxo-1,2,3,4-tetrahydropyrimidine-5-carboxylate (134h). Brown crystals. Mp 291–293 °C (MeCN). IR (KBr): 3415, 3300, 1650, 1433, 1245, 1097, 745 cm^{-1}. ^1H NMR (DMSO-d_6, 600 MHz): δ 11.68 (br s, 1H), 9.37 (br s, 1H), 8.34 (d, J = 5.1 Hz, 1H), 8.24 (m, 1H), 8.05 (d, J = 5.1 Hz, 1H), 7.75 (br s, 1H), 7.66 (m, 1H), 7.56 (m, 1H), 7.48 (m, 1H), 7.42 (m, 1H), 7.34 (m, 1H), 7.27 (m, 1H), 7.24 (m, 1H), 6.04 (d, J = 2.6 Hz, 1H), 3.15 (s, 3H) ppm. ^{13}C NMR (DMSO-d_6, 150 MHz): δ 165.4, 152.4, 148.6, 146.9, 140.9, 138.3, 137.4, 132.7, 132.4, 129.9, 128.9, 128.4, 128.3, 128.3, 127.5, 121.9, 120.8, 119.3, 114.3, 112.1, 99.2, 52.1, 50.8 ppm. HRMS (ESI) calcd. for $C_{23}H_{17}ClN_4O_3^+$ $[M]^+$ 432.0989; found: 432.0986.

Methyl 4-(6-methoxy-9*H*-β-carbolin-1-yl)-6-methyl-2-oxo-1,2,3,4-tetrahydropyrimidine-5-carboxylate (134i). Brown crystals. Mp 226–228 °C (MeCN). IR (KBr): 3368, 3219, 3108, 1707, 1662, 1497, 1341, 1246, 1093, 816 cm^{-1}. ^1H NMR (DMSO-d_6, 600 MHz): δ 11.42 (br s, 1H), 9.17 (br s, 1H), 8.21 (d, J = 5.2 Hz, 1H), 7.97 (d, J = 5.1 Hz, 1H), 7.76 (d, J = 2.5 Hz, 1H), 7.60 (t, J = 2.2 Hz, 1H), 7.54 (d, J = 8.8 Hz, 1H), 7.19 (dd,

J_1 = 2.5 Hz, J_2 = 8.8 Hz, 1H), 5.90 (d, J = 2.5 Hz, 1H), 3.86 (s, 3H), 3.34 (s, 3H), 2.26 (s, 3H) ppm. ^{13}C NMR (DMSO-d_6, 150 MHz): δ 166.2, 153.4, 152.6, 149.4, 147.4, 137.4, 135.8, 133.2, 128.1, 121.0, 118.3, 114.1, 112.9, 103.6, 97.8, 55.8, 51.8, 50.8, 18.2 ppm. HRMS (ESI) calcd. for $C_{19}H_{18}N_4O_4^+$ $[M]^+$ 366.1323; found: 366.1330.

General continuous-flow procedure for the preparation of derivatives of dihidro-β-carboline (68, 142–146). Prior to the reaction, the entire flow system was rinsed with MeCN and the BPR was set to 20 bar. The corresponding tryptamine (**29**, 0.50 mmol) and the appropriate carboxylic acid (0.50 mmol) were dissolved in anhydrous MeCN (see Figure 14 for concentration). To this solution, T3P® (50% in EtOAc, 2.0 eq) was added, and the mixture was stirred at room temperature until complete dissolution. The resulting solution was filtered and introduced into the flow reactor, which was operated under the specified temperature and residence time (see Figure 14 for reaction conditions). After collection of the reaction mixture, the solvent was removed in vacuo to afford the crude product. Purification by flash chromatography gave the desired 3,4-dihydro-β-carboline derivatives (**68**, **142–146**) in pure form. Analytical samples were obtained either by recrystallization or by conversion to the corresponding hydrochloride salts.

1-Methyl-4,9-dihydro-3*H*-β-carboline (68). Brown crystals. Mp 173–175 °C (EtOAc). (lit. [55] mp. 175–178 °C). IR (KBr): 2989, 1550, 1324, 1277, 736 cm^{-1}. ^{1}H NMR (DMSO-d_6, 600 MHz): δ 11.37 (br s, 1H), 7.55 (m, 1H), 7.43 (m, 1H), 7.20 (m, 1H), 7.05 (m, 1H), 3.70 (m, 2H), 2.75 (t, J = 8.4 Hz, 2H), 2.30 (t, J = 1.4 Hz, 3H) ppm. ^{13}C NMR (DMSO-d_6, 150 MHz): δ 157.3, 136.7, 129.4, 125.1, 123.7, 119.8, 119.6, 114.3, 112.5, 47.9, 22.3, 19.1 ppm. HRMS (ESI) calcd. for $C_{12}H_{13}N_2^+$ $[M+H]^+$ 185.1073; found: 185.1074.

1-*tert*-Butyl-4,9-dihydro-3*H*-β-carboline (142). Yellow crystals. Mp 176–178 °C (MeCN). (lit. [55] mp. 176–177 °C). IR (KBr): 3253, 1587, 1532, 1305, 1174, 1004, 735 cm^{-1}. ^{1}H NMR (DMSO-d_6, 600 MHz): δ 10.92 (br s, 1H), 7.54 (m, 1H), 7.50 (m, 1H), 7.19 (m, 1H), 7.04 (m, 1H), 3.67 (t, J = 8.2 Hz, 2H), 2.69 (t, J = 8.3 Hz, 2H), 1.32 (s, 9H) ppm. ^{13}C NMR (DMSO-d_6, 150 MHz): δ 166.0, 136.7, 127.1, 124.4, 123.6, 119.4, 119.3, 116.6, 112.7, 47.8, 38.5, 28.5, 18.9 ppm. HRMS (ESI) calcd. for $C_{15}H_{19}N_2^+$ $[M+H]^+$ 227.1543; found: 227.1544.

1-Phenyl-4,9-dihydro-3*H*-β-carboline (143). Yellow crystals. Mp 230–232 °C (EtOH). (lit. [55] mp. 231–232 °C). IR (KBr): 3056, 2934, 2833, 1540, 1322, 1289, 1152, 1012, 716 cm^{-1}. ^{1}H NMR (DMSO-d_6, 600 MHz): δ 11.13 (br s, 1H), 7.77 (m, 2H), 7.62 (m,

1H), 7.53 (m, 1H), 7.53 (m, 2H), 7.44 (m, 1H), 7.21 (m, 1H), 7.08 (m, 1H), 3.89 (t, J = 8.3 Hz, 2H), 2.87 (t, J = 8.2 Hz, 2H). ppm. ^{13}C NMR (DMSO-d_6, 150 MHz): δ 158.8, 137.7, 137.1, 129.9, 128.7, 128.2, 127.7, 125.0, 123.9, 119.8, 119.7, 116.6, 113.0, 48.6, 19.1 ppm. HRMS (ESI) calcd. for $C_{17}H_{14}N_2^+$ $[M]^+$ 246.1157; found: 246.1148.

6-Chloro-1-methyl-4,9-dihydro-3*H*-β-carboline (144). Yellow crystals. Mp 232–234 °C (EtOAc). IR (KBr): 3077, 3016, 1546, 1312, 1283, 979, 806 cm^{-1}. ^{1}H NMR (DMSO-d_6, 600 MHz): δ 11.57 (br s, 1H), 7.62 (d, J = 2.0 Hz, 1H), 7.43 (d, J = 8.7 Hz, 1H), 7.19 (dd, J_1 = 2.0 Hz, J_2 = 8.6 Hz, 1H), 3.70 (t, J = 8.4 Hz, 2H), 2.74 (t, J = 8.4 Hz, 2H), 2.29 (s, 3H) ppm. ^{13}C NMR (DMSO-d_6, 150 MHz): δ 157.0, 135.0, 130.6, 126.2, 124.2, 123.6, 119.0, 114.1, 113.8, 47.8, 22.2, 18.8 ppm. HRMS (ESI) calcd. for $C_{12}H_{11}ClN_2^+$ $[M]^+$ 218.0611; found: 218.0607.

6-Methoxy-1-(4-methoxyphenyl)-4,9-dihydro-3*H*-β-carboline (145). Yellow crystals. Mp 179–182 °C (MeOH). IR (KBr): 2935, 2826, 1607, 1590, 1536, 1512, 1451, 1296, 1250, 1210, 1178, 1115, 1037, 835 cm^{-1}. ^{1}H NMR (DMSO-d_6, 600 MHz): δ 10.95 (s, 1H), 7.73 (d, J = 8.8 Hz, 2H), 7.32 (d, J = 8.8 Hz, 1H), 7.08 (m, 1H), 7.07 (d, J = 8.8 Hz, 2H), 6.85 (dd, J_1 = 8.8 Hz, J_2 = 2.5 Hz, 1H), 3.83 (m, 5H), 3.79 (s, 3H), 2.82 (m, 2H) ppm. ^{13}C NMR (DMSO-d_6, 150 MHz): δ 160.7, 158.1, 153.9, 132.3, 130.3, 129.7, 128.4, 125.2, 116.1, 114.9, 114.0, 113.8, 100.2, 55.5, 55.5, 48.4, 19.3 ppm. HRMS (ESI) calcd. for $C_{19}H_{18}N_2O_2^+$ $[M]^+$ 306.1368; found: 306.1369.

1-Thiophen-2-yl-4,9-dihydro-3*H*-β-carboline (146). Yellow crystals. Mp 230–232 °C (DIPE). (lit. [103] mp. 234–236 °C). IR (KBr): 3424, 3059, 2939, 1578, 1534, 1429, 1368, 1318, 1281, 1167, 1131, 978, 855, 787, 750, 707 cm^{-1}. ^{1}H NMR (DMSO-d_6, 600 MHz): δ 11.34 (br s, 1H), 7.79 (dd, J_1 = 3.7 Hz, J_2 = 0.9 Hz, 1H), 7.72 (dd, J_1 =5.1 Hz, J_2 = 0.9 Hz, 1H), 7.63 (d, J=8.0 Hz, 1H), 7.51 (d, J = 8.2 Hz, 1H), 7.26 (dd, J_1 = 5.1 Hz, J_2 = 3.7 Hz, 1H), 7.24 (t, J = 8.1 Hz, 1H), 7.10 (t. J = 7.5 Hz, 1H), 3.83 (m, 2H), 2.84 (m, 2H) ppm. ^{13}C NMR (DMSO-d_6, 150 MHz): δ 152.7, 142.7, 137.4, 129.4, 128.7, 128.2, 126.9, 124.9, 124.2, 120.0, 119.8, 117.2, 113.1, 48.0, 19.1 ppm. HRMS (ESI) calcd. for $C_{15}H_{21}N_2S^+$ $[M]^+$ 252.0721; found: 252.0719.

6. CONCLUSIONS

This dissertation's research describes a comprehensive synthetic and mechanistic exploration of indole-based alkaloids and their structural analogues, combining experimental organic chemistry with computational analysis and pharmacological collaboration. Through systematic investigations, alternative synthetic methodologies were developed for the preparation of oxazolyl- and thiazolylindoles, β-carboline derivatives, and their corresponding natural product analogues.

In the first part of the work, novel oxazolyl- and thiazolylindoles were synthesized *via* Robinson–Gabriel synthesis and related cyclodehydration reactions. Thiazole and carbothioamide functionalities were linked to antiproliferative activity against HL-60 leukemia and C6 glioma cell lines, according to the study's identification of structure–activity relationships. These findings suggest that these heteroaromatic frameworks could serve as starting points for medicinal chemistry investigations.

Next, the focus shifted to the asymmetric syntheses of bacillamide alkaloids and their antipodes, allowing unambiguous stereochemical assignments supported by SC-XRD. The structural determination of bacillamide D and its enantiomer supplements the known natural product chemistry of these derivatives and provides a reference for future isolation studies.

The research then moves toward the total syntheses of complex β-carboline alkaloids such as orthoscuticelline B, brevicarine, and brevicolline, yielding competitive routes. The work also explored practical modifications driven by green chemistry principles, including the replacement of certain reagents and the application of continuous-flow procedures for key cyclizations.

Finally, computational studies provided mechanistic insight into the contrasting reactivity of the Robinson–Gabriel synthesis and Bischler–Napieralski reactions, offering a possible explanation for the observed reaction selectivity. The combined synthetic, biological, and theoretical findings discussed here advance knowledge of indole-based heterocycle chemistry and provide adaptable frameworks for the development of bioactive molecules with potential pharmaceutical relevance.

7. SUMMARY

This doctoral work describes the design, synthesis, and mechanistic study of indole-derived alkaloids and their synthetic analogues, combining classical and modern organic chemistry with computational modeling and biological evaluation. The project was inspired by the role of the indole scaffold in natural and synthetic bioactive compounds and by the interest in developing alternative synthetic methodologies.

Novel oxazolyl- and thiazolylindoles were prepared through optimized Robinson–Gabriel synthesis and thionation reactions, and their antiproliferative activities were evaluated *in vitro*. The thiazolyl and carbothioamide derivatives exhibited the highest activity and selectivity toward tumor cell lines. Enantioselective syntheses of bacillamides B–D and neobacillamide A were then achieved using asymmetric transfer hydrogenation and Mitsunobu reaction steps, with absolute configurations supported by SC-XRD, providing the first structural elucidations within this group of alkaloids.

Further studies resulted in concise syntheses of orthoscuticelline B, brevicarine, and brevicolline, including practical alternatives to earlier reported methods. The work also applied flow-based approaches to the synthesis of 1-substituted 3,4-dihydro-β-carbolines, exploring their synthetic scalability and easy operation. Complementary computational investigations offered a possible rationale for the different mechanistic pathways and energetic preferences of the key cyclization reactions, providing a theoretical framework for the selectivities observed throughout the project.

Overall, the results of this dissertation present synthetic strategies, mechanistic insights, and biological data related to the field of heterocyclic chemistry. The methodologies and compounds developed herein could provide a basis for future research aimed at the exploration of indole-based therapeutic agents.

8. REFERENCES

1. Sravanthi, T. V., & Manju, S. L. (2016). Indoles – A promising scaffold for drug development. European Journal of Pharmaceutical Sciences, 91, 1-10. https://doi.org/10.1016/j.ejps.2016.05.025

2. Omar, F., Tareq, A. M., Alqahtani, A. M., Dhama, K., Sayeed, M. A., Emran, T. B., & Simal-Gandara, J. (2021). Plant-based indole alkaloids: A comprehensive overview from a pharmacological perspective. Molecules, 26(8), 2297. https://doi.org/10.3390/molecules26082297

3. Dreicer, R., Chu, F., Cahn, D. J., Getzenberg, R. H., Rodriguez, D., Barnette, K. G., Steiner, M. S., Saltzstein, D. R., Tutrone, R. F., & Shore, N. D. (2022). Phase 3 VERACITY clinical study of sabizabulin in men with metastatic castration-resistant prostate cancer who have progressed on an androgen receptor targeting agent. Journal of Clinical Oncology, 40(16), TPS5102. https://doi.org/10.1200/JCO.2022.40.16_suppl.TPS5102

4. Dadras, A., Rezvanfar, M. A., Beheshti, A., Naeimi, S. S., & Siadati, S. A. (2022). An urgent industrial scheme both for total synthesis, and for pharmaceutical analytical analysis of umifenovir as an anti-viral API for treatment of COVID-19. Combinatorial Chemistry & High Throughput Screening, 25(5), 838-846. https://doi.org/10.2174/1386207324666210203175631

5. Nalamachu, S., & Wortmann, R. (2014). Role of indomethacin in acute pain and inflammation management: a review of the literature. Postgraduate Medicine, 126(4), 92-97. https://doi.org/10.3810/pgm.2014.07.2787

6. Wang, S. M., Han, C., Lee, S. J., Patkar, A. A., Masand, P. S., & Pae, C. U. (2016). Vilazodone for the treatment of depression: an update. Chonnam Medical Journal, 52(2), 91-100. https://doi.org/10.4068/cmj.2016.52.2.91

7. Wong, G. W., Boyda, H. N., & Wright, J. M. (2014). Blood pressure lowering efficacy of partial agonist beta blocker monotherapy for primary hypertension. Cochrane Database of Systematic Reviews, (11). https://doi.org/10.1002/14651858.CD007450.pub2

8. Brandes, J. L., Kudrow, D., Stark, S. R., O'Carroll, C. P., Adelman, J. U., O'Donnell, F. J., Alexander, W. J., Spruill, S. E., Barrett, P. S., & Lener, S. E. (2007). Sumatriptan-naproxen for acute treatment of migraine: a randomized trial. Jama, 297(13), 1443-1454. https://doi.org/10.1001/jama.297.13.1443

9. Shin, D. Y., Shin, H. J., Kim, G.-Y., Cheong, J., Choi, I.-W., Kim, S.-K., Moon, S.-K., Kang, H. S., & Choi, Y. H. (2008). Streptochlorin isolated from Streptomyces sp. Induces apoptosis in human hepatocarcinoma cells through a reactive oxygen species-mediated mitochondrial pathway. Journal of Microbiology and Biotechnology, 18(11), 1862-1868. https://doi.org/10.4014/jmb.0800.124

10. Jeong, S. Y., Ishida, K., Ito, Y., Okada, S., & Murakami, M. (2003). Bacillamide, a novel algicide from the marine bacterium, Bacillus sp. SY-1, against the harmful dinoflagellate, Cochlodinium polykrikoides. Tetrahedron Letters, 44(43), 8005-8007. https://doi.org/10.1016/j.tetlet.2003.08.115

11. Ma, W. H., & Qin, L. P. (2014). Chemical constituents of arabidopsis thaliana. Chemistry of Natural Compounds, 50(4), 776-777. https://doi.org/10.1007/s10600-014-1083-9

12. Smith, B. A., Neal, C. L., Chetram, M., Vo, B., Mezencev, R., Hinton, C., & Odero-Marah, V. A. (2013). The phytoalexin camalexin mediates cytotoxicity towards aggressive prostate cancer cells via reactive oxygen species. Journal of Natural Medicines, 67(3), 607-618. https://doi.org/10.1007/s11418-012-0722-3

13. Goodwin, S., Smith, A. F., & Horning, E. C. (1959). Alkaloids of Ochrosia elliptica Labill. Journal of the American Chemical Society, 81(8), 1903-1908. https://doi.org/10.1021/ja01517a031

14. Kohn, K. W., Waring, M. J., Glaubiger, D., & Friedman, C. A. (1975). Intercalative binding of ellipticine to DNA. Cancer Research, 35(1), 71-76.

15. Wright, C. W., Addae-Kyereme, J., Breen, A. G., Brown, J. E., Cox, M. F., Croft, S. L., Gökçek, Y., Kendrick, H., Phillips, R. M., & Pollet, P. L. (2001). Synthesis and evaluation of cryptolepine analogues for their potential as new antimalarial agents. Journal of Medicinal Chemistry, 44(19), 3187-3194. https://doi.org/10.1021/jm010929+

16. Quilico, A., & Panizzi, L. (1943). Chemische Untersuchungen über Aspergillus echinulatus, I. Mitteilung. Berichte der Deutschen Chemischen Gesellschaft (A and B Series), 76(4), 348-358. https://doi.org/10.1002/cber.19430760408

17. Makhloufi, H., Pinon, A., Champavier, Y., Saliba, J., Millot, M., Fruitier-Arnaudin, I., Liagre, B., Chemin, G., & Mambu, L. (2024). In Vitro Antiproliferative Activity of Echinulin Derivatives from Endolichenic Fungus Aspergillus sp. against Colorectal Cancer. Molecules, 29(17), 4117. https://doi.org/10.3390/molecules29174117

18. Zhang, Y. S., Li, J. D., & Yan, C. (2018). An update on vinpocetine: new discoveries and clinical implications. European Journal of Pharmacology, 819, 30-34. https://doi.org/10.1016/j.ejphar.2017.11.041

19. Dai, J., Dan, W., Schneider, U., & Wang, J. (2018). β-Carboline alkaloid monomers and dimers: Occurrence, structural diversity, and biological activities. European Journal of Medicinal Chemistry, 157, 622-656. https://doi.org/10.1016/j.ejmech.2018.08.027

20. Cohen, P. A., Wang, Y. H., Maller, G., DeSouza, R., & Khan, I. A. (2016). Pharmaceutical quantities of yohimbine found in dietary supplements in the USA. Drug Testing and Analysis, 8(3-4), 357-369. https://doi.org/10.1002/dta.1849

21. Trojánek, J., Štrouf, O., Holubek, J., & Čekan, Z. (1961). Structure of vincamine. Tetrahedron Letters, 2(20), 702-706. https://doi.org/10.1016/S0040-4039(01)91678-8

22. Fischhof, P. K., Möslinger-Gehmayr, R., Herrmann, W. M., Friedmann, A., & Ruβmann, D. L. (1996). Therapeutic efficacy of vincamine in dementia. Neuropsychobiology, 34(1), 29-35. https://doi.org/10.1159/000119288

23. Achor, R. W., Hanson, N. O., & Gifford, R. W. (1955). Hypertension treated with Rauwolfia serpentina (whole root) and with reserpine: controlled study disclosing occasional severe depression. Journal of the American Medical Association, 159(9), 841-845. https://doi.org/10.1001/jama.1955.02960260011004

24. Oikawa, Y., Yoshioka, T., Mohri, K., & Yonemitsu, O. (1979). Synthesis of pimprinine and related oxazolylindole alkaloids from N-acyl derivatives of tryptamine and tryptophan methyl ester by DDQ oxidation. Heterocycles, 12(11) 1457-1462. https://doi.org/10.3987/r-1979-11-1457

25. Koyama, Y., Yokose, K., & Dolby, L. J. (1981). Isolation, characterization and synthesis of pimprinine, pimprinethine and pimprinaphine, metabolites of Streptoverticillium olivoreticuli. Agricultural and Biological Chemistry, 45(5), 1285-1287. https://doi.org/10.1271/bbb1961.45.1285

26. Kumar, D., Sundaree, S., Patel, G., & Rao, V. S. (2008). A facile synthesis of naturally occurring 5-(3-indolyl) oxazoles. Tetrahedron Letters, 49(5), 867-869. https://doi.org/10.1016/j.tetlet.2007.11.173

27. Savelson, E., & Tepe, J. J. (2022). One-Pot Friedel–Crafts/Robinson–Gabriel Synthesis of the Indole-Oxazole Scaffold and Its Application to the Synthesis of Breitfussins C, G, and H. The Journal of Organic Chemistry, 88(2), 755-761. https://doi.org/10.1021/acs.joc.2c00033

28. Bracken, C., & Baumann, M. (2020). Development of a continuous flow Photoisomerization reaction converting Isoxazoles into diverse Oxazole products. The Journal of Organic Chemistry, 85(4), 2607-2617. https://doi.org/10.1021/acs.joc.9b03399

27. Nakagawa, M., Nishida, A., Fuwa, M., Saito, H., & Ltd, L. C. C. (1999, August 13). WO2001012626A1 - Indole compounds, process for the preparation of the same and uses thereof - Google Patents. https://patents.google.com/patent/WO2001012626A1/en#patentCitations

30. Pedras, M. S. C., & Abdoli, A. (2013). Metabolism of the phytoalexins camalexins, their bioisosteres and analogues in the plant pathogenic fungus Alternaria brassicicola. Bioorganic & Medicinal Chemistry, 21(15), 4541-4549. https://doi.org/10.1016/j.bmc.2013.05.026

31. Nicolaou, K. C., Hao, J., Reddy, M. V., Rao, P. B., Rassias, G., Snyder, S. A., Huang, X., Chen, D. Y. -k., Brenzovich, W. E., Giuseppone, N., Giannakakou, P., & O'Brate, A. (2004). Chemistry and biology of diazonamide A: second total synthesis and biological investigations. Journal of the American Chemical Society, 126(40), 12897-12906. https://doi.org/10.1021/ja040093a

32. Al-Azawe, S. S. (1988). Journal of the Iraqi Chemical Society, 13, 1.

33. Wang, B., Tao, Y., Liu, Q., Liu, N., Jin, Z., & Xu, X. (2017). Algicidal activity of bacillamide alkaloids and their analogues against marine and freshwater harmful algae. Marine Drugs, 15(8), 247. https://doi.org/10.3390/md15080247

34. Wang, Y., Liu, Q., Wei, Z., Liu, N., Li, Y., Li, D., Jin, Z., & Xu, X. (2018). Thiazole amides, a novel class of algaecides against freshwater harmful algae. Scientific Reports, 8(1), 8555. https://doi.org/10.1038/s41598-018-26911-6

35. Saalim, M., Liu, S., Bennett, S. D., Zaleta-Pinet, D. A., Poulin, R. X., & Clark, B. R. (2024). Precursor-Directed Biosynthesis of Antialgal Fluorinated Bacillamide Derivatives in Bacillus atrophaeus. Journal of Natural Products, 87(2), 388-395. https://doi.org/10.1021/acs.jnatprod.3c01178

36. Hohmann, M., Brunner, V., Johannes, W., Schum, D., Carroll, L. M., Liu, T., Sasaki, D., Bosch, J., Clavel, T., Sieber, S. A., Zeller, G., Tschurtschenthaler, M., Janßen, K.-P., & Gulder, T. M. (2024). Bacillamide D produced by Bacillus cereus from the mouse intestinal bacterial collection (miBC) is a potent cytotoxin in vitro. Communications Biology, 7(1), 655. https://doi.org/10.1038/s42003-024-06208-3

37. Figueira, V. B., Prabhakar, S., & Lobo, A. M. (2005). Synthesis of the algicide bacillamide. Arkivoc, 14, 14-9. https://doi.org/10.3998/ark.5550190.0006.e02

38. Kumara, S., & Aggarwal, R. (2018). A concise and efficient route to the total synthesis of bacillamide A and its analogues. Archivoc, 2018(3), 354-361. https://doi.org/10.24820/ark.5550190.p010.362

39. Socha, A. M., Long, R. A., & Rowley, D. C. (2007). Bacillamides from a hypersaline microbial mat bacterium. Journal of Natural Products, 70(11), 1793-1795. https://doi.org/10.1021/np070126a

40. Bray, C. D., & Olasoji, J. (2010). A total synthesis of (+)-bacillamide B. Synlett, 2010(04), 599-601. https://doi.org/10.1055/s-0029-1219153

41. Sun, X., Liu, Y., Liu, J., Gu, G., & Du, Y. (2015). Synthesis and structural reconfirmation of bacillamide B. Organic & Biomolecular Chemistry, 13(14), 4271-4277. https://doi.org/10.1039/C5OB00093A

42. Ivanova, V., Kolarova, M., Aleksieva, K., Gräfe, U., Dahse, H. M., & Laatsch, H. (2007). Microbiaeratin, a new natural indole alkaloid from a Microbispora aerata strain, isolated from Livingston Island, Antarctica. Preparative Biochemistry & Biotechnology, 37(2), 161-168. https://doi.org/10.1080/10826060701199122

43. Li, D., Yang, H. S., Cui, Q., Mao, S. J., & Xu, X. H. (2009). Synthesis of bacillamide 3 and its analogue. Chinese Chemical Letters, 20(10), 1195-1197. https://doi.org/10.1016/j.cclet.2009.05.014

44. Wang, W., Joyner, S., Khoury, K. A. S., & Dömling, A. (2010). (−)-Bacillamide C: the convergent approach. Organic & Biomolecular Chemistry, 8(3), 529-532. https://doi.org/10.1039/B918214D

45. Martínez, V., & Davyt, D. (2013). Total syntheses of bacillamide C and neobacillamide A; revision of their absolute configurations. Tetrahedron: Asymmetry, 24(24), 1572-1575. https://doi.org/10.1016/j.tetasy.2013.11.001

46. Yu, L. L., Li, Z. Y., Peng, C. S., Li, Z. Y., & Guo, Y. W. (2009). Neobacillamide A, a novel thiazole-containing alkaloid from the marine bacterium Bacillus vallismortis C89, associated with South China Sea sponge Dysidea avara. Helvetica Chimica Acta, 92(3), 607-612. https://doi.org/10.1002/hlca.200800349

47. Konda, Y., Suzuki, Y., Omura, S., & Onda, M. (1976). Alkaloid from Thermoactinomyces species. Chemical and Pharmaceutical Bulletin, 24(1), 92-96. https://doi.org/10.1248/cpb.24.92

48. Onda, M., & Konda, Y. (1978). Synthesis of the alkaloid from Thermoactinomyces species. Chemical and Pharmaceutical Bulletin, 26(7), 2167-2169. https://doi.org/10.1248/cpb.26.2167

49. Dean, B. M., Mijović, M. P. V., & Walker, J. (1961). 660. Chemistry of micrococcin P. Part VI. Racemisation of 2-(l-amino-2-methylpropyl) thiazole-4-carboxylic acid, and related studies. Journal of the Chemical Society (Resumed), 3394-3400. https://doi.org/10.1039/JR9610003394

50. Bischler, A., & Napieralski, B. (1893). Zur kenntniss einer neuen isochinolinsynthese. Berichte der Deutschen Chemischen Gesellschaft, 26(2), 1903-1908. https://doi.org/10.1002/cber.189302602143

51. Katritzky, A. R., Ramsden, C. A., Scriven, E. F., & Taylor, R. J. (2008). Comprehensive heterocyclic chemistry III. In V1 3-memb. Heterocycl., together with all Fused Syst. contain. a 3-memb. Heterocycl. Ring. V2 4-memb. Heterocycl. together with all Fused Syst. contain. a 4-memb. Heterocycl. Ring. V3 Five-memb. Rings with One Heteroat. together with their Benzo and other Carbocycl.-fused Deriv. V4 Five-memb. Rings with Two Heteroat., each with their Fused Carbocycl. Deriv. (pp. 1-13718). Elsevier. https://doi.org/10.1016/C2009-1-28335-3

52. Li, M., Yuan, Y., & Chen, Y. (2021). Bischler-Napieralski Cyclization: A Versatile Reaction towards Functional Aza-PAHs and Their Conjugated Polymers. Chinese Journal of Chemistry, 39(11), 3101-3115. https://doi.org/10.1002/cjoc.202100419

53. Keglevich, G. (Ed.). (2018). Organophosphorus Chemistry: Novel Developments. (pp. 148-157). De Gruyter. https://doi.org/10.1515/9783110535839

54. Szabó, T., Dancsó, A., Ábrányi-Balogh, P., Volk, B., & Milen, M. (2019). First reported propylphosphonic anhydride (T3P®) mediated Robinson–Gabriel cyclization. Synthesis of natural and unnatural 5-(3-indolyl) oxazoles. Tetrahedron Letters, 60(20), 1353-1356. https://doi.org/10.1016/j.tetlet.2019.04.024

55. Abranyi-Balogh, P., Földesi, T., Grün, A., Volk, B., Keglevich, G., & Milen, M. (2016). Synthetic study on the T3P®-promoted one-pot preparation of 1-substituted-3, 4-dihydro-β-carbolines by the reaction of tryptamine with carboxylic acids. Tetrahedron Letters, 57(18), 1953-1957. https://doi.org/10.1016/j.tetlet.2016.03.067

56. Ábrányi-Balogh, P., Volk, B., Keglevich, G., & Milen, M. (2016). Computational study on the synthesis of 1-phenyl-3, 4-dihydro-β-carboline: T3P®-promoted one-pot formation from tryptamine vs. POCl3-mediated ring closure of Nb-benzoyltryptamine. The first DFT investigation of the Bischler-Napieralski reaction. Computational and Theoretical Chemistry, 1097, 48-60. https://doi.org/10.1016/j.comptc.2016.10.008

57. Kleks, G., Duffy, S., Lucantoni, L., Avery, V. M., & Carroll, A. R. (2020). Orthoscuticellines A–E, β-carboline alkaloids from the bryozoan Orthoscuticella ventricosa collected in Australia. Journal of Natural Products, 83(2), 422-428. https://doi.org/10.1021/acs.jnatprod.9b00933

58. Yi, L., He, Y.-T., Tan, S., White, L. V., Lan, P., Gardiner, M. G., Pei, Z., Coote, M. L., & Banwell, M. G. (2022). Total syntheses of the structures assigned to the marine natural products orthoscuticellines A–E. The Journal of Organic Chemistry, 87(18), 12287-12296. https://doi.org/10.1021/acs.joc.2c01477

59. Abarca, B., Custodio, R., Cuadro, A. M., Sucunza, D., Domingo, A., Mendicuti, F., Alvarez-Builla, J., & Vaquero, J. J. (2014). Efficient synthesis of an indoloquinolizinium alkaloid selective DNA-binder by ring-closing metathesis. Organic Letters, 16(13), 3464-3467. https://doi.org/10.1021/ol5013668

60. Busqué, J., Pedrosa, M. M., Cabellos, B., & Muzquiz, M. (2010). Phenological changes in the concentration of alkaloids of Carex brevicollis in an alpine rangeland. Journal of Chemical Ecology, 36(11), 1244-1254. https://doi.org/10.1007/s10886-010-9865-4

61. Batizi, B., Pollák, P., Dancsó, A., Keglevich, P., Simig, G., Volk, B., & Milen, M. (2025). Studies on the syntheses of β-carboline alkaloids brevicarine and brevicolline. Beilstein Journal of Organic Chemistry, 21(1), 955-963. https://doi.org/10.3762/bjoc.21.79

62. Terent'eva, I. (1960). Moldavii Trudy Instituta Khimii Akademii Nauk Moldavskoi SSR, 21.

63. Szabó, T., Görür, F. L., Horváth, S., Volk, B., & Milen, M. (2022). Synthesis of racemic and enantiopure forms of β-carboline alkaloid brevicolline. Synthesis, 54(17), 3867-3873. https://doi.org/10.1055/s-0041-1737830

64. Vember, P. A., & Terentjeva, I. (1969). Brevicarine from brevicolline. Khimiya Prirodnykh Soedinenii. 5, 404-406.

65. Kuchkova, K., Semenov, A., & Terentjeva, I. (1970). Khimiya Geterotsiklicheskikh Soedinenii. 197.

66. Kuchkova, K., Semenov, A., & Terentjeva, I. (1971). Total synthesis of alkaloid brevicarine and its inferior homologue. Acta Chimica Academiae Scientiarum Hungaricae. 69, 367–371.

67. Powers, J. C. (1965). Synthesis of Piperidylindoles. The Journal of Organic Chemistry, 30(8), 2534-2540. https://doi.org/10.1021/jo01019a008

68. Müller, W. H., Preuß, R., & Winterfeldt, E. (1977). Reaktionen an Indolderivaten, XXXIII. Eine einfache und biogeneseorientierte Totalsynthese von Brevicollin und Brevicarin. Chemische Berichte, 110(7), 2424-2432. https://doi.org/10.1002/cber.19771100703

69. Marcu, G. A. (1965). Tr. Tret'ei Nauchn. Konferentsiya Molodykh Uchenykh Moldavii, Biologiya i Sel'skokhozyaistvennye Nauki, 2, 243.

70. Iasnetsov, V. S., & Sizov, P. I. (1972). Mechanism of action of brevicollin, thalictrimene and pachycarpine on the uterus. Farmakologiia i Toksikologiia, 35(2), 201-203.

71. Towers, G. H. N., & Abramowski, Z. (1983). UV-mediated genotoxicity of furanoquinoline and of certain tryptophan-derived alkaloids. Journal of Natural Products, 46(4), 576-581. https://doi.org/10.1021/np50028a027

72. Vember, P. A., & Terent'eva, I. V. (1969). Brevicarine from brevicolline. Chemistry of Natural Compounds, 5(5), 335-336. https://doi.org/10.1007/bf00595072

73. Bhajan, C., Soulange, J. G., Sanmukhiya, V. M. R., Olędzki, R., & Harasym, J. (2023). Phytochemical composition and antioxidant properties of Tambourissa ficus, a Mauritian endemic fruit. Applied Sciences, 13(19), 10908. https://doi.org/10.3390/app131910908

74. Dubey, A., Ghosh, N., & Singh, R. (2023). An in-depth and in vitro evaluation of the antioxidant and neuroprotective activity of aqueous and ethanolic extract of Asparagus racemosus Linn seed. Research Journal of Chemistry and Environment, 27(10), 46-66. https://doi.org/10.25303/2710rjce046066

75. Chalertpet, K., Sangkheereeput, T., Somjit, P., Bankeeree, W., & Yanatatsaneejit, P. (2023). Effect of Smilax spp. and Phellinus linteus combination on cytotoxicity and cell proliferation of breast cancer cells. BMC Complementary Medicine and Therapies, 23(1), 177. https://doi.org/10.1186/s12906-023-04003-x

76. Macaev, F., Stangaci, E., Duca, D., Duca, G., & De Chimie Al Academiei De Stiinte a Moldovei, I. (2008, July 15). MD4009B1 - Use of 1-methyl-4-(N-methylaminobutyl-4)- Beta -carboline as antituberculous remedy - Google Patents. https://patents.google.com/patent/MD4009B1/en

77. Riaz, A., Rasul, A., Hussain, G., Saadullah, M., Rasool, B., Sarfraz, I., Masood, M., Asrar, M., Jabeen, F., & Sultana, T. (2020). Resistomycin, a pentacyclic polyketide, inhibits the growth of triple negative breast cancer cells through induction of apoptosis and mitochondrial dysfunction. Pakistan Journal of Pharmaceutical Sciences, 33(3), 1233-1238. https://doi.org/10.36721/pjps.2020.33.3.sup.1233-1238.1

78. Min, D. J., Kim, S. J., & Hwang, J. S. (2007, October 31). Composition for external application containing PPARs activator from plant (WO Patent Application No. WO 066255 A1). World Intellectual Property Organization.

79. Denisenko, P. P., Vinogradova, T. V., & Semenov, A. A. (1988). Brevikarin dihydrochloride--a new original anti-arrhythmia agent. Farmakologiia i Toksikologiia, 51(2), 50-53.

80. Kireev, D., Wigle, T. J., Norris-Drouin, J., Herold, J. M., Janzen, W. P., & Frye, S. V. (2010). Identification of non-peptide malignant brain tumor (MBT) repeat antagonists by virtual screening of commercially available compounds. Journal of Medicinal Chemistry, 53(21), 7625-7631. https://doi.org/10.1021/jm1007374

81. Polledo, L., Marín, J. G., Martínez-Fernández, B., González, J., Alonso, J., Salceda, W., & García-Iglesias, M. J. (2012). Recurrent outbreaks of myelodysplasia in newborn calves. Journal of Comparative Pathology, 147(4), 479-485. https://doi.org/10.1016/j.jcpa.2012.03.002

82. Frisch, M. J., Trucks, G. W., Schlegel, H. B., Scuseria G. E., Robb, M. A., Cheeseman, J. R., Scalmani, G., Barone, V., Petersson, G. A., Nakatsuji, H., Li, X., Caricato, M., Marenich, A. V., Bloino, J., Janesko, B. G., Gomperts, R., Mennucci, B., Hratchian, H. P., Ortiz, J. V., Izmaylov, A. F., Sonnenberg, J. L., Williams-Young, D., Ding, F., Lipparini, F., Egidi, F., Goings, J., Peng, B., Petrone, A., Henderson, T., & Ranasinghe D. (2016). Gaussian 16 Revision C. 01, 2016. Gaussian Inc. Wallingford CT, 1, 572.

83. Zhao, Y., & Truhlar, D. G. (2008). The M06 suite of density functionals for main group thermochemistry, thermochemical kinetics, noncovalent interactions, excited states, and transition elements: two new functionals and systematic testing of four M06-class functionals and 12 other functionals. Theoretical Chemistry Accounts, 120(1), 215-241. https://doi.org/10.1007/s00214-007-0310-x

84. Petersson, A., Bennett, A., Tensfeldt, T. G., Al-Laham, M. A., Shirley, W. A., & Mantzaris, J. (1988). A complete basis set model chemistry. I. The total energies of closed-shell atoms and hydrides of the first-row elements. The Journal of Chemical Physics, 89(4), 2193-2218. https://doi.org/10.1063/1.455064

85. Marenich, A. V., Cramer, C. J., & Truhlar, D. G. (2009). Universal solvation model based on solute electron density and on a continuum model of the solvent defined by the bulk dielectric constant and atomic surface tensions. The Journal of Physical Chemistry B, 113(18), 6378-6396. https://doi.org/10.1021/jp810292n

86. Daina, A., Michielin, O., & Zoete, V. (2017). SwissADME: a free web tool to evaluate pharmacokinetics, drug-likeness and medicinal chemistry friendliness of small molecules. Scientific Reports, 7(1), 42717. https://doi.org/10.1038/srep42717

87. Daina, A., & Zoete, V. (2016). A boiled-egg to predict gastrointestinal absorption and brain penetration of small molecules. ChemMedChem, 11(11), 1117-1121. https://doi.org/10.1002/cmdc.201600182

88. Menche, D., Hassfeld, J., Li, J., Mayer, K., & Rudolph, S. (2009). Modular total synthesis of archazolid A and B. The Journal of Organic Chemistry, 74(19), 7220-7229. https://doi.org/10.1021/jo901565n

89. Han, A., & Inc, R. P. (2021, December 29). WO2023129518A1 - Tubulysins and protein-tubulysin conjugates - Google Patents. https://patents.google.com/patent/WO2023129518A1/en?oq=WO2023129518+

90. Schmidt, U., Gleich, P., Griesser, H., & Utz, R. (1986). Amino Acids and Peptides; 58 Synthesis of Optically Active 2-(1-Hydroxyalkyl)-thiazole-4-carboxylic Acids and 2-(1-Aminoalkyl)-thiazole-4-carboxylic Acids. Synthesis, 1986(12), 992-998. https://doi.org/10.1055/s-1986-31847

91. Clayden, J., Greeves, N., & Warren, S. (2012). Organic chemistry. (2nd ed. pp. 1114-1117.) Oxford university press.

92. Wolfe, S., & Hasan, S. K. (1970). Five-membered rings. II. Inter and intramolecular reactions of simple amines with N-substituted phthalimides. Methylamine as a reagent for removal of a phthaloyl group from nitrogen. Canadian Journal of Chemistry, 48(22), 3572-3579. https://doi.org/10.1139/v70-598

93. Terent'eva, I. V., Lazur'evskii, G. V., & Shirshova, T. I. (1969). The structure of brevicarine. Chemistry of Natural Compounds, 5(5), 330-334.

94. Aubry, C., Jenkins, P. R., Mahale, S., Chaudhuri, B., Maréchal, J. D., & Sutcliffe, M. J. (2004). New fascaplysin-based CDK4-specific inhibitors: design, synthesis and biological activity. Chemical Communications, (15), 1696-1697. https://doi.org/10.1039/B406076H

95. Redko, B., Albeck, A., & Gellerman, G. (2012). Facile synthesis and antitumor activity of novel N (9) methylated AHMA analogs. New Journal of Chemistry, 36(11), 2188-2191. https://doi.org/10.1039/C2NJ40567A

96. Inoue, H., Iijima, I., & Takeda, M. (1980). Synthesis of bridged 2-phenylcyclohexylamines as potential analgetics. Chemical and Pharmaceutical Bulletin, 28(4), 1022-1034. https://doi.org/10.1248/cpb.28.1022

97. Prabakaran, K., Zeller, M., Szalay, P. S., & Rajendra Prasad, K. J. (2012). Convenient Approaches towards the Synthesis of Novel Pyrano [2, 3-a] carbazoles. Journal of Heterocyclic Chemistry, 49(6), 1302-1309. https://doi.org/10.1002/jhet.910

98. Bingul, M., Arndt, G. M., Marshall, G. M., Black, D. S., Cheung, B. B., & Kumar, N. (2021). Synthesis and characterisation of novel tricyclic and tetracyclic furoindoles: Biological evaluation as SAHA enhancer against neuroblastoma and breast cancer cells. Molecules, 26(19), 5745. https://doi.org/10.3390/molecules26195745

99. Varga, P. R., & Keglevich, G. (2021). Synthesis of α-aminophosphonates and related derivatives; the last decade of the Kabachnik–Fields reaction. Molecules, 26(9), 2511. https://doi.org/10.3390/molecules26092511

100. Gábor, D., Pollák, P., Volk, B., Dancsó, A., Simig, G., & Milen, M. (2023). Catalyst-and Solvent-Free Room Temperature Synthesis of α-Aminophosphonates: Green Accomplishment of the Kabachnik–Fields Reaction. ChemistrySelect, 8(26), e202301460. https://doi.org/10.1002/slct.202301460

101. Bhagat, S., & Chakraborti, A. K. (2007). An extremely efficient three-component reaction of aldehydes/ketones, amines, and phosphites (Kabachnik− Fields reaction) for the synthesis of α-aminophosphonates catalyzed by magnesium perchlorate. The Journal of Organic Chemistry, 72(4), 1263-1270. https://doi.org/10.1021/jo062140i

102. Ignacio, J. M., Macho, S., Marcaccini, S., Pepino, R., & Torroba, T. (2005). A facile synthesis of 1, 3, 5-trisubstituted hydantoins via Ugi four-component condensation. Synlett, 2005(20), 3051-3054. https://doi.org/10.1055/s-2005-922745

103. Milen, M., Slegel, P., Keglevich, P., Keglevich, G., Simig, G., & Volk, B. (2015). Efficient synthesis of Nb-thioacyltryptamine derivatives by a three-component Willgerodt–Kindler reaction, and their transformation to 1-substituted-3, 4-dihydro-β-carbolines. Tetrahedron Letters, 56(42), 5697-5700. https://doi.org/10.1016/j.tetlet.2015.09.007

9. BIBLIOGRAPHY OF THE CANDIDATE'S PUBLICATIONS

9.1. PUBLICATIONS RELATED TO THE DISSERTATION

1.

Pollák, P., Garádi, Z., Volk, B., Dancsó, A., Simig, G., & Milen, M. (2025). Studies on the total syntheses of β-carboline alkaloids orthoscuticellines A and B. Natural Product Research, 39(13), 3677-3685.

https://doi.org/10.1080/14786419.2024.2306600

IF: 2.2; Q2

2.

Pollák, P., Szele, B., Varga, M., Paszternák, A., Varga, K., Dancsó, A., Simig, G., Volk, B., Tábi, T., & Milen, M. (2025). Synthesis and Structure–Activity Relationship Studies of Novel Oxazolyl-and Thiazolyl-Indoles and their Intermediates as Selective Antiproliferative Agents Against HL-60 Leukemia and C6 Glioma Cell Lines. ChemMedChem, 20(15), e202500030.

https://doi.org/10.1002/cmdc.202500030

IF: 3.4; Q1

3.

Pollák, P., Milen, M., Volk, B., & Ábrányi-Balogh, P. (2025). Comparative Computational Study on the Robinson–Gabriel Synthesis and Bischler–Napieralski Reaction: Density Functional Theory Investigation of T3P-Mediated Ring Closure. European Journal of Organic Chemistry, 28(21), e202400679.

https://doi.org/10.1002/ejoc.202400679

IF: 2.7; Q2

4.

Batizi, B., Pollák, P., Dancsó, A., Keglevich, P., Simig, G., Volk, B., & Milen, M. (2025). Studies on the syntheses of β-carboline alkaloids brevicarine and brevicolline. Beilstein Journal of Organic Chemistry, 21(1), 955-963.

https://doi.org/10.3762/bjoc.21.79

IF: 2.2; Q2

5.

Batizi, B., Pollák, P., Horváth, S., Karaghiosoff, K., Simig, G., Németh, G., Volk, B., & Milen, M. (2025). Synthesis of Bacillamide B–D and Neobacillamide A Alkaloids, and Their Antipodes: Unambiguous Assignment of Absolute Configurations and Direction of Optical Rotations. Asian Journal of Organic Chemistry, 14(12), e70255.
https://doi.org/10.1002/ajoc.70255

IF: 2.7; Q2

9.2. PUBLICATIONS UNRELATED TO THE DISSERTATION

6.

Gábor, D., Pollák, P., Volk, B., Dancsó, A., Simig, G., & Milen, M. (2023). Catalyst-and Solvent-Free Room Temperature Synthesis of α-Aminophosphonates: Green Accomplishment of the Kabachnik–Fields Reaction. ChemistrySelect, 8(26), e202301460.
https://doi.org/10.1002/slct.202301460

IF: 2.1; Q2

7.

Milen, M., John, T. M., Pollák, P., & Keglevich, G. (2025). The Direct use of Metallic Ore Minerals as Catalysts in Organic Syntheses. Current Organic Chemistry, 29(2), 97-107.
https://doi.org/10.2174/0113852728327246240821061535

IF: 2.1; Q3

8.

Milen, M., & Pollák, P. (2025, in press) A Biginelli-reakció és reprodukálhatóságának vizsgálata. Magyar Kémiai Folyóirat.

9.

Pollák, P., Barótfi, S., Csóka, I., & Budai-Szűcs, M. (2025). A mesterséges intelligencia szerepe a korai fázisú onkológiai klinikai vizsgálatok tervezésében és megvalósíthatóságában [The role of artificial intelligence in the design and feasibility of early-phase oncology clinical trials]. Orvosi Hetilap, 166(47), 1857-1868.
https://doi.org/10.1556/650.2025.33420

IF: 0.9; Q4

10.

Milen, M., Pollák, P., & Volk, B. (2026) Propylphosphonic Anhydride (T3P®)-Mediated Multicomponent Reactions. Tetrahedron, 194, 135157.

https://doi.org/10.1016/j.tet.2026.135157

IF: 2.2; Q3

10. ACKNOWLEDGEMENTS

I am deeply grateful to my external supervisors, **Mátyás Milen** and **Balázs Volk** (Egis Pharmaceuticals PLC), for their unwavering guidance and encouragement throughout my PhD studies. I owe special thanks to **Gyula Simig**, retired from Egis Pharmaceuticals PLC, for generously sharing his long-standing laboratory expertise. My appreciation also goes to **Gábor Németh** (Egis Pharmaceuticals PLC) for his expert industrial advice in organic and analytical chemistry, and to **István Mándity** (Semmelweis University) for his support in lecturing, funding applications, and flow chemistry. I am thankful to **Péter Ábrányi-Balogh** (HUN-REN TTK Medicinal Chemistry Research Group) for introducing me to computational chemistry and supervising that part of the project.

I also wish to express special appreciation to **Benedek Batizi**, whom I have had the pleasure of supervising from BSc through MSc studies. His commitment, creativity, and perseverance have significantly enriched our joint projects and made mentoring a truly rewarding experience.

I warmly thank the **Department of Organic Chemistry at Semmelweis University** for their collegial help in teaching and presenting my research, and all past and present collaborators from the **Department of Pharmacodynamics**, Department of Organic Chemistry at BME, and **Egis Pharmaceuticals PLC** – including Kamilla Varga, Máté Varga, Alexandra Paszternák, Tamás Tábi, Péter Keglevich, György Keglevich, Boglárka Szele, Zsófia Garádi, András Dancsó, and Simon Horváth – for their valuable contributions.

Finally, I express my heartfelt gratitude to my wife, parents, and grandparents, whose constant support, patience, and understanding have sustained me throughout this journey.

This work was prepared in the framework of 2020-1.1.2-PIACI-KFI-2020-00039 project with the support of the Ministry of Culture and Innovation from the National Research, Development, and Innovation Fund.

Project no. 2023-2.1.2-KDP-2023-00016 has been implemented with the support provided by the Ministry for Culture and Innovation of Hungary from the National Research, Development and Innovation Fund, financed under the KDP-2023 funding scheme.

SYNTHESIS OF INDOLE-BASED ALKALOIDS AND THEIR ANALOGUES

PhD thesis

Patrik Pollák

Semmelweis University Doctoral School

Pharmaceutical Sciences and Health Technologies Division

Supervisors:	Mátyás Milen, PhD Balázs Volk, DSc
Corporate expert:	Gábor Németh, PhD
Internal advisor:	István Mándity, habil. PhD
Official reviewers:	Gábor Krajsovszky, PhD Béla Mátravölgyi, PhD
Head of the Complex Examination Committee:	Romána Zelkó, DSc
Members of the Complex Examination Committee:	László Őrfi, PhD Tamás Gáti, PhD

Budapest
2026

TABLE OF CONTENTS

LIST OF ABBREVIATIONS

Ac – acetyl

ADME – absorption, distribution, metabolism, and excretion

API – active pharmaceutical ingredient

BBB – blood–brain barrier

Boc – *tert*-butyloxycarbonyl

BOILED – brain or intestina estimated permeation

BPR – back pressure regulator

CBS – Corey–Bakshi–Shibata

CCDC – Cambridge Crystallographic Data Centre

CDI – 1,1'-carbonyldiimidazole

Cy – cyclohexyl

DBU – 1,8-diazabicyclo[5.4.0]undec-7-ene

DCC – *N*,*N*′-dicyclohexylcarbodiimide

DCM – dichloromethane

DDQ – 2,3-dichloro-5,6-dicyano-1,4-benzoquinone

DFT – density functional theory

DIAD – diisopropyl azodicarboxylate

DIPE – diisopropyl ether

DIPEA – *N*,*N*-diisopropylethylamine

DMAP – 4-dimethylaminopyridine

DME – dimethoxyethane

DMF – *N*,*N*-dimethylformamide

DMSO – dimethyl sulfoxide

DPPA – diphenylphosphoryl azide

EDCI – 1-ethyl-3-(3-dimethylaminopropyl)carbodiimide

ee – enantiomeric excess

ESI – electrospray ionization

eq – equivalent

FT-IR – Fourier transform infrared

GI – gastrointestinal

HBTU – *N*-[(1*H*-benzotriazol-1-yloxy)(dimethylamino)methylene]-*N*-methylmethanaminium hexafluorophosphate *N*-oxide

HMTA – hexamethylenetetramine

HOBt – hydroxybenzotriazole

HPLC – high-performance liquid chromatography

HPLC-MS – high-performance liquid chromatography - mass spectrometry

Hz – Hertz

IBD – iodobenzene diacetate

IC_{50} – half maximal inhibitory concentration

ID – inner diameter

IR – infrared

LC – liquid chromatography

LED – light-emitting diode

logP – logarithm of the partition coefficient between *n*-octanol and water

Mp – melting point

MS – mass spectrometry

MW – microwave

ND – not determined

NMM – *N*-methylmorpholine

NMR – nuclear magnetic resonance

OD – outer diameter

PE – petroleum ether

Pn – *n*-pentyl

PTSA – *para*-toluenesulfonic acid

Py – pyridine-4-yl

QST3 – Synchronous Transit-Guided Quasi-Newton

R&D – research and development

Red-Al – sodium bis(2-methoxy-ethoxy)aluminium hydride

rt – room temperature

SAR – structure–activity relationship

SMD – solvation model based on density

$t_{1/2}$ – half-life of a reaction

T3P® – propanephosphonic acid anhydride

TBAF – tetrabutylammonium fluoride

TBDPS – *tert*-butyldiphenylsilyl

TEA – triethylamine

Tf – trifluoromethanesulfonate

TFA – trifluoroacetic acid

TFAA – trifluoroacetic anhydride

THF – tetrahydrofuran

TLC – thin-layer chromatography

TPSA – topological polar surface area

TS – transition state

Ts – tosyl

TsDPEN – *N*-tosyl-1,2-diphenyl-ethylenediamine

UPLC – ultra-performance liquid chromatography

UV – ultraviolet

SC-XRD – single crystal X-ray diffraction

1. INTRODUCTION

1.1. Indole-based drug substances and alkaloids

Nowadays, an increasing number of novel compounds containing the indole scaffold are being isolated from natural sources [1]. Furthermore, numerous synthetic indole-based drug candidates are currently undergoing preclinical research and human clinical trials [2]. Several representatives exhibit anticancer [3], antiviral [4], anti-inflammatory [5] activities and some compounds have also proven to be effective for the treatment of depression [6], high blood pressure [7] and migraine [8]. Figure 1 shows a few of the countless chemical structures of indole-containing compounds with medicinal chemistry relevance, which are active pharmaceutical ingredients (also known as drug substances) in clinical use or an investigational new drug. Vilazodone is a serotonin modulator for the treatment of major depressive disorder, pindolol is a non-selective beta blocker used in the treatment of hypertension, and sumatriptan is a serotonin receptor agonist for the treatment of migraine headaches. Indomethacin is a commonly used nonsteroidal anti-inflammatory drug (NSAID), umifenovir is sold and used as an antiviral medication for influenza in Russia and China, and sabazibulin, currently in phase III clinical trials for the treatment of metastatic castration-resistant prostate cancer.

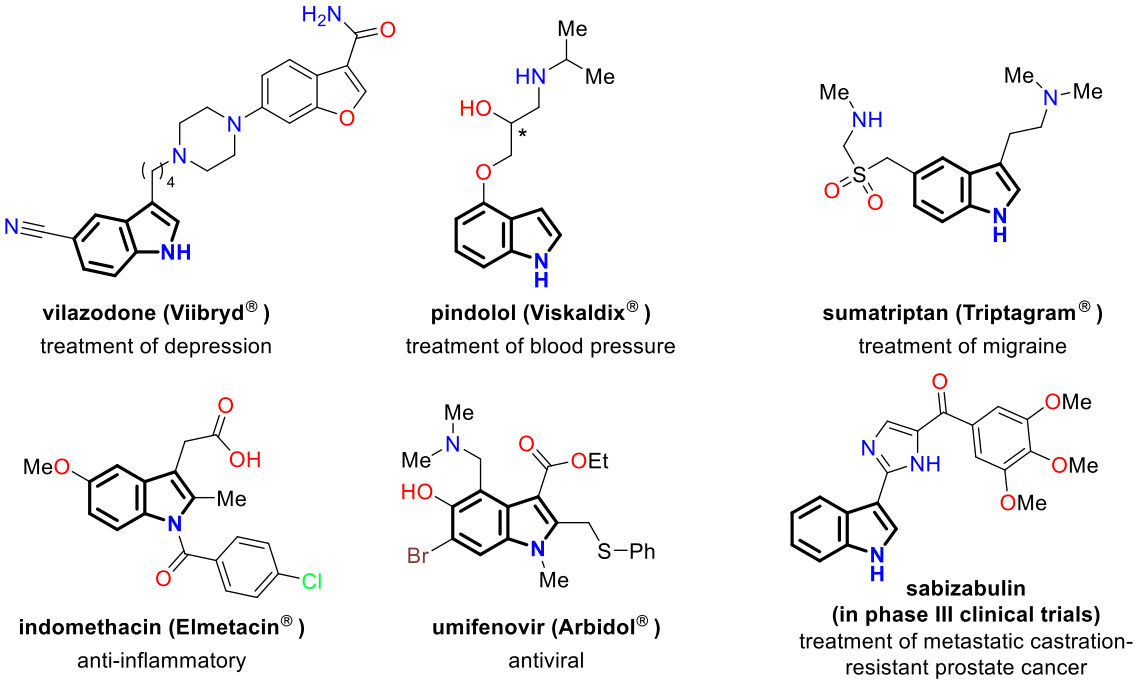

Figure 1. Representatives of indole-based drug substances

Alkaloids, which are defined as naturally occurring, biologically active nitrogen-containing compounds, represent a significant and pharmacologically important class of

drug substances. Figure 2 presents selected examples of indole-based alkaloid structures, several of which also incorporate heteroaromatic moieties such as 1,3-oxazole or 1,3-thiazole rings. Streptochlorin, a 1,3-oxazole-containing alkaloid isolated from the marine bacterium *Streptomyces staurosporeus*, has been reported to induce apoptosis in U937 leukemia cells [9]. Bacillamide A, a 1,3-thiazole-containing metabolite isolated in 2003 from *Bacillus sp.* SY-1, has been identified as an antialgal agent [10]. Camalexin, another 1,3-thiazole-containing compound, was first isolated from *Arabidopsis thaliana* [11] and has been described as a cytotoxic agent [12]. Ellipticine, isolated from *Ochrosia elliptica* [13], acts as a DNA intercalator [14]. Cryptolepinone, obtained from *Cryptolepis sanguinolenta*, has demonstrated antimalarial properties [15]. Finally, echinulin, isolated from *Aspergillus echinulatus* [16], has been reported to possess antiproliferative activity [17].

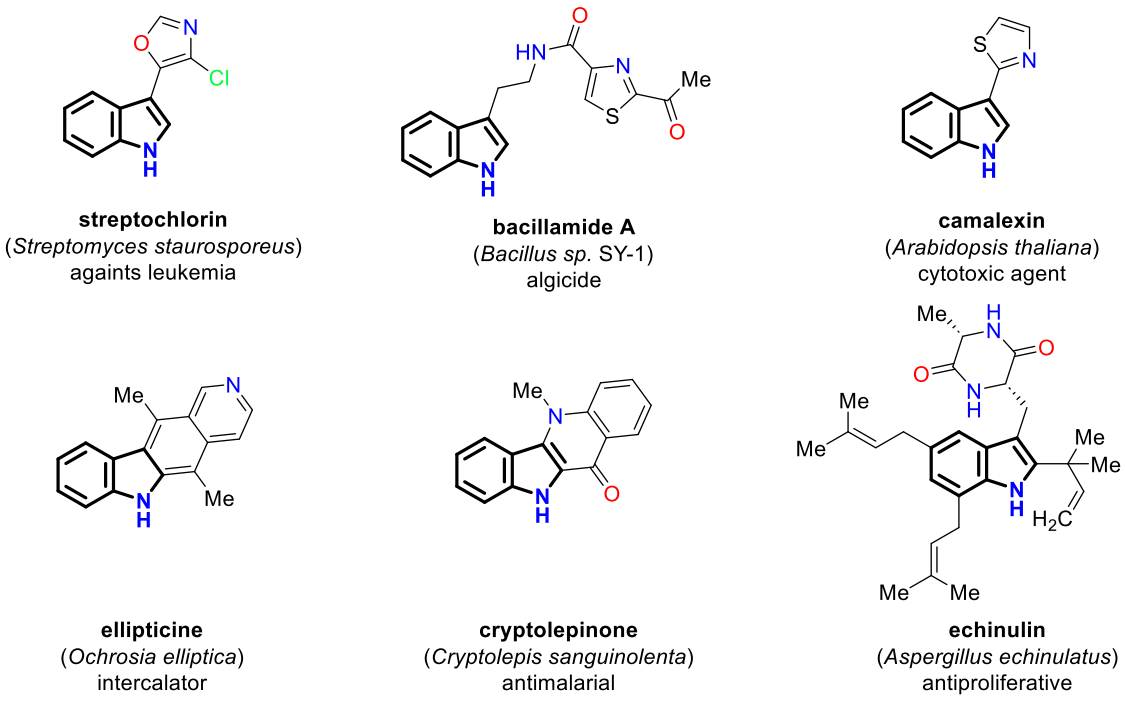

Figure 2. Representatives of indole-based alkaloids

β-Carbolines constitute a structurally distinct class of tricyclic pyridine-fused indole frameworks that are widely found in nature and exhibit remarkable pharmacological potential. This heteroaromatic scaffold is present in several clinically relevant drugs and investigational agents, including vinpocetine, tadalafil, and cipargamin (Figure 3). Notably, vinpocetine holds particular significance in the Hungarian pharmaceutical research, having been developed by Gedeon Richter Plc. (formerly Kőbánya Pharmaceutical Company). Initially synthesized as a semisynthetic derivative of the

natural alkaloid vincamine, vinpocetine is marketed as an over-the-counter medicine under the brand name Cavinton® for the treatment of cerebrovascular disorders [18].

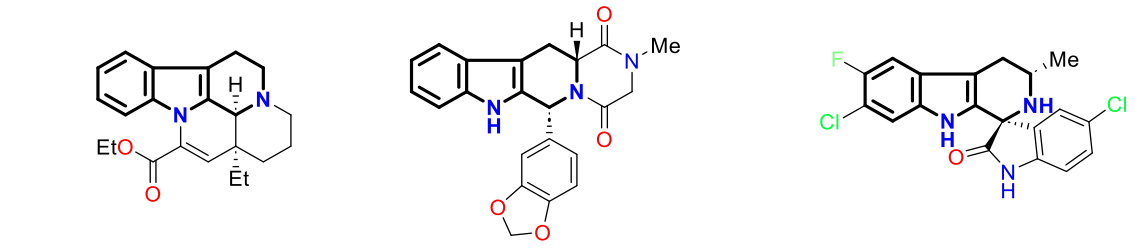

Figure 3. Drug substance representatives of β-carboline type

β-Carboline alkaloids are widely distributed in nature, occurring in diverse biological sources such as plants, foodstuffs, marine organisms, insects, mammals, and even human tissues and body fluids [19]. Representative examples are shown in Figure 4. Yohimbine, isolated from *Pausinystalia johimbe*, is clinically applied for the treatment of sexual dysfunction [20]. Vincamine, first isolated from *Vinca minor*, had its structure elucidated at the Department of Organic Chemistry, Semmelweis University [21,22], and has been utilized in the treatment of dementia [23]. Reserpine, a natural product present in *Rauvolfia serpentina*, has long been applied in the therapeutic control of hypertension [24].

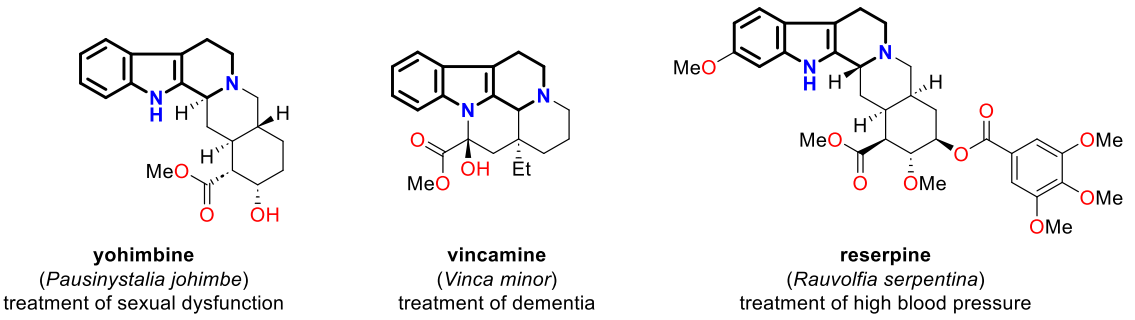

Figure 4. Representatives of β-carboline alkaloids

Given the remarkable biological relevance and structural diversity of indole-based alkaloids, numerous synthetic strategies have been developed to access various functionalized indole derivatives. Among these, the introduction of heteroaromatic substituents, such as oxazole and thiazole rings, has gained particular interest due to their impact on bioactivity and molecular recognition. Therefore, in the following section, the principal synthetic approaches towards oxazolyl- and thiazolylindole systems will be summarized.

1.2. Synthetic approaches towards oxazolyl- and thiazolylindoles

Several naturally occurring oxazolylindole derivatives, notably pimprinine (**1**, R = Me, Scheme 1) and its analogues, differ only in indole and/or oxazole ring substituents [25,26]. The most common synthetic route to the oxazolylindoles involves cyclodehydration (known as Robinson–Gabriel synthesis) of *N*-[2-(1*H*-indol-3-yl)-2-oxoethyl]carboxamides (**2**) in the final step, typically using $POCl_3$. Interestingly, in some cases it slowly occurs just upon boiling in THF. The amides (**2**) are prepared *via* oxidation of *N*-acyltryptamine derivatives (**3**) with DDQ.

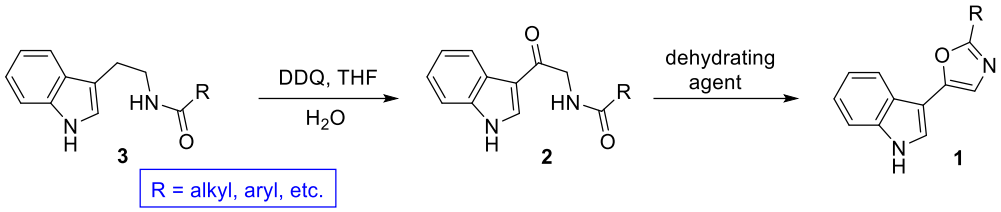

Scheme 1. Representative synthetic route leading to oxazolylindoles (**1**)

Koyama *et al.* reported the synthesis of ketones **2** from ethyl indole-3-carboxylate (**4**, Scheme 2). Reaction of **4** with isocyanomethyllithium in THF afforded 3-(1,3-oxazol-5-yl)-1*H*-indole (**5**), which, after acylation with various carboxylic anhydrides and subsequent hydrolysis, yielded ketones **2**. Cyclization of these intermediates in refluxing $POCl_3$ gave the corresponding substituted oxazolyl–indoles (**1**) [26].

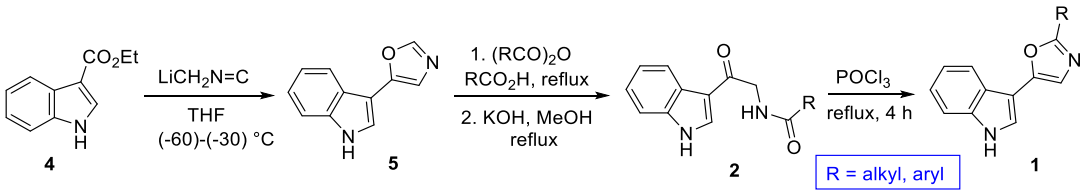

Scheme 2. Synthesis of oxazolylindoles (**5**) from ethyl indole-3-carboxylate (**4**)

Kumar *et al.* synthesized compounds **1** in a five-step sequence (24–32% overall yield) starting from 3-acetyl-1-phenylsulfonylindole (**6**) (Scheme 3). Oxidation with hydroxy(tosyloxy)iodobenzene afforded the tosyloxy derivative (**7**), which was aminated with HMTA to give amine **8**. Subsequent *N*-acylation yielded amides **9**, which underwent cyclodehydration in refluxing EtOH with PTSA to form 5-(3-indolyl)oxazole derivatives **10**. Final removal of the *N*-phenylsulfonyl group led to the target products (**1**) [27].

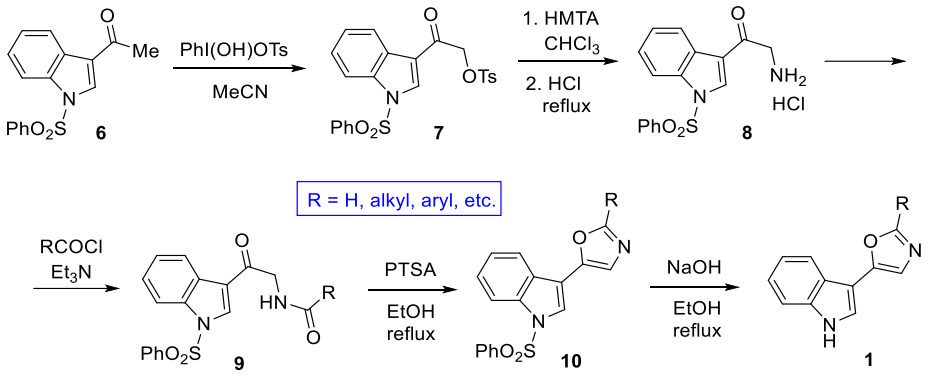

Scheme 3. Synthesis of oxazolylindoles (**1**) from 3-acetyl-1-phenylsulfonylindole (**6**)

A recent study reported the optimization of reaction conditions for the Friedel–Crafts synthesis of acylaminoketone **2** (R = Ph) *via* the reaction of indole (**11**) with 2-phenyl-1,3-oxazol-5(4*H*)-one (**12**), as well as of the Robinson–Gabriel cyclization of **2** (R = Ph) to 3-(2-phenyl-1,3-oxazol-5-yl)-1*H*-indole (**1**, R = Ph) (Scheme 4). Both transformations proceeded in good yields, enabling the development of an efficient one-pot procedure [28].

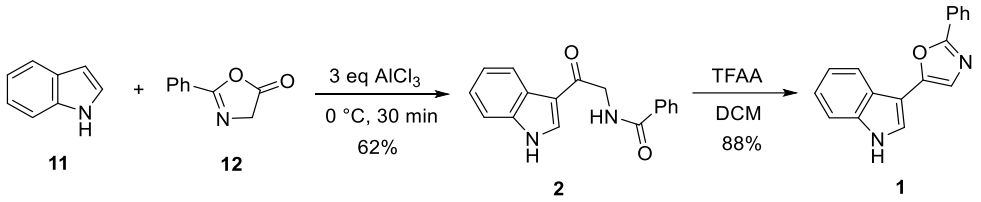

Scheme 4. Synthesis of phenyloxazolylindole **1** *via* Friedel–Crafts acylation of indole followed by Robinson–Gabriel cyclization

Regarding the synthesis of oxazolylindoles bearing a carboxyl group or its derivatives at the 2-position of the oxazole ring, only a single example has been reported. In this study, continuous-flow photoisomerization of isoxazole **13** furnished ethyl 5-(1*H*-indol-3-yl)-1,3-oxazole-2-carboxylate (**1**, Scheme 5) [29].

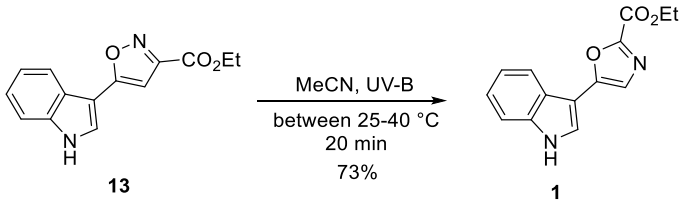

Scheme 5. The sole reported synthetic route to indolyloxazole-carboxylates

The synthesis of certain thiazolylindole derivatives has also been reported. According to a Japanese patent [30], ketone **14** was converted to thiazole **15** *via* treatment with

phosphorus pentasulfide (Scheme 6). Notably, the *in situ* cyclodehydration of intermediate **16** occurred under relatively mild conditions, in refluxing chloroform.

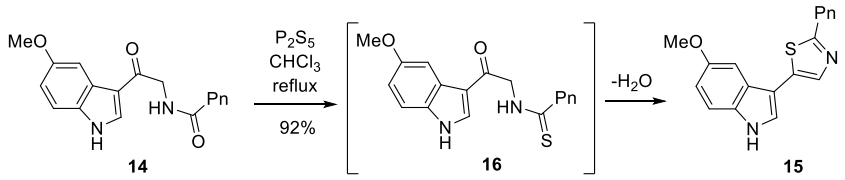

Scheme 6. Synthesis of thiazolylindole **15** from ketone **14**

Similarly, ketone **2** (R = H) reacted with Lawesson's reagent to afford thiazole **17** (R = H) *via* intermediate **18** (R = H, Scheme 7) [31].

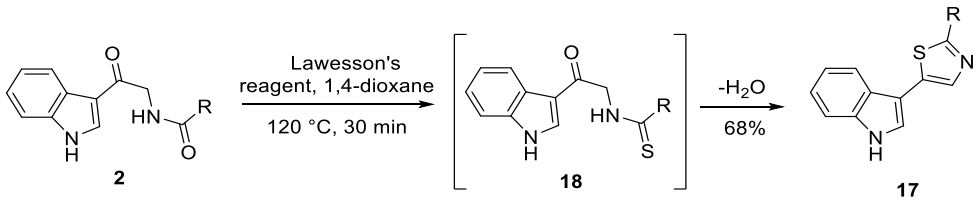

Scheme 7. Synthesis of thiazolylindole **17** (R = H)

Nicolaou *et al.* synthesized key intermediate **18** (R = Ph) *via* thiobenzoylation of amino-ketone **19**. Subsequent cyclization with $POCl_3$ and pyridine under mild conditions afforded thiazolylindole **17** (R = Ph) in good yield (Scheme 8) [32].

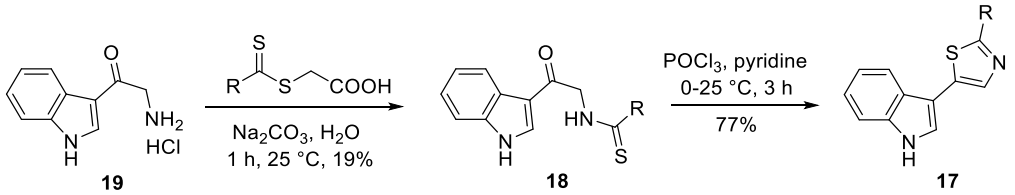

Scheme 8. Two-step synthesis of thiazolylindole **17** (R = Ph) from amino-ketone (**19**)

Al-Azawe reported the synthesis of thiazolylindole **17** (R = Py) *via* the reaction of 3-(2-bromoacetyl)indole (**20**) with pyridine-4-carbothioamide (**21**) (Scheme 9) [33].

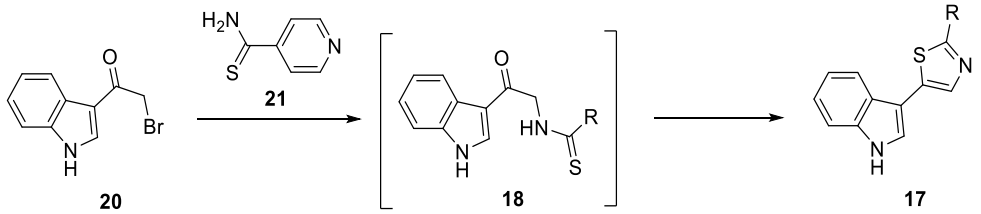

Scheme 9. Synthesis of thiazolylindole (**17**)

As several oxazolyl- and thiazolylindole frameworks occur naturally within bioactive secondary metabolites, these structural motifs have attracted attention in the context of marine and microbial alkaloids. One representative family is the bacillamides, which

combine indole and thiazole moieties in their molecular architecture. To place our synthetic work in a broader biological and chemical context, the next section provides an overview of the literature related to bacillamide-type indole alkaloids.

1.3. Literature summary of bacillamide alkaloids

Rising algal blooms have highlighted the algicidal [34–36] and recently discovered anticancer [37] activities of bacillamide alkaloids. The stereostructures and optical rotations of the chiral bacillamides are shown in Figure 5.

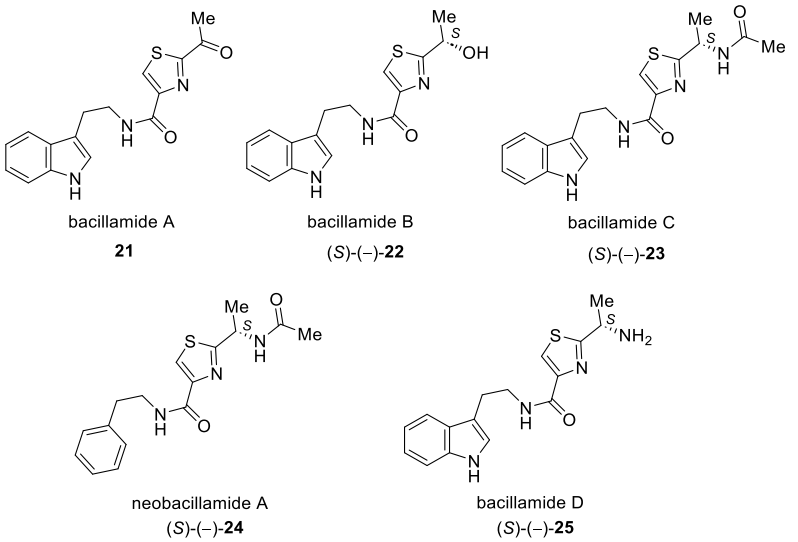

Figure 5. Structure of bacillamide and neobacillamide alkaloids

Okada *et al.* [10] isolated bacillamide A (**21**) from the marine bacterium *Bacillus sp.* SY-1 and elucidated its structure using spectroscopic data. The first synthesis, starting from 4-methylthiazole, was a multistep process with low yields and significant side-product formation due to the use of mixed anhydrides [38]. Later, a more practical route comprising cyclization of (*R*)-cysteine ethyl ester hydrochloride (**26**) with pyruvaldehyde (**27**), oxidation of the product with iodobenzene diacetate to yield ethyl 2-acetyl-1,3-thiazole-4-carboxylate (**28**), and amidation with tryptamine (**29a**) to afford bacillamide A (**21**) (Scheme 10) [39].

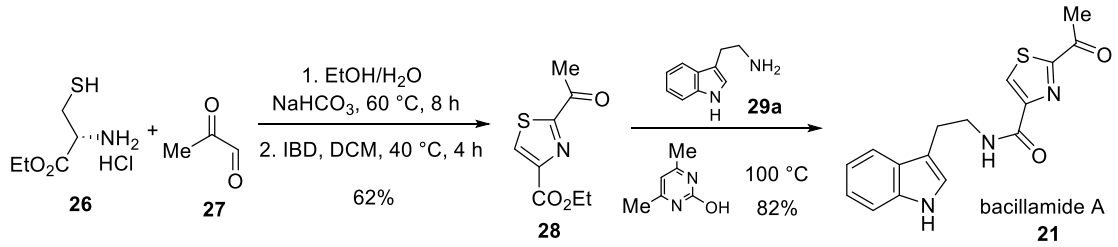

Scheme 10. Synthesis of bacillamide A alkaloid (**21**)

Rowley *et al.* isolated bacillamide B [(*S*)-**22**] from *Bacillus endophyticus*, reporting a positive optical rotation, $[\alpha]_D^{20} = +7.4$ (c 0.095, MeOH), and proposed structure **22** with *R* configuration at the asymmetric center based on circular dichroism comparison with a related compound of known configuration [40]. Bray *et al*. [41] synthesized compound (*S*)-**22** (Scheme 11), *via* reaction of (*S*)-lactic acid derivative **30** with ethyl bromopyruvate (**31**), formation to thiazole **32**, hydrolysis to **33**, and coupling with tryptamine (**29a**). The optical rotation of the product $[\alpha]_D^{20} = +10.1$ (c 0.10, MeOH), led to a revision of bacillamide B alkaloid's stereochemistry from *R* to *S*.

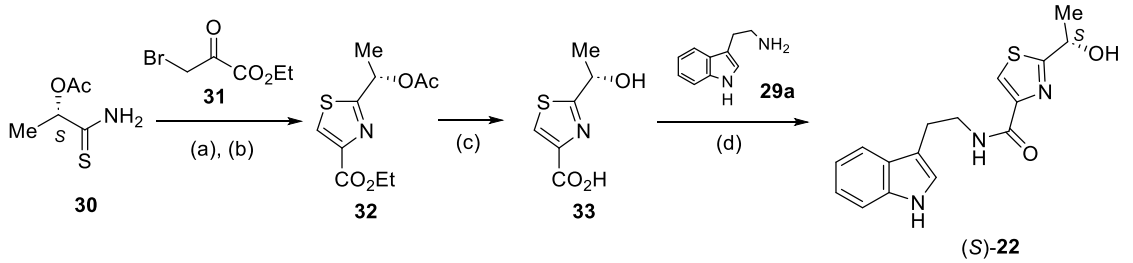

(a) compound **31**, ethyloxirane, *i*-PrOH, 60 °C, 30 min; (b) $(CF_3CO)_2O$, 20 °C, 30 min, 58% (for 2 steps); (c) 2 M LiOH, THF–MeOH; 20 °C, 24 h, 80%; (d) dipyridyl disulfide, Ph_3P, tryptamine (**29a**), CH_2Cl_2, 20 °C, 16 h, 54%.

Scheme 11. The synthesis of bacillamide B [(*S*)-**22**] from (*S*)-lactic acid derivative (**30**) [41]

To resolve the contradictory stereochemical data, Du *et al.* developed syntheses for both enantiomers of compound **22** [42], illustrated in Scheme 12 for (*S*)-**22**. *L*-Cystine (**34**) was converted to β-azidodisulfide **35**, which underwent amidation with tryptamine (**29a**) to afford intermediate **36**. Cyclization yielded thiazoline **38** (diastereomeric ratio not reported), which was dehydrogenated (**39**) and deprotected to give bacillamide B [(*S*)-**22**, $[\alpha]_D^{20} = -1.81$ (c 0.095, MeOH)]. The (*R*)-enantiomer showed $[\alpha]_D^{20} = +2.01$ (c 0.095, MeOH). Reproducing Bray's synthesis, they obtained $[\alpha]_D^{20} = -2.6$ (c 1.0, MeOH), contrary to the $[\alpha]_D^{20} = +10.1$ (c 0.10, MeOH) reported. Re-examination of natural bacillamide B gave $[\alpha]_D^{20} = -1.25$ (c 0.16, MeOH), contrasting with Rowley's $[\alpha]_D^{20} = +7.4$ (c 0.095, MeOH). These results strongly support (*S*)-**22** as the correct structure of bacillamide B.

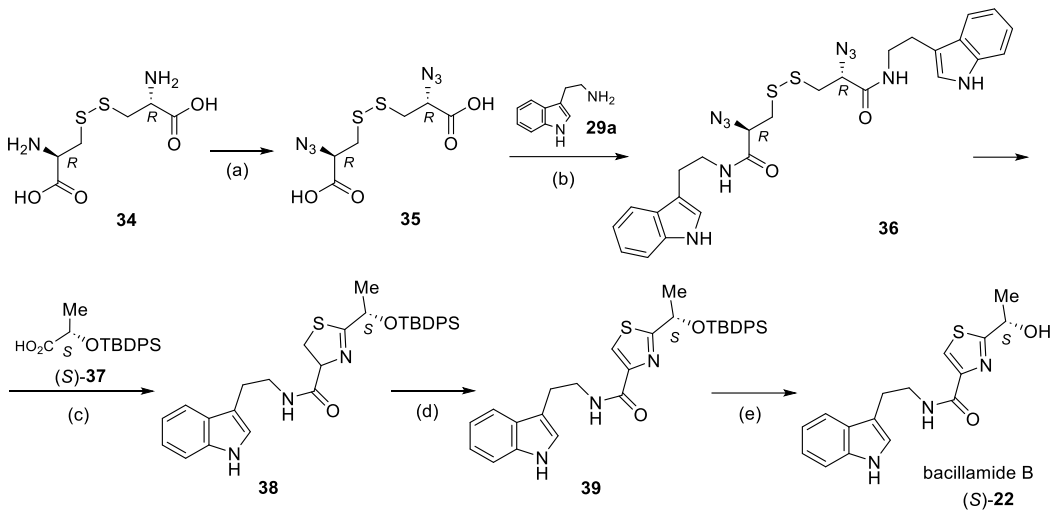

(a) TfN_3, $CuSO_4$, K_2CO_3, 83%; (b) tryptamine (**29a**), DCC, HOBt, rt, 5 h, 85%; (c) EDCI (4.0 eq), DIPEA (8.0 eq), compound **37** (4.0 eq) in DCM, PPh_3 (8.0 eq), reflux, 24 h, 75%; (d) DBU (5.0 eq), $BrCCl_3$ (5.0 eq), DCM, rt, 4 h, 67%; (e) TBAF (1.5 eq), THF, rt, 15 min, 85%.

Scheme 12. Synthesis of bacillamide B [(*S*)-**22**] from (*R*)-cystine (**34**) [42]

Laatsch *et al*. isolated bacillamide C [(*S*)-(–)-**23**], also known as microbiaeratin, from the culture filtrate of *Microbispora aerata* strain IMBAS-11A and elucidated its structure spectroscopically, without addressing stereochemistry or reporting optical rotation [43]. Rowley *et al*. obtained bacillamide C [(*S*)-(–)-**23**] from *Bacillus endophyticus*, measured an optical rotation of $[\alpha]_D^{24} = -15.2$ (c 0.082, MeOH), and proposed an *R* configuration at the asymmetric center based on circular dichroism, as with bacillamide B [40]. Xu *et al*. achieved the first synthesis of (*R*)-**23** and (*R*)-**25** enantiomers of bacillamides C and D, starting from (*R*)-alanine [(*R*)-**40**] (Scheme 13) [44]. This was converted *via* a multistep sequence to thioamide **41**, cyclized to thiazole **42**, hydrolyzed to **43**, and amidated with tryptamine (**29a**) to give compound **44**. Boc deprotection yielded (*R*)-**25**, which underwent *N*-acylation to afford (*R*)-**23**. However, optical rotations of the synthetic products were not determined, so comparison with the natural alkaloids could not be done.

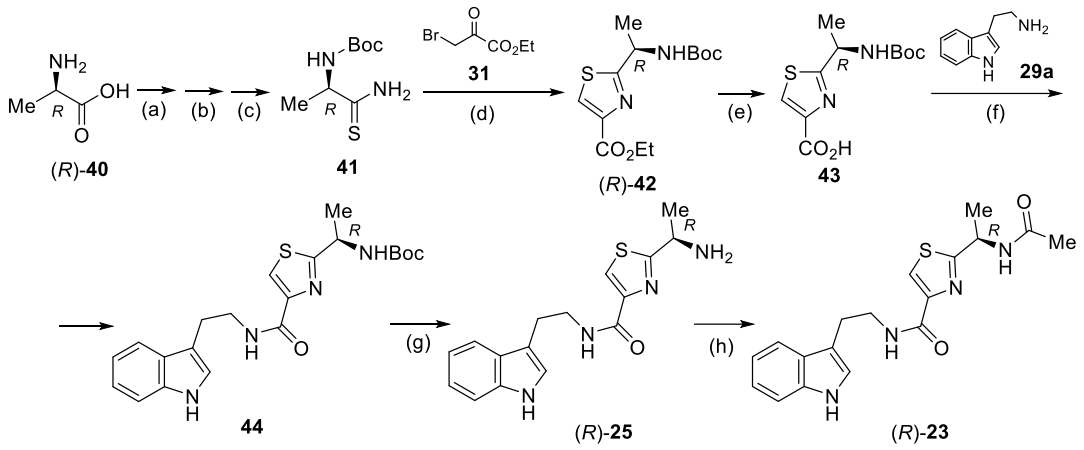

(a) NaOH, 0 °C, $(Boc)_2O$, rt, 92.7%; (b) $(Boc)_2O$, Py, NH_4HCO_3, rt, 92.2%; (c) DME, Lawesson's reagent, rt, 73.4%; (d) 1. $KHCO_3$, DME, −15 °C; 2. compound **31**; 3. TFAA, 2,6-lutidine, −15 °C, 88.7% (for 3 steps); (e) LiOH, THF/MeOH/H_2O; (f) 1. isobutyl chloroformate, NMM, CH_2Cl_2; 2. compound **29a**, NMM, CH_2Cl_2, 56.7% (for 3 steps); (g) AcCl, MeOH, EtOAc, 84.5%; (h) pyridine, Ac_2O, DMAP, 85.4%.

Scheme 13. Synthesis of (*R*)-**23** and (*R*)-**25**, antipodes of bacillamides C and D

Dömling *et al.* [45] reported the synthesis of racemic bacillamide C [(*R*,*S*)-**23**] and its (*R*)-enantiomer [(*R*)-**23**]. The key intermediate thiazole **49** was prepared *via* a multicomponent Ugi reaction (**45**–**48**) employing (*R*)-1-(4-methoxyphenyl)ethylamine (**47**) as the chiral component (Scheme 14). The resulting 1:1 diastereomeric mixture of thiazoles **49** was separated chromatographically. Removal of the chiral auxiliary from (*R*,*R*)-**49** gave ester **50**, which was amidated with tryptamine (**29a**) to yield (*R*)-**23**, exhibiting $[\alpha]_D^{24} = -15.5$ (c 0.155, MeOH). However, as the diastereomers were not rigorously identified, it remains uncertain whether (*R*,*R*)-**49** or (*S*,*R*)-**49** was used in the synthesis, rendering the optical rotation assignment potentially unreliable.

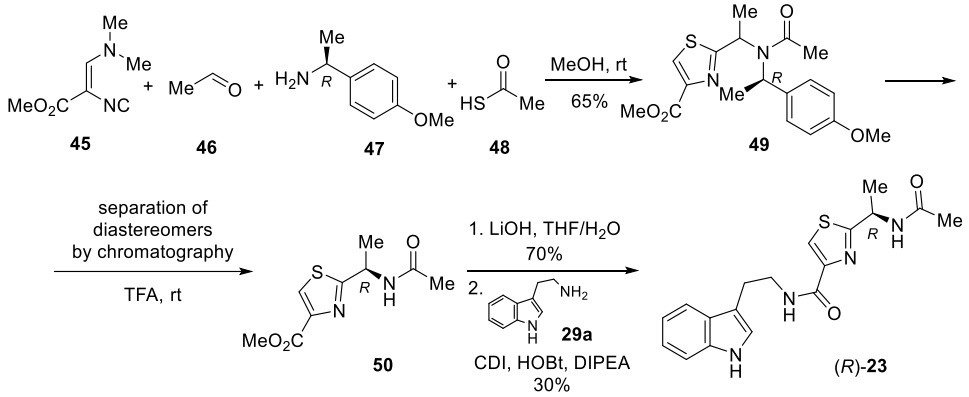

Scheme 14. Synthesis of (*R*)-**23**, antipode of bacillamide C

To resolve the uncertain stereochemical assignment of natural bacillamide C [(*S*)-**23**] [40], Davyt *et al.* synthesized both enantiomers [(*S*)-**23**, (*R*)-**23**] starting from Boc-

protected (*R*)- and (*S*)-alanine (**51**) [46]. Protected (*S*)-alanine (**51**) was converted to nitrile **52**, which reacted with (*R*)-cysteine ethyl ester hydrochloride (**26**) to afford thiazole (*S*)-**42** (Scheme 15). Boc deprotection, *N*-acetylation (**53**), ester hydrolysis (**54**), and amidation with tryptamine (**29a**) yielded bacillamide C [(*S*)-**23**]. These results confirmed that the natural product has (*S*) configuration and a negative optical rotation, $[\alpha]_D^{24} = -23.6$ (c 4.99, MeOH), with its levorotatory character also verified by a biosynthetically produced sample [36].

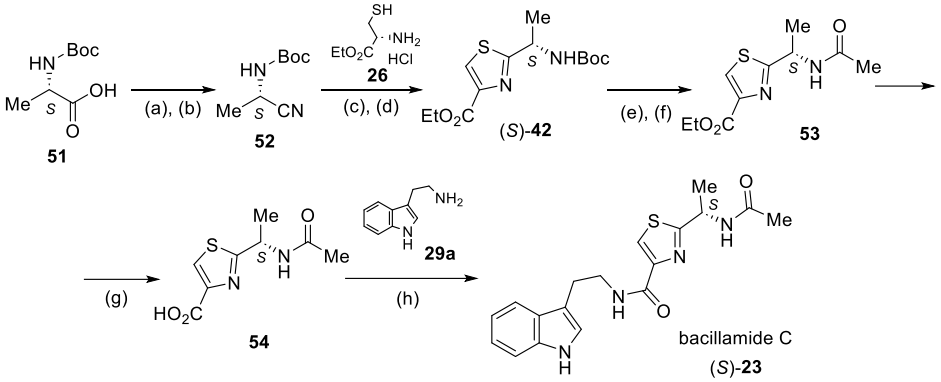

(a) NH_3 gas, $ClCO_2Et$, Et_3N, THF, −10 °C; (b) TFAA, Py, THF, rt, 70% (for two steps); (c) **26**, phosphate buffer pH 7, MeOH, 60 °C; (d) DBU, $BrCCl_3$, CH_2Cl_2, −10 °C, 66% (for two steps); (e) TFA, CH_2Cl_2, rt; (f) Ac_2O, Py, rt, 81% (for two steps); (g) 10% aqueous KOH, THF, rt, 80%; (h) tryptamine (**29a**), HBTU, DIPEA, 0 °C to rt, 29%.

Scheme 15. Synthesis of bacillamide C alkaloid [(*S*)-**23**]

Neobacillamide A [(*S*)-**24**] was isolated from the bacterium *Bacillus vallismortis* C89, and its structure was elucidated by Guo *et al* [47]. Based on previously misassigned literature data [40,43], the authors incorrectly determined the absolute configuration of the levorotatory compound $\{[\alpha]_D^{20} = -16.0$ (c 0.10, MeOH)$\}$. Enantiospecific synthesis of both enantiomers *via* reaction of compound **54** and its antipode with β-phenylethylamine (**55**, Scheme 16) demonstrated that the levorotatory product, neobacillamide A [(*S*)-**24**, $[\alpha]_D^{24} = -24.1$ (c 7.37, MeOH)] was obtained.

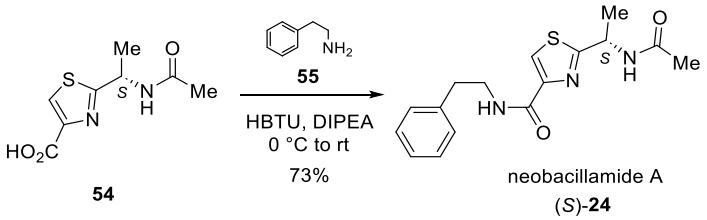

Scheme 16. Synthesis of neobacillamide A alkaloid [(*S*)-**24**]

Bacillamide D [(*S*)-**25**] was the first of the bacillamide alkaloid family to be identified and isolated in 1976 from *Thermoactinomyces* strain TM-6. Its structure was confirmed

by chemical transformations and spectroscopic methods available at that time, and an (*S*) configuration was tentatively assigned to the asymmetric center based on its negative optical rotation, $[\alpha]_D^{20} = -6.0$ (c 1.0, MeOH) [48]. The proposed structure was later confirmed by a synthesis starting from (*S*)-alanine [(*S*)-**40**, Scheme 17] [49]. Conversion to thiazole (**56**) according to established procedures [50] was carried out, followed by *N*-benzyloxycarbonylation (**57**), amidation with tryptamine (**29a**) to give **58**, and deprotection to yield bacillamide D with an optical rotation of $[\alpha]_D^{20} = -2.6$ (c 1.0, EtOH).

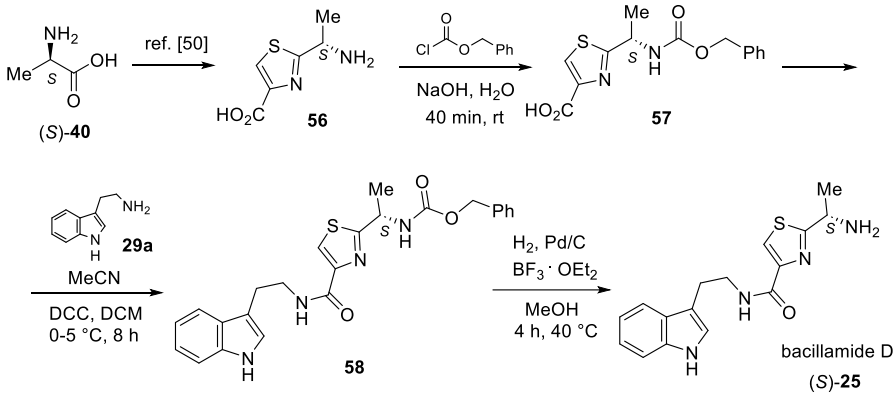

Scheme 17. Synthesis of bacillamide D alkaloid [(*S*)-**25**]

As noted above, Xu *et al.* synthesized (*R*)-**25**, the antipode of bacillamide D [(*S*)-**25**], from (*R*)-alanine [(*R*)-**40**] without reporting optical rotation (Scheme 13) [44] and later prepared (*S*)-**25** from (*S*)-alanine [(*S*)-**40**] [35]. More recently, Gulder *et al.* [37] isolated bacillamide D [(*S*)-**25**] from a bacterial source and converted it to bacillamide C [(*S*)-**23**] by *N*-acetylation. They reported $[\alpha]_D^{20} = -14.7$ (c 2.92, MeOH) for isolated (*S*)-**25** and $[\alpha]_D^{20} = -40.2$ (c 1.02, MeOH) for the synthesized (*S*)-**23**.

1.4. Application of the Bischler–Napieralski reaction in β-carboline synthesis

While the bacillamides illustrate the synthetic and stereochemical challenges associated with thiazolylindole systems, β-carboline alkaloids represent another major subclass of indole-derived natural products with distinct biosynthetic origins and pharmacological profiles. Their synthesis often relies on classical heterocyclization reactions forming the pyridine-fused indole core. One of the most versatile and widely used transformations for this purpose is the Bischler–Napieralski cyclization, which has played a pivotal role in the preparation of β-carboline derivatives. The present section therefore discusses the application of this reaction in β-carboline synthesis.

Discovered in 1893, the Bischler–Napieralski reaction is the key method for synthesizing 3,4-dihydro-β-carbolines (**60**) from tryptamine (**29a**) *via* the corresponding acyltryptamines (tryptamides, **59**, Scheme 18) [51]. Cyclization is typically promoted by dehydrating agents such as $POCl_3$, PCl_5, P_2O_5, etc. [52,53].

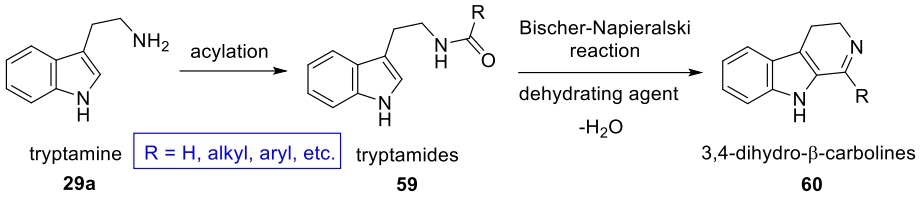

Scheme 18. Preparation of 3,4-dihydro-β-carbolines (**60**) from tryptamine (**29a**) by acylation and subsequent Bischler–Napieralski reaction

Propylphosphonic anhydride (PPAA or T3P®, **61**) is a low-toxicity (compared to other reagents with similar activity), highly soluble coupling agent and water scavenger enabling facile work-up (Scheme 19) [54]. Our research group previously applied T3P® in microwave-assisted Robinson–Gabriel (**62** to **63**) and Bischler–Napieralski reactions of tryptamine derivatives (Scheme 19) [55–57].

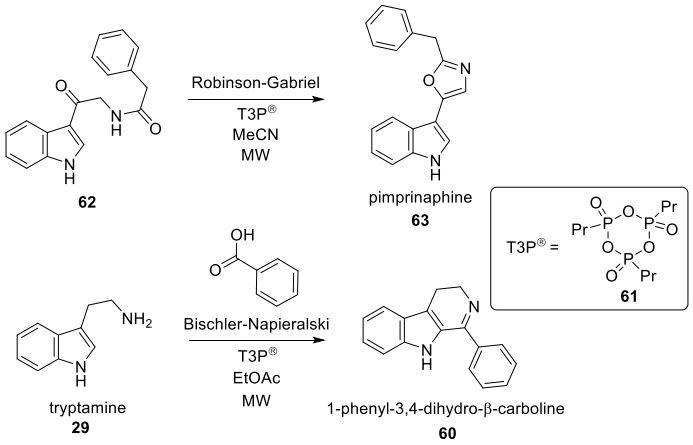

Scheme 19. MW-assisted Robinson–Gabriel synthesis and one-pot acylation-Bischler–Napieralski reaction promoted by T3P®

Microwave treatment of *N*-[2-(1*H*-indol-3-yl)-2-oxoethyl]acetamide (**64**) with T3P® yielded pimprinine (**66**) *via* Robinson–Gabriel synthesis, however there is no data reported about the appropriate Bischler–Napieralski product (**65**) in the literature [55]. In contrast, the analogous reaction of *N*-acetyltryptamine (**67**) is reported to afford harmalan (**68**) through a Bischler–Napieralski pathway (Scheme 20) [56]. In order to clarify the basis of this noteworthy observation, we undertook additional analyses, the outcomes of which are reported in the Results section.

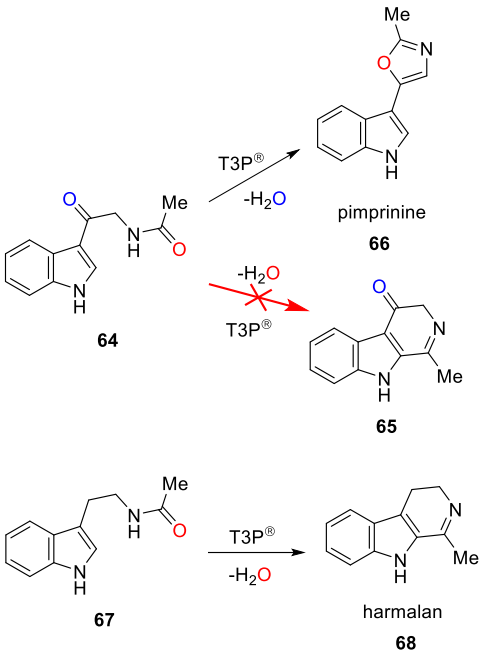

Scheme 20. Experimentally found reactions of **64** and **67** with T3P® reagent

1.5. Overview of β-carboline alkaloids orthoscuticellines A and B

The synthetic utility of the Bischler–Napieralski reaction becomes particularly evident in the preparation of complex natural β-carbolines, including the orthoscuticelline alkaloids. These marine-derived compounds exhibit unique dimeric structures and intriguing stereochemical properties. Consequently, an overview of orthoscuticellines A and B, including their isolation, structural elucidation, and previous synthetic efforts, is provided in the present section.

Several alkaloids, including bis-β-carboline orthoscuticellines A (**69**, meso) and B (**70**, racemate), were recently isolated from the marine bryozoan *Orthoscuticella ventricosa* and structurally characterized (Figure 6) [58]. Both showed modest activity against *Plasmodium falciparum*, the causative agent of malaria.

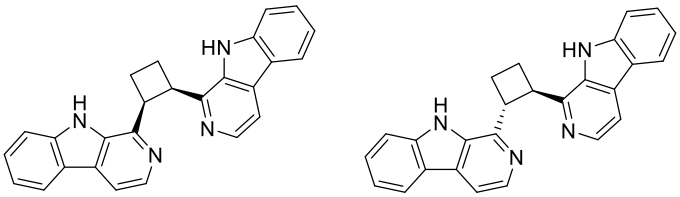

69 (meso form)
orthoscuticelline A

(±)-*trans*-**70**
orthoscuticelline B

Figure 6. Chemical structures of orthoscuticelline A (**69**) and B (**70**) alkaloids

Compounds **69** and (±)-*trans*-**70** were first synthesized by Banwell *et al.* in 2022 [59]. Blue LED irradiation of 1-vinyl-β-carboline (**71**), prepared in four steps from tryptamine

(**29a**) [60], with an iridium(III) catalyst in acetonitrile resulted in a 1:3 mixture of cycloadducts **69** and (±)-*trans*-**70** (Scheme 21) in good yield. The isomers were separated, fully characterized, and the *trans* stereochemistry of (±)-*trans*-**70** was confirmed by SC-XRD. However, the NMR spectra of the isolated compound [58] exhibited significant deviations from those of the synthetic analogue [59], with no explanation provided in the publication.

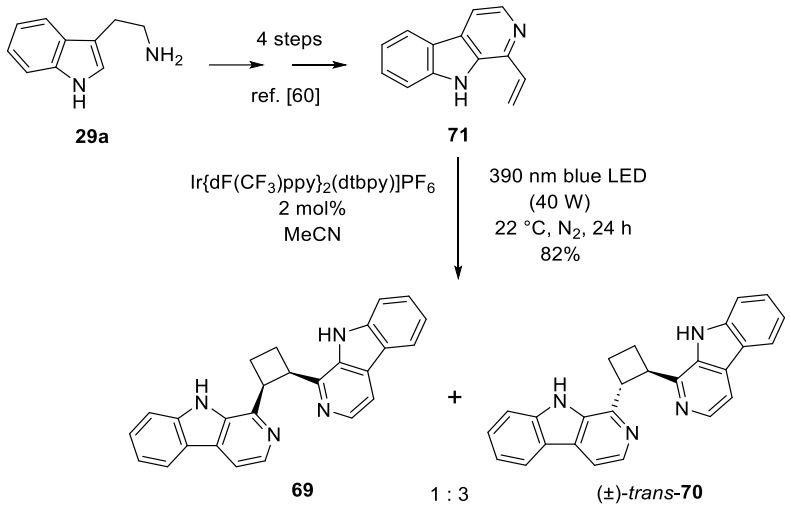

Scheme 21. First total synthesis of orthoscuticelline A (**69**) and B (**70**) alkaloids

Since the photochemical method proved unsuitable for the selective preparation of *cis*- or *trans*-1,2-disubstituted cyclobutanes and the reason for the difference in the NMR spectra was not clear, we aimed the development of an alternative, practical synthetic route to access both stereoisomers, **69** and (±)-*trans*-**70**.

1.6. Literature survey of brevicarine and brevicolline β-carboline alkaloids

Beyond orthoscuticellines, several other β-carboline alkaloids, such as brevicarine and brevicolline, further demonstrate the structural and biosynthetic diversity of this class. Their study also highlights the recurring challenges in regioselective cyclization and oxidation steps characteristic of β-carboline formation. This final section of the introduction therefore summarizes the literature on brevicarine and brevicolline alkaloids, providing additional context for the synthetic investigations presented in this dissertation.

Carex brevicollis DC, a sedge prevalent in Central and South-Eastern Europe, contains several alkaloids, predominantly β-carboline alkaloids (*S*)-brevicolline [(*S*)-**72**] and brevicarine (**73**, Figure 7) [61–63].

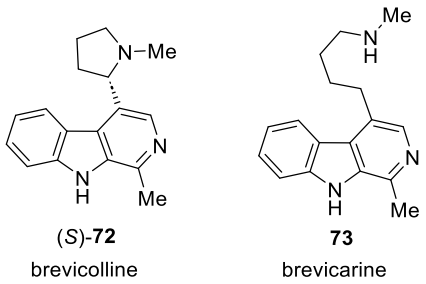

Figure 7. Structure of brevicolline [(*S*)-**72**] and brevicarine (**73**) alkaloids

In a recent study, our research group reported the total synthesis of racemic brevicolline [(±)-**72**] (Scheme 22) [64], enabled by a newly developed triflate intermediate (**74**) suitable for C–C bond formation at position 4 of the β-carboline *via* cross-coupling. Sonogashira coupling of **74** with *N*-(3-butynyl)phthalimide (**75**) afforded **76**, which, after phthalimide cleavage with methylhydrazine, yielded butynylamine **77**. The synthesis proceeded *via* the cyclization to dihydropyrrole **78**, and subsequent reduction to **79**, which upon *N*-methylation led to (±)-**72**. Resolution *via* chiral chromatography then yielded the natural product (*S*)-brevicolline [(*S*)-**72**].

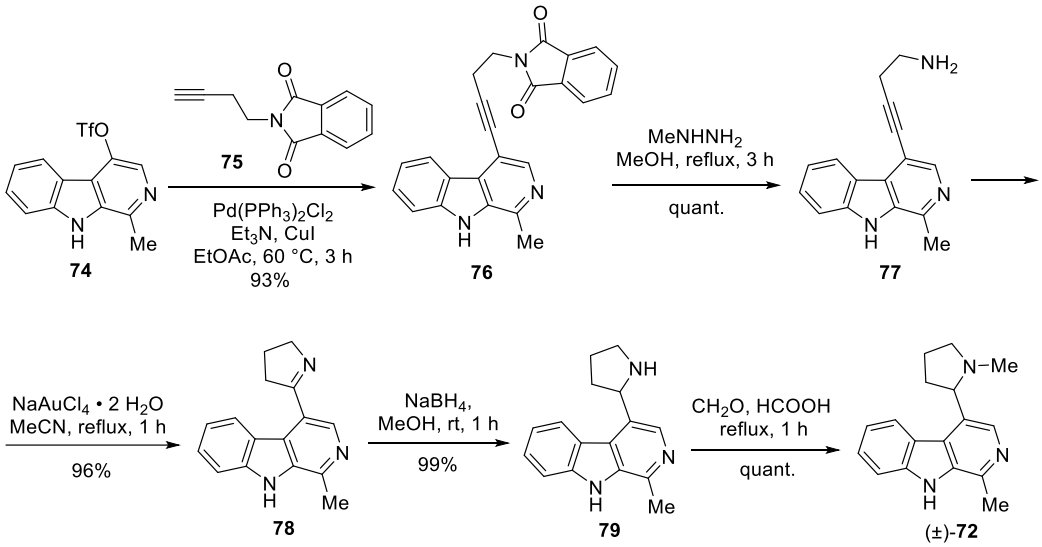

Scheme 22. Synthesis of racemic brevicolline [(±)-**72**] from key triflate intermediate (**74**)

To extend this work, we pursued the synthesis of brevicarine (**73**), a structurally related alkaloid. The first reported semi-synthetic route involved a short sequence from naturally derived (*S*)-brevicolline [(*S*)-**72**] (Scheme 23) [65]. Heating (*S*)-**72** in benzoyl chloride induced pyrrolidine ring opening and *N*-benzoylation to give **80**, which upon debenzoylation yielded **81**. Catalytic hydrogenation of its side-chain C=C bond furnished brevicarine (**73**).

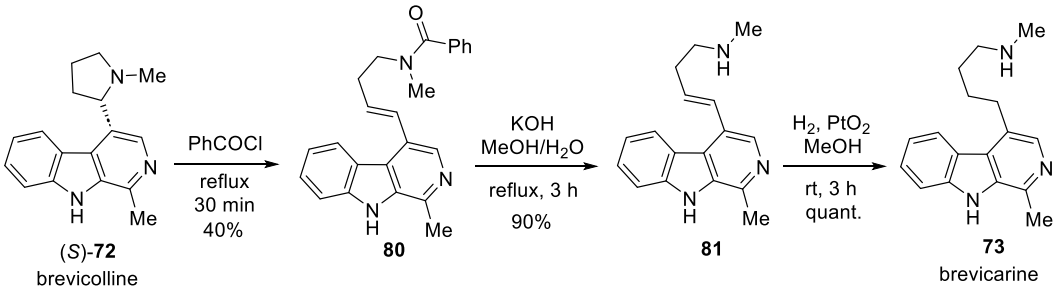

Scheme 23. Semi-synthesis of brevicarine (**73**) from isolated brevicolline [(*S*)-**72**]

The first total synthesis of brevicarine (**73**) is outlined in Scheme 24 [66,67]. Condensation of indole (**82**) with 1-methylpiperidone (**83**) afforded **84** [68], which underwent *N*-alkylation with benzyl bromide to give quaternary ammonium salt **85**. Reaction of **85** with the potassium salt of **86** yielded ring-opened derivative **87**. Subsequent removal of the benzylsulfanyl group, Beckmann rearrangement of the oxime derived from ketone **88**, and cyclization produced β-carboline **89**, which was dehydrogenated and debenzylated to brevicarine (**73**), obtained as the dihydrochloride salt.

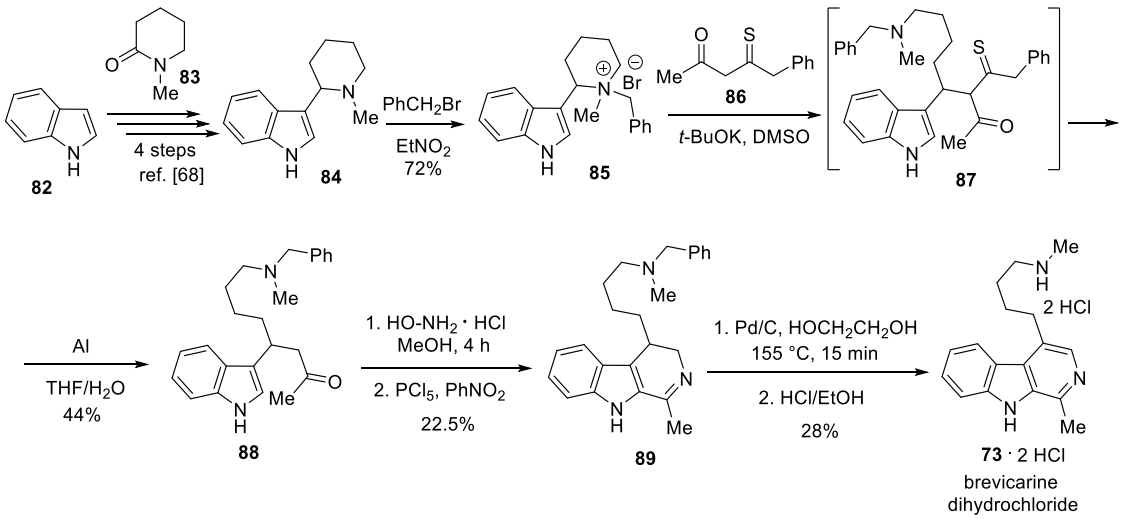

Scheme 24. The first total synthesis of brevicarine (**73**) alkaloid

Müller *et al.* developed an alternative synthesis of brevicarine (**73**, Scheme 25). Treatment of nitrovinylindole (**90**) with *N*-methylpyrrole (**91**) afforded compound **92**, which was hydrogenated under harsh conditions (100 °C, 130 bar) to reduce both the pyrrole ring and the nitro group [69]. *N*-Acetylation yielded a mixture of diastereomeric racemates (**93**), which was cyclized to β-carboline derivatives **94**. Heating **94** in pivalic acid with catalytic trifluoroacetic acid furnished brevicarine (**73**).

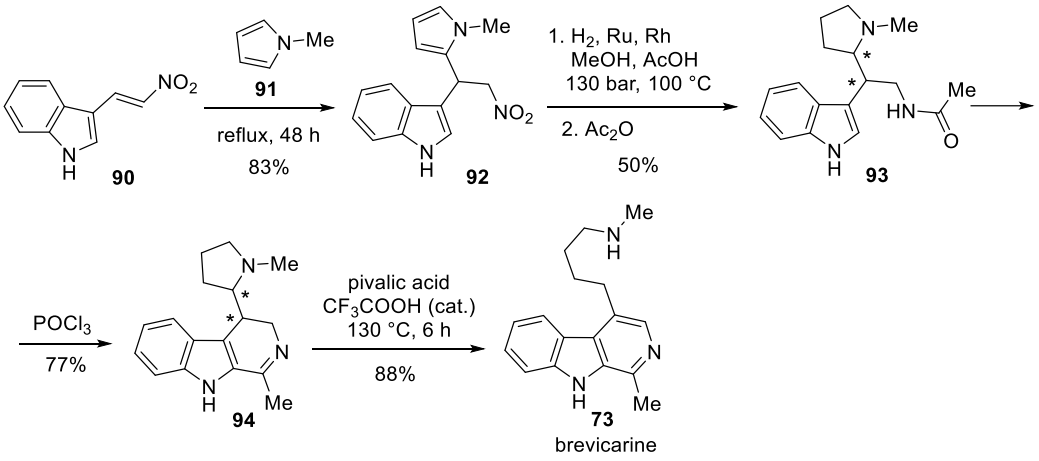

Scheme 25. Synthesis of brevicarine (**73**) from nitrovinylindole (**90**)

The sedge *Carex brevicollis* DC has long been known to induce smooth muscle contraction [62], an effect likely related to the oxytocic activity of (*S*)-brevicolline [(*S*)-**72**], studied in pregnant mammals [70,71]. First isolated in 1960 [63], (*S*)-brevicolline exhibits antibacterial and antifungal activity through photosensitization [72] and has been used in human obstetrics and veterinary infertility treatment [62]. Synthetic and biogenetic studies, including the conversion of (*S*)-**72** to brevicarine (**73**) (Scheme 23), suggest that (*S*)-brevicolline may serve as a biosynthetic precursor of brevicarine in plants [65].

Brevicarine (**73**), first isolated in 1967 from *Carex brevicollis* DC [73], has since been identified in several other natural sources, including *Tambourissa ficus* (Mauritian endemic fruit) [74], *Asparagus racemosus* (linn seed) [75], and extracts of *Phellinus linteus smilax corbularia* and *Phellinus linteus smilax glabra* [76]. Reported pharmacological activities include antioxidant [74], antibacterial against *Mycobacterium tuberculosis* [77], antiproliferative against triple-negative breast cancer [78], anti-Parkinson [75], and skin anti-inflammatory effects [79]. The dihydrochloride salt has shown superior *in vivo* antiarrhythmic efficacy in rats, cats, and rabbits compared to quinidine and novocainamide [80]. *N*-Methylbrevicarine, a semi-synthetic derivative, has demonstrated *in silico* activity as a non-peptide malignant brain tumor antagonist, with hits on three MBT-containing proteins [81]. While *Carex brevicollis* DC has been reported to exhibit teratogenic effects in animals [61,82], possibly linked to its β-carboline alkaloids, further evidence is required. Given their high medicinal potential, the total synthesis of these alkaloids and related analogues remains essential for structural confirmation and securing material for pharmacological evaluation.

2. OBJECTIVES

The primary objective of my PhD research, conducted at the Directorate of Drug Substance Development at Egis Pharmaceuticals PLC and under the academic affiliations of Department of Organic Chemistry and Center of Pharmacology and Drug Research & Development, Semmelweis University, was to contribute to the synthesis and development of novel bioactive compounds with potential pharmaceutical applications. The work was carried out within the framework of the Cooperative Doctoral Program, emphasizing research, development, and innovation, with a strong focus on applicability in industrial settings.

The central aim of the project was the synthesis of natural alkaloids (namely bacillamides, orthoscuticellines A–B, brevicarine, brevicolline) and structurally modified synthetic analogues (oxazolyl- and thiazolylindoles, 1-substituted β-carbolines), with a particular emphasis on compounds containing the indole scaffold as an important skeleton in many biologically active molecules. In line with the growing interest in indole alkaloids as sources of new drug candidates, I set out to develop and optimize synthetic routes that enable the efficient production of such compounds. Where possible, efforts were made to improve existing synthetic methodologies with attention to the principles of green chemistry.

Another key objective was to support pharmacological evaluation of the synthesized new compounds through interdisciplinary collaboration. These studies aimed to assess antiproliferative and cytotoxic activities, providing feedback for further compound optimization and SAR studies in the project of oxazolyl- and thiazolylindoles and 1-substituted β-carbolines.

A further aim was to develop a continuous-flow synthesis of 1-substituted β-carbolines and dihydro-isoquinolines *via* the Bischler–Napieralski reaction and also to model T3P®-induced cyclization reactions in order to understand why, in most cases, the Robinson–Gabriel synthesis proceeds more readily than the Bischler–Napieralski reaction.

Beyond the scientific goals, I prioritized mentoring younger students and fostering knowledge transfer. I involved undergraduate and MSc students in ongoing projects, giving them hands-on experience in an industrial R&D environment and complementing their academic training with practical skills, thereby strengthening the bridge between university education and pharmaceutical industry needs.

3. METHODS

3.1. Reagents, solvents and purification methods

All reagents and solvents were purchased from commercial sources and used without further purification. Purifications by flash column chromatography were carried out using Merck 107736 silica gel 60 H with a hexane–EtOAc, PE–EtOAc, or DCM–MeOH solvent system. Analytical samples of synthesized compounds were obtained by recrystallization from the solvents or solvent mixtures given in the publications or in chapter Discussion. For enantiomer separations, chiral chromatography has been used, the parameters of which are given in the corresponding publications.

3.2. Analytical techniques for compound characterization

Reactions were monitored by TLC carried out on silica gel plates (60 F_{254}) using UV light as visualizing agent, or by HPLC-MS on a Shimadzu LC-40 HPLC equipments (Kyoto, Japan) equipped with diode array detector and an LCMS-2020 quadrupole mass spectrometer. Column: Acquity UPLC bridged ethylene hybrid (BEH) C_{18} 50 × 3 mm, 1.7 μm. All melting points were determined on a Büchi B-540 capillary melting point apparatus and are uncorrected. IR spectra were obtained on a Bruker Alpha FT-IR spectrometer in transmission mode in KBr pellets or film. ^{1}H NMR, ^{13}C NMR and ^{31}P NMR spectra were recorded in $CDCl_3$ or DMSO-d_6 or CD_3OD solution in 5 mm tubes at room temperature, on a Bruker Avance III HD (600, 150 and 242 MHz for ^{1}H, ^{13}C and ^{31}P NMR spectra, respectively) or a Bruker Avance III (400, 100 and 162 MHz for ^{1}H, ^{13}C and ^{31}P NMR spectra, respectively) spectrometer with the deuterium signal of the solvent as the lock and TMS as the internal standard. Chemical shifts (δ) and coupling constants (J) are given in ppm and in Hz, respectively. The following abbreviations are used to designate multiplicities: s = singlet, d = doublet, t = triplet, q = quartet, m = multiplet, br = broad. High-resolution mass spectra (HRMS) were recorded on a Bruker Q-TOF MAXIS Impact mass spectrometer coupled with a Waters I-Class UPLC system (for $[M+H]^+$) or on an Agilent 7250 Q-TOF mass spectrometer coupled to an Agilent 8890 gas chromatographic system (for $[M]^+$). Chiral stationary phase HPLC measurements were carried out using an Agilent 1200 HPLC instrument. SC-XRD measurements were carried out on a Rigaku R-Axis Spider instrument with image plate detector. SC-XRD structures of compounds have been uploaded to the CCDC database.

3.3. Computational chemistry software

The DFT level computations at the M062X/6–31+G (d,p) level of theory were performed considering the solvent effect (SMD implicit solvent model) of DMF (dielectric constant is 36.71) by the Gaussian 16 program package [83–86] at 120°C. This was followed by single point calculations at the M062X/6-311++G (3df,3pd) level of theory to result in more accurate energy values. The geometries of the molecules were optimized in all cases, and frequency calculations were also performed to assure that the structures are in a local minimum or in a saddle point. The transition states were optimized with the QST3 or the TS (berny) method. Transition states were identified by having one imaginary frequency in the Hessian matrix, and IRC calculations were performed in order to prove that the transition states connect two corresponding minima.

3.4. Flow chemistry apparatus

The continuous flow experiments were performed in a laboratory scale flow reactor system which comprises syringe pumps (manufacturer: H-ION, HI-SY100, 2×5 mL syringe, 0.01–3.50 mL min^{-1}), heated coil reactor (reactor volume: 5 mL, 1.8 mm ID, 1/8" OD, SS316L material, 1.96 m length), back-pressure regulator (manufacturer: H-ION, HI-BP100, 316Ti material, 0.0–100.0 bar) and cooling loop (volume: 0.5 mL, 1 mm ID, 1/16" OD, 0.64 m length) (Figure 8). Before usage and after the reactions, the system was washed thoroughly with MeOH–MeCN 1:1 solution (1 mL min^{-1}). Samples have been collected after reaching stationary conditions (ca. 2 h).

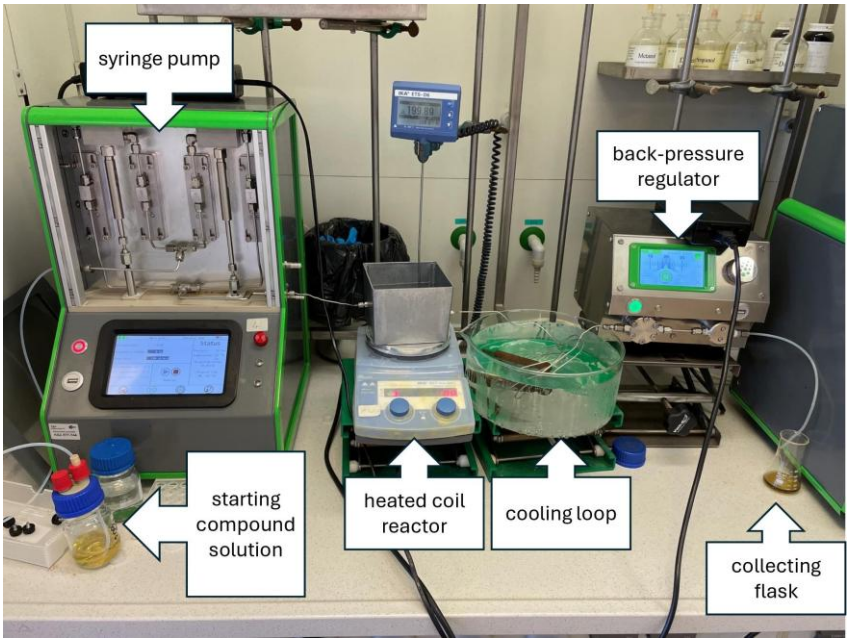

Figure 8. Flow reactor system

4. RESULTS

General procedure for the preparation of α-aminophosphonate derivatives of β-carboline (132a–j). The appropriate β-carboline aldehyde (**135a** or **135b**, 0.5 mmol), aniline derivative (**136**, 0.5 mmol), phosphite (**137**, 0.5 mmol) and $Mg(ClO_4)_2$ (10 mol%, 0.05 mmol) were stirred in neat at 80 °C for 2−4 hours (for reaction times, see Scheme 38). After the reaction was complete (or when no more progress was observed in the reaction), the residue was dissolved in a DCM–MeOH 1:1 mixture and it was purified by flash column chromatography on silica gel (DCM–MeOH) to afford pure α-aminophosphonates **132a–j** (for yields, see Scheme 38).

Diethyl [9*H*-β-carbolin-1-yl(phenylamino)methyl]phosphonate (132a). Colourless crystals. Mp 173–175 °C (MeCN) IR (KBr): 3216, 3172, 1601, 1237, 1050, 1020, 971, 752, 742 cm^{-1}. ^1H NMR ($CDCl_3$, 600 MHz): δ 10.25 (br s, 1H), 8.43 (d, J = 5.2 Hz, 1H), 7.97 (m, 1H), 7.87 (dd, J_1 = 1.2 Hz, J_2 = 5.1 Hz, 1H), 7.32 (m, 1H), 7.15 (m, 1H), 7.14 (m, 1H), 7.11 (m, 2H), 6.85 (m, 2H), 6.69 (m, 1H), 5.84 (t, J = 7.3 Hz, 1H), 5.48 (dd, J_1 = 7.0 Hz, J_2 = 20.9 Hz, 1H), 4.17 (m, 1H), 4.12 (m, 1H), 4.07 (m, 1H), 3.96 (m, 1H), 1.26 (t, J = 7.0 Hz, 3H), 1.12 (t, J = 7.0 Hz, 3H) ppm. ^{13}C NMR ($CDCl_3$, 150 MHz): δ 146.9, 140.8, 138.3, 138.1, 134.4, 130.2, 129.1, 128.2, 121.2, 119.7, 118.7, 114.5, 114.2, 111.9, 64.0, 58.1, 57.1, 16.4, 16.2 ppm. ^{31}P NMR ($CDCl_3$, 162 MHz): δ 22.4 ppm. HRMS (ESI) calcd. for $C_{22}H_{25}N_3O_3P^+$ $[M+H]^+$ 410.1628; found: 410.1625.

Diethyl {9*H*-β-carbolin-1-yl[(4-fluorophenyl)amino]methyl}phosphonate (132b). Colourless crystals. Mp 191–193 °C (MeCN) IR (KBr): 3217, 1506, 1237, 1053, 1019, 968, 742 cm^{-1}. ^1H NMR ($CDCl_3$, 400 MHz): δ 10.20 (br s, 1H), 8.43 (d, J = 5.2 Hz, 1H), 8.00 (m, 1H), 7.88 (dd, J_1 = 1.7 Hz, J_2 = 5.2 Hz, 1H), 7.37 (m, 1H), 7.23 (m, 1H), 7.17 (m, 1H), 6.81 (m, 2H), 6.77 (m, 2H), 5.69 (t, J = 7.1 Hz, 1H), 5.38 (dd, J_1 = 7.1 Hz, J_2 = 20.7 Hz, 1H), 4.13 (m, 1H), 4.08 (m, 2H), 3.96 (m, 1H), 1.25 (t, J = 7.1 Hz, 3H), 1.12 (t, J = 7.1 Hz, 3H) ppm. ^{13}C NMR ($CDCl_3$, 100 MHz): δ 156.5, 143.2, 140.9, 138.1, 134.4, 130.3, 128.4, 121.4, 121.3, 119.9, 115.6, 115.3, 114.6, 112.0, 64.0, 64.0, 58.3, 16.4, 16.2 ppm. ^{31}P NMR ($CDCl_3$, 162 MHz): δ 22.3 ppm. HRMS (ESI) calcd. for $C_{22}H_{24}FN_3O_3P^+$ $[M+H]^+$ 428.1534; found: 428.1538.

Diethyl {9*H*-β-carbolin-1-yl[(4-chlorophenyl)amino]methyl}phosphonate (132c). Yellow crystals. Mp 188–190 °C (DIPE) IR (KBr): 3455, 3220, 2994, 1625, 1599, 1491, 1325, 1236, 1201, 1051, 1020, 965 cm^{-1}. ^1H NMR (DMSO-d_6, 600 MHz): δ 11.71 (s, 1H), 8.34 (d, J = 5.2 Hz, 1H), 8.23 (d, J = 7.9 Hz, 1H), 8.07 (d, J = 4.8 Hz, 1H), 7.66 (d,

J = 8.2 Hz, 1H), 7.58 (t, *J* = 7.6 Hz, 1H), 7.26 (t, *J* =7.4 Hz, 1H), 7.06 (d, *J* = 8.9 Hz, 2H), 6.88 (d, *J* = 8.9 Hz, 2H), 6.53 (dd, J_1 = 10.0 Hz, J_2 = 4.6 Hz, 1H), 5.69 (dd, J_1 = 23.0 Hz, J_2 =10.0 Hz, 1H), 4.04 (m, 2H), 3.89 (m, 1H), 3.70 (m, 1H), 1.17 (t, *J* = 7.0 Hz, 3H), 0.91 (t, *J* = 7.0 Hz, 3H) ppm. ^{13}C NMR (DMSO-d_6, 150 MHz): δ 146.4, 140.6, 139.5, 137.8, 134.2, 128.7, 128.6, 128.4, 122.1, 120.8, 120.7, 119.7, 115.1, 114.5, 112.0, 62.9, 62.6, 54.0, 16.5, 16.2 ppm. ^{31}P NMR (DMSO-d_6, 242 MHz): δ 21.2 ppm. HRMS (ESI) calcd. for $C_{22}H_{23}ClN_3O_3P^+$ $[M]^+$ 443.1166; found: 443.1171.

Diethyl {[(4-bromophenyl)amino](9*H*-β-carbolin-1-yl)methyl}phosphonate (132d). Colourless crystals. Mp 197–200 °C (MeCN) IR (KBr): 3335, 3241, 2982, 1594, 1503, 1216, 1060, 1028, 968, 812, 738 cm^{-1}. ^{1}H NMR ($CDCl_3$, 600 MHz): δ 10.32 (br s, 1H), 8.43 (d, *J* = 4.8 Hz, 1H), 7.96 (d, *J* = 7.8 Hz, 1H), 7.88 (d, *J* = 4.8 Hz, 1H), 7.32 (m, 1H), 7.17 (m, 1H), 7.13 (m, 1H), 7.11 (m, 1H), 6.73 (d, *J* = 9.0 Hz, 2H) 5.99 (br s, 1H), 5.48 (d, *J* = 19.8 Hz, 1H), 4.15 (m, 3H), 3.99 (m, 1H), 2.26 (br s, 1H), 1.26 (t, *J* = 7.2 Hz, 3H), 1.14 (t, *J* = 7.2 Hz, 3H) ppm. ^{13}C NMR ($CDCl_3$, 150 MHz): δ 145.8, 141.0, 137.6, 134.2, 131.8, 128.5, 121.3, 121.1, 119.9, 115.7, 114.7, 111.8, 110.4, 64.2, 57.6, 56.6, 16.4, 16.2 ppm. ^{31}P NMR ($CDCl_3$, 242 MHz): δ 21.7 ppm. HRMS (ESI) calcd. for $C_{22}H_{24}BrN_3O_3P^+$ $[M+H]^+$ 488.0733; found: 488.0736.

Diethyl {9*H*-β-carbolin-1-yl[(4-methylphenyl)amino]methyl}phosphonate (132e). Colourless crystals. Mp 138–140 °C (MeCN) IR (KBr): 3354, 3220, 2981, 1614, 1518, 1215, 1059, 1029, 965, 812, 740 cm^{-1}. ^{1}H NMR ($CDCl_3$, 600 MHz): δ 10.15 (br s, 1H), 8.43 (d, *J* = 4.8 Hz, 1H), 8.00 (d, *J* = 7.2 Hz, 1H), 7.87 (d, J_1 = 4.2 Hz, 1H), 7.39 (m, 1H), 7.26 (m, 1H), 7.16 (m, 1H), 6.91 (d, *J* = 7.8 Hz, 2H), 6.75 (d, *J* = 8.4 Hz, 2H), 5.58 (s, 1H), 5.40 (d, *J* = 20.4 Hz, 1H), 4.11 (m, 3H), 3.92 (m, 1H), 2.16 (s, 3H), 1.25 (t, *J* = 7.2 Hz, 3H), 1.10 (t, *J* = 6.6 Hz, 3H) ppm. ^{13}C NMR ($CDCl_3$, 150 MHz): δ 144.6, 140.9, 138.5, 138.1, 134.4, 130.2, 128.3, 128.1, 121.3, 119.8, 114.4, 112.0, 63.9, 58.7, 57.7, 20.3, 16.4, 16.2 ppm. ^{31}P NMR ($CDCl_3$, 242 MHz): δ 22.5 ppm. HRMS (ESI) calcd. for $C_{23}H_{27}N_3O_3P^+$ $[M+H]^+$ 424.1785; found: 424.1789.

Diethyl {9*H*-β-carbolin-1-yl[(4-methoxyphenyl)amino]methyl}phosphonate (132f). Colourless crystals. Mp 162–165 °C (MeCN) IR (KBr): 3208, 3096, 1625, 1512, 1236, 1033, 960, 828, 748 cm^{-1}. ^{1}H NMR ($CDCl_3$, 600 MHz): δ 10.19 (br s, 1H), 8.43 (d, *J* = 4.8 Hz, 1H), 8.00 (d, *J* = 7.8 Hz, 1H), 7.87 (m, 1H), 7.38 (m, 1H), 7.27 (m, 1H), 7.17 (m, 1H), 6.78 (m, 2H), 6.68 (m, 2H), 5.44 (br s, 1H), 5.37 (d, *J* = 21.0 Hz, 1H), 4.16 (m, 2H), 4.11 (m, 1H), 3.93 (m, 1H), 3.66 (s, 3H), 1.26 (t, *J* = 7.2 Hz, 3H), 1.11 (t, *J* = 7.2 Hz, 3H)

ppm. ^{13}C NMR ($CDCl_3$, 150 MHz): δ 152.9, 140.9, 138.6, 138.1, 134.4, 130.2, 128.3, 121.3, 119.8, 115.7, 114.6, 114.4, 112.0, 63.9, 59.4, 58.3, 55.6, 16.4, 16.2 ppm. ^{31}P NMR ($CDCl_3$, 242 MHz): δ 22.5 ppm. HRMS (ESI) calcd. for $C_{23}H_{27}N_3O_4P^+$ $[M+H]^+$ 440.1734; found: 440.1737.

Diethyl (9*H*-β-carbolin-1-yl{[4-(trifluoromethyl)phenyl]amino}methyl)phosphonate (132g). Brown crystals. Mp 204–206 °C (DIPE) IR (KBr): 3425, 3252, 1616, 1535, 1433, 1326, 1108, 1059, 825 cm^{-1}. ^{1}H NMR (DMSO-d_6, 600 MHz): δ 11.75 (br s, 1H), 8.36 (d, J = 5.2 Hz, 1H), 8.25 (m, 1H), 8.09 (d, J = 5.0 Hz, 1H), 7.68 (m, 1H), 7.59 (m, 1H), 7.37 (d, J = 8.6 Hz, 2H), 7.27 (m, 1H), 7.07 (dd, J_1 = 4.2 Hz, J_2 = 9.6 Hz, 1H), 7.03 (d, J = 8.6 Hz, 1H), 5.83 (dd, J_1 = 9.6 Hz, J_2 = 22.6 Hz, 1H), 4.04 (m, 2H), 3.90 (m, 1H), 3.74 (m, 1H), 1.16 (t, J = 7.0 Hz, 3H), 0.92 (t, J = 7.0 Hz, 3H) ppm. ^{13}C NMR (DMSO-d_6, 150 MHz): δ 150.7, 140.6, 139.1, 137.8, 134.1, 128.7, 128.5, 126.3, 125.3, 122.1, 120.7, 119.7, 117.1, 114.6, 113.0, 112.1, 62.9, 62.7, 53.4, 16.5, 16.2 ppm. ^{31}P NMR (DMSO-d_6, 242 MHz): δ 20.8 ppm. HRMS (ESI) calcd. for $C_{23}H_{23}F_3N_3O_3P^+$ $[M]^+$ 477.1429; found: 477.1418.

Bis(1-methylethyl) [9*H*-β-carbolin-1-yl(phenylamino)methyl]phosphonate (132h). Colourless crystals. Mp 210–213 °C (DIPE) IR (KBr): 3333, 3217, 3174, 1603, 1503, 1214, 1018, 999, 748 cm^{-1}. ^{1}H NMR (DMSO-d_6, 600 MHz): δ 11.69 (br s, 1H), 8.32 (d, J = 5.2 Hz, 1H), 8.22 (m, 1H), 8.04 (d, J = 5.1 Hz, 1H), 7.66 (m, 1H), 7.57 (m, 1H), 7.24 (m, 1H), 7.01 (m, 2H), 6.85 (m, 2H), 6.53 (m, 1H), 6.19 (dd, J_1 = 5.0 Hz, J_2 = 10.2 Hz, 1H), 5.59 (dd, J_1 = 10.3 Hz, J_2 = 23.9 Hz, 1H), 4.66 (m, 1H), 4.28 (m, 1H), 1.24 (d, J = 6.2 Hz, 3H), 1.20 (d, J = 6.2 Hz, 3H), 1.09 (d, J = 6.1 Hz, 3H), 0.62 (d, J = 6.1 Hz, 3H) ppm. ^{13}C NMR (DMSO-d_6, 150 MHz): δ 147.5, 140.5, 140.2, 137.6, 134.2, 129.0, 128.5, 128.2, 122.0, 120.6, 119.6, 117.5, 114.3, 113.7, 112.0, 71.4, 71.2, 54.6, 24.2, 24.1, 23.7, 23.0 ppm. ^{31}P NMR (DMSO-d_6, 242 MHz): δ 10.9 ppm. HRMS (ESI) calcd. for $C_{24}H_{29}N_3O_3P^+$ $[M+H]^+$ 438.1947; found: 438.1942.

Dibutyl [9*H*-β-carbolin-1-yl(phenylamino)methyl]phosphonate (132i). Yellow oil. IR (KBr): 3220, 3170, 1602, 1502, 1247, 1212, 1063, 1029, 995, 743 cm^{-1}. ^{1}H NMR (DMSO-d_6, 600 MHz): δ 11.73 (br s, 1H), 8.32 (d, J = 5.2 Hz, 1H), 8.22 (m, 1H), 8.05 (dd, J_1 = 1.2 Hz, J_2 = 5.2 Hz, 1H), 7.65 (m, 1H), 7.57 (m, 1H), 7.25 (m, 1H), 7.02 (m, 2H), 6.86 (m, 2H), 6.54 (m, 1H), 6.23 (dd, J_1 = 4.6 Hz, J_2 = 10.1 Hz, 1H), 5.70 (dd, J_1 = 10.1 Hz, J_2 = 23.1 Hz, 1H), 3.98 (m, 2H), 3.82 (m, 1H), 3.61 (m, 1H), 1.50 (m, 2H), 1.23 (m, 2H), 1.20 (m, 2H), 0.98 (m, 2H), 0.77 (t, J = 7.4 Hz, 3H), 0.59 (t, J = 7.4 Hz, 3H)

ppm. ^{13}C NMR (DMSO-d_6, 150 MHz): δ 147.4, 140.6, 139.9, 137.7, 134.2, 129.0, 128.5, 128.3, 122.0, 120.7, 119.6, 117.6, 114.4, 113.7, 112.0, 66.4, 66.0, 54.0, 32.2, 31.9, 18.3, 18.1, 13.6, 13.4 ppm. ^{31}P NMR (DMSO-d_6, 242 MHz): δ 21.5 ppm. HRMS (ESI) calcd. for $C_{26}H_{32}N_3O_3P^+$ $[M]^+$ 465.2191; found: 465.2194.

Diethyl {[(4-bromophenyl)amino](6-methoxy-9*H*-β-carbolin-1-yl)methyl}phosphonate (132j). Yellow crystals. Mp 220–223 °C (MeCN) IR (KBr): 3279, 2965, 1672, 1225, 1069, 1013, 967, 746, 576 cm^{-1}. ^{1}H NMR ($CDCl_3$, 600 MHz): δ 10.13 (br s, 1H), 8.39 (d, J = 5.4 Hz, 1H), 7.83 (m, 1H), 7.39 (m, 1H), 7.18 (m, 2H), 6.99 (m, 2H), 6.72 (d, J =9.0 Hz, 2H), 5.96 (br s, 1H), 5.42 (dd, J_1 = 6.0 Hz, J_2 = 27.0 Hz, 1H), 4.14 (m, 3H), 4.08 (m, 1H), 3.88 (s, 3H), 1.25 (t, J = 6.6 Hz, 3H), 1.14 (t, J = 7.2 Hz, 3H) ppm. ^{13}C NMR ($CDCl_3$, 150 MHz): δ 154.0, 145.8, 137.7, 137.4, 135.9, 134.9, 131.8, 130.2, 121.5, 118.6, 115.7, 114.6, 112.7, 110.4, 102.9, 64.1, 64.1, 61.8, 57.6, 56.6, 55.9, 16.4, 16.2 ppm. ^{31}P NMR ($CDCl_3$, 242 MHz): δ 21.5 ppm. HRMS (ESI) calcd. for $C_{23}H_{26}BrN_3O_4P^+$ $[M+H]^+$ 518.0839; found: 518.0841.

General procedure for the preparation of α-acylamino-α-aryl carboxamide derivatives of β-carboline (133a–j). The appropriate β-carboline aldehyde (**135a** or **135b**, 0.250 mmol), aniline derivative (**136**, 0.275 mmol), alkyl isocyanide (**138**, 0.275 mmol) and carboxylic acid (**139**, 0.275 mmol) were stirred in MeOH (2 mL) at room temperature for 24−72 hours (for reaction times, see Scheme 39). After the reaction was complete (or when no more progress was observed in the reaction), water was added, it was extracted with EtOAc and washed with brine. The organic layer was dried over Na_2SO_4 and purified by flash column chromatography on silica gel (DCM–MeOH) to afford pure α-acylamino-α-aryl carboxamides **133a–j** (for yields, see Scheme 39).

2-[Acetyl(phenyl)amino]-*N*-*tert*-butyl-2-(9*H*-β-carbolin-1-yl)acetamide (133a). Colourless crystals. Mp 205–207 °C (hexane). IR (KBr): 3369, 3249, 3057, 1675, 1656, 1495, 1375, 1083, 749, 700 cm^{-1}. ^{1}H NMR ($CDCl_3$, 600 MHz): δ 10.26 (br s, 1H), 9.68 (br s, 1H), 8.20 (d, J = 5.4 Hz, 1H), 8.12 (d, J = 7.8 Hz, 1H), 7.94 (d, J = 4.8 Hz, 1H), 7.62 (m, 1H), 7.59 (m, 1H), 7.31 (m, 1H), 7.26 (m, 1H), 7.20 (m, 2H), 7.20 (br s, 2H), 7.00 (s, 1H), 1.88 (s, 3H), 1.28 (s, 9H) ppm. ^{13}C NMR ($CDCl_3$, 150 MHz): δ 172.7, 165.9, 140.4, 139.6, 138.9, 136.1, 135.2, 129.6, 128.9, 128.8, 128.7, 121.5, 121.3, 120.1, 114.7, 112.4, 58.5, 51.1, 28.4, 22.7 ppm. HRMS (ESI) calcd. for $C_{25}H_{27}N_4O_2^+$ $[M+H]^+$ 415.2129; found: 415.2134.

***N*-[2-(*tert*-Butylamino)-1-(9*H*-β-carbolin-1-yl)-2-oxoethyl]-2,2-dimethyl-*N*-phenyl-propanamide (133b).** Yellow crystals. Mp 76–78 °C (hexane). IR (KBr): 3310, 1670, 1621, 1591, 1495, 1364, 1198, 745, 703 cm^{-1}. ^1H NMR ($CDCl_3$, 600 MHz): δ 10.24 (br s, 1H), 9.53 (br s, 1H), 8.13 (d, J = 5.1 Hz, 1H), 8.12 (m, 1H), 7.88 (d, J = 5.2 Hz, 1H), 7.63 (br s, 1H), 7.61 (m, 1H), 7.58 (m, 1H), 7.30 (m, 1H), 7.29 (br s, 1H), 7.18 (m, 1H), 7.09 (s, 1H), 6.83 (br s, 1H), 5.86 (br s, 1H), 1.34 (s, 9H), 1.02 (s, 9H) ppm. ^{13}C NMR ($CDCl_3$, 150 MHz): δ 180.0, 166.9, 140.3, 139.7, 138.8, 136.0, 135.3, 131.5, 130.8, 129.3, 128.7, 128.6, 128.4, 127.6, 121.5, 121.2, 120.0, 114.6, 112.2, 61.1, 51.2, 41.6, 29.6, 28.5, 27.1 ppm. HRMS (ESI) calcd. for $C_{28}H_{32}N_4O_2^+$ $[M]^+$ 456.2520; found: 456.2532.

***N*-[2-(*tert*-Butylamino)-1-(9*H*-β-carbolin-1-yl)-2-oxoethyl]-*N*-phenylbenzamide (133c).** Colourless crystals. Mp 121–123 °C (hexane). IR (KBr): 3272, 3055, 1673, 1619, 1555, 1493, 1369, 1078, 694 cm^{-1}. ^1H NMR ($CDCl_3$, 600 MHz): δ 10.34 (br s, 1H), 9.67 (br s, 1H), 8.24 (d, J = 5.2 Hz, 1H), 8.13 (m, 1H), 7.94 (d, J = 5.2 Hz, 1H), 7.64 (m, 1H), 7.59 (m, 1H), 7.31 (m, 1H), 7.28 (m, 2H), 7.18 (s, 1H), 7.17 (m, 1H), 7.09 (m, 2H), 7.03 (m, 1H), 6.98 (m, 2H), 6.74 (br s, 2H), 1.31 (s, 9H) ppm. ^{13}C NMR ($CDCl_3$, 150 MHz): δ 172.8, 166.1, 140.5, 139.5, 139.5, 136.4, 135.4, 135.2, 129.9, 129.8, 129.7, 128.8, 128.5, 128.3, 127.7, 127.6, 121.5, 121.3, 120.1, 114.9, 112.4, 59.8, 51.2, 31.6, 28.4, 22.6, 14.1 ppm. HRMS (ESI) calcd. for $C_{30}H_{28}N_4O_2^+$ $[M]^+$ 476.2207; found: 476.2217.

2-[Acetyl(4-fluorophenyl)amino]-*N*-*tert*-butyl-2-(9*H*-β-carbolin-1-yl)acetamide (133d). Yellow crystals. Mp 104–106 °C (hexane). IR (KBr): 3248, 2968, 1647, 1507, 1387, 1217, 1124, 727 cm^{-1}. ^1H NMR ($CDCl_3$, 600 MHz): δ 10.26 (br s, 1H), 9.6 (br s, 1H), 8.21 (d, J = 5.4 Hz, 1H), 8.13 (d, J = 7.8 Hz, 1H), 7.96 (d, J = 4.8 Hz, 1H), 7.61 (m, 2H), 7.31 (m, 1H), 6.99 (s, 1H), 6.89 (br s, 1H), 1.88 (s, 3H), 1.29 (s, 9H) ppm. ^{13}C NMR ($CDCl_3$, 150 MHz): δ 209.8, 208.5, 172.7, 165.9, 163.2, 161.5, 140.7, 138.9, 135.6, 135.1, 134.9, 131.5, 130.2, 129.2, 121.6, 121.1, 120.4, 115.9, 115.0, 112.4, 58.8, 51.3, 42.8, 32.5, 30.0, 28.4, 25.2, 22.7, 18.8 ppm. HRMS (ESI) calcd. for $C_{25}H_{26}FN_4O_2^+$ $[M+H]^+$ 433.2034; found: 433.2041.

2-[Acetyl(4-chlorophenyl)amino]-*N*-*tert*-butyl-2-(9*H*-β-carbolin-1-yl)acetamide (133e). Yellow crystals. Mp 198–200 °C (hexane). IR (KBr): 3283, 2975, 1668, 1556, 1486, 1379, 1303, 1224, 1079, 752 cm^{-1}. ^1H NMR ($CDCl_3$, 600 MHz): δ 10.17 (br s, 1H), 9.66 (br s, 1H), 8.21 (d, J = 5.4 Hz, 1H), 8.13 (d, J = 7.8 Hz, 1H), 7.95 (d, J = 4.8 Hz, 1H), 7.61 (m, 2H), 7.31 (m, 1H), 7.18 (br s, 2H), 6.99 (s, 1H), 1.88 (s, 3H), 1.30 (s, 9H) ppm. ^{13}C NMR ($CDCl_3$, 150 MHz): δ 172.5, 165.7, 140.4, 139.3, 137.4, 136.2, 135.2,

134.7, 131.1, 129.8, 129.2, 128.9, 121.4, 120.2, 114.9, 112.4, 58.3, 51.2, 28.4, 22.7 ppm. HRMS (ESI) calcd. for $C_{25}H_{26}ClN_4O_2^+$ $[M]^+$ 449.1739; found: 449.1738.

2-[Acetyl(4-bromophenyl)amino]-*N*-*tert*-butyl-2-(9*H*-β-carbolin-1-yl)acetamide (133f). Yellow crystals. Mp 212–214 °C (hexane). IR (KBr): 3177, 3098, 1593, 1503, 1291, 1251, 1201, 1042, 971, 789 cm^{-1}. ^1H NMR ($CDCl_3$, 600 MHz): δ 10.16 (br s, 1H), 9.67 (br s, 1H), 8.21 (d, J = 4.8 Hz, 1H), 8.13 (d, J = 7.8 Hz, 1H), 7.95 (d, J = 5.4 Hz, 1H), 7.61 (m, 2H), 7.33 (m, 3H), 6.99 (s, 1H), 1.88 (s, 3H), 1.72 (s, 1H), 1.30 (s, 9H) ppm. ^{13}C NMR ($CDCl_3$, 150 MHz): δ 172.4, 165.7, 140.4, 139.3, 138.0, 136.3, 135.2, 132.3, 131.4, 129.8, 128.9, 122.9, 121.5, 121.3, 120.2, 114.9, 112.4, 58.2, 51.2, 28.4, 22.7 ppm. HRMS (ESI) calcd. for $C_{25}H_{26}BrN_4O_2^+$ $[M+H]^+$ 493.1234; found: 493.1233.

2-[Acetyl(4-methylphenyl)amino]-*N*-*tert*-butyl-2-(9*H*-β-carbolin-1-yl)acetamide (133g). Yellow crystals. Mp 218–220 °C (hexane). IR (film): 3290, 2967, 1646, 1561, 1388, 1226, 909, 730 cm^{-1}. ^1H NMR ($CDCl_3$, 600 MHz): δ 10.27 (br s, 1H), 9.71 (br s, 1H), 8.20 (d, J = 4.8 Hz, 1H), 8.13 (d, J = 7.8 Hz, 1H), 7.93 (d, J = 5.4 Hz, 1H), 7.62 (m, 1H), 7.58 (m, 1H), 7.30 (m, 1H), 7.00 (s, 1H), 6.98 (br s, 1H), 2.29 (s, 3H), 1.87 (s, 3H), 1.30 (s, 9H) ppm. ^{13}C NMR ($CDCl_3$, 150 MHz): δ 172.9, 166.0, 140.4, 139.7, 138.6, 136.2, 136.1, 135.2, 129.6, 129.2, 128.7, 121.5, 121.3, 114.7, 112.4, 58.3, 51.1, 28.4, 22.6, 21.1 ppm. HRMS (ESI) calcd. for $C_{26}H_{29}N_4O_2^+$ $[M+H]^+$ 429.2285; found: 429.2290.

2-[Acetyl(4-methoxyphenyl)amino]-*N*-*tert*-butyl-2-(9*H*-β-carbolin-1-yl)acetamide (133h). Yellow crystals. Mp 145–147 °C (hexane). IR (KBr): 3284, 2965, 1625, 1510, 1389, 1249, 1035, 732 cm^{-1}. ^1H NMR ($CDCl_3$, 600 MHz): δ 10.26 (br s, 1H), 9.73 (br s, 1H), 8.20 (d, J = 5.4 Hz, 1H), 8.13 (d, J = 7.8 Hz, 1H), 7.93 (d, J = 5.4 Hz, 1H), 7.62 (m, 1H), 7.58 (m, 1H), 7.30 (m, 1H), 6.68 (s, 1H), 3.74 (s, 3H), 1.88 (s, 3H), 1.31 (s, 9H) ppm. ^{13}C NMR ($CDCl_3$, 150 MHz): δ 173.2, 166.0, 159.4, 140.4, 139.7, 136.1, 135.2, 131.6, 130.7, 129.6, 128.7, 121.5, 121.3, 120.1, 114.7, 114.0, 112.4, 58.4, 55.3, 51.1, 28.4, 22.6 ppm. HRMS (ESI) calcd. for $C_{26}H_{29}N_4O_3^+$ $[M+H]^+$ 445.2234; found: 445.2235.

2-[Acetyl(phenyl)amino]-2-(9*H*-β-carbolin-1-yl)-*N*-pentylacetamide (133i). Yellow crystals. Mp 66–68 °C (hexane). IR (KBr): 3294, 3061, 1650, 1626, 1494, 1383, 747, 700 cm^{-1}. ^1H NMR ($CDCl_3$, 600 MHz): δ 10.29 (br s, 1H), 9.72 (br s, 1H), 8.21 (d, J = 5.2 Hz, 1H), 8.14 (m, 1H), 7.95 (d, J = 5.2 Hz, 1H), 7.63 (m, 1H), 7.60 (m, 1H), 7.31 (m, 1H), 7.28 (m, 1H), 7.20 (br s, 2H), 7.00 (br s, 2H), 3.26 (m, 1H), 3.20 (m, 1H), 1.88 (s, 3H), 1.38 (m, 2H), 1.25 (m, 2H), 1.15 (m, 2H), 0.84 (t, J = 7.3 Hz, 3H) ppm. ^{13}C NMR ($CDCl_3$, 150 MHz): δ 172.7, 167.0, 140.5, 139.4, 138.9, 136.2, 135.2, 129.8, 129.5, 129.1,

128.9, 128.8, 121.5, 121.3, 120.1, 114.9, 112.4, 58.2, 39.4, 29.0, 28.7, 22.8, 22.3, 14.0 ppm. HRMS (ESI) calcd. for $C_{26}H_{28}N_4O_2^+$ $[M]^+$ 428.2207; found: 428.2217.

2-[Acetyl(phenyl)amino]-*N*-*tert*-butyl-2-(6-methoxy-9*H*-β-carbolin-1-yl)acetamide (133j). Colourless crystals. Mp 193–195 °C (Et_2O). IR (KBr): 3424, 3283, 1675, 1626, 1586, 1494, 1211, 1071, 707 cm^{-1}. ^1H NMR ($CDCl_3$, 600 MHz): δ 10.13 (br s, 1H), 9.70 (br s, 1H), 8.16 (d, J = 5.3 Hz, 1H), 7.89 (d, J = 5.3 Hz, 1H), 7.55 (d, J = 2.4 Hz, 1H), 7.53 (d, J = 8.8 Hz, 1H), 7.28 (m, 2H), 7.25 (dd, J_1 = 2.5 Hz, J_2 = 8.9 Hz, 1H), 7.20 (br s, 2H), 7.20 (br s, 1H), 6.98 (s, 1H), 3.94 (s, 3H), 1.88 (s, 3H), 1.27 (s, 9H) ppm. ^{13}C NMR ($CDCl_3$, 150 MHz): δ 172.7, 165.9, 154.2, 139.8, 138.9, 135.8, 135.6, 135.4, 129.7, 129.4, 128.9, 128.7, 121.6, 118.9, 114.6, 113.2, 103.2, 58.4, 56.0, 51.1, 28.4, 22.7 ppm. HRMS (ESI) calcd. for $C_{26}H_{28}N_4O_3^+$ $[M]^+$ 444.2156; found: 444.2153.

General procedure for the preparation of 3,4-dihydropyrimidin-2(1*H*)-one derivatives of β-carboline (134a–i). The appropriate β-carboline aldehyde (**135a** or **135b**, 0.50 mmol), urea (0.50 mmol), β-ketoester (**140**, 0.90 mmol) and $CeCl_3$ (20 mol%, 0.10 mmol) were stirred in the appropriate solvent (2 mL) at 75 °C for 24−48 hours (for reaction times and solvent, see Scheme 40). After the reaction was complete (or when no more progress was observed in the reaction) the residue was dissolved in a DCM–MeOH 1:1 mixture and it was purified by flash column chromatography on silica gel (DCM–MeOH) to afford pure 3,4-dihydropyrimidin-2(1*H*)-ones **134a–i** (for yields, see Scheme 40).

Methyl4-(9*H*-β-carbolin-1-yl)-6-methyl-2-oxo-1,2,3,4-tetrahydropyrimidine-5-carboxylate (134a). Brown crystals. Mp 290–292 °C (MeCN). IR (KBr): 3310, 3222, 1686, 1658, 1430, 1239, 1103, 746 cm^{-1}. ^1H NMR (DMSO-d_6, 600 MHz): δ 11.61 (br s, 1H), 9.19 (br s, 1H), 8.26 (d, J = 5.2 Hz, 1H), 8.00 (d, J = 5.1 Hz, 1H), 7.63 (m, 1H), 7.62 (m, 1H), 7.55 (m, 1H), 7.23 (m, 1H), 5.94 (d, J = 2.5 Hz, 1H), 3.35 (s, 3H), 2.26 (s, 3H) ppm. ^{13}C NMR (DMSO-d_6, 150 MHz): δ 166.2, 152.6, 149.4, 147.3, 140.9, 138.1, 132.6, 128.3, 128.2, 121.9, 120.8, 119.3, 114.1, 112.0, 97.8, 51.8, 50.8, 18.3 ppm. HRMS (ESI) calcd. for $C_{18}H_{16}N_4O_3^+$ $[M]^+$ 336.1217; found: 336.1219.

Methyl 4-(9*H*-β-carbolin-1-yl)-2-oxo-6-propyl-1,2,3,4-tetrahydropyrimidine-5-carboxylate (134b). Brown crystals. Mp 168–170 °C (MeCN). IR (KBr): 3241, 1697, 1642, 1431, 1233, 1213, 1097, 746 cm^{-1}. ^1H NMR (DMSO-d_6, 600 MHz): δ 11.60 (br s, 1H), 9.14 (br s, 1H), 8.25 (d, J = 5.1 Hz, 1H), 8.21 (m, 1H), 7.99 (d, J = 4.6 Hz, 1H), 7.64 (m, 1H), 7.59 (br s, 1H), 7.55 (m, 1H), 7.23 (m, 1H), 5.93 (s, 1H), 3.34 (s, 3H), 2.78 (m, 1H),

2.53 (m, 1H), 1.58 (m, 2H), 0.94 (t, J = 7.4 Hz, 3H) ppm. ^{13}C NMR (DMSO-d_6, 150 MHz): δ 165.9, 153.6, 152.8, 147.4, 140.8, 138.1, 132.6, 128.3, 128.2, 121.9, 120.8, 119.3, 114.1, 112.0, 97.5, 51.8, 50.8, 45.9, 32.5, 21.8, 13.8 ppm. HRMS (ESI) calcd. for $C_{20}H_{20}N_4O_3^+$ $[M]^+$ 364.1535; found: 364.1538.

Ethyl 4-(9*H*-β-carbolin-1-yl)-2-oxo-6-phenyl-1,2,3,4-tetrahydropyrimidine-5-carboxylate (134c). Brown crystals. Mp 195–197 °C (MeCN). IR (KBr): 3296, 1693, 1693, 1496, 1430, 1371, 1330, 1244, 1189, 1097 cm^{-1}. ^{1}H NMR (DMSO-d_6, 600 MHz): δ 11.67 (s, 1H), 9.24 (br s, 1H), 8.34 (d, J = 5.1 Hz, 1H), 8.23 (d, J = 7.8 Hz, 1H), 8.04 (d, J = 5.1 Hz, 1H), 7.71 (br s, 1H), 7.64 (d, J = 8.2 Hz, 1H), 7.56 (t, J = 7.6 Hz, 1H), 7.40 (m, 1H), 7.39 (m, 2H), 7.30 (m, 2H), 7.24 (t, J = 7.4 Hz, 1H), 6.03 (d, J = 2.4 Hz, 1H), 3.56 (q, J = 7.1 Hz, 2H), 0.52 (t, J = 7.1 Hz, 3H) ppm. ^{13}C NMR (DMSO-d_6, 150 MHz): δ 165.5, 152.6, 149.9, 147.2, 140.8, 138.2, 135.7, 132.7, 128.9, 128.6, 128.3, 128.2, 127.9, 121.9, 120.8, 119.3, 114.2, 112.0, 99.1, 59.0, 52.2, 13.4 ppm. HRMS (ESI) calcd. for $C_{24}H_{20}N_4O_3^+$ $[M]^+$ 412.1530; found: 412.1539.

***tert*-Butyl 4-(9*H*-β-carbolin-1-yl)-6-methyl-2-oxo-1,2,3,4-tetrahydropyrimidine-5-carboxylate (134d).** Gray crystals. Mp 238–240 °C (MeCN). IR (KBr): 3444, 3301, 3242, 3099, 1691, 1636, 1323, 1233, 1093, 741 cm^{-1}. ^{1}H NMR (DMSO-d_6, 600 MHz): δ 11.64 (br s, 1H), 9.00 (br s, 1H), 8.26 (d, J = 5.2 Hz, 1H), 8.21 (m, 1H), 7.99 (d, J = 5.2 Hz, 1H), 7.59 (m, 1H), 7.58 (br s, 1H), 7.53 (m, 1H), 7.22 (m, 1H), 5.92 (br s, 1H), 2.25 (s, 3H), 0.95 (s, 9H) ppm. ^{13}C NMR (DMSO-d_6, 150 MHz): δ 165.3, 152.2, 148.2, 147.5, 140.7, 137.9, 132.9, 128.2, 128.0, 121.9, 120.8, 119.2, 113.9, 112.0, 99.2, 78.8, 52.2, 27.8, 18.2 ppm. HRMS (ESI) calcd. for $C_{21}H_{22}N_4O_3^+$ $[M]^+$ 378.1686; found: 378.1680.

1-Methylethyl 4-(9*H*-β-carbolin-1-yl)-6-methyl-2-oxo-1,2,3,4-tetrahydropyrimidine-5-carboxylate (134e). Grey crystals. Mp 263–265 °C (MeCN). IR (KBr): 3454, 3343, 3167, 3065, 1687, 1636, 1457, 1425, 1372, 1236, 1096, 740 cm^{-1}. ^{1}H NMR (DMSO-d_6, 600 MHz): δ 11.67 (br s, 1H), 9.11 (br s, 1H), 8.26 (d, J = 5.2 Hz, 1H), 8.21 (m, 1H), 7.99 (d, J = 5.1 Hz, 1H), 7.65 (br s, 1H), 7.62 (m, 1H), 7.54 (m, 1H), 7.22 (m, 1H), 5.96 (d, J = 1.9 Hz, 1H), 4.59 (m, 1H), 2.27 (s, 3H), 0.99 (d, J = 6.2 Hz, 3H), 0.33 (d, J = 6.2 Hz, 3H) ppm. ^{13}C NMR (DMSO-d_6, 150 MHz): δ 165.1, 152.3, 149.1, 147.7, 140.7, 138.0, 132.8, 128.2, 127.9, 121.9, 120.8, 119.2, 113.9, 111.9, 98.3, 65.8, 55.1, 51.8 39.8, 39.6, 30.9, 21.7, 21, 18.1 ppm. HRMS (ESI) calcd. for $C_{20}H_{20}N_4O_3^+$ $[M]^+$ 364.1535; found: 364.1536.

Ethyl 4-(9*H*-β-carbolin-1-yl)-6-ethyl-2-oxo-1,2,3,4-tetrahydropyrimidine-5-carboxylate (134f). Brown crystals. Mp 258–260 °C (MeCN). IR (KBr): 3425, 3310, 3227, 3118, 1695, 1661, 1633, 1225, 1097, 748 cm^{-1}. ^1H NMR (DMSO-d_6, 600 MHz): δ 11.63 (br s, 1H), 9.14 (br s, 1H), 8.26 (d, J = 5.1 Hz, 1H), 8.21 (m, 1H), 7.99 (d, J = 5.2 Hz, 1H), 7.62 (m, 1H), 7.61 (br s, 1H), 7.54 (m, 1H), 7.22 (m, 1H), 5.94 (d, J = 2.5 Hz, 1H), 3.77 (m, 2H), 2.89 (m, 1H), 2.45 (m, 1H), 1.14 (t, J = 7.4 Hz, 3H), 0.71 (t, J = 7.1 Hz, 3H) ppm. ^{13}C NMR (DMSO-d_6, 150 MHz): δ 165.3, 154.9, 152.8, 147.6, 140.8, 138.1, 132.7, 128.3, 128.0, 121.9, 120.8, 119.2, 114.0, 111.9, 97.2, 59.1, 51.7, 24.4, 13.8, 13.3 ppm. HRMS (ESI) calcd. for $C_{20}H_{20}N_4O_3^+$ $[M]^+$ 364.1530; found: 364.1528.

Ethyl 4-(9*H*-β-carbolin-1-yl)-6-(1-methylethyl)-2-oxo-1,2,3,4-tetrahydropyrimidine-5-carboxylate (134g). Brown crystals. Mp 236–238 °C (MeCN). IR (KBr): 3372, 2966, 1694, 1664, 1646, 1444, 1326, 1127, 1097 cm^{-1}. ^1H NMR (DMSO-d_6, 600 MHz): δ 11.63 (s, 1H), 8.78 (br s, 1H), 8.26 (d, J = 5.1 Hz, 1H), 8.21 (d, J = 7.9 Hz, 1H), 7.99 (d, J = 5.1 Hz, 1H), 7.62 (m, 2H), 7.54 (~t, J = 8.1 Hz, 1H), 7.22 (t, J = 7.8 Hz, 1H), 5.96 (d, J = 2.6 Hz, 1H), 4.20 (m, 1H), 3.75 (m, 2H), 1.17 (d, J = 7.0 Hz, 3H), 1.16 (d, J = 7.0 Hz, 3H), 0.66 (t, J = 7.1 Hz, 3H) ppm. ^{13}C NMR (DMSO-d_6, 150 MHz): δ 165.7, 157.5, 153.0, 147.6, 140.7, 138.2, 132.7, 128.2, 128.0, 121.9, 120.8, 119.2, 114.0, 111.9, 96.8, 59.2, 51.7, 27.0, 19.5, 19.3, 13.7 ppm. HRMS (ESI) calcd. for $C_{21}H_{22}N_4O_3^+$ $[M]^+$ 378.1692; found: 378.1693.

Methyl 4-(9*H*-β-carbolin-1-yl)-6-(2-chlorophenyl)-2-oxo-1,2,3,4-tetrahydropyrimidine-5-carboxylate (134h). Brown crystals. Mp 291–293 °C (MeCN). IR (KBr): 3415, 3300, 1650, 1433, 1245, 1097, 745 cm^{-1}. ^1H NMR (DMSO-d_6, 600 MHz): δ 11.68 (br s, 1H), 9.37 (br s, 1H), 8.34 (d, J = 5.1 Hz, 1H), 8.24 (m, 1H), 8.05 (d, J = 5.1 Hz, 1H), 7.75 (br s, 1H), 7.66 (m, 1H), 7.56 (m, 1H), 7.48 (m, 1H), 7.42 (m, 1H), 7.34 (m, 1H), 7.27 (m, 1H), 7.24 (m, 1H), 6.04 (d, J = 2.6 Hz, 1H), 3.15 (s, 3H) ppm. ^{13}C NMR (DMSO-d_6, 150 MHz): δ 165.4, 152.4, 148.6, 146.9, 140.9, 138.3, 137.4, 132.7, 132.4, 129.9, 128.9, 128.4, 128.3, 128.3, 127.5, 121.9, 120.8, 119.3, 114.3, 112.1, 99.2, 52.1, 50.8 ppm. HRMS (ESI) calcd. for $C_{23}H_{17}ClN_4O_3^+$ $[M]^+$ 432.0989; found: 432.0986.

Methyl 4-(6-methoxy-9*H*-β-carbolin-1-yl)-6-methyl-2-oxo-1,2,3,4-tetrahydropyrimidine-5-carboxylate (134i). Brown crystals. Mp 226–228 °C (MeCN). IR (KBr): 3368, 3219, 3108, 1707, 1662, 1497, 1341, 1246, 1093, 816 cm^{-1}. ^1H NMR (DMSO-d_6, 600 MHz): δ 11.42 (br s, 1H), 9.17 (br s, 1H), 8.21 (d, J = 5.2 Hz, 1H), 7.97 (d, J = 5.1 Hz, 1H), 7.76 (d, J = 2.5 Hz, 1H), 7.60 (t, J = 2.2 Hz, 1H), 7.54 (d, J = 8.8 Hz, 1H), 7.19 (dd,

J_1 = 2.5 Hz, J_2 = 8.8 Hz, 1H), 5.90 (d, J = 2.5 Hz, 1H), 3.86 (s, 3H), 3.34 (s, 3H), 2.26 (s, 3H) ppm. ^{13}C NMR (DMSO-d_6, 150 MHz): δ 166.2, 153.4, 152.6, 149.4, 147.4, 137.4, 135.8, 133.2, 128.1, 121.0, 118.3, 114.1, 112.9, 103.6, 97.8, 55.8, 51.8, 50.8, 18.2 ppm. HRMS (ESI) calcd. for $C_{19}H_{18}N_4O_4^+$ $[M]^+$ 366.1323; found: 366.1330.

General continuous-flow procedure for the preparation of derivatives of dihidro-β-carboline (68, 142–146). Prior to the reaction, the entire flow system was rinsed with MeCN and the BPR was set to 20 bar. The corresponding tryptamine (**29**, 0.50 mmol) and the appropriate carboxylic acid (0.50 mmol) were dissolved in anhydrous MeCN (see Figure 14 for concentration). To this solution, T3P® (50% in EtOAc, 2.0 eq) was added, and the mixture was stirred at room temperature until complete dissolution. The resulting solution was filtered and introduced into the flow reactor, which was operated under the specified temperature and residence time (see Figure 14 for reaction conditions). After collection of the reaction mixture, the solvent was removed in vacuo, residue was dissolved in DCM and extraction with 10% NaOH solution, drying and evaporation afforded the crude product. Purification by flash chromatography gave the desired 3,4-dihydro-β-carboline derivatives (**68**, **142–146**) in pure form. Analytical samples were obtained either by recrystallization or by conversion to the corresponding hydrochloride salts.

1-Methyl-4,9-dihydro-3*H*-β-carboline (68). Brown crystals. Mp 173–175 °C (EtOAc). (lit. [56] mp. 175–178 °C). IR (KBr): 2989, 1550, 1324, 1277, 736 cm^{-1}. ^{1}H NMR (DMSO-d_6, 600 MHz): δ 11.37 (br s, 1H), 7.55 (m, 1H), 7.43 (m, 1H), 7.20 (m, 1H), 7.05 (m, 1H), 3.70 (m, 2H), 2.75 (t, J = 8.4 Hz, 2H), 2.30 (t, J = 1.4 Hz, 3H) ppm. ^{13}C NMR (DMSO-d_6, 150 MHz): δ 157.3, 136.7, 129.4, 125.1, 123.7, 119.8, 119.6, 114.3, 112.5, 47.9, 22.3, 19.1 ppm. HRMS (ESI) calcd. for $C_{12}H_{13}N_2^+$ $[M+H]^+$ 185.1073; found: 185.1074.

1-*tert*-Butyl-4,9-dihydro-3*H*-β-carboline (142). Yellow crystals. Mp 176–178 °C (MeCN). (lit. [56] mp. 176–177 °C). IR (KBr): 3253, 1587, 1532, 1305, 1174, 1004, 735 cm^{-1}. ^{1}H NMR (DMSO-d_6, 600 MHz): δ 10.92 (br s, 1H), 7.54 (m, 1H), 7.50 (m, 1H), 7.19 (m, 1H), 7.04 (m, 1H), 3.67 (t, J = 8.2 Hz, 2H), 2.69 (t, J = 8.3 Hz, 2H), 1.32 (s, 9H) ppm. ^{13}C NMR (DMSO-d_6, 150 MHz): δ 166.0, 136.7, 127.1, 124.4, 123.6, 119.4, 119.3,

116.6, 112.7, 47.8, 38.5, 28.5, 18.9 ppm. HRMS (ESI) calcd. for $C_{15}H_{19}N_2^+$ $[M+H]^+$ 227.1543; found: 227.1544.

1-Phenyl-4,9-dihydro-3*H*-β-carboline (143). Yellow crystals. Mp 230–232 °C (EtOH). (lit. [56] mp. 231–232 °C). IR (KBr): 3056, 2934, 2833, 1540, 1322, 1289, 1152, 1012, 716 cm^{-1}. ^1H NMR (DMSO-d_6, 600 MHz): δ 11.13 (br s, 1H), 7.77 (m, 2H), 7.62 (m, 1H), 7.53 (m, 1H), 7.53 (m, 2H), 7.44 (m, 1H), 7.21 (m, 1H), 7.08 (m, 1H), 3.89 (t, J = 8.3 Hz, 2H), 2.87 (t, J = 8.2 Hz, 2H). ppm. ^{13}C NMR (DMSO-d_6, 150 MHz): δ 158.8, 137.7, 137.1, 129.9, 128.7, 128.2, 127.7, 125.0, 123.9, 119.8, 119.7, 116.6, 113.0, 48.6, 19.1 ppm. HRMS (ESI) calcd. for $C_{17}H_{14}N_2^+$ $[M]^+$ 246.1157; found: 246.1148.

6-Chloro-1-methyl-4,9-dihydro-3*H*-β-carboline (144). Yellow crystals. Mp 232–234 °C (EtOAc). IR (KBr): 3077, 3016, 1546, 1312, 1283, 979, 806 cm^{-1}. ^1H NMR (DMSO-d_6, 600 MHz): δ 11.57 (br s, 1H), 7.62 (d, J = 2.0 Hz, 1H), 7.43 (d, J = 8.7 Hz, 1H), 7.19 (dd, J_1 = 2.0 Hz, J_2 = 8.6 Hz, 1H), 3.70 (t, J = 8.4 Hz, 2H), 2.74 (t, J = 8.4 Hz, 2H), 2.29 (s, 3H) ppm. ^{13}C NMR (DMSO-d_6, 150 MHz): δ 157.0, 135.0, 130.6, 126.2, 124.2, 123.6, 119.0, 114.1, 113.8, 47.8, 22.2, 18.8 ppm. HRMS (ESI) calcd. for $C_{12}H_{11}ClN_2^+$ $[M]^+$ 218.0611; found: 218.0607.

6-Methoxy-1-(4-methoxyphenyl)-4,9-dihydro-3*H*-β-carboline (145). Yellow crystals. Mp 179–182 °C (MeOH). IR (KBr): 2935, 2826, 1607, 1590, 1536, 1512, 1451, 1296, 1250, 1210, 1178, 1115, 1037, 835 cm^{-1}. ^1H NMR (DMSO-d_6, 600 MHz): δ 10.95 (s, 1H), 7.73 (d, J = 8.8 Hz, 2H), 7.32 (d, J = 8.8 Hz, 1H), 7.08 (m, 1H), 7.07 (d, J = 8.8 Hz, 2H), 6.85 (dd, J_1 = 8.8 Hz, J_2 = 2.5 Hz, 1H), 3.83 (m, 5H), 3.79 (s, 3H), 2.82 (m, 2H) ppm. ^{13}C NMR (DMSO-d_6, 150 MHz): δ 160.7, 158.1, 153.9, 132.3, 130.3, 129.7, 128.4, 125.2, 116.1, 114.9, 114.0, 113.8, 100.2, 55.5, 55.5, 48.4, 19.3 ppm. HRMS (ESI) calcd. for $C_{19}H_{18}N_2O_2^+$ $[M]^+$ 306.1368; found: 306.1369.

1-Thiophen-2-yl-4,9-dihydro-3*H*-β-carboline (146). Yellow crystals. Mp 230–232 °C (DIPE). (lit. [87] mp. 234–236 °C). IR (KBr): 3424, 3059, 2939, 1578, 1534, 1429, 1368, 1318, 1281, 1167, 1131, 978, 855, 787, 750, 707 cm^{-1}. ^1H NMR (DMSO-d_6, 600 MHz): δ 11.34 (br s, 1H), 7.79 (dd, J_1 = 3.7 Hz, J_2 = 0.9 Hz, 1H), 7.72 (dd, J_1 =5.1 Hz, J_2 = 0.9 Hz, 1H), 7.63 (d, J=8.0 Hz, 1H), 7.51 (d, J = 8.2 Hz, 1H), 7.26 (dd, J_1 = 5.1 Hz, J_2 = 3.7 Hz, 1H), 7.24 (t, J = 8.1 Hz, 1H), 7.10 (t. J = 7.5 Hz, 1H), 3.83 (m, 2H), 2.84 (m, 2H) ppm. ^{13}C NMR (DMSO-d_6, 150 MHz): δ 152.7, 142.7, 137.4, 129.4, 128.7, 128.2, 126.9,

124.9, 124.2, 120.0, 119.8, 117.2, 113.1, 48.0, 19.1 ppm. HRMS (ESI) calcd. for $C_{15}H_{21}N_2S^+$ $[M]^+$ 252.0721; found: 252.0719.

5. DISCUSSION

5.1. Synthesis and SAR studies of novel oxazolyl- and thiazolylindoles

Following an extensive review of the literature, we selected tryptamine (**29a**) as the starting scaffold for the synthesis of the target molecules, employing a Robinson–Gabriel cyclization to construct the oxazole or thiazole ring systems [88]. Condensation of tryptamine (**29a**) and 5-chlorotryptamine (**29b**) with methyl 2-chloro-2-oxoacetate (**95**) furnished oxalamide esters **96a** and **96b** (Scheme 26, pathway A). Subsequent treatment of these intermediates with aqueous ammonia, methylamine, or cyclohexylamine produced the corresponding bis-amides **97a–d**. Oxidation of intermediates **97a** and **97b** with DDQ yielded the α-acylamino ketones **98a** and **98b**, which underwent cyclization to give the target oxazole derivatives **99a** and **99b**. For the cyclization step, TFA and TFAA were used at room temperature for $R^1 = R^2 = H$, whereas $POCl_3$ at 80 °C was required for R^1=H and R^2 = Me. Under the latter conditions, treatment of **98a** (R^1 = H) with $POCl_3$ led to the carbonitrile **100** instead of the amide.

Another synthetic sequence was developed to access oxazoles **99c–e**. In this route, intermediate **96a** was first oxidized with DDQ to ketone **101**, which was subsequently cyclized to indolyloxazole-carboxylic ester **102**, a key intermediate for medicinal chemistry library synthesis. Direct amidation of compound **102** with appropriate amines in methanol at ambient temperature led to oxazole-carboxamides **99c–e**. Finally, conversion of oxazole-carboxamides **99a–e** into the corresponding carbothioamides **103a–e** was achieved in generally high yields by reaction with Lawesson's reagent.

An alternative synthetic pathway (Scheme 26, pathway B) to 1,3-oxazole-2-carbothioamides **103b** and **103c** was established by employing Zavarzin's method to introduce the thioamide functionality [89,90]. In this approach, 2-chloroacetamide **104**, prepared by the reaction of tryptamine (**29a**) with chloroacetyl chloride, was treated with methylamine or isopropylamine and elemental sulfur, affording 2-oxocarbothioamides **105a** and **105b**. Subsequent DDQ-mediated oxidation yielded the corresponding ketones **106a** and **106b**, which underwent cyclization with $POCl_3$ to furnish the desired products **103b** and **103c**. The application of the Robinson–Gabriel cyclization strategy was justified over the Suzuki coupling by the accessibility of cost-effective starting materials,

the opportunity to study mechanistic phenomena such as the spontaneous cyclization of thioamides, and the feasibility of late-stage scaffold diversification.

The molecular structure of the methylamido derivative **103b** (R^1 = H, R^2 = Me) was unambiguously confirmed by SC-XRD as well.

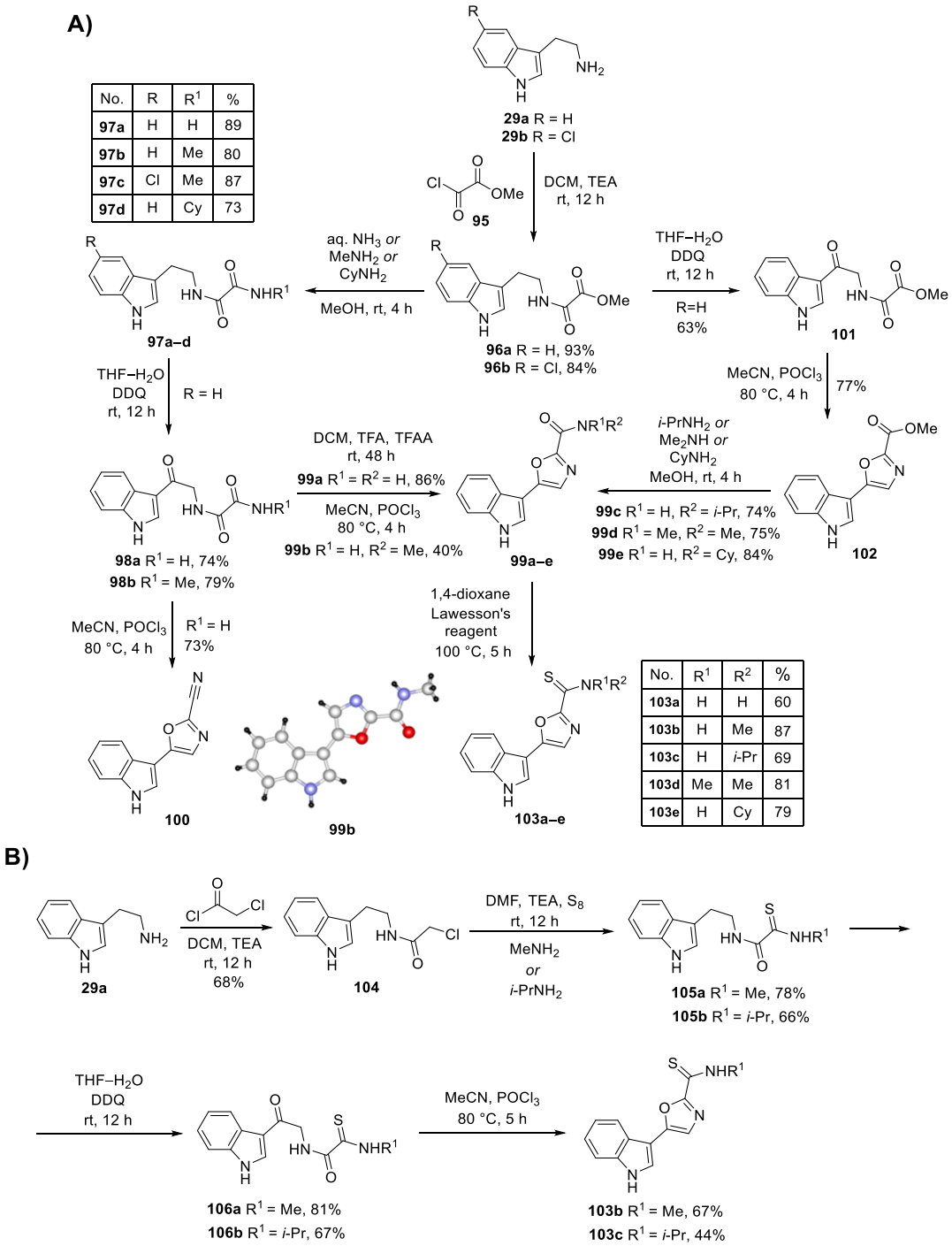

Scheme 26. Synthetic routes leading to indolyloxazole-carboxamides (**99a–e**) and -carbothioamides (**103a–e**)

For the initial step in the synthesis of key intermediates **107a–f** for thiazolylindoles **108a–f** and **109a,b** (Scheme 27), we adopted the procedure of Zavarzin *et al.* for the convenient preparation of 2-(substituted-amino)-2-thioxoacetamides, which involves treating 2-chloroacetamide with the appropriate amine and elemental sulfur. In our hands, the reaction proved highly effective, providing 2-thioxoacetamides **107a–f** in generally good yields.

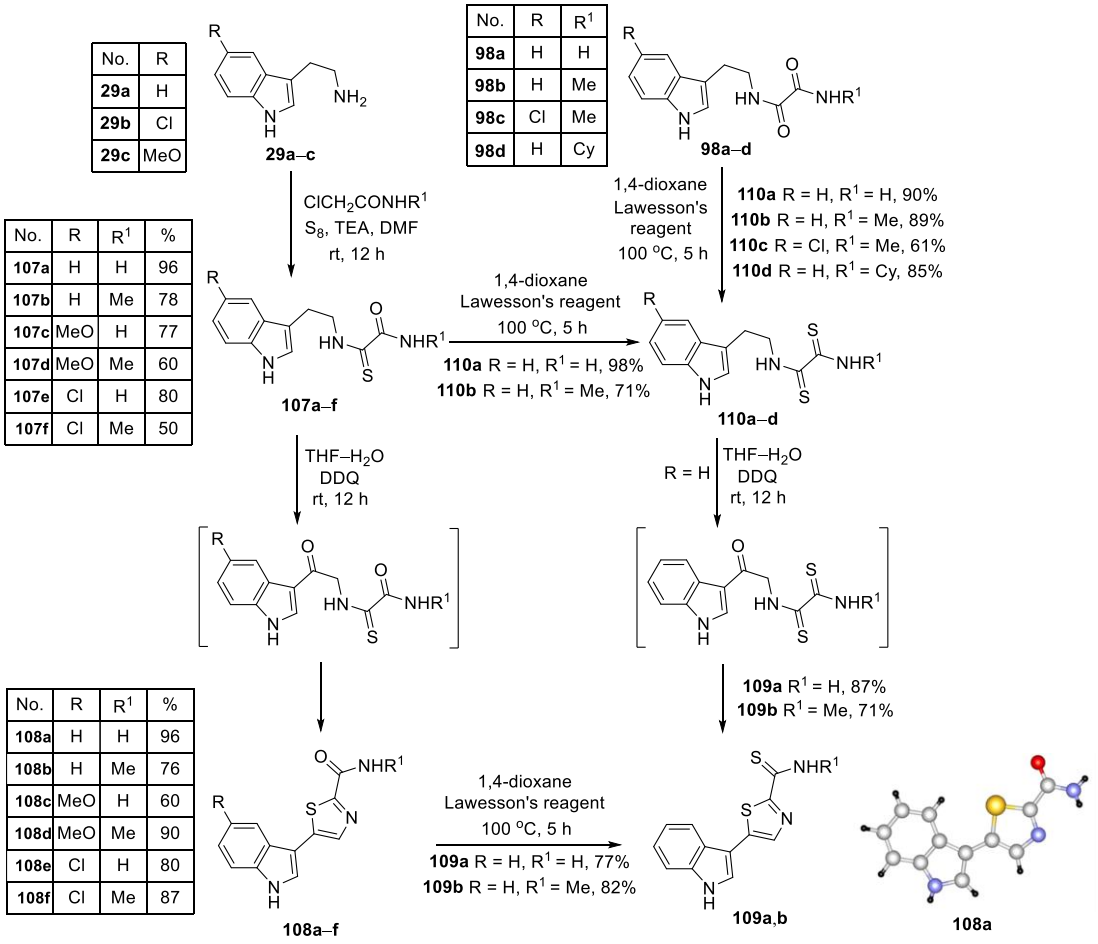

Scheme 27. Synthesis of indolylthiazole-carboxamides (**108a–f**) and -carbothioamides (**109a,b**)

Unexpectedly, DDQ oxidation of **107a–f** in THF at room temperature furnished thiazolylindoles **108a–f** directly, indicating that the ring closure occurred under these mild conditions without the need for a dehydrating reagent – an outcome previously not documented. Based on the observations, the cyclization occurring without a dehydrating agent can be attributed to the thioacetamide group situated at the 2-aminoethyl side chain of the tryptamine moiety. Under these conditions, thiazole ring formation invariably proceeds *via* a mechanism consistent with the Robinson–Gabriel synthesis. Further

conversion of amides **108a** and **108b** with Lawesson's reagent afforded the corresponding thioamides **109a** and **109b**. The structure of **109a** (R^1 = H) was confirmed by SC-XRD.

Alternatively, **109a** and **109b** could also be obtained *via* DDQ oxidation of bis-thioamide precursors **110a** and **110b**, themselves prepared by treating either **98a–d** or **107a**,**b** with Lawesson's reagent. The application of the Robinson–Gabriel cyclization strategy was justified over the Suzuki coupling by the accessibility of cost-effective starting materials, the opportunity to study mechanistic phenomena such as the spontaneous cyclization of thioamides, and the feasibility of late-stage scaffold diversification.

In silico ADME profiles of the synthesized compounds were evaluated using SwissADME [91]. Key parameters (molecular weight, H-bond donors, rotatable bonds, Lipinski compliance, TPSA, logP values, solubility, GI absorption, BBB permeability, and lead-likeness) have been studied. All compounds meet Lipinski's rule of five and most show favorable lipophilicity and lead-like properties. BOILED-Egg analysis indicated high GI absorption for all derivatives and predicted good BBB penetration for several ones [92].

The pharmacological evaluation of all synthesized compounds was carried out in collaboration with our partner laboratory, which tested their antiproliferative effects on 3T3 fibroblasts, HL-60 leukemia cells, and C6 glioma cells. The results indicate that only a subset of compounds, primarily thiazoles and oxazoles bearing a thioamide group, reduced cancer cell counts significantly, whereas most acyclic derivatives and oxazoles with a carboxamide group appeared to inhibit proliferation without marked cytotoxicity (Figure 9).

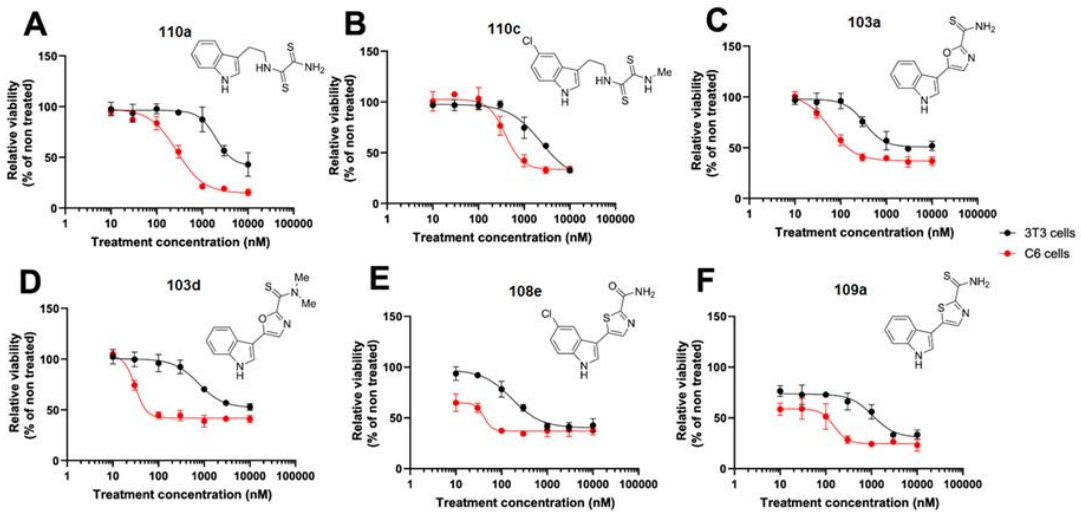

Figure 9. Dose-response curves of the most prominent compounds on C6 and 3T3 cells

Key SAR trends are summarized in Figure 10: thiazole scaffolds were generally more active than oxazoles; carbothioamide substitution further enhanced activity; and chlorine atoms increased both potency and selectivity towards cancer cells. Notably, these compounds and their intermediates present numerous opportunities for further structural optimization.

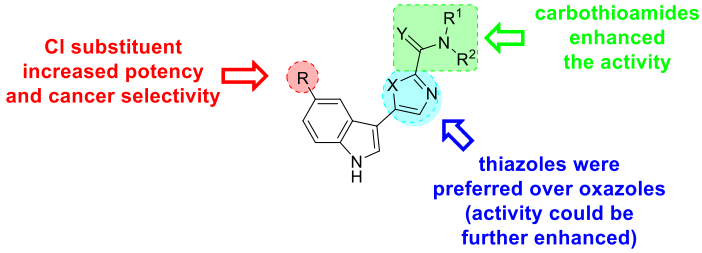

Figure 10. SAR of the prepared compounds

5.2. Synthesis of bacillamide alkaloids

Having established efficient synthetic pathways towards oxazolyl- and thiazolylindole frameworks and identified preliminary structure-activity relationships among these novel compounds, our attention was next directed towards naturally occurring analogues featuring similar heteroaromatic motifs. Among such systems, the bacillamide family of indole and thiazole containing alkaloids represent an intriguing target due to their distinctive biological profiles and unresolved stereochemical questions. Therefore, in the following section, we focused on the asymmetric synthesis of bacillamide alkaloids and their analogues to clarify their absolute configurations and enable stereochemical benchmarking for future studies.

Given the potential ecological relevance of naturally occurring bacillamide alkaloids as algicidal agents, and the complex yet sometimes inconsistent data available on their stereochemistry, we undertook the synthesis of both enantiomeric forms of bacillamides B–D as well as neobacillamide A [93]. For each compound, we determined the absolute configuration and optical rotation. This provides a reference framework: should a natural product of this class be isolated in the future, its optical rotation (or chiral chromatographic behaviour) can be directly compared, enabling straightforward stereochemical assignment. To complement this, chiral stationary phase HPLC methods were developed, making enantiomer separation and retention time comparison a practical tool for stereochemical determination.

As a preliminary step towards the enantioselective syntheses and the development of chiral analytical methods, we first prepared the racemic forms of the target molecules. In the following sections, the asymmetric syntheses are described which afforded the enantiomerically enriched final products.

The main intermediates in the syntheses of bacillamides B–D and neobacillamide A are the enantiomeric forms of 2-(1-hydroxyethyl)thiazole (**33**), which were accessed *via* asymmetric transfer hydrogenation or asymmetric hydride transfer reaction of ketone **28**. When employing (*S*)-Me-CBS or (*R*)-Me-CBS as catalysts [94], the reactions afforded 69–71% yields with *ee* limited to 53–73% (Scheme 28). To improve stereoselectivity, we turned to a Noyori-type catalyst, RuCl(*S*,*S*)-Tsdpen, and its enantiomer [95], which provided the corresponding alcohols in 95–96% *ee*. An alternative synthetic route to (*S*)-**33** has been reported in the literature [96], supporting the expected stereochemical outcome on the basis of the reaction mechanism [97]. A summary of the asymmetric synthesis results is presented in Table 1.

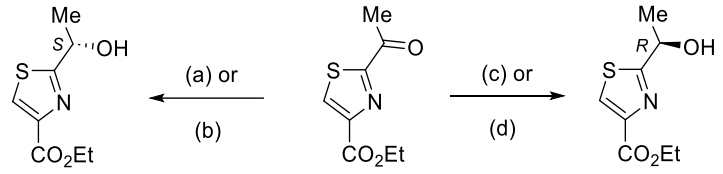

(*S*)-(–)-**33** **28** (see Scheme 10) (*R*)-(+)-**33**

(a) (*R*)-Me-CBS (10 mol%), $NaBH_4$, Me_2SO_4, THF, 0 °C to rt, 69%, *ee* 73%;
(b) RuCl[(*S*,*S*)-Tsdpen](mesitylene) (5 mol%), HCOONa, MeOH, 0 °C to rt, 81%, *ee* 95%;
(c) (*S*)-Me-CBS (10 mol%), $NaBH_4$, Me_2SO_4, THF, 0 °C to rt, 71%, *ee* 53%;
(d) RuCl[(*R*,*R*)-Tsdpen](mesitylene) (5 mol%), HCOONa, MeOH, 0 °C to rt, 84%, *ee* 96%.

Scheme 28. Enantioselective synthesis of 2-(1-hydroxyethyl)thiazole **33**

Table 1. Summary of the syntheses of 2-(1-hydroxyethyl)thiazole **33**

catalyst	(*S*)-Me-CBS	(*R*)-Me-CBS	RuCl[(*S*,*S*)-Tsdpen](mesitylene)	RuCl[(*R*,*R*)-Tsdpen](mesitylene)
appropriate product according to mechanism[95]	(*R*)-(+)-**33**	(*S*)-(–)-**33**	(*S*)-(–)-**33**	(*R*)-(+)-**33**
purity by chiral stationary phase HPLC	*ee* 53%	*ee* 73%	*ee* 95%	*ee* 96%
yield of reduction	71%	69%	81%	84%
measured optical rotation	ND	ND	$[\alpha]_D^{25} = -19.3$ (*c* 1.20, $CHCl_3$)	$[\alpha]_D^{23} = +20.8$ (*c* 1.20, $CHCl_3$)
literature optical rotation	–	–	$[\alpha]_D^{20} = -19.9$ (*c* 1.20, $CHCl_3$)	–

In the following section, the four synthetic pathways (routes **A–D**) depicted in Scheme 29 are discussed, taking into account that several of the individual transformations are chemically analogous. In route **A**, the thiazole ester [(*R*)-(+)-**33**] was condensed with tryptamine (**29a**), furnishing the antipode of bacillamide B [(*R*)-(+)-**22**] in 65% yield with 95% *ee*. Subsequent conversion of this intermediate into bacillamide D [(*S*)-(–)-**25**] was achieved in two steps with an overall yield of 51% and an *ee* of 87%. The process involved a Mitsunobu reaction to generate the azido intermediate with inverted configuration [(*S*)-**111**], which was directly reduced to yield the target compound. The structure of bacillamide D [(*S*)-(–)-**25**] was confirmed by SC-XRD (Figure 11). Furthermore, *N*-acetylation of bacillamide D [(*S*)-(–)-**25**] led to bacillamide C [(*S*)-(–)-**23**] in 88% yield. These results, corroborated by X-ray analysis, are consistent with the structural and optical rotation data reported by Davyt *et al.* [46] for bacillamide C [(*S*)-(–)-**23**].

For the synthesis of neobacillamide A (Scheme 29, route **B**), the thiazole ester [(*R*)-(+)-**33**] was subjected to amidation with β-phenylethylamine (**55**), affording amide (*R*)-(+)-**112** in 79% yield. Subsequent transformation to azido derivative (*S*)-**113**, involving inversion at the stereogenic center, and its subsequent reduction furnished amine (*S*)-(–)-**114** in 40% overall yield for the two steps. Final *N*-acetylation provided neobacillamide A [(*S*)-(–)-**24**] in 80% yield with an *ee* of 78%.

Bacillamide B [(*S*)-(–)-**22**] was synthesized *via* amidation of the corresponding thiazole ester [(*S*)-(–)-**33**, Scheme 29, route **C**] with tryptamine (**29a**), yielding the product in 89% yield and 96% *ee*. The literature contains inconsistent data regarding the sign of optical rotation of bacillamide B; our measurements are in agreement with those reported by Du *et al.* [42].

Azidation of bacillamide B [(*S*)-(–)-**22**], accompanied by inversion of configuration to give intermediate (*R*)-**111**, followed by reduction, produced the enantiomer of bacillamide D [(*R*)-(+)-**25**] in 48% yield with 91% *ee*. The structure of this compound was confirmed by SC-XRD (Figure 12). Subsequent *N*-acetylation led to the corresponding antipode of bacillamide C [(*R*)-(+)-**23**] in 84% yield.

Finally, the enantiomeric counterpart of neobacillamide A [(*R*)-(+)-**24**, Scheme 29, route **D**] was obtained by amidation of the thiazole ester [(*S*)-(–)-**33**] with β-phenylethylamine (**55**) to form (*S*)-(–)-**112** in 77% yield. Conversion through azide intermediate (*R*)-**113** and reduction afforded amine (*R*)-(+)-**114** in 76% combined yield, which was then *N*-acetylated to yield the target compound in 87% yield with 91% *ee*.

It is noteworthy that the observed decrease in *ee* could be attributable to the partial SN_1 character during the Mitsunobu reaction, where the chiral center is directly involved. Furthermore, minor fluctuations in reaction conditions (such as temperature and reaction time) may have increased this effect and the cumulative impact of which became apparent only in the final products, such as in the case of neobacillamide A ((*R*)-(+)-**24**, *ee* 78%), due to the lack of systematic chiral stationary phase HPLC monitoring for every intermediate stage.

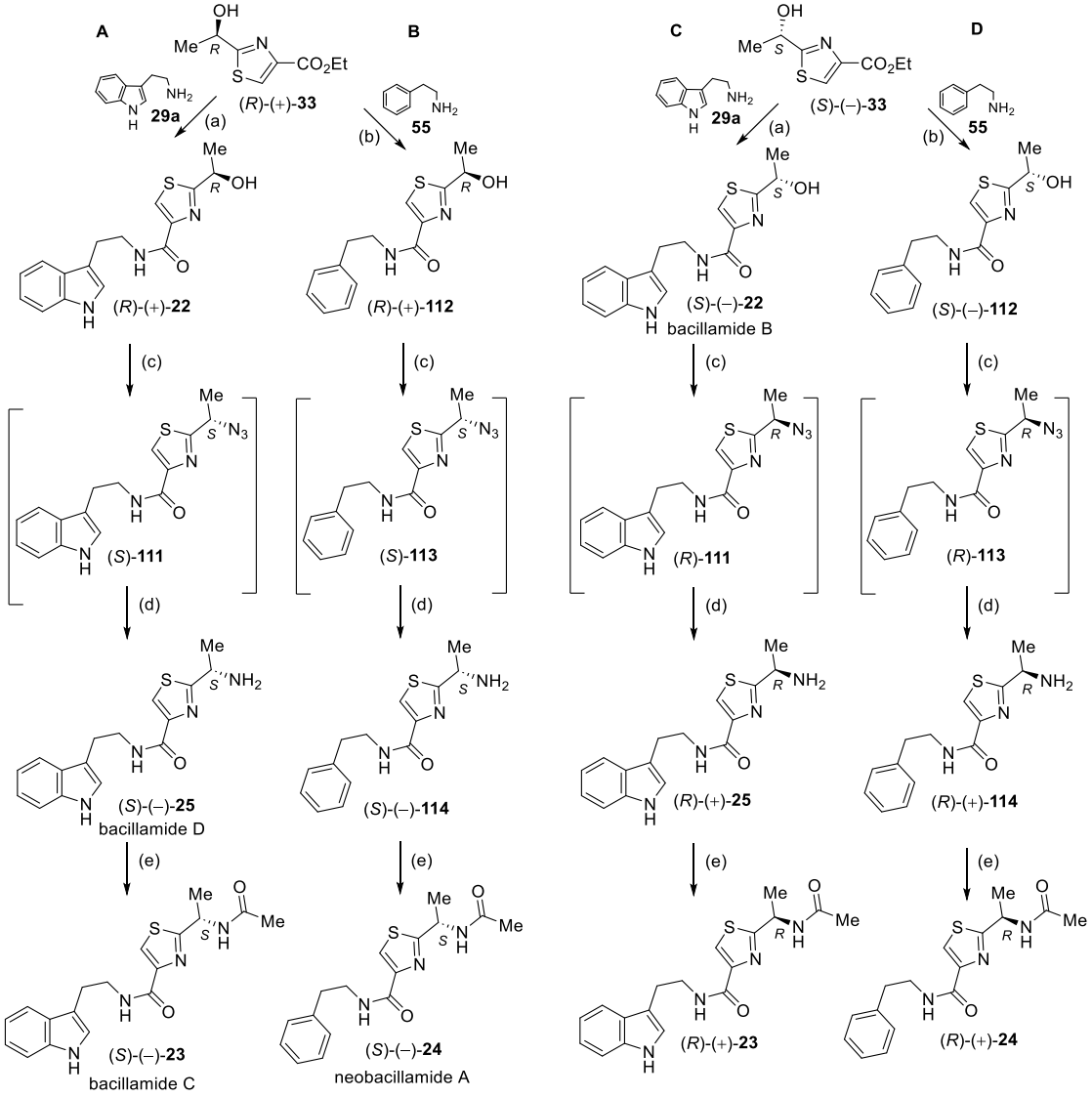

Route A: (a) tryptamine (**29a**), 4,6-dimethylpyrimidin-2-ol, 105 °C, 6 h, 65%, *ee* 95%; (c) PPh_3, DIPEA, DIAD, THF, DPPA; (d) $NaBH_4$, $NiCl_2 \cdot 6\ H_2O$, MeOH, rt, 51% (for two steps), *ee* 87%; (e) acetyl chloride, TEA, DCM, 88%, *ee* 84%. **Route B** (b) β-phenylethylamine (**55**), 4,6-dimethylpyrimidin-2-ol, 105 °C, 12 h, 79%; (c) PPh_3, DIPEA, DIAD, THF, DPPA; (d) $NaBH_4$, $NiCl_2 \cdot 6\ H_2O$, MeOH, rt, 40% (for two steps); (e) acetyl chloride, TEA, DCM, 80%, *ee* 78%. **Route C** (a) tryptamine (**29a**), 4,6-dimethylpyrimidin-2-ol, 105 °C, 6 h, 89%, *ee* 96%; (c) PPh_3, DIPEA, DIAD, THF, DPPA; (d) $NaBH_4$, $NiCl_2 \cdot 6\ H_2O$, MeOH, rt, 48% (for two steps), *ee* 91%; (e) acetyl chloride, TEA, DCM, 84%, *ee* 90%. **Route D** (b) β-phenylethylamine (**55**), 4,6-dimethylpyrimidin-2-ol, 105 °C, 12 h, 77%; (c) PPh_3, DIPEA, DIAD, THF, DPPA; (d) $NaBH_4$, $NiCl_2 \cdot 6\ H_2O$, MeOH, rt, 76% (for two steps); (e) acetyl chloride, TEA, DCM, 87%, *ee* 91%.

Scheme 29. Synthesis of bacillamide B [(*S*)-(–)-**22**], bacillamide C [(*S*)-(–)-**23**], bacillamide D [(*S*)-(–)-**25**], neobacillamide A [(*S*)-(–)-**24**], and their antipodes.

To the best of our knowledge no SC-XRD analysis of the molecular structures of bacillamides A–D or neobacillamide A has been reported in the literature. In order to prove the configurations of bacillamide D (*S*) and bacillamide D antipode (*R*) and to obtain structural information on the shape of the molecules, crystalline picrate salts [(*S*)-(–)-**25** · $(O_2N)_3C_6H_2OH$] and [(*R*)-(+)-**25** · $(O_2N)_3C_6H_2OH$] have been prepared, yielding crystals suitable for SC-XRD (Figures 11 and 12). The measurements confirm the absolute configuration at the carbon atom of the aminoethyl group attached to the thiazole ring, displaying proper Flack parameters.

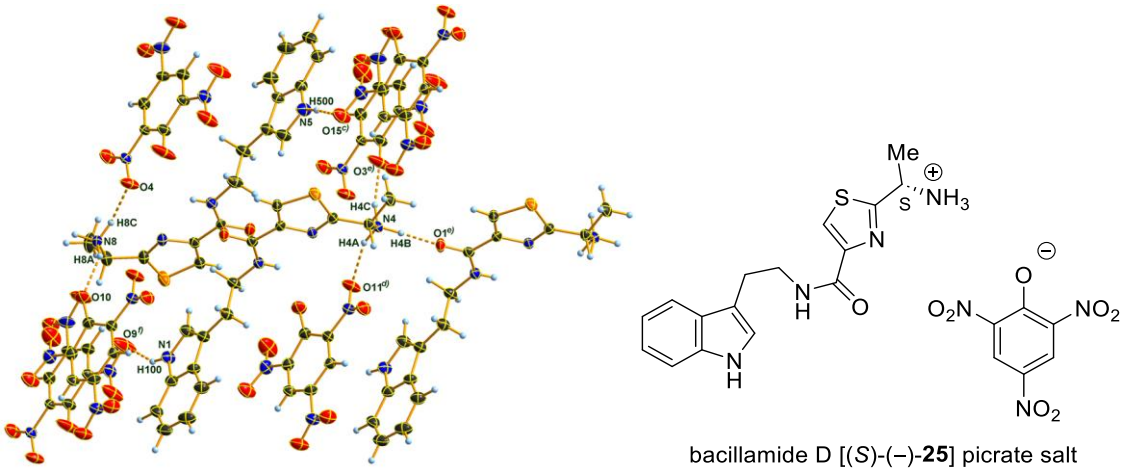

Figure 11. X-ray structure of the picrate salt of bacillamide D [(*S*)-(–)-**25** · $(O_2N)_3C_6H_2OH$]

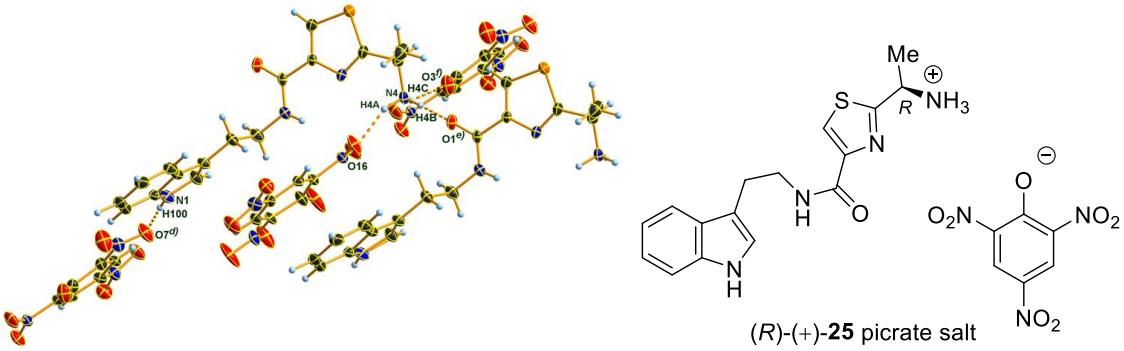

Figure 12. X-ray structure of the picrate salt of bacillamide D antipode [(*R*)-(+)-**25** · $(O_2N)_3C_6H_2OH$].

5.3. Studies on the syntheses of orthoscuticellines A and B

While the synthesis and stereochemical analysis of the bacillamides provided valuable insights into thiazolylindole chemistry and enantioselective transformations, our attention

next turned to a structurally distinct group of marine-derived β-carboline dimers: the orthoscuticellines. These compounds represent a unique case where two β-carboline cores are linked through a cyclobutane unit, posing both synthetic and mechanistic challenges. Building upon the knowledge gained from Bischler–Napieralski cyclizations in the bacillamide project, this section explores our synthetic strategies towards orthoscuticellines A and B.

The synthesis of orthoscuticelline B [(±)-*trans*-**70**] was accomplished in three steps with an overall yield of 58% (Scheme 30) [98]. Condensation of tryptamine (**29a**) with (±)-*trans*-1,2-cyclobutanedicarboxylic acid [(±)-*trans*-**115**] in the presence of T3P® as a coupling agent afforded the corresponding dicarboxamide (±)-*trans*-**116** in 83% yield. Subsequent Bischler–Napieralski cyclization produced the bis(dihydro-β-carboline)-substituted cyclobutane derivative (±)-*trans*-**117**, which was then oxidized with DDQ (performed in pressure-bearing vial) to furnish the target molecule, orthoscuticelline B [(±)-*trans*-**70**]. Remarkably, the trans stereochemistry remained completely intact throughout the sequence, and no formation of the corresponding *cis* isomers was observed in any of the reaction steps.

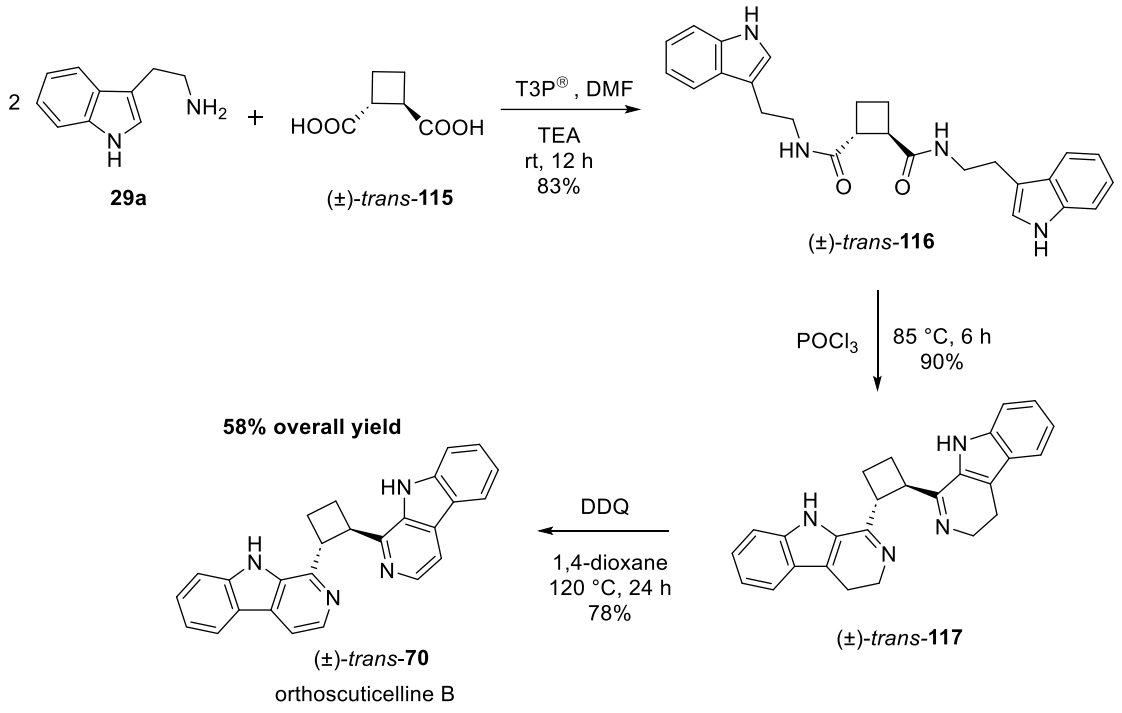

Scheme 30. Synthesis of alkaloid orthoscuticelline B [(±)-*trans*-**70**]

The synthesis of the *cis*-cyclobutane-1,2-dicarboxylic acid (*cis*-**115**, meso form) derivative orthoscuticelline A (**69**) was designed following an analogous strategy to that used for the trans isomer (Scheme 31). In the initial step, condensation of tryptamine

(**29a**) with *cis*-**115** yielded the corresponding *cis*-dicarboxamide (*cis*-**116**). The reaction afforded a significantly lower yield (47%) than that obtained for the trans analogue (83%, Scheme 30), which can be attributed to the concurrent formation of the side-product **118** (meso form) in 19% yield, resulting from the mono-condensation of *cis*-**115** with a single equivalent of tryptamine (**29a**). Subsequent Bischler–Napieralski cyclization of *cis*-**116** produced the bis(dihydro-β-carboline)-substituted cyclobutane intermediate *cis*-**117**. However, the final dehydrogenation (performed in pressure-bearing vial) step unexpectedly yielded the *trans*-cyclobutane-1,2-dicarboxylic acid (*trans*-**115**) derivative orthoscuticelline B (**70**) instead of the desired orthoscuticelline A (**69**). Attempts to perform the oxidation under milder conditions or using alternative reagents, including oxalyl chloride with iron(III) chloride, T3P®, trifluoromethanesulfonic anhydride (Tf_2O), and polyphosphoric acid (PPA), failed to provide the expected product.

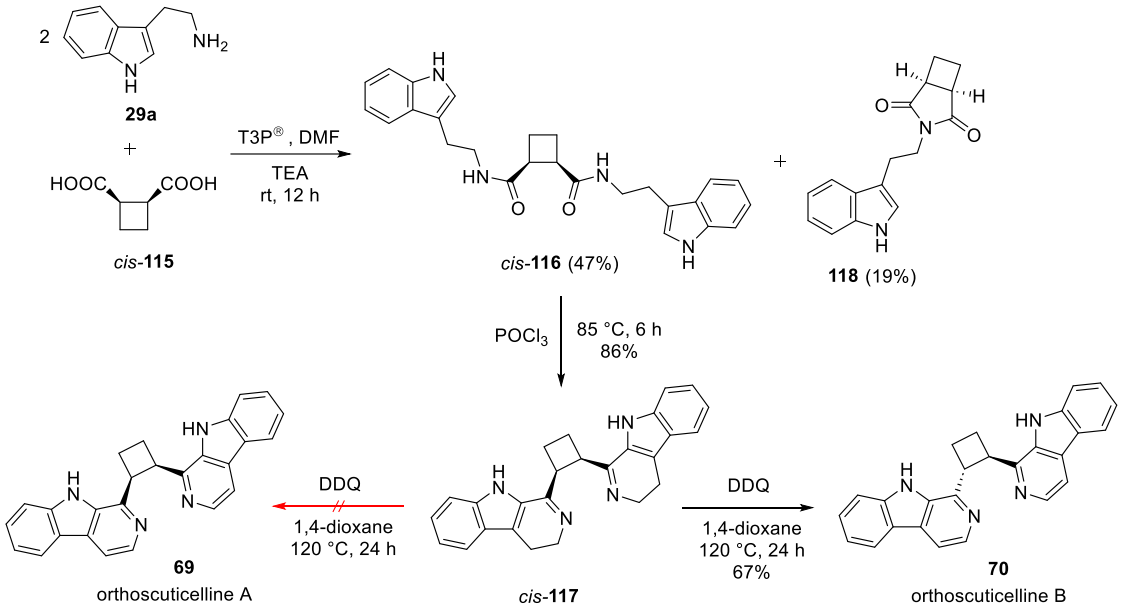

Scheme 31. Synthetic plan for alkaloid orthoscuticelline A (**69**)

The formation of unexpected product **70** is attributable to the conversion of the *cis*-**117** dihydro intermediate into the corresponding thermodynamically more stable (±)-*trans*-**117** isomer through tautomerization of the dihydro-β-carboline ring system (Scheme 32). Experimental evidence supporting this hypothesis was obtained when compound *cis*-**117**, upon stirring overnight at room temperature in 1,4-dioxane, was found to undergo isomerization to yield the (±)-*trans*-**117** derivative.

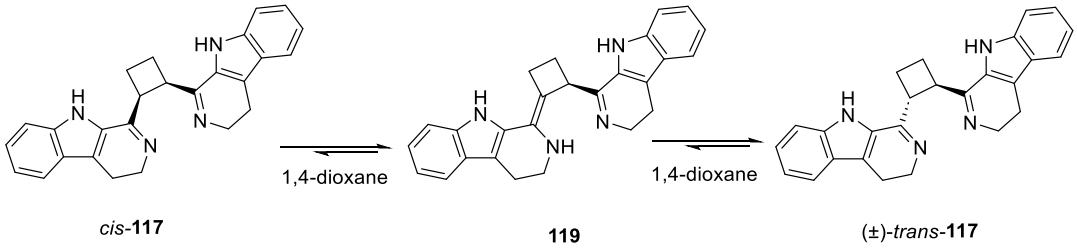

Scheme 32. Proposed tautomerism of *cis*-**117** to (±)-*trans*-**117**

Consequently, an alternative synthetic strategy was explored for the preparation of the *cis* isomer, orthoscuticelline A (**69**), instead of the previously attempted Bischler–Napieralski route. Starting from *cis*-cyclobutane-1,2-dicarboxylic acid (*cis*-**115**), the corresponding *cis*-cyclobutane-1,2-dialdehyde (*cis*-**120**) was obtained in two steps following literature procedures, i.e. *via* acyl chloride formation using thionyl chloride ($SOCl_2$) and subsequent reduction of the diester intermediate (*cis*-**119**) with Red-Al (Scheme 33). However, when conventional Pictet–Spengler cyclization conditions were applied, none of the tested methods afforded the desired tetrahydro derivative (*cis*-**121**) even after 48 hours. The unsuccessful trials included the use of various Brønsted acids (H_2SO_4, trifluoroacetic acid), Lewis acids ($BF_3 \cdot Et_2O$, trimethylsilyl chloride), and other reagents such as 2,4,6-trichloro-1,3,5-triazine, T3P®, and hexafluoro-2-propanol. Following these unsuccessful attempts, the total synthesis of orthoscuticelline A (**69**) was discarded.

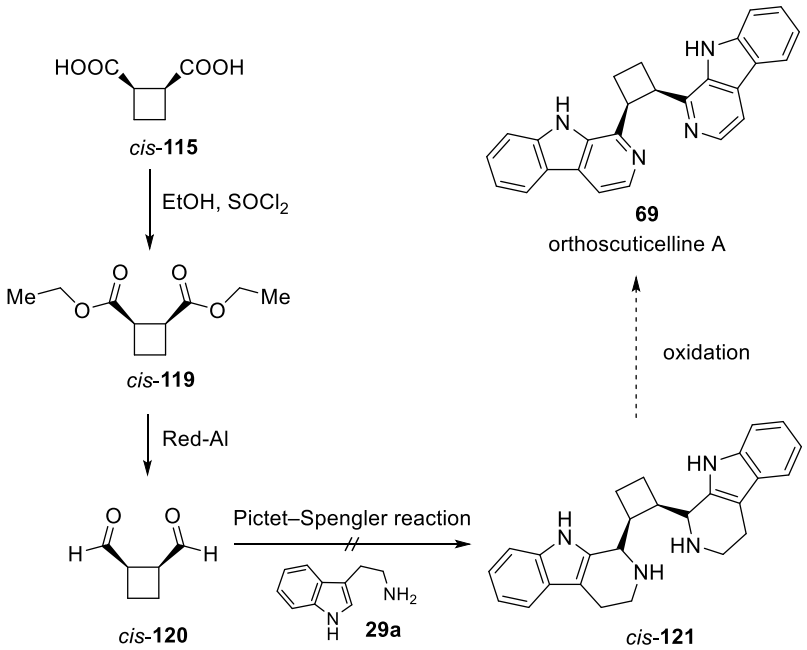

Scheme 33. Alternative synthesis plan for orthoscuticelline A (**69**)

Whereas the initial isolation of orthoscuticelline B [(±)-*trans*-**70**] in the literature from approximately 25 g of freeze-dried bryozoan material yielded only 0.2 mg of product (0.001%) [58], and the first reported total synthesis afforded 31.9 mg of a mixture of orthoscuticellines A (**69**) and B (**70**) over five synthetic steps (overall yield of 7% for **69** and 20% for **70**) [59], our optimized synthetic route provided 77 mg of pure orthoscuticelline B (**70**) starting from commercially available tryptamine (**29a**) in only three steps with an overall yield of 58%.

The NMR spectroscopic data of our synthesized (±)-*trans*-**70** were identical to those reported for the synthetic compound by Yi *et al.* [59]. In contrast, the NMR data published by Kleks *et al.* [58] showed significant deviations from those of the synthetic sample. We hypothesized that these discrepancies originated from the formation of a trifluoroacetate salt, as TFA has been used during the isolation procedure in that study. To test this assumption, NMR spectra of our product were recorded in DMSO-d_6 with incremental additions of TFA (0–2 eq). Pronounced changes were observed in both the ^{1}H and ^{13}C NMR chemical shifts with increasing acid concentration. Upon the addition of 0.5 eq of TFA, the resulting spectra matched precisely those reported by Kleks *et al.* [58], thereby confirming our hypothesis.

5.4. Studies on the syntheses of brevicarine and brevicolline

The orthoscuticelline studies highlighted the potential and limitations of classical cyclization reactions in constructing complex β-carboline architectures. To further expand this structural space and connect marine and terrestrial alkaloid chemistry, we next investigated brevicarine and brevicolline, two plant-derived β-carboline alkaloids exhibiting notable pharmacological activities. Their synthesis did not only allow us to compare different β-carboline-forming strategies but also to evaluate scalable, environmentally conscious modifications applicable to natural product synthesis [99].

In this work, our objective was to establish a novel and scalable synthetic route to brevicarine (**73**) and to design an alternative pathway for the synthesis of brevicolline [(*S*)-**72**], both utilizing a common key intermediate (**74**) [64]. The synthesis of brevicarine (**73**, Scheme 34) commenced with the catalytic hydrogenation of the alkyne moiety in phthaloyl-protected intermediate **76**, affording compound **122**. Subsequent cleavage of the phthalimide protecting group using methylamine furnished the corresponding amine **123**. Alternatively, a modified, environmentally benign protocol was developed, in which the removal of the phthaloyl group from compound **76** to yield amine **77** was achieved

with methylamine instead of the previously applied, highly toxic methylhydrazine [100]. This was followed by catalytic reduction of the triple bond, providing the same amine intermediate **123**.

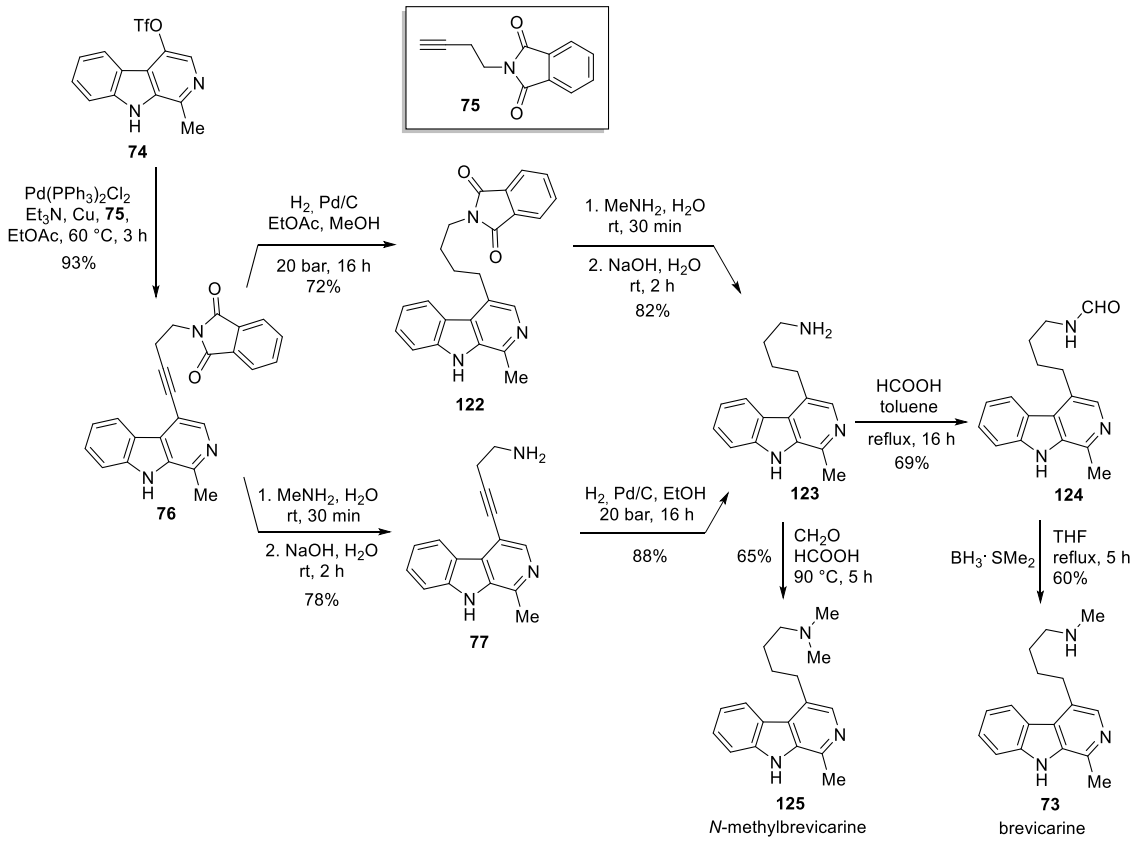

Scheme 34. New synthetic variants for the preparation of brevicarine alkaloid (**73**) and its synthetic derivative *N*-methylbrevicarine (**125**)

Attempts to achieve *N*-monomethylation of the primary amino group in compound **123** through direct alkylation with methyl iodide or *via* the Eschweiler–Clarke reductive amination using formaldehyde and formic acid proved unsuccessful, as the reaction consistently yielded a considerable amount of the undesired dimethylated side-product, even when only one equivalent of the alkylating reagent was employed. Ultimately, a successful strategy was developed to circumvent overmethylation: the methyl group was introduced indirectly by *N*-formylation of compound **123** to afford the formamide intermediate **124**, followed by reduction of the formyl functionality with borane-dimethyl sulfide complex, giving brevicarine (**73**) as its dihydrochloride salt. On the basis of these findings, the Eschweiler–Clarke methylation of primary amine **123** was subsequently applied to prepare *N*-methylbrevicarine (**125**), a close structural analogue of natural alkaloid **73** [101].

Although a preliminary ^{1}H NMR spectrum of isolated brevicarine base (**73**) and partial signal assignments were reported as early as 1969 [101], the data were incomplete. The chemical shifts described in that early report, however, are fully consistent with those of our synthetic compound. Subsequent publications [65,69,70] confirmed the structure of brevicarine by IR and MS analyses or through its characteristic reactivity but did not include comprehensive NMR characterization. In the present work, we provided the complete and unambiguous assignment of all ^{1}H and ^{13}C NMR resonances for both the free base and the dihydrochloride salt of brevicarine (**73**).

During our investigations aimed at developing an improved and efficient synthetic route to brevicarine (**73**), an unexpected reaction outcome was observed (Scheme 35). According to literature precedents, the reduction of carbamate **126**, prepared from amine **123** *via* ethoxycarbonylation, was anticipated to yield brevicarine (**73**) upon treatment with $LiAlH_4$ [102,103]. Contrary to expectations, the reaction proceeded only as far as the *N*-formyl intermediate (**124**), and no formation of brevicarine (**73**) was detected by LC–MS analysis [104].

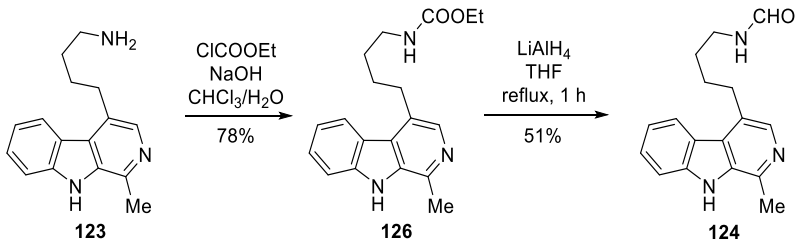

Scheme 35. Synthesis of carbamate **126** and its subsequent reduction with $LiAlH_4$

In designing an alternative synthetic approach towards racemic brevicolline [(±)-**72**], our primary objective was to achieve direct coupling of the pyrrole moiety to compound **74**, rather than constructing the pyrrole ring *via* intramolecular cyclization, as outlined in Scheme 22. The Suzuki–Miyaura cross-coupling reaction of **74** with pyrrole boronic ester **127** proceeded smoothly, affording the pyrrolo-β-carboline derivative **128** in excellent yield (Scheme 36). However, attempts to selectively hydrogenate the pyrrole ring of **128** under various catalytic conditions were unsuccessful. When the reaction was performed under mild conditions (ambient temperature, 15 bar H_2) using platinum(IV) oxide monohydrate (Adams' catalyst, $PtO_2 \cdot H_2O$) as the catalyst, a complete reduction occurred, yielding the overhydrogenated tetrahydro derivative **129**, corresponding to the partially saturated form of racemic brevicolline [(±)-**72**], in 91% yield.

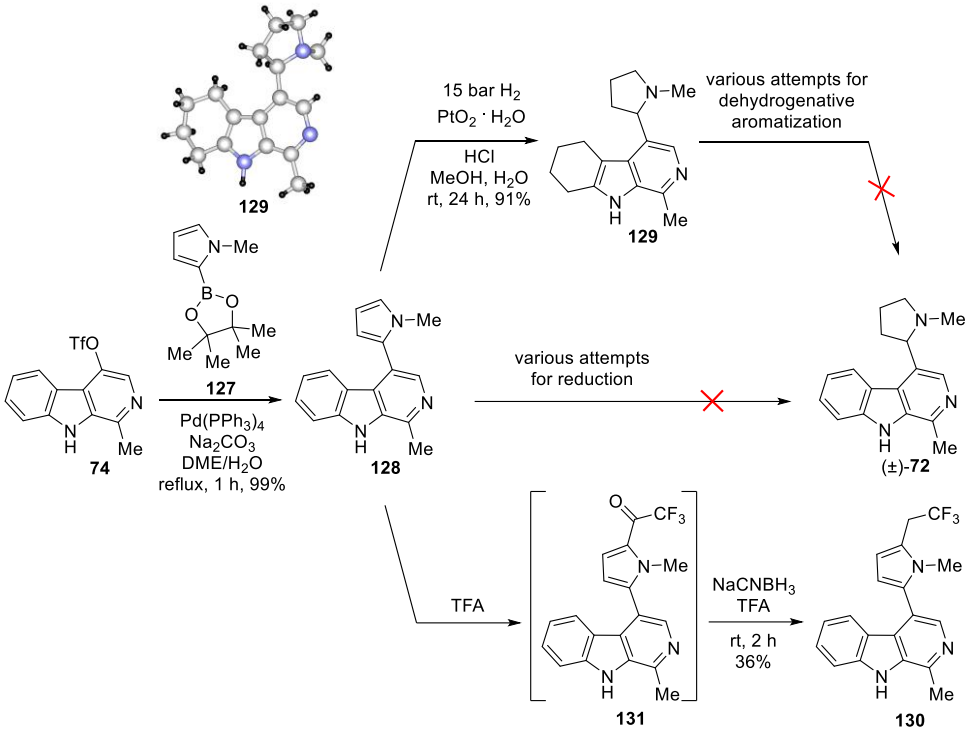

Scheme 36. Experiments on the synthesis of racemic brevicolline [(±)-**72**], and the formation of unexpected products

The structure of compound **129** was further confirmed by SC-XRD analysis. Variation of the hydrogenation catalyst using $Pd(OH)_2$, Ru, or Rh did not alter the course of the reaction; in all cases, compound **129** was obtained exclusively, and the formation of brevicolline [(±)-**72**] could not be detected. Interestingly, attempts to convert compound **129** into brevicolline [(±)-**72**] *via* dehydrogenative aromatization using a range of oxidizing agents (DDQ, Pd/C, MnO_2, $CuCl_2$, I_2, elemental sulfur, and $KMnO_4$) were likewise unsuccessful.

Based on literature precedents [102,103], we next explored the selective reduction of the pyrrole ring in compound **128** with $NaCNBH_3$ in TFA. Unexpectedly, this reaction afforded the trifluoroethylated derivative **130**. The formation of this product can be rationalized by analogy to previously reported examples of TFA-mediated trifluoroacetylation of aromatic systems [105,106]. In our case, however, both trifluoroacetylation of the pyrrole moiety in **128** and subsequent reduction of the resulting carbonyl intermediate **131** with $NaCNBH_3$ occurred in a single reaction vessel – a transformation not previously described in the literature. It is noteworthy that when the same reaction was performed in acetic acid instead of TFA, no conversion was observed

(**128** did not react), whereas replacing $NaCNBH_3$ with $NaBH_4$ in TFA again led to the formation of compound **130**.

5.5. Synthesis of 1-substituted β-carbolines *via* multicomponent reactions and SAR studies thereof

Having completed the synthesis of complex β-carboline natural products, our focus shifted towards the development of structurally simplified analogues amenable to high-throughput derivatization and pharmacological screening. To this end, we explored multicomponent reactions as versatile tools for the rapid construction of 1-substituted β-carboline derivatives. These reactions allowed the systematic investigation of substituent effects and the establishment of preliminary structure-activity relationships within a chemically diverse compound library. The mentioned compounds represent novel chemical entities, their comprehensive structural characterization and analytical data are reported here for the first time.

In view of the valuable pharmacological potential associated with these structural motifs, we set out to synthesize a series of derivatives of 1-formyl-β-carbolines (**135**), namely α-aminophosphonates (**132**), α-acylamino-α-aryl carboxamides (**133**), and 2-oxo-1,2,3,4-tetrahydropyrimidine-5-acyl derivatives (**134**), employing the Kabachnik–Fields, Ugi, and Biginelli multicomponent reactions, respectively (Scheme 37). The target compounds were designed to incorporate structural features that have frequently been associated with diverse and significant biological activities in the literature.

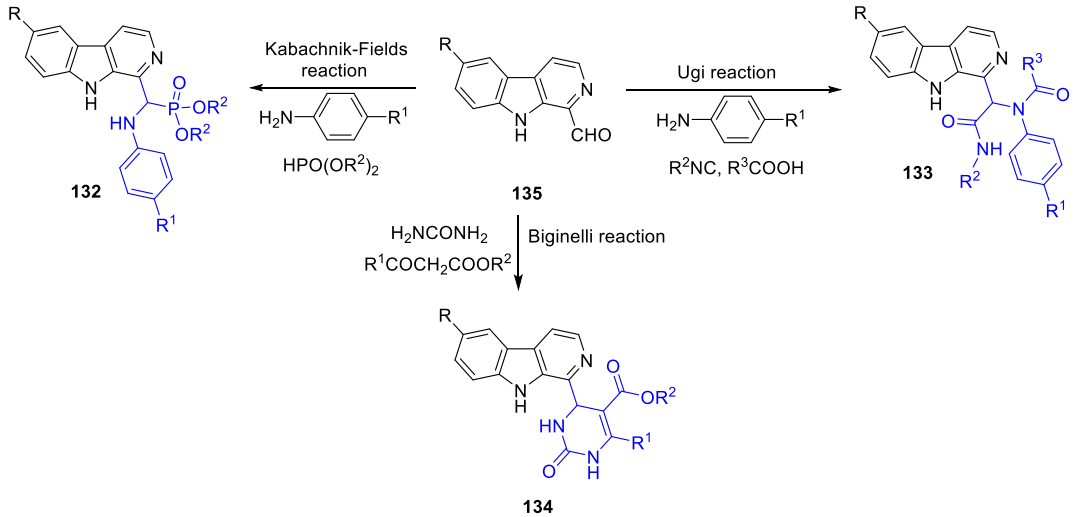

Scheme 37. Multicomponent reactions of 1-formyl-β-carbolines (**135**)

The most widely employed method for the synthesis of α-aminophosphonates is the one-pot, three-component Kabachnik–Fields reaction, which involves the condensation

of a carbonyl compound, a primary or secondary amine, and a phosphite. This transformation has been performed under a broad range of experimental conditions, utilizing various catalysts and solvents [107]. More recently, our group reported a broadly applicable, catalyst- and solvent-free procedure for the Kabachnik–Fields synthesis of α-aminophosphonates under ambient conditions [108]. In the present work, α-aminophosphonates (**132**) incorporating a β-carboline scaffold were synthesized by reacting 1-formyl-β-carbolines (**135**) with aniline or substituted anilines (**136**) and dialkyl phosphites (**137**) in a three-component Kabachnik–Fields condensation carried out at 80 °C in the presence of 10 mol% magnesium perchlorate [109] as the catalyst (Scheme 38).

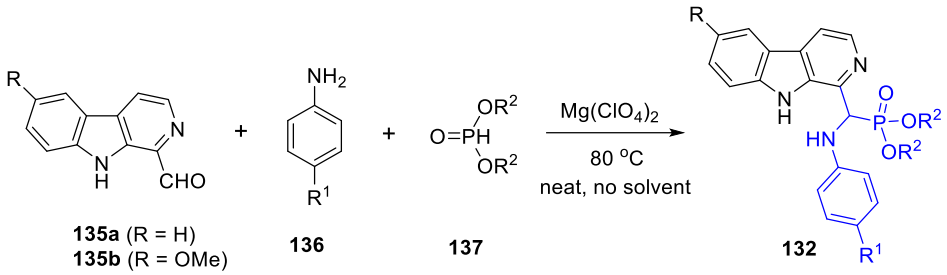

132	R	R^1	R^2	reaction time (h)	yield (%)
a	H	H	Et	2	92
b	H	F	Et	2	94
c	H	Cl	Et	2	80
d	H	Br	Et	4	74
e	H	Me	Et	3	97
f	H	MeO	Et	2.5	98
g	H	CF_3	Et	2	49
h	H	H	*i*-Pr	2	73
i	H	H	Bu	4	49
j	MeO	Br	Et	2	89

Scheme 38. Synthesis of α-aminophosphonate derivatives of β-carboline (**132**)

α-Acylamino-α-aryl carboxamides (**133**) can be synthesized *via* the Ugi multicomponent reaction, which involves the condensation of four components: an amine, an aldehyde or ketone, an isocyanide, and a carboxylic acid. By varying these starting materials, a wide range of substitution patterns can be achieved. In the present work, β-carboline-based α-acylamino-α-aryl carboxamide derivatives (**133**) were obtained through Ugi condensation of 1-formyl-β-carbolines (**135**), aniline or substituted anilines (**136**), alkyl isocyanides (**138**), and carboxylic acids (**139**). The reactions were performed in methanol at room temperature [110] and afforded the desired products in good yields (Scheme 39).

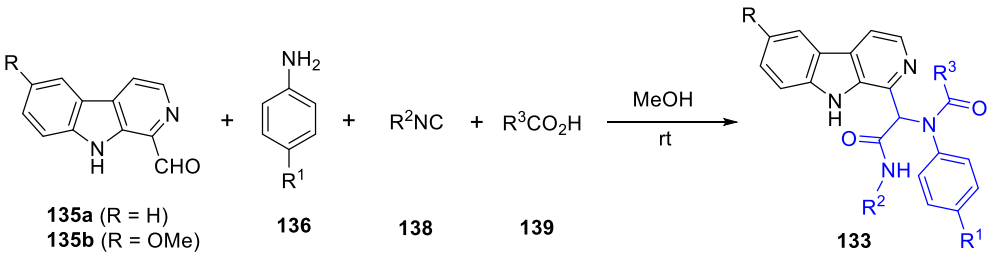

135a (R = H)
135b (R = OMe)

136 **138** **139** **133**

133	R	R^1	R^2	R^3	reaction time (h)	yield (%)
a	H	H	*t*-Bu	Me	24	82
b	H	H	*t*-Bu	*t*-Bu	72	93
c	H	H	*t*-Bu	Ph	48	74
d	H	F	*t*-Bu	Me	48	76
e	H	Cl	*t*-Bu	Me	72	60
f	H	Br	*t*-Bu	Me	48	33
g	H	Me	*t*-Bu	Me	72	90
h	H	MeO	*t*-Bu	Me	48	77
i	H	H	Pn	Me	72	91
j	MeO	H	*t*-Bu	Me	72	80

Scheme 39. Synthesis of α-acylamino-α-aryl carboxamide derivatives of β-carboline (**133**)

The Biginelli reaction is an acid-catalyzed three-component condensation between an aldehyde, a β-ketoester, and urea, leading to the formation of 2-oxo-4-aryl-1,2,3,4-tetrahydropyrimidine-5-carboxylic acid derivatives. In the present work, 2-oxo-1,2,3,4-tetrahydropyrimidine-5-carboxylic acid derivatives bearing a β-carbolin-1-yl substituent at the 4-position (**134**) were synthesized *via* Biginelli reactions by reacting 1-formyl-β-carbolines (**135**) with urea and β-ketoesters (**140**) in various alcohol solvents in the presence of 20 mol% cerium(III) chloride [111] as the catalyst (Scheme 40).

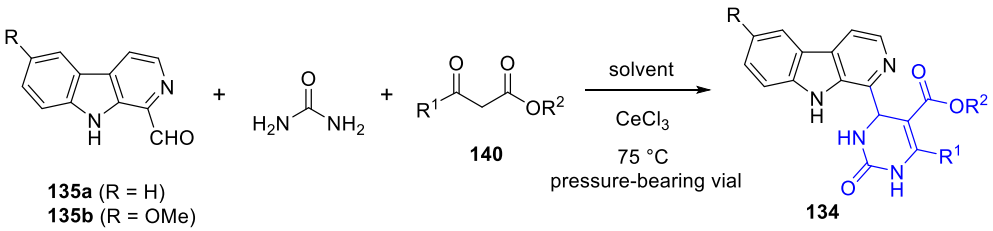

135a (R = H)
135b (R = OMe)

140 **134**

134	R	R^1	R^2	solvent	reaction time (h)	yield (%)
a	H	Me	Me	MeOH	24	59
b	H	Pr	Me	MeOH	24	57
c	H	Ph	Et	EtOH	40	26
d	H	Me	*t*-Bu	*t*-BuOH	24	28
e	H	Me	*i*-Pr	*i*-PrOH	24	82
f	H	Et	Et	EtOH	24	77
g	H	*i*-Pr	Et	EtOH	24	53
h	H	2-Cl-C_6H_4	Me	MeOH	48	35
i	MeO	Me	Me	MeOH	24	33

Scheme 40. Synthesis of 3,4-dihydropyrimidin-2(1*H*)-one derivatives of β-carboline (**134**)

Due to the limitations on dissertation length, only the most promising representatives from each compound class synthesized *via* multicomponent reactions are presented and discussed below. The antiproliferative activities of these compounds were evaluated against two cancer cell lines, HL-60 human promyelocytic leukemia and C6 rat glioma, as well as 3T3 mouse fibroblast cells used as a non-cancerous control to assess selectivity. The HL-60 model represents disseminated hematological malignancies that require systemic pharmacotherapy, while the C6 glioma model serves as a representative for brain tumors, which remain a major therapeutic challenge due to limited efficacy of current treatment options.

Among the compounds tested, Kabachnik–Fields product **132e** exhibited potent activity against HL-60 cells with an IC_{50} of 62.53 nM and demonstrated a 9.0-fold selectivity relative to 3T3 fibroblasts, while showing no measurable activity against C6 glioma cells. Conversely, the Ugi product **133g** showed pronounced cytotoxicity towards C6 cells (IC_{50} = 60.27 nM) with 24.9-fold selectivity and was inactive against HL-60 cells. The Biginelli derivative **134e** displayed dual activity, with IC_{50} values of 136.2 nM on HL-60 cells (14.0-fold selectivity) and 91.83 nM on C6 cells (20.8-fold selectivity). These findings highlight the potential of structurally diverse β-carboline derivatives obtained *via* multicomponent reactions as selective antiproliferative agents with distinct cell-line-specific profiles. Additional *in silico* target docking studies, along with ADME measurements, are currently being conducted.

5.6. Flow synthesis of 1-substituted 3,4-dihydro-β-carbolines

Encouraged by the promising biological results obtained for certain 1-substituted β-carbolines, we next sought to translate batch reactions into continuous-flow processes to enhance efficiency, reproducibility, and scalability. This section presents our efforts towards establishing a robust flow synthesis of 3,4-dihydro-β-carboline intermediates, emphasizing the optimization of reaction parameters and the potential for sustainable production at larger scale.

For the development of a two-step flow synthesis of β-carboline derivatives, harmalan (**68**) was selected as a model compound, starting from tryptamine (**29a**) through T3P® mediated *N*-acetylation to *N*-acetyltryptamine (**67**), followed by Bischler–Napieralski cyclization to yield the corresponding 1-methyl-3,4-dihydro-β-carboline (**68**, Scheme 41).

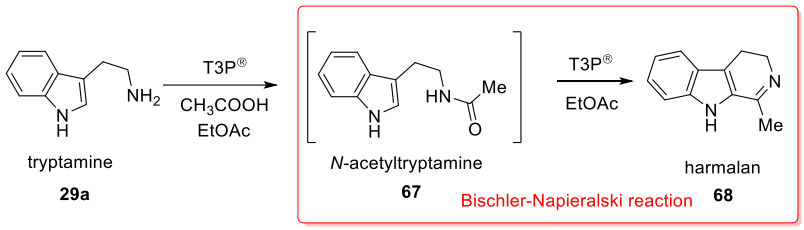

Scheme 41. Synthesis of 1-methyl-3,4-dihydro-β-carboline from tryptamine

Preliminary batch optimization studies were carried out to evaluate the effects of solvent, T3P® excess, temperature, and concentration on reaction efficiency. Initially, DMF was employed as the reaction medium; however, when the reaction time was extended to 1–2 hours, a significant amount of an undesired side-product (**141**) was detected in the mixture and gas formation was observed. The side-product was isolated and characterized, revealing that harmalan (**68**) undergoes overreaction with DMF at elevated temperature in the presence of T3P® (Scheme 42).

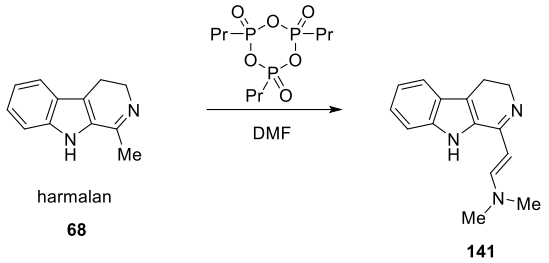

Scheme 42. Unexpected side-product formation from harmalan (**68**)

A solvent mixture of ethyl acetate and acetonitrile was selected after extensive screening, as it provided complete solubility for all reactants and products while eliminating side-product formation observed in DMF. The use of T3P® is advantageous over more aggressive reagents like $POCl_3$ due to its lower toxicity and milder reaction profile. Furthermore, T3P® enables a streamlined process by promoting both the acylation and subsequent cyclization in a single step, while the MeCN/EtOAc solvent system ensures optimal flow compatibility and heat transfer. The model reaction in batch employed tryptamine (**29a**) and a representative carboxylic acid as substrates in a 1:1 ratio, using 2 eq T3P® (50% in EtOAc) as both coupling and cyclization reagent. 0.18 M substrate concentration was needed for full dissolution. The reactions were carried out in the same continuous-flow apparatus described in the Methods section, employing a 5-mL stainless steel coil reactor equipped with a back-pressure regulator (20 bar) to permit operation at 200 °C (Figure 13). Both consecutive reaction steps were performed within

the same coil, immersed in an oil bath and magnetically stirred to ensure uniform temperature distribution.

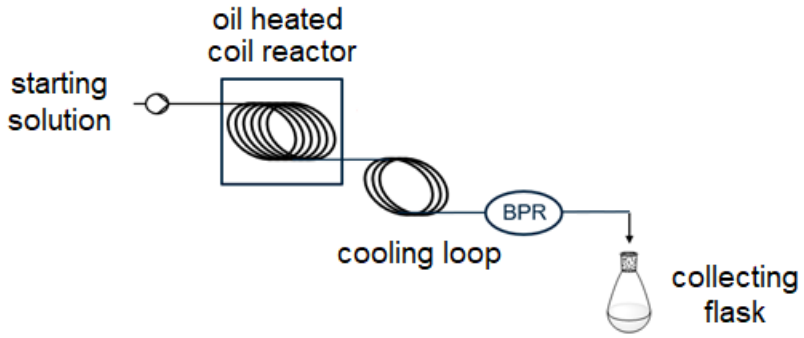

Figure 13. Continuous-flow setup for two-step synthesis of 3,4-dihydro-β-carbolines

The best performance was achieved for the model compound harmalan (**68**) under the following conditions: 200 °C, 20 bar, and a residence time of 4 minutes giving 90% yield (Figure 14). The continuous-flow process demonstrated excellent reproducibility, with consistent yields across multiple runs and no need for chromatographic purification. In most cases of scope expansion, the products could be isolated in high yields by simple solvent evaporation, basic extraction and, with only occasional chromatography required when small amounts of intermediates remained (Figure 14).

Compared to the model compound, we extended the reaction by enabling functionalization at both the 1- and 6-positions, thereby broadening the structural diversity and expanding the reaction scope. In some cases (compounds **143**, **145**, **146**), additional MeCN was needed for complete dissolution of the substrates, which can be observed on the concentration data. The high pressure and temperature conditions employed here would be challenging and potentially hazardous in batch mode, but are readily and safely achieved under continuous-flow conditions, illustrating one of the key advantages of the technique. Compounds **68** and **142-144** and **146** were synthesized previously using batch methods, however their continuous-flow technology synthesis is reported here for the first time, with their formal analytical characterization of their base forms. Compound **145** is reported here the first time.

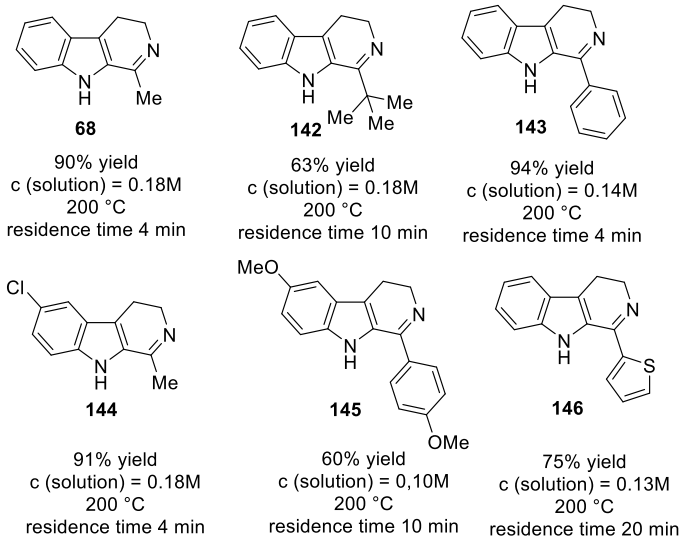

Figure 14. 3,4-Dihydro-β-carbolines prepared with flow system

Overall, this work represents the first reported flow synthesis of 3,4-dihydro-β-carbolines starting from tryptamines, providing a reproducible and scalable method with significantly reduced reaction time, simplified workup, and enhanced process safety. The modularity of the approach also allows facile structural diversification by varying the amine or acid components, thereby offering a versatile platform for the rapid generation of β-carboline analogues with potential pharmacological relevance.

5.7. Computational study on the Robinson–Gabriel synthesis and Bischler–Napieralski reaction

To complement the experimental observations obtained from both batch and flow reactions, computational investigations were undertaken to elucidate the mechanistic features governing the key cyclization steps. In particular, DFT calculations were applied to compare the energetics of the Robinson–Gabriel and Bischler–Napieralski reactions, thereby providing theoretical insights that rationalize the distinct outcomes observed in our synthetic studies [112]. The results of these computational analyses are discussed in this section.

To gain insight into the mechanisms of the Robinson–Gabriel and Bischler–Napieralski reactions (for the experimentally found reactions of **64** and **67** with T3P® reagent see Scheme 20 in the Introduction section), DFT calculations were performed using two model substrates, *N*-acetyl-β-oxotryptamine (**64**, Scheme 43) and *N*-acetyltryptamine (**67**, Scheme 44). The computational analysis aimed to rationalize the observed formation of the oxazole product (**66**, Scheme 43) *via* the Robinson–Gabriel

pathway and the absence of the corresponding 3,4-dihydro-β-carboline-4-one (**68**, harmalan, Scheme 44) in the Bischler–Napieralski route.

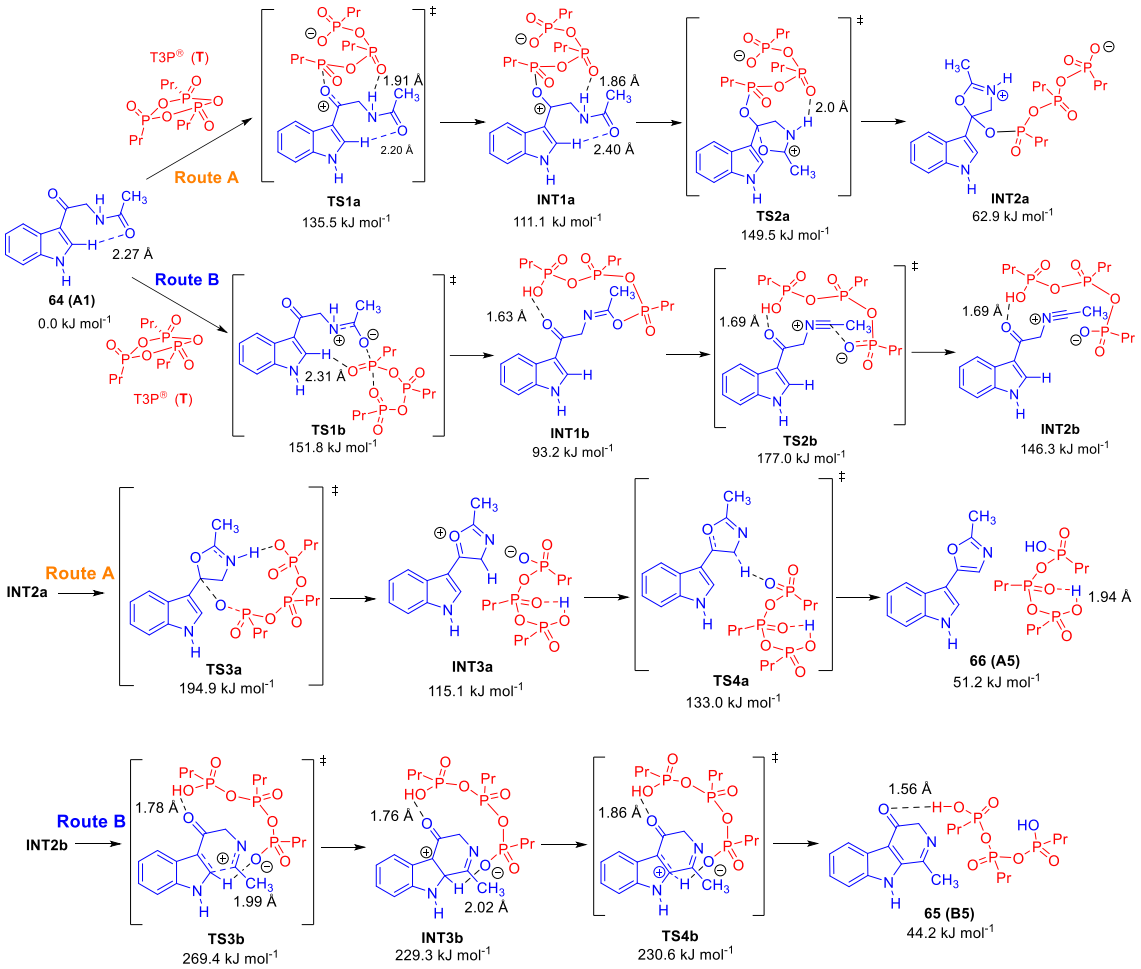

Scheme 43. DFT mapped mechanisms of the Robinson–Gabriel and Bischler–Napieralski reactions from *N*-acetyl-β-oxotryptamine (**64**)

Both mechanisms begin with activation of the amide by T3P®, leading to phosphorus–oxygen adducts. For the β-oxotryptamine model, the carbonyl oxygen proved more reactive than the amide oxygen, favoring the Robinson–Gabriel pathway. Comparison of the calculated activation barriers indicated that the cyclization step forming the oxazole intermediate required substantially less energy than the corresponding step in the Bischler–Napieralski route, which involves nitrilium ion attack on the indole ring.

The overall energy profile revealed that the rate-determining step in the proposed but experimentally unobserved Bischler–Napieralski pathway (TS3b, 269 kJ mol^{-1}) was considerably higher than that of the feasible Robinson–Gabriel cyclization (TS3a, 195 kJ mol^{-1}), explaining why only the latter occurs under the applied conditions. The computed intermediate energies further confirmed that the oxazole ring formation (TS3a) is

exothermic (formation of intermediate INT2a compared to INT1a) and thermodynamically more favorable than β-carboline formation (TS3b).

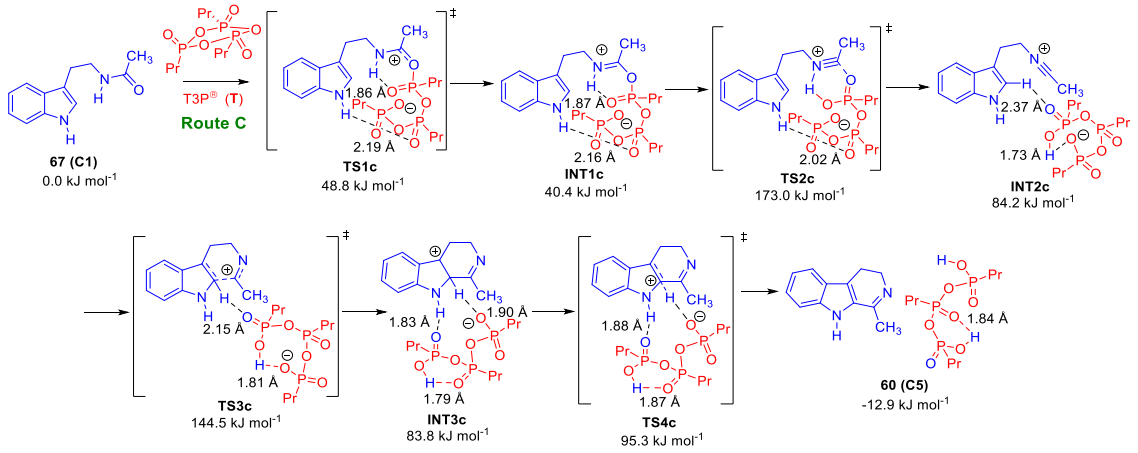

Scheme 44. DFT mapped mechanisms of the Bischler–Napieralski reactions from *N*-acetyltryptamine (**67**)

To evaluate the influence of the carbonyl substituent, the Bischler–Napieralski reaction of *N*-acetyltryptamine (**67**) was also modeled. In this case, the absence of the electron-withdrawing keto group significantly lowered the activation barrier of the cyclization step (144 kJ mol^{-1}), confirming that the carbonyl group in β-oxotryptamine deactivates the indole ring towards electrophilic attack in the Bischler–Napieralski pathway.

The combined energy profiles (Figure 15) clearly demonstrate that the Robinson–Gabriel reaction proceeds *via* a kinetically and thermodynamically more favorable route, while the Bischler–Napieralski pathway of *N*-acetyl-β-oxotryptamine (**64**) is hindered by prohibitively high activation energies, rendering product formation experimentally unfeasible (A6, B6 and C6 are the final products in their lowest energy conformer form without any interactions between them).

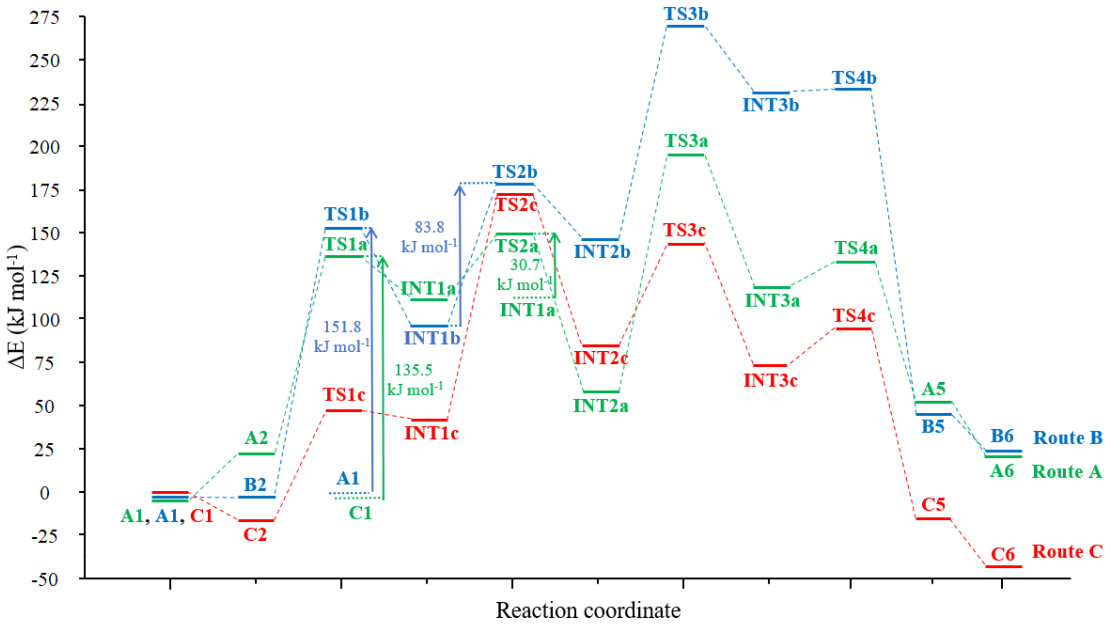

Figure 15. Summarizing diagram for the energetics of the Robinson–Gabriel synthesis (Route A: A1 to A6, green) and Bischler–Napieralski reactions (Route B: A1 to B6, blue and Route C: C1 to C6, red)

To compare the kinetics of the two experimentally feasible reactions, time-resolved HPLC-MS measurements were performed under identical conditions (120°C) to monitor the consumption of *N*-acetyl-β-oxotryptamine (**64**) and *N*-acetyltryptamine (**67**) and the formation of the corresponding Robinson–Gabriel and Bischler–Napieralski products. The Robinson–Gabriel reaction reached 50% conversion after approximately 20 minutes and was complete within 100 minutes, while the Bischler–Napieralski cyclization exhibited a similar profile with a $t_{1/2}$ of 16 minutes and full conversion after about 90 minutes. These comparable reaction rates are consistent with the similar activation barriers calculated for the rate-determining steps (Robinson–Gabriel reaction: TS3a 195 kJ mol^{-1} and Bischler–Napieralski cyclization: TS2c 173 kJ mol^{-1}). While the calculated activation energies appear higher than typically expected for a reaction occurring at 120 °C, it should be noted that such values often reflect the tendency of DFT methods to overestimate activation barriers. Therefore, these results are primarily intended to provide a comparative analysis of energetic trends and mechanistic pathways.

The computational and experimental results are in good agreement, indicating that the electron-withdrawing effect of the keto group in *N*-acetyl-β-oxotryptamine (**64**) alters the charge distribution in the nitrilium intermediate, thereby disfavoring β-carboline ring formation under the applied conditions.

6. CONCLUSIONS

This dissertation's research describes a comprehensive synthetic and mechanistic exploration of indole-based alkaloids and their structural analogues, combining experimental organic chemistry with computational analysis and pharmacological collaboration. Through systematic investigations, alternative synthetic methodologies were developed for the preparation of oxazolyl- and thiazolylindoles, β-carboline derivatives, and their corresponding natural product analogues.

In the first part of the work, novel oxazolyl- and thiazolylindoles were synthesized *via* Robinson–Gabriel synthesis and related cyclodehydration reactions. Thiazole and carbothioamide functionalities were linked to antiproliferative activity against HL-60 leukemia and C6 glioma cell lines, according to the study's identification of structure–activity relationships. These findings suggest that these heteroaromatic frameworks could serve as starting points for medicinal chemistry investigations.

Next, the focus shifted to the asymmetric syntheses of bacillamide alkaloids and their antipodes, allowing unambiguous stereochemical assignments supported by SC-XRD. The structural determination of bacillamide D and its enantiomer supplements the known natural product chemistry of these derivatives and provides a reference for future isolation studies.

The research then moves toward the total syntheses of complex β-carboline alkaloids such as orthoscuticelline B, brevicarine, and brevicolline, yielding competitive routes. The work also explored practical modifications driven by green chemistry principles, including the replacement of certain reagents and the application of continuous-flow procedures for key cyclizations.

Finally, computational studies provided mechanistic insight into the contrasting reactivity of the Robinson–Gabriel synthesis and Bischler–Napieralski reactions, offering a possible explanation for the observed reaction selectivity. The combined synthetic, biological, and theoretical findings discussed here advance knowledge of indole-based heterocycle chemistry and provide adaptable frameworks for the development of bioactive molecules with potential pharmaceutical relevance.

7. SUMMARY

This doctoral work describes the design, synthesis, and mechanistic study of indole-derived alkaloids and their synthetic analogues, combining classical and modern organic chemistry with computational modeling and biological evaluation. The project was inspired by the role of the indole scaffold in natural and synthetic bioactive compounds and by the interest in developing alternative synthetic methodologies.

Novel oxazolyl- and thiazolylindoles were prepared through optimized Robinson–Gabriel synthesis and thionation reactions, and their antiproliferative activities were evaluated *in vitro*. The thiazolyl and carbothioamide derivatives exhibited the highest activity and selectivity toward tumor cell lines. Enantioselective syntheses of bacillamides B–D and neobacillamide A were then achieved using asymmetric transfer hydrogenation and Mitsunobu reaction steps, with absolute configurations supported by SC-XRD, providing the first structural elucidations within this group of alkaloids.

Further studies resulted in concise syntheses of orthoscuticelline B, brevicarine, and brevicolline, including practical alternatives to earlier reported methods. The work also applied flow-based approaches to the synthesis of 1-substituted 3,4-dihydro-β-carbolines, exploring their synthetic scalability and easy operation. Complementary computational investigations offered a possible rationale for the different mechanistic pathways and energetic preferences of the key cyclization reactions, providing a theoretical framework for the selectivities observed throughout the project.

Overall, the results of this dissertation present synthetic strategies, mechanistic insights, and biological data related to the field of heterocyclic chemistry. The methodologies and compounds developed herein could provide a basis for future research aimed at the exploration of indole-based therapeutic agents.

8. REFERENCES

1. Sravanthi, T. V., & Manju, S. L. (2016). Indoles – A promising scaffold for drug development. European Journal of Pharmaceutical Sciences, 91, 1-10. https://doi.org/10.1016/j.ejps.2016.05.025

2. Omar, F., Tareq, A. M., Alqahtani, A. M., Dhama, K., Sayeed, M. A., Emran, T. B., & Simal-Gandara, J. (2021). Plant-based indole alkaloids: A comprehensive overview from a pharmacological perspective. Molecules, 26(8), 2297. https://doi.org/10.3390/molecules26082297

3. Dreicer, R., Chu, F., Cahn, D. J., Getzenberg, R. H., Rodriguez, D., Barnette, K. G., Steiner, M. S., Saltzstein, D. R., Tutrone, R. F., & Shore, N. D. (2022). Phase 3 VERACITY clinical study of sabizabulin in men with metastatic castration-resistant prostate cancer who have progressed on an androgen receptor targeting agent. Journal of Clinical Oncology, 40(16), TPS5102. https://doi.org/10.1200/JCO.2022.40.16_suppl.TPS5102

4. Dadras, A., Rezvanfar, M. A., Beheshti, A., Naeimi, S. S., & Siadati, S. A. (2022). An urgent industrial scheme both for total synthesis, and for pharmaceutical analytical analysis of umifenovir as an anti-viral API for treatment of COVID-19. Combinatorial Chemistry & High Throughput Screening, 25(5), 838-846. https://doi.org/10.2174/1386207324666210203175631

5. Nalamachu, S., & Wortmann, R. (2014). Role of indomethacin in acute pain and inflammation management: a review of the literature. Postgraduate Medicine, 126(4), 92-97. https://doi.org/10.3810/pgm.2014.07.2787

6. Wang, S. M., Han, C., Lee, S. J., Patkar, A. A., Masand, P. S., & Pae, C. U. (2016). Vilazodone for the treatment of depression: an update. Chonnam Medical Journal, 52(2), 91-100. https://doi.org/10.4068/cmj.2016.52.2.91

7. Wong, G. W., Boyda, H. N., & Wright, J. M. (2014). Blood pressure lowering efficacy of partial agonist beta blocker monotherapy for primary hypertension. Cochrane Database of Systematic Reviews, (11). https://doi.org/10.1002/14651858.CD007450.pub2

8. Brandes, J. L., Kudrow, D., Stark, S. R., O'Carroll, C. P., Adelman, J. U., O'Donnell, F. J., Alexander, W. J., Spruill, S. E., Barrett, P. S., & Lener, S. E. (2007). Sumatriptan-naproxen for acute treatment of migraine: a randomized trial. Jama, 297(13), 1443-1454. https://doi.org/10.1001/jama.297.13.1443

9. Shin, D. Y., Shin, H. J., Kim, G.-Y., Cheong, J., Choi, I.-W., Kim, S.-K., Moon, S.-K., Kang, H. S., & Choi, Y. H. (2008). Streptochlorin isolated from Streptomyces sp. Induces apoptosis in human hepatocarcinoma cells through a reactive oxygen species-mediated mitochondrial pathway. Journal of Microbiology and Biotechnology, 18(11), 1862-1868. https://doi.org/10.4014/jmb.0800.124

10. Jeong, S. Y., Ishida, K., Ito, Y., Okada, S., & Murakami, M. (2003). Bacillamide, a novel algicide from the marine bacterium, Bacillus sp. SY-1, against the harmful dinoflagellate, Cochlodinium polykrikoides. Tetrahedron Letters, 44(43), 8005-8007. https://doi.org/10.1016/j.tetlet.2003.08.115

11. Ma, W. H., & Qin, L. P. (2014). Chemical constituents of arabidopsis thaliana. Chemistry of Natural Compounds, 50(4), 776-777. https://doi.org/10.1007/s10600-014-1083-9

12. Smith, B. A., Neal, C. L., Chetram, M., Vo, B., Mezencev, R., Hinton, C., & Odero-Marah, V. A. (2013). The phytoalexin camalexin mediates cytotoxicity towards aggressive prostate cancer cells via reactive oxygen species. Journal of Natural Medicines, 67(3), 607-618. https://doi.org/10.1007/s11418-012-0722-3

13. Goodwin, S., Smith, A. F., & Horning, E. C. (1959). Alkaloids of Ochrosia elliptica Labill. Journal of the American Chemical Society, 81(8), 1903-1908. https://doi.org/10.1021/ja01517a031

14. Kohn, K. W., Waring, M. J., Glaubiger, D., & Friedman, C. A. (1975). Intercalative binding of ellipticine to DNA. Cancer Research, 35(1), 71-76.

15. Wright, C. W., Addae-Kyereme, J., Breen, A. G., Brown, J. E., Cox, M. F., Croft, S. L., Gökçek, Y., Kendrick, H., Phillips, R. M., & Pollet, P. L. (2001). Synthesis and evaluation of cryptolepine analogues for their potential as new antimalarial agents. Journal of Medicinal Chemistry, 44(19), 3187-3194. https://doi.org/10.1021/jm010929+

16. Quilico, A., & Panizzi, L. (1943). Chemische Untersuchungen über Aspergillus echinulatus, I. Mitteilung. Berichte der Deutschen Chemischen Gesellschaft (A and B Series), 76(4), 348-358. https://doi.org/10.1002/cber.19430760408

17. Makhloufi, H., Pinon, A., Champavier, Y., Saliba, J., Millot, M., Fruitier-Arnaudin, I., Liagre, B., Chemin, G., & Mambu, L. (2024). In Vitro Antiproliferative Activity of Echinulin Derivatives from Endolichenic Fungus Aspergillus sp. against Colorectal Cancer. Molecules, 29(17), 4117. https://doi.org/10.3390/molecules29174117

18. Zhang, Y. S., Li, J. D., & Yan, C. (2018). An update on vinpocetine: new discoveries and clinical implications. European Journal of Pharmacology, 819, 30-34. https://doi.org/10.1016/j.ejphar.2017.11.041

19. Dai, J., Dan, W., Schneider, U., & Wang, J. (2018). β-Carboline alkaloid monomers and dimers: Occurrence, structural diversity, and biological activities. European Journal of Medicinal Chemistry, 157, 622-656. https://doi.org/10.1016/j.ejmech.2018.08.027

20. Cohen, P. A., Wang, Y. H., Maller, G., DeSouza, R., & Khan, I. A. (2016). Pharmaceutical quantities of yohimbine found in dietary supplements in the USA. Drug Testing and Analysis, 8(3-4), 357-369. https://doi.org/10.1002/dta.1849

21. Clauder, O., Gesztes, K., & Szász, K. (1962). Studies on the structure of vincamine. Tetrahedron Letters, 3(24), 1147-1154. https://doi.org/10.1016/S0040-4039(00)70977-4

22. Trojánek, J., Štrouf, O., Holubek, J., & Čekan, Z. (1961). Structure of vincamine. Tetrahedron Letters, 2(20), 702-706. https://doi.org/10.1016/S0040-4039(01)91678-8

23. Fischhof, P. K., Möslinger-Gehmayr, R., Herrmann, W. M., Friedmann, A., & Ruβmann, D. L. (1996). Therapeutic efficacy of vincamine in dementia. Neuropsychobiology, 34(1), 29-35. https://doi.org/10.1159/000119288

24. Achor, R. W., Hanson, N. O., & Gifford, R. W. (1955). Hypertension treated with Rauwolfia serpentina (whole root) and with reserpine: controlled study disclosing occasional severe depression. Journal of the American Medical Association, 159(9), 841-845. https://doi.org/10.1001/jama.1955.02960260011004

25. Oikawa, Y., Yoshioka, T., Mohri, K., & Yonemitsu, O. (1979). Synthesis of pimprinine and related oxazolylindole alkaloids from N-acyl derivatives of tryptamine and tryptophan methyl ester by DDQ oxidation. Heterocycles, 12(11) 1457-1462. https://doi.org/10.3987/r-1979-11-1457

26. Koyama, Y., Yokose, K., & Dolby, L. J. (1981). Isolation, characterization and synthesis of pimprinine, pimprinethine and pimprinaphine, metabolites of Streptoverticillium olivoreticuli. Agricultural and Biological Chemistry, 45(5), 1285-1287. https://doi.org/10.1271/bbb1961.45.1285

27. Kumar, D., Sundaree, S., Patel, G., & Rao, V. S. (2008). A facile synthesis of naturally occurring 5-(3-indolyl) oxazoles. Tetrahedron Letters, 49(5), 867-869. https://doi.org/10.1016/j.tetlet.2007.11.173

28. Savelson, E., & Tepe, J. J. (2022). One-Pot Friedel–Crafts/Robinson–Gabriel Synthesis of the Indole-Oxazole Scaffold and Its Application to the Synthesis of Breitfussins C, G, and H. The Journal of Organic Chemistry, 88(2), 755-761. https://doi.org/10.1021/acs.joc.2c00033

29. Bracken, C., & Baumann, M. (2020). Development of a continuous flow Photoisomerization reaction converting Isoxazoles into diverse Oxazole products. The Journal of Organic Chemistry, 85(4), 2607-2617. https://doi.org/10.1021/acs.joc.9b03399

30. Nakagawa, M., Nishida, A., Fuwa, M., Saito, H., & Ltd, L. C. C. (1999, August 13). WO2001012626A1 - Indole compounds, process for the preparation of the same and uses thereof - Google Patents. https://patents.google.com/patent/WO2001012626A1/en#patentCitations

31. Pedras, M. S. C., & Abdoli, A. (2013). Metabolism of the phytoalexins camalexins, their bioisosteres and analogues in the plant pathogenic fungus Alternaria brassicicola. Bioorganic & Medicinal Chemistry, 21(15), 4541-4549. https://doi.org/10.1016/j.bmc.2013.05.026

32. Nicolaou, K. C., Hao, J., Reddy, M. V., Rao, P. B., Rassias, G., Snyder, S. A., Huang, X., Chen, D. Y. -k., Brenzovich, W. E., Giuseppone, N., Giannakakou, P., & O'Brate, A. (2004). Chemistry and biology of diazonamide A: second total synthesis and biological investigations. Journal of the American Chemical Society, 126(40), 12897-12906. https://doi.org/10.1021/ja040093a

33. Al-Azawe, S. S. (1988). Synthesis of 2,5-disubstituted thiazoles and their reactions with Grignard reagents. Journal of the Iraqi Chemical Society, 13, 1.

34. Wang, B., Tao, Y., Liu, Q., Liu, N., Jin, Z., & Xu, X. (2017). Algicidal activity of bacillamide alkaloids and their analogues against marine and freshwater harmful

algae. Marine Drugs, 15(8), 247. https://doi.org/10.3390/md15080247

35. Wang, Y., Liu, Q., Wei, Z., Liu, N., Li, Y., Li, D., Jin, Z., & Xu, X. (2018). Thiazole amides, a novel class of algaecides against freshwater harmful algae. Scientific Reports, 8(1), 8555. https://doi.org/10.1038/s41598-018-26911-6

36. Saalim, M., Liu, S., Bennett, S. D., Zaleta-Pinet, D. A., Poulin, R. X., & Clark, B. R. (2024). Precursor-Directed Biosynthesis of Antialgal Fluorinated Bacillamide Derivatives in Bacillus atrophaeus. Journal of Natural Products, 87(2), 388-395. https://doi.org/10.1021/acs.jnatprod.3c01178

37. Hohmann, M., Brunner, V., Johannes, W., Schum, D., Carroll, L. M., Liu, T., Sasaki, D., Bosch, J., Clavel, T., Sieber, S. A., Zeller, G., Tschurtschenthaler, M., Janßen, K.-P., & Gulder, T. M. (2024). Bacillamide D produced by Bacillus cereus from the mouse intestinal bacterial collection (miBC) is a potent cytotoxin in vitro. Communications Biology, 7(1), 655. https://doi.org/10.1038/s42003-024-06208-3

38. Figueira, V. B., Prabhakar, S., & Lobo, A. M. (2005). Synthesis of the algicide bacillamide. Arkivoc, 14, 14-9. https://doi.org/10.3998/ark.5550190.0006.e02

39. Kumara, S., & Aggarwal, R. (2018). A concise and efficient route to the total synthesis of bacillamide A and its analogues. Archivoc, 2018(3), 354-361. https://doi.org/10.24820/ark.5550190.p010.362

40. Socha, A. M., Long, R. A., & Rowley, D. C. (2007). Bacillamides from a hypersaline microbial mat bacterium. Journal of Natural Products, 70(11), 1793-1795. https://doi.org/10.1021/np070126a

41. Bray, C. D., & Olasoji, J. (2010). A total synthesis of (+)-bacillamide B. Synlett, 2010(04), 599-601. https://doi.org/10.1055/s-0029-1219153

42. Sun, X., Liu, Y., Liu, J., Gu, G., & Du, Y. (2015). Synthesis and structural reconfirmation of bacillamide B. Organic & Biomolecular Chemistry, 13(14), 4271-4277. https://doi.org/10.1039/C5OB00093A

43. Ivanova, V., Kolarova, M., Aleksieva, K., Gräfe, U., Dahse, H. M., & Laatsch, H. (2007). Microbiaeratin, a new natural indole alkaloid from a Microbispora aerata strain, isolated from Livingston Island, Antarctica. Preparative Biochemistry & Biotechnology, 37(2), 161-168. https://doi.org/10.1080/10826060701199122

44. Li, D., Yang, H. S., Cui, Q., Mao, S. J., & Xu, X. H. (2009). Synthesis of bacillamide 3 and its analogue. Chinese Chemical Letters, 20(10), 1195-1197. https://doi.org/10.1016/j.cclet.2009.05.014

45. Wang, W., Joyner, S., Khoury, K. A. S., & Dömling, A. (2010). (−)-Bacillamide C: the convergent approach. Organic & Biomolecular Chemistry, 8(3), 529-532. https://doi.org/10.1039/B918214D

46. Martínez, V., & Davyt, D. (2013). Total syntheses of bacillamide C and neobacillamide A; revision of their absolute configurations. Tetrahedron: Asymmetry, 24(24), 1572-1575. https://doi.org/10.1016/j.tetasy.2013.11.001

47. Yu, L. L., Li, Z. Y., Peng, C. S., Li, Z. Y., & Guo, Y. W. (2009). Neobacillamide A, a novel thiazole-containing alkaloid from the marine bacterium Bacillus vallismortis C89, associated with South China Sea sponge Dysidea avara.

Helvetica Chimica Acta, 92(3), 607-612. https://doi.org/10.1002/hlca.200800349

48. Konda, Y., Suzuki, Y., Omura, S., & Onda, M. (1976). Alkaloid from Thermoactinomyces species. Chemical and Pharmaceutical Bulletin, 24(1), 92-96. https://doi.org/10.1248/cpb.24.92

49. Onda, M., & Konda, Y. (1978). Synthesis of the alkaloid from Thermoactinomyces species. Chemical and Pharmaceutical Bulletin, 26(7), 2167-2169. https://doi.org/10.1248/cpb.26.2167

50. Dean, B. M., Mijović, M. P. V., & Walker, J. (1961). 660. Chemistry of micrococcin P. Part VI. Racemisation of 2-(l-amino-2-methylpropyl) thiazole-4-carboxylic acid, and related studies. Journal of the Chemical Society (Resumed), 3394-3400. https://doi.org/10.1039/JR9610003394

51. Bischler, A., & Napieralski, B. (1893). Zur kenntniss einer neuen isochinolinsynthese. Berichte der Deutschen Chemischen Gesellschaft, 26(2), 1903-1908. https://doi.org/10.1002/cber.189302602143

52. Katritzky, A. R., Ramsden, C. A., Scriven, E. F., & Taylor, R. J. (2008). Comprehensive heterocyclic chemistry III. In V1 3-memb. Heterocycl., together with all Fused Syst. contain. a 3-memb. Heterocycl. Ring. V2 4-memb. Heterocycl. together with all Fused Syst. contain. a 4-memb. Heterocycl. Ring. V3 Five-memb. Rings with One Heteroat. together with their Benzo and other Carbocycl.-fused Deriv. V4 Five-memb. Rings with Two Heteroat., each with their Fused Carbocycl. Deriv. (pp. 1-13718). Elsevier. https://doi.org/10.1016/C2009-1-28335-3

53. Li, M., Yuan, Y., & Chen, Y. (2021). Bischler-Napieralski Cyclization: A Versatile Reaction towards Functional Aza-PAHs and Their Conjugated Polymers. Chinese Journal of Chemistry, 39(11), 3101-3115. https://doi.org/10.1002/cjoc.202100419

54. Keglevich, G. (Ed.). (2018). Organophosphorus Chemistry: Novel Developments. (pp. 148-157). De Gruyter. https://doi.org/10.1515/9783110535839

55. Szabó, T., Dancsó, A., Ábrányi-Balogh, P., Volk, B., & Milen, M. (2019). First reported propylphosphonic anhydride (T3P®) mediated Robinson–Gabriel cyclization. Synthesis of natural and unnatural 5-(3-indolyl) oxazoles. Tetrahedron Letters, 60(20), 1353-1356. https://doi.org/10.1016/j.tetlet.2019.04.024

56. Abranyi-Balogh, P., Földesi, T., Grün, A., Volk, B., Keglevich, G., & Milen, M. (2016). Synthetic study on the T3P®-promoted one-pot preparation of 1-substituted-3,4-dihydro-β-carbolines by the reaction of tryptamine with carboxylic acids. Tetrahedron Letters, 57(18), 1953-1957. https://doi.org/10.1016/j.tetlet.2016.03.067

57. Ábrányi-Balogh, P., Volk, B., Keglevich, G., & Milen, M. (2016). Computational study on the synthesis of 1-phenyl-3,4-dihydro-β-carboline: T3P®-promoted one-pot formation from tryptamine vs. POCl3-mediated ring closure of Nb-benzoyltryptamine. The first DFT investigation of the Bischler-Napieralski reaction. Computational and Theoretical Chemistry, 1097, 48-60. https://doi.org/10.1016/j.comptc.2016.10.008

58. Kleks, G., Duffy, S., Lucantoni, L., Avery, V. M., & Carroll, A. R. (2020). Orthoscuticellines A–E, β-carboline alkaloids from the bryozoan Orthoscuticella ventricosa collected in Australia. Journal of Natural Products, 83(2), 422-428. https://doi.org/10.1021/acs.jnatprod.9b00933

59. Yi, L., He, Y.-T., Tan, S., White, L. V., Lan, P., Gardiner, M. G., Pei, Z., Coote, M. L., & Banwell, M. G. (2022). Total syntheses of the structures assigned to the marine natural products orthoscuticellines A–E. The Journal of Organic Chemistry, 87(18), 12287-12296. https://doi.org/10.1021/acs.joc.2c01477

60. Abarca, B., Custodio, R., Cuadro, A. M., Sucunza, D., Domingo, A., Mendicuti, F., Alvarez-Builla, J., & Vaquero, J. J. (2014). Efficient synthesis of an indoloquinolizinium alkaloid selective DNA-binder by ring-closing metathesis. Organic Letters, 16(13), 3464-3467. https://doi.org/10.1021/ol5013668

61. Busqué, J., Pedrosa, M. M., Cabellos, B., & Muzquiz, M. (2010). Phenological changes in the concentration of alkaloids of Carex brevicollis in an alpine rangeland. Journal of Chemical Ecology, 36(11), 1244-1254. https://doi.org/10.1007/s10886-010-9865-4

62. Lazurjevski, G., & Terentjeva, I. (1976). 1,4-Substituted β-Carbolines from Carex brevicollis DC. Heterocycles, 4(11), 1783. https://doi.org/10.3987/r-1976-11-1783

63. Terent'eva, I. (1960). Moldavii Trudy Instituta Khimii Akademii Nauk Moldavskoi SSR, 21.

64. Szabó, T., Görür, F. L., Horváth, S., Volk, B., & Milen, M. (2022). Synthesis of racemic and enantiopure forms of β-carboline alkaloid brevicolline. Synthesis, 54(17), 3867-3873. https://doi.org/10.1055/s-0041-1737830

65. Vember, P. A., & Terentjeva, I. (1969). Brevicarine from brevicolline. Khimiya Prirodnykh Soedinenii. 5, 404-406.

66. Kuchkova, K., Semenov, A., & Terentjeva, I. (1970). Khimiya Geterotsiklicheskikh Soedinenii. 197.

67. Kuchkova, K., Semenov, A., & Terentjeva, I. (1971). Total synthesis of alkaloid brevicarine and its inferior homologue. Acta Chimica Academiae Scientiarum Hungaricae. 69, 367–371.

68. Powers, J. C. (1965). Synthesis of Piperidylindoles. The Journal of Organic Chemistry, 30(8), 2534-2540. https://doi.org/10.1021/jo01019a008

69. Müller, W. H., Preuß, R., & Winterfeldt, E. (1977). Reaktionen an Indolderivaten, XXXIII. Eine einfache und biogeneseorientierte Totalsynthese von Brevicollin und Brevicarin. Chemische Berichte, 110(7), 2424-2432. https://doi.org/10.1002/cber.19771100703

70. Marcu, G. A. (1965). Tr. Tret'ei Nauchn. Konferentsiya Molodykh Uchenykh Moldavii, Biologiya i Sel'skokhozyaistvennye Nauki, 2, 243.

71. Iasnetsov, V. S., & Sizov, P. I. (1972). Mechanism of action of brevicollin, thalictrimene and pachycarpine on the uterus. Farmakologiia i Toksikologiia, 35(2), 201-203.

72. Towers, G. H. N., & Abramowski, Z. (1983). UV-mediated genotoxicity of furanoquinoline and of certain tryptophan-derived alkaloids. Journal of Natural Products, 46(4), 576-581. https://doi.org/10.1021/np50028a027

73. Vember, P. A., & Terent'eva, I. V. (1969). Brevicarine from brevicolline. Chemistry of Natural Compounds, 5(5), 335-336. https://doi.org/10.1007/bf00595072

74. Bhajan, C., Soulange, J. G., Sanmukhiya, V. M. R., Olędzki, R., & Harasym, J. (2023). Phytochemical composition and antioxidant properties of Tambourissa ficus, a Mauritian endemic fruit. Applied Sciences, 13(19), 10908. https://doi.org/10.3390/app131910908

75. Dubey, A., Ghosh, N., & Singh, R. (2023). An in-depth and in vitro evaluation of the antioxidant and neuroprotective activity of aqueous and ethanolic extract of Asparagus racemosus Linn seed. Research Journal of Chemistry and Environment, 27(10), 46-66. https://doi.org/10.25303/2710rjce046066

76. Chalertpet, K., Sangkheereeput, T., Somjit, P., Bankeeree, W., & Yanatatsaneejit, P. (2023). Effect of Smilax spp. and Phellinus linteus combination on cytotoxicity and cell proliferation of breast cancer cells. BMC Complementary Medicine and Therapies, 23(1), 177. https://doi.org/10.1186/s12906-023-04003-x

77. Macaev, F., Stangaci, E., Duca, D., Duca, G., & De Chimie Al Academiei De Stiinte a Moldovei, I. (2008, July 15). MD4009B1 - Use of 1-methyl-4-(N-methylaminobutyl-4)- Beta -carboline as antituberculous remedy - Google Patents. https://patents.google.com/patent/MD4009B1/en

78. Riaz, A., Rasul, A., Hussain, G., Saadullah, M., Rasool, B., Sarfraz, I., Masood, M., Asrar, M., Jabeen, F., & Sultana, T. (2020). Resistomycin, a pentacyclic polyketide, inhibits the growth of triple negative breast cancer cells through induction of apoptosis and mitochondrial dysfunction. Pakistan Journal of Pharmaceutical Sciences, 33(3), 1233-1238. https://doi.org/10.36721/pjps.2020.33.3.sup.1233-1238.1

79. Min, D. J., Kim, S. J., & Hwang, J. S. (2007, October 31). Composition for external application containing PPARs activator from plant (WO Patent Application No. WO 066255 A1). World Intellectual Property Organization.

80. Denisenko, P. P., Vinogradova, T. V., & Semenov, A. A. (1988). Brevikarin dihydrochloride--a new original anti-arrhythmia agent. Farmakologiia i Toksikologiia, 51(2), 50-53.

81. Kireev, D., Wigle, T. J., Norris-Drouin, J., Herold, J. M., Janzen, W. P., & Frye, S. V. (2010). Identification of non-peptide malignant brain tumor (MBT) repeat antagonists by virtual screening of commercially available compounds. Journal of Medicinal Chemistry, 53(21), 7625-7631. https://doi.org/10.1021/jm1007374

82. Polledo, L., Marín, J. G., Martínez-Fernández, B., González, J., Alonso, J., Salceda, W., & García-Iglesias, M. J. (2012). Recurrent outbreaks of myelodysplasia in newborn calves. Journal of Comparative Pathology, 147(4), 479-485. https://doi.org/10.1016/j.jcpa.2012.03.002

83. Frisch, M. J., Trucks, G. W., Schlegel, H. B., Scuseria G. E., Robb, M. A., Cheeseman, J. R., Scalmani, G., Barone, V., Petersson, G. A., Nakatsuji, H., Li, X., Caricato, M., Marenich, A. V., Bloino, J., Janesko, B. G., Gomperts, R., Mennucci, B., Hratchian, H. P., Ortiz, J. V., Izmaylov, A. F., Sonnenberg, J. L., Williams-Young, D., Ding, F., Lipparini, F., Egidi, F., Goings, J., Peng, B., Petrone, A., Henderson, T., & Ranasinghe D. (2016). Gaussian 16 Revision C. 01, 2016. Gaussian Inc. Wallingford CT, 1, 572.

84. Zhao, Y., & Truhlar, D. G. (2008). The M06 suite of density functionals for main group thermochemistry, thermochemical kinetics, noncovalent interactions, excited states, and transition elements: two new functionals and systematic testing of four M06-class functionals and 12 other functionals. Theoretical Chemistry Accounts, 120(1), 215-241. https://doi.org/10.1007/s00214-007-0310-x

85. Petersson, A., Bennett, A., Tensfeldt, T. G., Al-Laham, M. A., Shirley, W. A., & Mantzaris, J. (1988). A complete basis set model chemistry. I. The total energies of closed-shell atoms and hydrides of the first-row elements. The Journal of Chemical Physics, 89(4), 2193-2218. https://doi.org/10.1063/1.455064

86. Marenich, A. V., Cramer, C. J., & Truhlar, D. G. (2009). Universal solvation model based on solute electron density and on a continuum model of the solvent defined by the bulk dielectric constant and atomic surface tensions. The Journal of Physical Chemistry B, 113(18), 6378-6396. https://doi.org/10.1021/jp810292n

87. Milen, M., Slegel, P., Keglevich, P., Keglevich, G., Simig, G., & Volk, B. (2015). Efficient synthesis of Nb-thioacyltryptamine derivatives by a three-component Willgerodt–Kindler reaction, and their transformation to 1-substituted-3, 4-dihydro-β-carbolines. Tetrahedron Letters, 56(42), 5697-5700. https://doi.org/10.1016/j.tetlet.2015.09.007

88. Pollák, P., Szele, B., Varga, M., Paszternák, A., Varga, K., Dancsó, A., Simig, G., Volk, B., Tábi, T., & Milen, M. (2025). Synthesis and Structure–Activity Relationship Studies of Novel Oxazolyl-and Thiazolyl-Indoles and their Intermediates as Selective Antiproliferative Agents Against HL-60 Leukemia and C6 Glioma Cell Lines. ChemMedChem, 20(15), e202500030. https://doi.org/10.1002/cmdc.202500030

89. Zavarzin, I. V., Yarovenko, V. N., Shirokov, A. V., Smirnova, N. G., Es'kov, A. A., & Krayushkin, M. M. (2003). Synthesis and reactivity of monothio-oxamides. Arkivoc, 13, 205-223. https://doi.org/10.3998/ark.5550190.0004.d22

90. Krayushkin, M. M., Yarovenko, V. N., & Zavarzin, I. V. (2004). Synthesis and reactivity of monothiooxamides and thiohydrazides of oxamic acids. Russian chemical bulletin, 53(3), 517-527. https://doi.org/10.1023/B:RUCB.0000035631.82058.9c

91. Daina, A., Michielin, O., & Zoete, V. (2017). SwissADME: a free web tool to evaluate pharmacokinetics, drug-likeness and medicinal chemistry friendliness of small molecules. Scientific Reports, 7(1), 42717. https://doi.org/10.1038/srep42717

92. Daina, A., & Zoete, V. (2016). A boiled-egg to predict gastrointestinal absorption and brain penetration of small molecules. ChemMedChem, 11(11), 1117-1121. https://doi.org/10.1002/cmdc.201600182

93. Batizi, B., Pollák, P., Horváth, S., Karaghiosoff, K., Simig, G., Németh, G., Volk, B., & Milen, M. (2025). Synthesis of Bacillamide B–D and Neobacillamide A Alkaloids, and Their Antipodes: Unambiguous Assignment of Absolute Configurations and Direction of Optical Rotations. Asian Journal of Organic Chemistry, 14(12), e70255. https://doi.org/10.1002/ajoc.70255

94. Menche, D., Hassfeld, J., Li, J., Mayer, K., & Rudolph, S. (2009). Modular total synthesis of archazolid A and B. The Journal of Organic Chemistry, 74(19), 7220-7229. https://doi.org/10.1021/jo901565n

95. Han, A., & Inc, R. P. (2021, December 29). WO2023129518A1 - Tubulysins and protein-tubulysin conjugates - Google Patents. https://patents.google.com/patent/WO2023129518A1/en?oq=WO2023129518+

96. Schmidt, U., Gleich, P., Griesser, H., & Utz, R. (1986). Amino Acids and Peptides; 58 Synthesis of Optically Active 2-(1-Hydroxyalkyl)-thiazole-4-carboxylic Acids and 2-(1-Aminoalkyl)-thiazole-4-carboxylic Acids. Synthesis, 1986(12), 992-998. https://doi.org/10.1055/s-1986-31847

97. Clayden, J., Greeves, N., & Warren, S. (2012). Organic chemistry. (2nd ed. pp. 1114-1117. ISBN: 9780199270293) Oxford university press.

98. Pollák, P., Garádi, Z., Volk, B., Dancsó, A., Simig, G., & Milen, M. (2025). Studies on the total syntheses of β-carboline alkaloids orthoscuticellines A and B. Natural Product Research, 39(13), 3677-3685. https://doi.org/10.1080/14786419.2024.2306600

99. Batizi, B., Pollák, P., Dancsó, A., Keglevich, P., Simig, G., Volk, B., & Milen, M. (2025). Studies on the syntheses of β-carboline alkaloids brevicarine and brevicolline. Beilstein Journal of Organic Chemistry, 21(1), 955-963. https://doi.org/10.3762/bjoc.21.79

100. Wolfe, S., & Hasan, S. K. (1970). Five-membered rings. II. Inter and intramolecular reactions of simple amines with N-substituted phthalimides. Methylamine as a reagent for removal of a phthaloyl group from nitrogen. Canadian Journal of Chemistry, 48(22), 3572-3579. https://doi.org/10.1139/v70-598

101. Terent'eva, I. V., Lazur'evskii, G. V., & Shirshova, T. I. (1969). The structure of brevicarine. Chemistry of Natural Compounds, 5(5), 330-334.

102. Aubry, C., Jenkins, P. R., Mahale, S., Chaudhuri, B., Maréchal, J. D., & Sutcliffe, M. J. (2004). New fascaplysin-based CDK4-specific inhibitors: design, synthesis and biological activity. Chemical Communications, (15), 1696-1697. https://doi.org/10.1039/B406076H

103. Redko, B., Albeck, A., & Gellerman, G. (2012). Facile synthesis and antitumor activity of novel N (9) methylated AHMA analogs. New Journal of Chemistry, 36(11), 2188-2191. https://doi.org/10.1039/C2NJ40567A

104. Inoue, H., Iijima, I., & Takeda, M. (1980). Synthesis of bridged 2-phenylcyclohexylamines as potential analgetics. Chemical and Pharmaceutical Bulletin, 28(4), 1022-1034. https://doi.org/10.1248/cpb.28.1022

105. Prabakaran, K., Zeller, M., Szalay, P. S., & Rajendra Prasad, K. J. (2012). Convenient Approaches towards the Synthesis of Novel Pyrano [2,3-*a*] carbazoles. Journal of Heterocyclic Chemistry, 49(6), 1302-1309. https://doi.org/10.1002/jhet.910

106. Bingul, M., Arndt, G. M., Marshall, G. M., Black, D. S., Cheung, B. B., & Kumar, N. (2021). Synthesis and characterisation of novel tricyclic and tetracyclic furoindoles: Biological evaluation as SAHA enhancer against neuroblastoma and breast cancer cells. Molecules, 26(19), 5745. https://doi.org/10.3390/molecules26195745

107. Varga, P. R., & Keglevich, G. (2021). Synthesis of α-aminophosphonates and related derivatives; the last decade of the Kabachnik–Fields reaction. Molecules, 26(9), 2511. https://doi.org/10.3390/molecules26092511

108. Gábor, D., Pollák, P., Volk, B., Dancsó, A., Simig, G., & Milen, M. (2023). Catalyst-and Solvent-Free Room Temperature Synthesis of α-Aminophosphonates: Green Accomplishment of the Kabachnik–Fields Reaction. ChemistrySelect, 8(26), e202301460. https://doi.org/10.1002/slct.202301460

109. Bhagat, S., & Chakraborti, A. K. (2007). An extremely efficient three-component reaction of aldehydes/ketones, amines, and phosphites (Kabachnik− Fields reaction) for the synthesis of α-aminophosphonates catalyzed by magnesium perchlorate. The Journal of Organic Chemistry, 72(4), 1263-1270. https://doi.org/10.1021/jo062140i

110. Ignacio, J. M., Macho, S., Marcaccini, S., Pepino, R., & Torroba, T. (2005). A facile synthesis of 1, 3, 5-trisubstituted hydantoins via Ugi four-component condensation. Synlett, 2005(20), 3051-3054. https://doi.org/10.1055/s-2005-922745

111. Jazinizadeh, T., Yazdani-Elah-Abadi, A., Maghsoodlou, M. T., & Heydari, R. (2020). $CeCl_3$-catalyzed a highly efficient and eco-friendly synthesis of new and densely functionalized thiazolo [3,2-*a*] pyrimidins *via* Biginelli-type reaction. Polycyclic Aromatic Compounds. https://doi.org/10.1080/10406638.2018.1481111

112. Pollák, P., Milen, M., Volk, B., & Ábrányi-Balogh, P. (2025). Comparative Computational Study on the Robinson–Gabriel Synthesis and Bischler–Napieralski Reaction: Density Functional Theory Investigation of T3P-Mediated Ring Closure. European Journal of Organic Chemistry, 28(21), e202400679. https://doi.org/10.1002/ejoc.202400679

9. BIBLIOGRAPHY OF THE CANDIDATE'S PUBLICATIONS

9.1. PUBLICATIONS RELATED TO THE DISSERTATION

1.

Pollák, P., Garádi, Z., Volk, B., Dancsó, A., Simig, G., & Milen, M. (2025). Studies on the total syntheses of β-carboline alkaloids orthoscuticellines A and B. Natural Product Research, 39(13), 3677-3685.

https://doi.org/10.1080/14786419.2024.2306600

IF: 2.2; Q2

2.

Pollák, P., Szele, B., Varga, M., Paszternák, A., Varga, K., Dancsó, A., Simig, G., Volk, B., Tábi, T., & Milen, M. (2025). Synthesis and Structure–Activity Relationship Studies of Novel Oxazolyl-and Thiazolyl-Indoles and their Intermediates as Selective Antiproliferative Agents Against HL-60 Leukemia and C6 Glioma Cell Lines. ChemMedChem, 20(15), e202500030.

https://doi.org/10.1002/cmdc.202500030

IF: 3.4; Q1

3.

Pollák, P., Milen, M., Volk, B., & Ábrányi-Balogh, P. (2025). Comparative Computational Study on the Robinson–Gabriel Synthesis and Bischler–Napieralski Reaction: Density Functional Theory Investigation of T3P-Mediated Ring Closure. European Journal of Organic Chemistry, 28(21), e202400679.

https://doi.org/10.1002/ejoc.202400679

IF: 2.7; Q2

4.

Batizi, B., Pollák, P., Dancsó, A., Keglevich, P., Simig, G., Volk, B., & Milen, M. (2025). Studies on the syntheses of β-carboline alkaloids brevicarine and brevicolline. Beilstein Journal of Organic Chemistry, 21(1), 955-963.

https://doi.org/10.3762/bjoc.21.79

IF: 2.2; Q2

5.

Batizi, B., Pollák, P., Horváth, S., Karaghiosoff, K., Simig, G., Németh, G., Volk, B., & Milen, M. (2025). Synthesis of Bacillamide B–D and Neobacillamide A Alkaloids, and Their Antipodes: Unambiguous Assignment of Absolute Configurations and Direction of Optical Rotations. Asian Journal of Organic Chemistry, 14(12), e70255.
https://doi.org/10.1002/ajoc.70255

IF: 2.7; Q2

9.2. PUBLICATIONS UNRELATED TO THE DISSERTATION

6.

Gábor, D., Pollák, P., Volk, B., Dancsó, A., Simig, G., & Milen, M. (2023). Catalyst-and Solvent-Free Room Temperature Synthesis of α-Aminophosphonates: Green Accomplishment of the Kabachnik–Fields Reaction. ChemistrySelect, 8(26), e202301460.
https://doi.org/10.1002/slct.202301460

IF: 2.1; Q2

7.

Milen, M., John, T. M., Pollák, P., & Keglevich, G. (2025). The Direct use of Metallic Ore Minerals as Catalysts in Organic Syntheses. Current Organic Chemistry, 29(2), 97-107.
https://doi.org/10.2174/0113852728327246240821061535

IF: 2.1; Q3

8.

Milen, M., & Pollák, P. (2026) A Biginelli-reakció és reprodukálhatóságának vizsgálata. Magyar Kémiai Folyóirat. 132(1-2), 48-51.
https://doi.org/10.24100/MKF.2026.01-02.48-51

9.

Pollák, P., Barótfi, S., Csóka, I., & Budai-Szűcs, M. (2025). A mesterséges intelligencia szerepe a korai fázisú onkológiai klinikai vizsgálatok tervezésében és megvalósíthatóságában [The role of artificial intelligence in the design and feasibility of early-phase oncology clinical trials]. Orvosi Hetilap, 166(47), 1857-1868. https://doi.org/10.1556/650.2025.33420

IF: 0.9; Q4

10.

Milen, M., Pollák, P., & Volk, B. (2026) Propylphosphonic Anhydride (T3P®)-Mediated Multicomponent Reactions. Tetrahedron, 194, 135157. https://doi.org/10.1016/j.tet.2026.135157

IF: 2.2; Q3

10. ACKNOWLEDGEMENTS AND FUNDING

I am deeply grateful to my external supervisors, **Mátyás Milen** and **Balázs Volk** (Egis Pharmaceuticals PLC), for their unwavering guidance and encouragement throughout my PhD studies. I owe special thanks to **Gyula Simig**, retired from Egis Pharmaceuticals PLC, for generously sharing his long-standing laboratory expertise. My appreciation also goes to **Gábor Németh** (Egis Pharmaceuticals PLC) for his expert industrial advice in organic and analytical chemistry, and to **István Mándity** (Semmelweis University) for his support in lecturing, funding applications, and flow chemistry. I am thankful to **Péter Ábrányi-Balogh** (HUN-REN TTK Medicinal Chemistry Research Group) for introducing me to computational chemistry and supervising that part of the project.

I also wish to express special appreciation to **Benedek Batizi**, whom I have had the pleasure of supervising from BSc through MSc studies. His commitment, creativity, and perseverance have significantly enriched our joint projects and made mentoring a truly rewarding experience.

I warmly thank the **Department of Organic Chemistry at Semmelweis University** for their collegial help in teaching and presenting my research, and all past and present collaborators from the **Department of Pharmacodynamics**, Department of Organic Chemistry at BME, and **Egis Pharmaceuticals PLC** – including Kamilla Varga, Máté Varga, Alexandra Paszternák, Tamás Tábi, Péter Keglevich, György Keglevich, Boglárka Szele, Zsófia Garádi, András Dancsó, and Simon Horváth – for their valuable contributions.

Finally, I express my heartfelt gratitude to my wife, parents, and grandparents, whose constant support, patience, and understanding have sustained me throughout this journey.

This work was prepared in the framework of 2020-1.1.2-PIACI-KFI-2020-00039 project with the support of the Ministry of Culture and Innovation from the National Research, Development, and Innovation Fund.

Project no. 2023-2.1.2-KDP-2023-00016 has been implemented with the support provided by the Ministry for Culture and Innovation of Hungary from the National Research, Development and Innovation Fund, financed under the KDP-2023 funding scheme.